Francisco Rodríguez
Manuel Berenguel
José Luis Guzmán
Armando Ramírez-Arias

Modeling and Control of Greenhouse Crop Growth

AIC

Springer

Advances in Industrial Control

Series editors

Michael J. Grimble, Glasgow, UK
Michael A. Johnson, Kidlington, UK

More information about this series at http://www.springer.com/series/1412

Francisco Rodríguez · Manuel Berenguel
José Luis Guzmán · Armando Ramírez-Arias

Modeling and Control of Greenhouse Crop Growth

Springer

Francisco Rodríguez
Manuel Berenguel
José Luis Guzmán
Departamento de Informática
Universidad de Almería
Almería
Spain

Armando Ramírez-Arias
Matemáticas e Informática (CITE III)
Universidad de Almería
Almería
Spain

To María del Mar and Mar

F. Rodríguez

To Antonio Román Díaz

M. Berenguel

To Aurelia and Jimena

J.L. Guzmán

To Carmen

A. Ramírez-Arias

Series Editors' Foreword

The series *Advances in Industrial Control* aims to report and encourage technology transfer in control engineering. The rapid development of control technology has impact on all areas of the control discipline. New theory, new controllers, actuators, sensors, new industrial processes, computer methods, new applications, new philosophies…, new challenges. Much of this development work resides in industrial reports, feasibility study papers, and in the reports of advanced collaborative projects. The series offers an opportunity for researchers to present an extended exposition of such new work in all aspects of industrial control for wider and rapid dissemination.

As every amateur gardener will know when growing tomatoes, if we use the tomato feed too early the plants put all their energy into producing foliage giving bushy plants with well-hidden flowers; and once the flowers have set, if we water the plants too much the swelling fruits will split and spoil. Getting the timing and quantities correct for a straightforward amateur gardening problem like this is a simple example of agrosystem control in action. The sensor–controller–actuator combination is the gardener who as "sensor" will observe the weather and look at the forecast weather, study the soil condition and plant condition, then as "controller" decide the actions and quantities needed and finally as "actuator" administer, water and tomato feed appropriately. The gardener's supervisory role will involve pest control and cultivar maintenance, for example, looking for pest infestations, and removing side shoots if necessary. A key feature to note is the labor-intensive nature of agrosystem control.

The simple example given above was for growing tomatoes, but all the operations are a microcosm of those needed in the large-scale production of commercial crops. Two particular features of consumer choice in vegetables are for uniformly high-quality fruit and for vegetables (and flowers) out of season, both of which are achieved for many vegetable and flower types using the controlled environments of greenhouses and poly-tunnels. In this commercial situation creating a uniform growing environment and a uniformity of high quality plant development thereby minimizing the cost of production and maximizing the grower's profit are key

motivators for the use of automatic control in greenhouse crop production. This is the system context for this first ever volume in the *Advances in Industrial Control* monograph series that reports the use of automatic control for these agrosystems, entitled *Modeling and Control of Greenhouse Crop Growth* and written by Francisco Rodríguez, Manuel Berenguel, José Luis Guzmán and Armando Ramírez-Arias.

The monograph follows the time-honored steps in an automatic control system study: system description, modeling and model validation, control studies, and applications. The particular application studied is the greenhouse crop growth of tomatoes. One immediate impression gained from the monograph is the complexity of the glasshouse crop growth system that is under control and, furthermore, that this complexity is further complicated by different time horizons for the overall system goals. Ultimately the authors propose a multi-layer hierarchical structure for the system control, decision-making, and supervision. Within this structure the authors investigate a wide range of control techniques for several different operational processes. These control techniques include adaptive control, model predictive control, event-based control, and fuzzy-logic control. However, the authors' signature achievement is the use of hierarchical control to accommodate the complexity of the glasshouse crop growth system and a multiobjective optimization solution to satisfying the many conflicting objectives inherent in the control system design.

In conclusion, this is the first monograph in the *Advances in Industrial Control* series on an important commercial agrosystem process. The volume will be of considerable interest to a wide range of readers from both the control and agricultural-crop-growing communities. The Series Editors hope that the work reported will inspire more monograph and textbook contributions on the control of these important and interesting systems.

Glasgow, Scotland, UK   M.J. Grimble
                                                                                      M.A. Johnson

Preface

Modern agriculture is nowadays subject to regulations in terms of quality and environmental impact and thus it is a field where the application of automatic control techniques has increased during the last few years. The greenhouse production agrosystem is a complex of physical, chemical, and biological processes, taking place simultaneously, reacting with different response times and patterns to environmental factors, and characterized by many interactions, which must be controlled to obtain the best results for the grower. Crop growth is the most important process and is mainly influenced by surrounding environmental climatic variables (Photosynthetically Active Radiation—PAR, temperature, humidity, and CO_2 concentration of the inside air), the amount of water and fertilizers supplied by irrigation, pests and diseases, and culture labors such as pruning and pesticide treatments, among others. A greenhouse is ideal for crop growing since it constitutes a closed environment in which climate and fertigation can be controlled (with different control problems and objectives). Empirically, the water and nutrients requirements of the different crop species are known and, in fact, the first automated systems were those that control these variables. On the other hand, the market price fluctuations and the environmental rules to improve water-use efficiency or to reduce fertilizer residues in the soil (such as the nitrate contents) are other aspects to be taken into account. Therefore, the optimal production process in a greenhouse agrosystem may be summarized as the problem of reaching the following objectives: an optimal crop growth (bigger production with better quality), reduction of the associated costs (mainly fuel, electricity, and fertilizers), reduction of residues (mainly pesticides and ions in soil), and the improvement of water use efficiency.

Many of these objectives are addressed in this book, where the major topics and key features are:

- Discussion and presentation of the greenhouse crop growth problem and the new challenges related to modeling and control issues, including a state of the art.
- Modeling of the different subsystems involved in the greenhouse crop grow control. Different modeling techniques are described to show how the resulting models can be used for simulation or control design purposes. Furthermore,

suggestions and ideas about how to develop and use physical and/or black-box models for the different subsystems are also described.

- Development of basic and advanced control strategies to control the different variables of the climate and irrigation control problems. First, basic control strategies such as PID control and feedforward compensators (which are widely used in commercial tools) are summarized. Moreover, advanced control techniques, such as event-based, robust, and predictive control, are described to improve the performance of the basic control strategies.
- A multiobjective optimization problem is proposed and tested for greenhouse crop growth management, obtaining tradeoff solutions of three objectives: maximization of economic benefits, fruit quality, and water-use efficiency. This optimization scheme has been integrated into a hierarchical control architecture performing the automatic generation of setpoints for daytime and night-time temperatures and electrical conductivity along a whole crop cycle (using a receding horizon strategy). The obtained results show logical trajectories both in short and long crop cycles.

The book summarizes research performed by the authors on modeling, simulation, control, and optimization of greenhouse crop production during more than 10 years providing real results in an industrial greenhouse. It includes recent research results mainly concerned with greenhouse crop growth problems. It can be useful for a wide range of readers in the academic field, as graduate students working on their Master's or Ph.Ds. in automatic control and agricultural engineering. Furthermore, suggestions are included for the greenhouse management, which will be useful for practitioners and companies.

The book is organized as follows: Chap. 1 gives a brief introduction to the greenhouse crop growth system justifying the need for automation. Furthermore, it is devoted to describe a typical automated greenhouse and the timescales involved: climate, crop growth, weather, and market. Chapter 2 is focused on climate dynamical models, based both on mass and energy balances (fundamental models) and obtained from data. Crop growth models are also developed in Chap. 2, as they play an important role in the optimization problem. In this book, tomato has been selected as representative crop so that the influence of both inside greenhouse climate and irrigation on tomato crop growth are studied. Implementation and disturbance forecast issues are also discussed in terms of parameters identification, and model calibration and validation, including sensitivity analysis. The problem of determining the trajectories to control greenhouse crop growth has traditionally been solved by using constrained optimization or applying artificial intelligence techniques. The economic profit has been used as the main criterion in most research on optimization approaches to obtain adequate climatic control setpoints for the crop growth. This book addresses the problem of greenhouse crop growth through a hierarchical control architecture governed by a high-level multiobjective optimization approach, where the solution to this problem is to find reference trajectories for diurnal and nocturnal temperatures (climate-related setpoints) and electrical conductivity (fertirrigation-related setpoints). The objectives are to

maximize profit, fruit quality, and water-use efficiency, these being currently fostered by international rules. Chapter 3 briefly describes control techniques used in the regulation layer of the hierarchical control scheme to cope with climate and irrigation control, including: PID control, feedforward control, gain scheduling control, adaptive control, event-based control, robust control, fuzzy logic control, and model predictive control. Chapter 4 is the core of the book. Taking into account the different models explained in Chap. 2 and the time scales involved, the main hierarchical control problem is introduced. The different control objectives are explained, starting with the solution of the optimization problem based on maximizing profits and afterwards introducing other objectives, such as maximization of water-use efficiency or quality. The solution of the multiobjective optimization problem is explained and also its role in the multilevel hierarchical control architecture is described. Finally, Chap. 5 summarizes some advices and suggestions for greenhouse users.

The text is composed of material collected from articles written by the authors, technical reports and lectures given to graduate students. The book is complemented with an extensive use of illustrations, tables and real examples which are helpful to understand the text. For this reason, the book can be of interest to engineers (agricultural, industrial, chemical, etc.) and process control engineers and researchers, as well as Ph.D. students in the engineering field.

Almería, Spain, July 2014   Francisco Rodríguez
Chapingo, México   Manuel Berenguel
                                                                     José Luis Guzmán
                                                            Armando Ramírez-Arias

Acknowledgments

Ciencia y Empleo de la Junta de Andalucía.[4] We gratefully acknowledge these institutions for their support.

The experiments described in the book could not have been carried out without the help of the Fundación Cajamar-Estación Experimental Las Palmerillas and their staff.

Finally, the authors thank their families for their support, patience, and understanding of family time lost during the writing of the book.

Almería, Chapingo, May 2014   Francisco Rodríguez
                                                                       Manuel Berenguel
                                                                        José Luis Guzmán
                                                                   Armando Ramírez-Arias

---

[4] Proyecto de Excelencia ControlCrop TEP 06174.

Contents

Acronyms

2DoF	Two degrees of freedom
AC	Adaptive control
AI	Artificial intelligence
AIC	Akaike's information criterion
ANN	Artificial neural networks
AR	Auto-regressive
ARIMA	Auto-regressive integrated moving average
ARIMAX	Auto-regressive integrated moving average with exogenous inputs
ARMA	Auto-regressive moving average
ARMAX	Auto-regressive moving average with exogenous inputs
ARX	Auto-regressive with exogenous inputs
AW	AntiWindup
BBCH	Biologische Bundesanstalt, Bundessortenamt and Chemical Scale
BIBO	Bounded-input bounded-output
BJ	Box-Jenkins
CARIMA	Controlled auto-regressive integrated moving average
CC	Cascade control
DAE	Differential algebraic equation
DES	Double exponential smoothing
DHA	Discrete hybrid automata
DKF	Discrete Kalman filter
DKFDF	Discrete Kalman filter with data fusion
DMC	Dynamic matrix control
DTC	Dead time compensator
EB	Event-based
EBC	Event-based control
EC	Electrical conductivity
EKF	Extended Kalman filter
ET	Evapotranspiration
EWMA	Exponentially weighted moving average
FDR	Frequency domain reflectometry

FF	Feedforward
FIR	Finite impulse response
FL	Feedback linearization
FLC	Fuzzy logic control
FOPDT	First order plus dead time
GA	Genetic algorithms
GM	Gain margin
GPC	Generalized predictive control
GS	Gain scheduling
HC	Hybrid control
IAE	Integral of the absolute error
ISE	Integral of the square of the error
ITAE	Integral of time multiplied by the absolute error
ITSE	Integral of time multiplied by the squared error
KBS	Knowledge-based system
KF	Kalman filter
KFDF	Kalman filter with data fusion
LAI	Leaf area index
LMIs	Linear matrix inequalities
LS	Least squares
LTI	Linear time invariant
MIMO	Multiple-inputs multiple-outputs
MIQP	Mixed integer quadratic programming
MISO	Multiple-inputs single-output
MLD	Mixed logical dynamical
MLP	Multi layer perceptron
MPC	Model-based predictive control
MSE	Mean squared error
NARX	Nonlinear auto-regressive with exogenous inputs
NC	Nonlinear control
NFIR	Nonlinear finite impulse response
NFT	Nutrient film technique
NLP	Nonlinear programming
NMPC	Nonlinear model predictive control
ODE	Ordinary differential equation
OE	Output error
OMT	Object modeling technique
PAR	Photosynthetically active radiation
PDC	Parallel distributed compensation
PDE	Partial differential equation
PDF	Pseudo derivative feedback
PI	Proportional-integral
PID	Proportional-integral-derivative
PM	Phase margin
PRBS	Pseudo random binary sequence

PRMS	Pseudo random multilevel sequence
PVC	Polyvinyl chloride
PWM	Pulse width modulation
QFT	Quantitative feedback theory
QP	Quadratic programming
RBFN	Radial basis functions network
RBS	Random binary sequence
RC	Robust control
RLS	Recursive least squares
RMSE	Root mean squared error
SCADA	Supervisory control and data acquisition
SISO	Single-input single-output
SLA	Specific leaf area
SP	Smith predictor
SQP	Sequential quadratic programming
SSE	Sum of squared errors
STC	Self-tuning control
TB	Time-based
TDC	Time delay compensation
TDL	Tapped delay lines
TDR	Time domain reflectometry
TS	Training set
T–S	Takagi–Sugeno model
VPD	Vapor pressure deficit
VS	Validation set
WSN	Wireless sensor network
WUE	Water use efficiency
ZN	Ziegler–Nichols
ZOH	Zero order hold

Symbols and Operators

$I\!N$	Set of natural numbers
$I\!R$	Set of real numbers
Z	Set of integers
$\arg(\cdot)$	Argument
$\det(\cdot)$	Matrix determinant
$(\cdot)^{\mathrm{T}}$	Transpose of $(\cdot)$
$\mathbf{I}$	Identity matrix of appropriate dimensions
$\sin(\cdot)$	Sine function
$\cos(\cdot)$	Cosine function
$\exp(\cdot), e^{(\cdot)}$	Exponential function
$\log(\cdot)$	Natural logarithm function
$\underline{\cdot}, \min(\cdot)$	Minimum of a set

$\overline{}$, $\max(\cdot)$	Maximum of a set
s	Complex variable used in Laplace Transform
z^{-1}	Backward shift operator
z	Forward shift operator and complex variable used in Z-Transform
$\Delta = 1 - z^{-1}$	Increment
$\forall$	For all
$\| \cdot \|$	$C^{n \times m}$ Norm
$\| \cdot \|_2$	$L_2^{n \times m}$ Norm
$\| \cdot \|_\infty$	∞ Norm
$\doteq$	Definition
$E[\cdot]$	Expectation operator
$\hat{}$	Expected value
$\bar{}$	Mean value
$\hat{X}(t+j\|t)$	Expected value of $X(t+j)$ with available information at instant t
$\wedge$	Logical AND
$\vee$	Logical OR
$\neg$	Logical NOR

Variables and Parameters Related to Greenhouse Physical Models

The notation used is composed of three elements ($T_{sb1,sb2}$): a symbol (T) that denotes the type of variables or constants, a first subscripts ($_{sb1}$) that identifies the name of the variable or constant and the physical process involved, and the second subscript ($_{sb2}$), that defines the greenhouse elements and the relation between them (separate by an hyphenation) or indicates a property of the variables or constants.

Type of Variables or Constants

c System constants or coefficients (–)
D Disturbance variable (–)
M Water mass flux (kg m^{-2} s^{-1})
Q Heat flux (W m^{-2})
t Time (continuous and discrete) (s, samples)
U Control input variables (–)
V Algebraic variable (–)
X State variable (–)
Y Output variable (–)

Second Subscript Notating Elements

a   Greenhouse internal air (–)
cr   Crop (–)
cv   Cover (–)
e   Greenhouse external conditions (–)
g   Greenhouse (–)

in   Inside/Incoming (–)
heat   Heating system (–)
out   Outside/Outcoming (–)
p   Pools of the NFT irrigation system (–)
s1   First soil layer (–)
s2   Second soil layer (–)
shd   Shade screen (–)
sky   Sky (upper hemisphere) (–)
ss   Soil surface (–)
wh   Whitening (–)

First Subscript and Second Subscript Modifiers
Physical Processes (Q, M, V, U)

cd   Condensation flux (–)
cl   Characteristic length (m)
cnd   Conduction flux (–)
cnv   Convection flux (–)
ef   Efficiency (–)
evp   Evaporation flux (–)
gen   Generated (–)
loss   Leakage when vents are closed (m^3 s^{-1})
phot   Photosynthesis (–)
rad   Long wave radiation flux (W m^{-2})
sol   Solar absorption (W m^{-2})
tot   Total amount of (–)
trp   Transpiration flux (kg s^{-1} m^{-2})
ven   Ventilation flux (m^3 s^{-1})

Type of Variables or Constants Variables (X, V, D)

cnv   Convection coefficient $V_{cnv,x-y}$: Convection coefficient between elements
        x and y (W m^{-2} K^{-1})
CO_2 CO_2 concentration (ppm)
H_a Absolute humidity (kg_{water} kg_{air}^{-1})
H_r Relative humidity (%)
hsat   Water concentration at saturation (kg_{water} kg_{air}^{-1})

LAI   Leaf Area Index (m^2 m^{-2})
lt   Latent heatvap: Vaporization air latent heat (J kg^{-1})
r   Resistance; bl: Boundary layer (s m^{-1}), s: Stomatal (s m^{-1}),
        trp: Transpiration (s m^{-1})
rn   Net radiation (W m^{-2})
rp   Par radiation (W m^{-2})
rs   Solar radiation (W m^{-2})

First Subscript and Second Subscript Modifiers Variables (X, V, D)

ssvp   Slope of saturated vapor pressure curve (Hpa s^{-1})
T Temperature (°C, K)
Texth Exhaust temperature (°C, K)
tsw   Short wave transmission (–)
ven   Position of the ventilation (°, rad, %), area—lat: Sidewall ventilation area
        (m^2), area—roof: Roof ventilation area (m^2), flux: Volumetric flow rate
        (m^3 s^{-1}), hef: Effective height (m), reg: Regime (–)
vpd   Vapor pressure deficit (Hpa)
vpsat   Saturation Vapor pressure (Hpa)
wd   Wind direction (°, rad)
ws   Wind speed (m s^{-1})

Constants (c)

alw   Long wave absorptivity (–)
area   Surface of (m^2)
asw   Short wave absorptivity (–)
cl   Characteristic length (m)
cnd   Conduction flux, $c_{cnd,x-y}$: Conduction coefficient between elements x
        and y (W m^{-1} K^{-1})
cnv   Convection flux, $c_{cnv,x-y}$: Convection coefficient parameters
d   Deep of (m)
den   Density of (kg m^{-3})
elw   Long wave emissivity (–)
extlw   Long wave crop extinction coefficient (–)
extsw   Short wave crop extinction coefficient (–)
evp   Evaporation from the pools (kg W^{-1} s^{-1}), 1: Net radiation calibration
        factor (kg Hpa^{-1} m^{-2} s^{-1}), 2: Humidity calibration factor (–)

vf   View factors for long wave radiation (–)
gv   Gravity constant (m s^{-2})
loss   Leakage when vents are closed, hw: Leakage with high wind speed
          (m^3 s^{-1}), lw: Leakage with low wind speed (m^3 s^{-1})
psyco   Psychometric constant (Hpa)
sb   Stefan–Boltzmann constant (W K^{-4} m^{-2})
sph   Specific heat coefficient (J kg^{-1} K^{-1})
th   Thickness of (m)
tlw   Long wave transmission (–)
ven   Ventilation, areap: Greenhouse section area perpendicular to vent flux
          (m^2), d: Discharge coefficient (–), l: Length of (m), max: Maximimun
          aperture (°), n: Number of (–), w: Width of (m), wd: Wind coefficient (–)
vol   Volume of (m^3)
ws   Wind speed, lim: Limit of (m s^{-1}), hw: High wind coefficient (m s^{-1}),
          lw: Low wind coefficient (m s^{-1})

Variables and Parameters Related to Crop Growth and Irrigation Models

$c_{con,phot}$ Photosynthesis coefficient conversion (s m^{-1})
c_{csol} Solutes concentration (mol m^{-3})
$c_{den,w}$ Density of water (kg m^{-3})
c_{df} Constant representing the drainage fraction (–)
c_E Growth efficiency (g$_{dry weight}$ g$_{CH_2O}^{-1}$)
c_{extlw} Light extinction coefficient (–)
c_{khr} Parameter affecting resistance between soil and root (–)
c_{kwrs} Parameter affecting resistance between soil and root (kg$_{dry weight}$ kg$_{water}^{-1}$)
c_{ky} Sensitivity to evapotranspiration deficit factor (–)
$c_{LAI,max}$ LAI when the set of leaves of the plant reaches its maximum (m^2 m^{-2})
c_m Light transmission coefficient through leaves (–)
c_{MF} Conversion factor between fresh and dry matter (–)
c_{nw} Water electric conductivity parameter (m^{-1} d)
c_{prr} Parameter that affects the pressure component of the hydric potential
                 within the root (kg$_{dry weight}$ kg$_{water}^{-1}$)
c_R Universal constant for gases (J mol^{-1} K^{-1})
c_{rsr} Parameter affecting resistance between soil and root (m s^{-1})
c_{sor} Parameter affecting resistance between soil and root (m^2)
c_{suwa} Constant threshold of EC over which there is a decrease
                 of water absorption (mS cm^{-1})
c_{srwa} Reduction coefficient of water absorption per unit of EC (m^3 mS^{-1} cm)

c_{w1}	Parameters of shape from the water retention curve (–)
c_{w2}	Parameters of shape from the water retention curve (–)
c_{w3}	Parameters of shape from the water retention curve (–)
c_z	Level in relation to the reference point (m)
c_ε	Parameter of rigidity of the cell wall (Pa)
D_{mc}	Content of dry matter in mature fruits (%)
f_{neor}	Nonstructural osmotically active fraction of dry matter for root (–)
f_{neoc}	Nonstructural osmotically active fraction of dry matter for canopy (–)
F_r	Irrigation supplied (kg m^{-2} min^{-1})
$F_{w_{r-c}}$	Water flow from root to shoot (kg m^{-2} min^{-1})
$F_{w_{s-r}}$	Water flow from substrate or soil to root (kg m^{-2} min^{-1})
$F_{w_{dr}}$	Excess flow or drainage (kg m^{-2} min^{-1})
F_{w_s}	Water flow in the soil or substrate (kg m^{-2} min^{-1})
GR_n	Net aboveground growth rate (g m^{-2} d^{-1})
g_{wrc}	Conductivity of the flow from root to shoot (m s^{-1})
K_F	Number of nodes since the first fruit appears until it matures (nodes)
K_{rSe}	Relative hydraulic conductivity (kg m^{-3} s)
K_s	Hydraulic conductivity at saturation (kg m^{-3} s)
K_{so}	Soil hydraulic conductivity (kg m^{-3} s^{-1})
M_{ner}	Nonstructural root dry matter (kg m^{-2})
M_{er}	Structural root dry matter (kg m^{-2})
N_b	Parameter in expolinear equation (node)
N_{FF}	Number of nodes/plant when first fruit appears (nodes)
N_{f1}	Number of nodes when the first fruit appears (nodes)
N_m	Maximum rate of nodes appearance (node d^{-1})
p_1	Loss of leaf dry weight per node (g node^{-1})
Q_{10}	Sensitivity of respiration to temperature (–)
r_m	Maintenance respiration coefficient (g$_{CH_2O}$ g$^{-1}_{dry\ weight}$ min^{-1})
r_{wsr}	Resistance to the flow from soil to root (s m^{-1})
R_y	Reduction of yield per unit of X_{CE} (% (mS cm)$^{-1}$)
S_e	Effective water content of the substrate or saturation in relation to sensible heat content (–)
S_t	Threshold of electric conductivity above which there is a yield decrease (mS cm^{-1})
T_{crit}	Mean daytime temperature above which fruit abortion starts (°C)
T_s	Absolute temperature (K)
$V_{abs,cr}(t)$	Water absorbed by the plants (m^3)
$V_{den,r}$	Density of roots (kg m^{-3})
$V_{dr}(t)$	Drainage volume (m^3)
V_{ET}	Evapotranspiration (kg water m^{-2} min^{-1})
$V_{ET_{max}}$	Maximum evapotranspiration (kg water m^{-2} min^{-1})
$V_{ff}(t)$	Fruit firmness (%)
V_{fot}	Photosynthesis (g$_{CH_2O}$ m^{-2} min^{-1})

$V_{fs}(t)$	Fruit size (%)
$V_{lt,vap}$	Latent heat of evaporation (J kg^{-1})
V_{max}	Maximum increase in vegetative tissue per node (g$_{dry\ weight}$ node^{-1})
V_{res}	Respiration (g$_{CH_2O}$ m^{-2} min^{-1})
V_R	Yield obtained with limited irrigation (kg m^{-2})
V_{Rmax}	Yield obtained under non limited irrigation (kg m^{-2})
V_{rn}	Net radiation available for the canopy (W m^{-2})
$V_{ssol}(t)$	Soluble solids concentration in the fruit (%)
$V_{ta}(t)$	Titratable acidity in fruits (%)
$V_{w,s}(t)$	Water content in the substrate (m^3)
X_{EC}	Electrical conductivity (mS cm^{-1})
X_F	Dry matter of fruits (g m^{-2})
X_{FF}	Fresh weight of fruits (kg m^{-2})
X_{LAI}	Leaf area index (m^2 m^{-2})
X_{LDW}	Dry matter of the leaf area (g m^{-2})
X_{MF}	Dry matter of mature fruits (g m^{-2})
X_N	Number of nodes (–)
X_{NT}	Number of trusses (–)
X_{SLA}	Specific leaf area (cm^{-2} g^{-1})
$\bar{X}_{Td,a}$	Average daily temperature (°C)
$X_{T,day}$	Average temperature of the daylight hours (°C)
X_W	Total dry weight (kg m^{-2})
X_{wc}	Mass of water in the shoot (kg water m^{-2})
X_{wr}	Mass of water in the roots (kg water m^{-2})
X_{wss}	Mass of water in the soil (kg water m^{-2})
α_e	Light efficiency (μmol$_{CO_2}$ μmol$^{-1}_{absorbed\ photon}$)
α_F	Maximum partitioning of new growth to fruit (fraction d^{-1})
α_v	Tuning parameter in ventilation rate equation (–)
β_l	Coefficient in expolinear equation (node^{-1})
β_v	Tuning parameter in ventilation rate equation (–)
δ_l	Maximum leaf area expansion per node (m^2 leaf node^{-1})
μ_S	Molal storage mass (kg mol^{-1})
ν	Vegetative-fruit transition coefficient (–)
ψ_e	Enclosing potential (Pa)
ψ_g	Gravitational potential (Pa)
ψ_{hc}	Potential of canopy (Pa)
ψ_{hr}	Potential of root (Pa)
ψ_{hs}	Potential of soil or substrate (Pa)
ψ_m	Matric potential (Pa)
ψ_n	Pneumatic potential (Pa)
ψ_{os}	Osmotic potential (Pa)
ψ_{osr}	Osmotic potential of root (Pa)
ψ_{osc}	Osmotic potential of canopy (Pa)

ψ_{pr}	Potential of pressure (Pa)
ψ_{prr}	Potential of pressure of root (Pa)
ψ_{prc}	Potential of pressure of canopy (Pa)
θ_r	Relative water content in the substrate (–)
θ_{mx}	Field capacity or container capacity (–)
ρ	Plants density (plants m^{-2})
τ_{CO_2}	Carbon dioxide efficiency ($g_{dry\ weight}\ node^{-1}$)

Other Variables and Parameters Related to Control Algorithms

Type of Variables or Constants

a	Pole of FOPDT discrete time transfer function (–)
A	CARIMA model polynomial in z^{-1} (–)
b	Numerator of FOPDT discrete time transfer function (–)
B	CARIMA model polynomial in z^{-1} (–)
c_k	Static gain of linear FOPDT model (–)
c_{Kp}	Proportional gain of PID controller (–)
$c_{Kpven,max}$	Maximum value of the proportional gain (–)
$c_{Kpven,min}$	Minimum value of the proportional gain (–)
$c_{T_{aw}}$	Tracking time constant of antiwindup scheme (s, min)
c_{T_d}	Derivative time of PID controller (s, min)
c_{T_i}	Integral time of PID controller (s, min)
c_{t_r}	Time delay of FOPDT model (s, min)
c_τ	Time constant of linear FOPDT model (s, min)
$c_{Tvenmin,wsmin}$	Minimum outside temperature for vents opening without wind (°C)
$c_{Tvenmin,wsmax}$	Minimum outside temperature for vents opening with maximum allowed wind speed (°C)
$c_{Tvenmax,wsmin}$	Outside temperature for maximum vents opening without wind (°C)
$c_{Tvenmax,wsmax}$	Outside temperature for maximum vents opening with maximum allowed wind speed (°C)
D	CARIMA model polynomial in z^{-1} (–)
D_m	Measured disturbance signal (–)
$\mathbf{D}_m$	Vector of future disturbances (–)
e	White noise signal (–)
E	Tracking error in feedback control (–)
E_{ee}	Electrical energy consumed by the heating system (W m^{-2})
E_u	Input side event (–)

E_y	Output side event (–)
F	Vector containing the free response of the system (–)
f_i	Free response coefficients of the system (–)
G	Matrix containing step response coefficients from the input (–)
g_i	Coefficients of **G** (–)
H	Matrix containing step response coefficients from the disturbance (–)
H_{heat}	Fuel consumption of the heating system (kg m^{-2})
h_i	Coefficients of **H** (–)
$M(t)$	Estimated trend in DES method (–)
N	Number/Prediction horizon (samples)
N_1	Minimum Prediction horizon (samples)Truncation order of a first order Volterra model
N_2	Maximum prediction horizon (samples)Truncation order of a second order Volterra model
N_d	Disturbance estimation horizon (samples)
N_u	Control horizon (samples)
N_t	Truncation order of a second order Volterra model (samples)
q_0	Parameter of discrete time PI controller (–)
q_1	Parameter of discrete time PI controller (–)
S	Unadjusted forecast in DES method (–)
t_{base}	Base sampling time in EBC (s)
t_f	Variable sampling time in EBC (s)
t_h	Harvesting time (d)
t_i	Initial time of crop cycle (d)
t_k	Time associated to an event (s)
t_{max}	Maximum sampling time in EBC (s)
T_{ref}	Setpoint temperature (°C)
t_s	Sample time (s, min)
U	Vector of actual and future control signals (–)
$U_{\text{sf}}(t)$	Supplied fertilizers in irrigation (m^3 m^{-2})
$U_{\text{sw}}(t)$	Supplied water to the crop (m^3 m^{-2})
V_{cos}	Greenhouse production associated costs (€, \$)
$V_{\text{ecos}}(t)$	Electricity costs (€ W^{-1}, \$ W^{-1})
$V_{\text{fcos}}(t)$	Fuel costs (€ kg^{-1}, \$ kg^{-1})
$V_{\text{fecos}}(t)$	Fertilizer cost (€ m^{-3}, \$ € m^{-3})
$V_{\text{price,cr}}$	Sales prices of the production at harvesting dates (€, \$)
$V_{\text{wcos}}(t)$	Water cost (€, m^{-3}, \$ m^{-3})
W	Generic reference trajectory (–)
w_{ff}	Optimization weighting parameter related to fruit firmness (–)
w_{fs}	Optimization weighting parameter related to fruit size (–)
w_{ssol}	Optimization weighting parameter related to soluble solids concentration in the fruit (–)

w_{ta}	Optimization weighting parameter related to titratable acidity in fruits (–)
$\mathbf{Y}$	Vector of future estimated outputs of the system (–)
α	Discrete variable allowing the commutation between dynamics in MLD (–)
α_d	Smoothing parameter for data in DES method (–)
α_v	Tuning parameter of the simplified ventilation flux model ($\%^{-1}$)
β_u	Parameter determining the deadband for the actuator (–)
β_v	Tuning parameter of the simplified ventilation flux model (–)
β_y	Parameter determining the deadband for the sensor (–)
δ	Weighting factor for future tracking errors (–)
γ_d	Smoothing parameter for trend in DES method (–)
λ	Weighting factor for control effort (–)
μ_i	Normalized membership functions (–)
Φ	Nonlinear mapping (–)
ρ	Tracking specifications for QFT design (–)
φ_i	Logical variables to determine a condition (–)
ω	Frequency (rad s^{-1})
σ	Discrete component of the state in MDL description (–)

Chapter 1
Introduction

1.1 The Greenhouse Crop Growth System

A greenhouse is an enclosure that allows owners to control climatic, nutrition, biotic, and cultural management variables that influence crop growth and development, so that optimal conditions are obtained at different stages of crop growth. Moreover, it permits producing off-season horticultural crops. The aim is to produce the maximum amount of a product with the highest quality and at minimal cost.

The diverse elements composing a greenhouse and the multiple relationships established inside make it a complex system, in which energy, mass, and information flows (inherent to the genetic material of plants and that provided by people), are dynamic and of different magnitudes. The crop is its main element as it is subjected to the influence of different variables, such as weather variations (temperature, humidity, photosynthetic active radiation -PAR-, and carbon dioxide -CO_2-), nutrition (water and nutrients), biotic (pests, diseases, viruses, bacteria, and weeds), and cultural management (pruning, spraying). These variables interact with each other with a high level of complexity, so that it is necessary to examine and identify them in subsystems. To achieve detailed knowledge of all the interactions and processes, models (mainly dynamic ones) are an important support tool to explain the observed behavior. Greenhouse subsystems have been dynamically characterized by different authors at different levels: Climate [57, 134, 177, 360, 422, 441, 461], water behavior in soil, or substrate [23, 145, 179, 293, 405], nutrition [179, 411], and pests and diseases [335], among others.

An important aspect is the economic one, from two points of view. First, the purchase prices at origin (paid to the farmer) fluctuate throughout the crop cycle. So, the ideal decision policy should be to obtain the production and sell when prices are the highest, trying to delay or advance crop growth to harvest at the optimal date. Moreover, to implement this policy it must be considered that the time interval in which delay/advance actions can be taken over the crop growth is limited to a range from 1 to 2 weeks, depending on the kind of crop. Second, obtaining optimal climate and fertigation conditions involves economic cost in terms of energy (electricity and
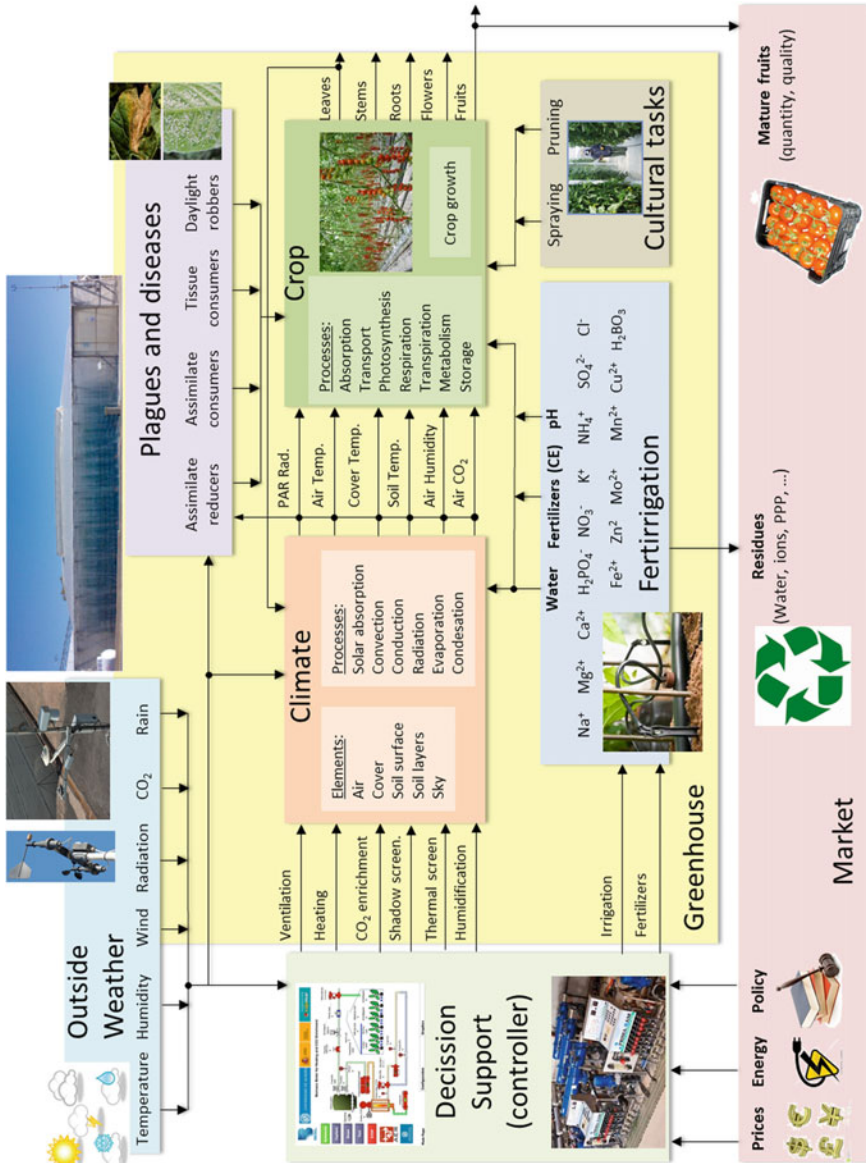
Fig. 1.1 Conceptual diagram of greenhouse production

fuel), water, and fertilizers. Therefore, the ideal situation from the economic point of view is not only maximizing production, but also optimizing the benefit defined as the difference between incomes proceeding from the sale of the products and the associated costs.

Figure 1.1 shows the subsystems, processes, and variables in their relationship with crop: The inputs are variables that can be controlled (inside climate, water, nutrients, and so on), disturbances are those variables affecting crop growth that cannot be manipulated, but can be measured so that their impact on the system can be accounted for (e.g., outside weather conditions, pests, and diseases), and the outputs are the variables to be controlled, distinguishing two types: Those that are the target of production (fruits, leaves, flowers, stems, or roots) and pollutant waste ones (e.g., waste of phytosanitary plant protection products). In addition, elements such as market or environmental regulations that influence control decisions on the input variables are shown. The integration of these elements is a major challenge for the greenhouse potential, which not only helps users in understanding the interactions between the different elements, but also allows them to control it.

This book proposes a comprehensive solution to the problem of optimal greenhouse production from an approach that includes climate, water, and nutritional elements (understanding the latter as the synthesis of nutrients expressed as electrical conductivity), considering economic aspects and energy efficiency.

1.2 The Need for Automation of Crop Growth in Greenhouses

As mentioned above, a greenhouse is ideal for crop growing since it constitutes a closed environment where climate and fertigation variables can be controlled. Although working in a closed environment facilitates the environmental control task, adequate control strategies are required to keep the main variables within the required limits, besides the process disturbances. Therefore, greenhouses should be equipped with sensors and actuators to be used by the control algorithms to interact with the process in order to fulfill the required control specifications.

The use of computers in greenhouses has allowed farmers to control the most important variables and to adapt the control parameters in an automatic manner. However, commercial computers are commonly used as an interface with actuators, and the control strategies are based on empirical rules according to the farmer experience [28]. Nowadays, most of the advanced control systems for climatic control include too many heuristic rules with, in many cases, hundreds of parameters to be tuned. The main problems in such controllers are the following [441]:

- The setpoint temperature tracking problem is affected by interactions between the different control loops and control devices (that are not usually taken into account).
- The setpoint values for the different climatic variables are not defined from a scientific point of view, and thus the energy usage in greenhouses is usually inefficient.

- The energy efficiency and actuator performance are difficult to be evaluated because of the large number of parameters and decision rules.

Currently, in most advanced control systems, many of them still under research, the control task is performed based on mathematical models that describe the dynamical behavior of the greenhouse, as usually done in the process industry [378]. The main idea of the advanced control techniques relies on using an objective function, based on climatic and crop models, and optimization techniques to determine the optimal trajectories of the main variables in the greenhouse control crop problem [107, 177, 201, 360, 383, 421, 441]. Some of these techniques have been used experimentally in greenhouses obtaining important energy savings [431]. However, although satisfactory results have been obtained in these experiments, the estimation of the economic benefit is still a challenge because of the small number of performed tests. Thus, more detailed tests in commercial facilities during several seasons are required to analyze the real impact of these control methodologies [429].

The complexity of the greenhouse production problem, with different simultaneous processes (physical, chemical, and biological) and with different timescales and patterns [178] make it difficult to account for this problem from an optimal control point of view. These different dynamics and timescales are associated to internal greenhouse climate, fast crop dynamics (i.e., transpiration, photosynthesis, and respiration), and slow crop development (i.e., crop growth and fruit changes). Hence, a multilayer hierarchical control architecture has been commonly proposed and used [88, 360, 362, 440], where setpoints for the different layers are calculated from the previous optimization problem. For instance, Fig. 1.2 shows the architecture proposed in this book, which has three layers. The upper layer solves the optimization problem defined by different objectives. The outputs of this layer are the growth trajectories to be followed by the crop in order to maximize the benefit. The second layer obtains the growth trajectories from the upper layer and calculates the low-level setpoints (greenhouse air temperature and electrical conductivity—EC—trajectories in this case) for the greenhouse crop, according to long-term and short-term weather predictions. Finally, the lower layer includes the controllers trying to minimize the error between the setpoints calculated by the second layer and the measured variables in the greenhouse system. A full description of the three layers is given in what follows:

- Upper layer (market or tactical control layer). Taking into account the long-term objectives (market prices, harvesting dates, and required quality) and the long-term predictions of the growth state using the modified Tomgro model presented in Sect. 2.2.1 [341] (for the estimation of yield and profits), the optimization is performed to calculate the setpoint trajectories for the crop growth. This layer usually receives the name of tactical control and is difficult to implement since it requires adequate market models, which often have high degrees of uncertainty.
- Middle layer (crop or plant growth layer). In this layer, the daytime and nighttime setpoints of the inside greenhouse temperature and the EC along the considered control horizon (typically 65 days for a short season −260 decision variables–or 120 days for a long season −480 decision variables) are calculated. Models for
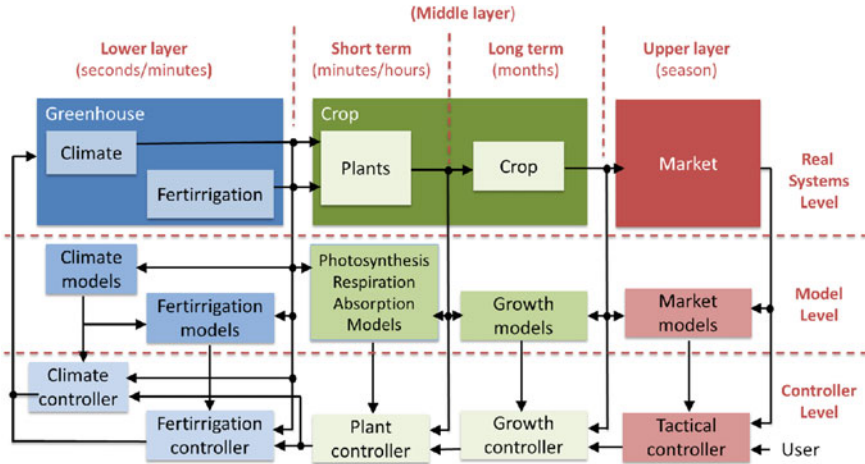
Fig. 1.2 Multilayer hierarchical control for greenhouse crop growth

irrigation have also been developed for control and optimization purposes [340], as presented in Sect. 2.2.2. The long-term weather prediction is performed using different kinds of disturbance models, as will be presented in Sect. 2.4. Starting from a short-term weather prediction (with low uncertainty), the long-term one is generated using a data window from the historical database. To account for the inherent uncertainty, a receding horizon approach is implemented online. The short-term weather prediction (with less uncertainty) is taking as the basis for generating the estimation. This layer is divided into two levels:

- Short-term growth control. There are physiological processes taking place in a temporal horizon of hours, such as photosynthesis or crop respiration, which directly influence the crop growth. In this level, the setpoints to be sent to the lower layer for the next day are calculated based on short-term weather predictions (that has a lesser degree of uncertainty), the actual state of the crop, and the short-term grower goals (considering his/her skill and the crop status).
- Long-term growth control. It includes the decisions on the global production schedule of the crop. These decisions are based on the growing rate and vegetative features obtained from the grower experience and models to set the specific climatic setpoint values. The main variables to be considered are the dry matter and leaves production, which correspond to the slower timescale of the crop growth process. Thus, the climatic and irrigation setpoints are computed according to a given harvesting date or a deserved growth trajectory.

• Lower layer (greenhouse or climate control and nutrition layer). Using the temperature and EC setpoints from the upper layers, the controllers compute the adequate control signals to be sent to the actuators. The control algorithms developed include a wide range from proportional-integral-derivative (PID) control,

feedforward control (FF), adaptive control (AC), model predictive control (MPC), and hybrid control (HC) [342, 362, 400, 406, 431]. This layer also uses simplified models for control design purposes.

Most research on greenhouse optimal control only considers one objective in the optimization problem solved in the upper layer, mainly focused on increasing the grower incomes [88, 177, 199, 360, 362, 440, 441, 458], only minimizing the CO_2 supply [145], including the temperature integral in the control decision-maker [231], or by minimizing the amount of nitrates in the crops [201, 259].

Although these control methods focus on only one objective, the greenhouse control problem includes different objectives that have to be optimized at the same time, existing conflicts among them. Thus, this multiobjective approach requests a different meaning for the optimal solution, where the solution satisfying one objective at the expense of others is the most common to be used. The aim of a multiobjective optimization problem is to find a set of feasible solutions that satisfy constraints and optimize the different objective functions [96]. The criterion maximizing profit in the greenhouse control problem is the most common solution in the literature [177, 302, 360, 382, 431, 441, 448]. However, other requirements related to environmental criteria [397, 424], efficient usage of water (mainly in arid regions) [47, 308, 424], pests, and diseases support under adequate climatic control [229, 230, 231, 380], product quality control [102, 125, 187, 201, 259, 411, 467], energy saving [47, 86, 98, 195, 304, 412, 433, 465, 494], or the pollution reduction problems, are becoming popular [308].

Before the work of [343], there was only one attempt in the literature combining more than one objective, specifically temperature and fertilization control problems [201]. However, in that work, the long-term weather predictions during the growing stage are considered constant (which can lead to a high level of uncertainty in the optimization problem). It is supposed that the temperature and nitrate profiles resulting from the optimization process are always reached (which it is not always ensured since there is a strong dependence on the current weather conditions), the water supply is not considered an objective (this being an important issue in arid regions), and only numerical simulation examples are provided. On the other hand, a preliminary multiobjective solution combining tracking and energy consumption problems is proposed in [193]. However, too many simplifications are performed in the model used for the optimization problem and very simple simulation results are shown. Thus, there is a lack of contributions combining the main objectives (to maximize profits, fruit crop quality, and water-use efficiency) in the same optimization problem and on the other hand, most of them are based on simulation results or short-time real experiments.

Therefore, based on the previous discussion, it can be concluded that adequate solution for the greenhouse crop growth problem is reached by considering different simultaneous objectives, such as will be presented in Chap. 5 [343]. However, the use of several objectives makes the optimization problem more complex since many of them may conflict, such as product quality maximization and incomes, cost reduction, and/or pollution minimization problems [88, 250, 411]. Other approaches not treated

in this book are related to the application of knowledge-based systems (KBS) and expert systems to manage greenhouse crop production [368, 473].

1.3 General Features and Structures of Automated Greenhouses

When the greenhouse system is analyzed from an automatic control point of view, the following variables must be considered in the greenhouse crop growth control problem:

- Controlled variables. Those variables that directly influence the crop growth. On one hand, climatic variables, such as PAR radiation, inner temperature, and CO_2 concentration. The relative humidity must be also controlled because it affects indirectly CO_2 absorption by assisting in pest growth. On the other hand, the fertilization variables are water supply, EC, and pH.
- Disturbance variables. Those variables that affect the controlled variables but cannot be manipulated. In this case, these variables are the external climatic ones (temperature, relative humidity, solar radiation, rain, and wind speed and direction), the crop transpiration (which is based on the crop stage), and a set of different variables describing the greenhouse elements (roof, soil surface, etc.)
- Manipulated variables. Those variables used to compensate for or to exploit the effect of disturbances and that are associated with the process actuators. The climatic actuators depend on each latitude where the greenhouse is located, being the most common ones: Natural ventilation, shade screen, heating system, fogging system, and CO_2 enrichment systems. In the case of the fertigation process, these systems are those used to supply water and fertilizers.

Hence, there exist a large number of coupled control loops composed of (Fig. 1.3):

- Process. Variable to be controlled (e.g., temperature).
- Measurement system. To measure the current value of each variable (e.g., temperature sensor), measurable disturbances, and actuator state.
- Controller. The system that compares the desired reference value (setpoint) with the current value of the controlled variable, and then takes the corresponding action based on this comparison (e.g., computer and control software to regulate the temperature variations).
- Actuators. Devices governed by the controller to keep the controlled variable within the desired limits (e.g., natural ventilation, heating system).

Thus, three tasks are performed continuously in each implemented control loop: To measure, compare, and act.

In this book, the results shown were obtained for tomato crop in different greenhouses located in the province of Almería (South–East Spain). Their main features are shown in Appendix A [339, 355, 373, 376]. This is a region with mild climatic conditions.
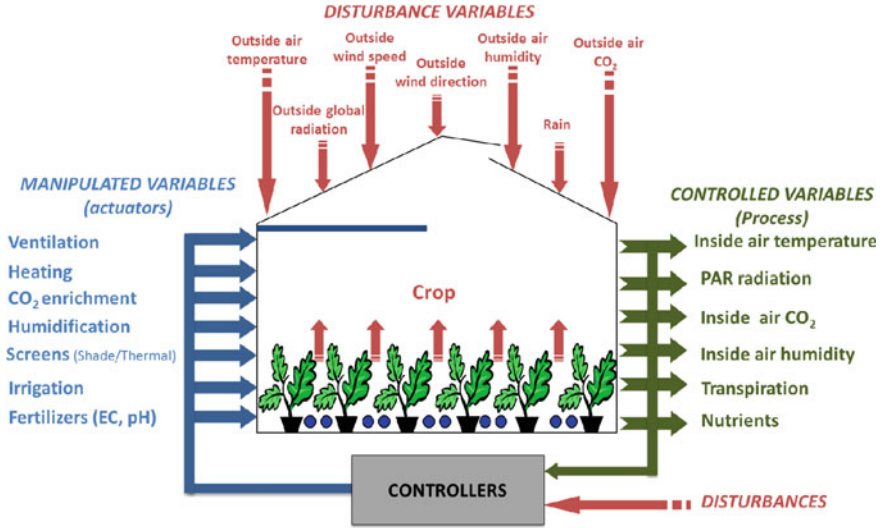
Fig. 1.3 Greenhouse climate control scheme

The data shown in this book were taken at a frequency of 1 min for all the measured variables and control actions. The control systems for the ventilation, heating, and fertigation systems were adapted to manage the control signal by relays from a personal computer.

The tomato crop growth variables were measured manually in eight plants randomly located in the greenhouse [339]. The following measurements were taken at a frequency of 8 days: Number of nodes, number of nodes of the first bunch, flower birth, curdle of fruits, number of nodes within the first fruit, number of nodes with the curdle of the first fruit, and its growth dynamics. On the other hand, six different plants were selected every 23 days to measure the leaf area, dry weight, and biomass of the different plant elements (roots, stems, leaves, flowers, and fruits), where destructive methods were used to estimate their values.

Chapter 2
The Greenhouse Dynamical System

2.1 Climate Dynamic Models

As pointed out in [324], when a complex system is modeled, one of the questions that arises is to discern whether models based on first principles or empirical models based on experimental data are to be used. The former generally provide detailed information of the process than empirical models, but they are usually more complex requiring longer times and deep knowledge in the design phase. Although models based on first principles can be used within model-based control structures, they are generally used for simulation purposes, while empirical ones are used for control tasks. These two approaches (and combinations) can be found within the framework of greenhouse climate variables modeling. This section presents the development of climate dynamic models based on first principles and on input–output data.

2.1.1 First Principles-Based Models

2.1.1.1 General Considerations

The dynamic behavior of the microclimate inside a greenhouse is a combination of physical processes involving energy transfer (radiation and heat) and mass balance (water vapor and CO_2 fluxes). These processes depend on the outside environmental conditions, structure of the greenhouse, type and state of the crop, and on the effect of the control actuators (typically ventilation and heating to modify inside temperature and humidity conditions, shading and artificial lighting to change internal radiation, CO_2 enrichment to influence photosynthesis and fogging/cooling for humidity enrichment).

The development of models of a dynamic system is a complex process that depends on the characteristics of the dynamics of the process object of study. This section deals with models based on physical principles as this is not a completely solved

problem. These models have been developed in different parts of the world since the 1960s of the last century, applied to several greenhouse structures (many of them of small size and used for research purposes), with different climatic actuators, cover material, and crops. Among them, it is interesting to emphasize several works related to that presented in this chapter, performed by the following authors:

- North and Central Europe: Bot [57], Udink ten Cate [461], Halleaux [167], Young et al. [483], van Henten [177], Tchamitchan et al. [447, 448], Tap et al. [441–443], Speetjens et al. [416]. It is interesting to highlight the work of Vanthoor et al. [468], in which a general methodology for any latitude is developed, using a similar approach as that proposed in this book.
- Mediterranean area: Kindelan [217], Cormary and Nicolas [99], Chaabane [83], Manera et al. [264], Boisson [55], Ioslovich el al. [202], Boulard et al. [62], Zhang et al. [489], Senent et al. [384], Wang and Boulard [476], and Tavares et al. [446].
- Central and North America: Takakura el al. [436, 437], Ahmadi et al. [3–5], Halleaux [167], Trigui et al. [459, 460], Leal-Iga [244], Bot et al. [198].
- South of Asia: Sharme et al. [392].

Although all these models are based on the same physical principles, they show differences in the approaches used when adapted to the particular conditions in each area. All these works describe the basic equations of the mathematical models and include some results, but they do not describe the complete methodology used for the implementation, calibration, and validation of the models. Other approaches can be found in [140, 306].

To model the climate that is generated inside a greenhouse based on physical, physiological, biological, and chemical principles, mass and energy balances have to be applied to all its constitutive elements. The main subsystems are [305]:

- *Cover*: It is a solid and homogeneous medium which partially transmits solar and thermal radiation. Its main objective is to isolate the internal atmosphere of the external weather conditions, making a bridge between the two environments.
- *Crop*: It is a living organism that is an open thermodynamic system that extracts energy from the surrounding environment to create and maintain its own essential management.
- *Air*: It is a gaseous medium joining the different solid elements in the greenhouse.
- *Soil*: It is a porous medium in which can be distinguished a solid phase (soil and organic matter), a liquid phase (water), and a gaseous phase (vapor and air). It is responsible for the greenhouse thermal inertia, absorbing energy during the day and emitting it overnight. Actually, it is divided into:

  - Surface, that is, the interface with the rest of the greenhouse.
  - Lower layers, that separate layers of ground that have different thermal characteristics related by conduction processes.

Therefore, the variables that describe the greenhouse climate are: Air temperature, water content in the air, CO_2 concentration in the air, temperatures of the outer and

inner surface of the cover, crop temperature, soil surface temperature, and temperature of each of the layers in which the soil is divided. Among these elements, the various energy and mass transport processes occur (conduction, convection, radiation, condensation, evaporation, and transpiration). Moreover, these processes are affected by other climatic variables as air speed inside the greenhouse and apparent temperature of the sky, which is defined as the temperature of a black hemisphere exchanging thermal radiation with the different elements of the greenhouse according to the Stefan–Boltzmann law, in the same amount as the actual exchange that occurs between the greenhouse and the atmosphere [58].

Other devices to consider when modeling greenhouse climate are installed actuators (those used to modify climatic variables) that constitute the inputs to the system and that can be artificially manipulated. As discussed above, there is a wide variety of climatic actuators, although the most common in warm climates are natural ventilation, heating systems, shading and thermal screens, humidifiers, and CO_2 enrichment systems.

In a greenhouse, the Principle of Continuity between its elements applies [278], so that the heat and mass transfer processes in each can be studied using mass and energy balances.

The energy balance in a given volume (vol) is described by the following differential equation:

$$\frac{dQ_{\text{tot,vol}}}{dt} = c_{\text{h,vol}} \frac{dX_{\text{T,vol}}}{dt} = Q_{\text{in,vol}} - Q_{\text{out,vol}} + Q_{\text{gen,vol}} \qquad (2.1)$$

where $Q_{\text{tot,vol}}$ (J) is the total amount of energy accumulated in the volume, $Q_{\text{in,vol}}$ and $Q_{\text{out,vol}}$ (J s^{-1}) are the energy per time unit entering and leaving the volume, respectively, and $Q_{\text{gen,vol}}$ (J s^{-1}) is the energy generated inside the volume. The left-hand term represents the change in energy per time unit t in the considered volume, which is directly related to temperature, $X_{\text{T,vol}}$ (K), through the heat capacity $c_{\text{h,vol}}$ (J K^{-1}).

The same considerations can be done with the mass balances in a volume (related with concentration, $X_{\text{c,vol}}$ (kg m^{-3}) and volume c_{vol} (m^3)), in such a way that the variation with time of the mass within a determined volume, $M_{\text{tot,vol}}$ (kg), is equal to the difference between the input, $M_{\text{in,vol}}$ and output, $M_{\text{out,vol}}$, flows (kg s^{-1}), plus the mass generated per time unit inside the volume, $M_{\text{gen,vol}}$ (kg s^{-1}), following the next balance:

$$\frac{dM_{\text{tot,vol}}}{dt} = c_{\text{vol}} \frac{dX_{\text{c,vol}}}{dt} = M_{\text{in,vol}} - M_{\text{out,vol}} + M_{\text{gen,vol}} \qquad (2.2)$$

Therefore, greenhouse climate is defined by a system of ordinary differential equations (ODEs) describing the mass and energy balances:

- Energy balances in: Outer and inner surfaces of the cover, inside air, crop, soil surface, and soil layers (typically from 2 to 5).
- Mass balances: Of water vapor and CO_2 concentration in the greenhouse air.
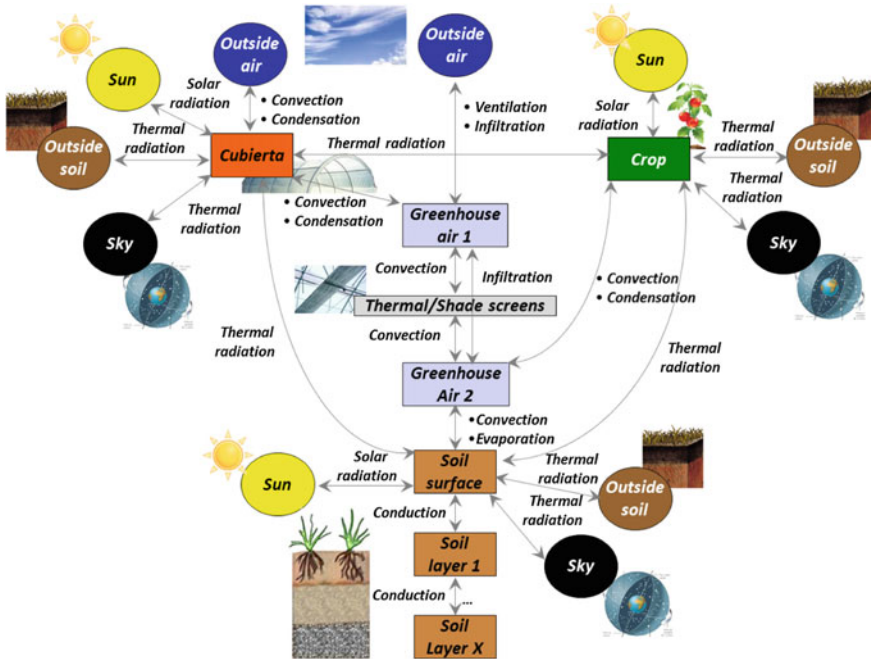
Fig. 2.1 Relationship between greenhouse elements

The number of equations to be solved depends on the known or measured variables, that is, on the boundary conditions. All authors agree to adopt as boundary conditions all the greenhouse climate disturbances, i.e., outdoor climate, soil temperature at a given depth, and wind speed inside. As the interest is in modeling inside air variables (temperature, humidity, and CO_2 concentration), if the variables describing the other elements are measured, they can be used as boundary conditions, thus reducing the complexity of the modeling problem as the number of ODEs is reduced. However, due to technical or economic reasons, sometimes several of these variables are not measured, being necessary to estimate them.

Therefore, to model climate variables in the volume of air that is in direct contact with the crop, the system is divided into the following elements: Cover, crop, soil surface, soil layers, and volume of air between the cover and the ground surface. If a shading screen is installed, the volume of air between the cover and the ground surface is divided into the corresponding two air volumes. Moreover, the surrounding conditions of the system are defined by four elements: Sun, sky dome, outside air, and ground outside the greenhouse.

Among these elements, energy transport phenomena are produced by heat transfer (conduction, convection, absorption, reflection and transmission of solar radiation, emission, absorption, reflection, and transmission of thermal radiation), mass transfer

(condensation of water vapor, evaporation of water vapor, crop transpiration) and the effects of. actuation systems

To summarize, the relationship among the most used actuation systems, the elements of the greenhouse and the outer systems are:

- *Natural ventilation*: It affects the thermal, vapor, and CO_2 balances in indoor air as it mixes with the outside.
- *Shade screen*: It reduces the amount of radiation that reaches the crop and the soil surface. A convection process between the air and the surfaces of the shade occurs. It also may produce condensation phenomena on its surfaces. Finally, as it is composed of porous material, an infiltration phenomenon occurs between the two volumes of air it defines.
- *Thermal screen*: It is a less porous element than the shade screen and also reduces the loss of thermal radiation from the ground and crop.
- *Heating*: If hot water pipes are used (see Sect. 3.1.2.2), convection processes with the surrounding air and thermal radiation exchange processes with soil, crop, cover, screen, outside ground, and sky dome occur.
- *Humidifiers*: They increase the concentration of water vapor in the air, they cause a reduction in the temperature therein.
- CO_2 *enrichment systems*. They increase the concentration of CO_2 in the air.

The dynamics of the climatic variables in a greenhouse are complex due to the following facts [361, 363]:

- Presence of different timescales, from minutes to months.
- Presence of nonlinearities, both static and dynamic.
- Time-varying parameters.
- The system is subjected to strong disturbances (measurable and nonmeasurable ones).
- High degree of correlation among variables.
- Combination of continuous and discrete variables.
- Presence of unmodeled dynamics.
- Changing dynamics depending on the greenhouse characteristics and geographical area.

It is thus a complex system and, although the physical processes taking place in a greenhouse are known, a number of assumptions have to be made to simplify the problem. The hypotheses accepted by most authors are [305]:

- *Cover*: Its material is homogeneous, with constant thermodynamic and optical properties and negligible heat capacity. A descriptive temperature is considered on each side.
- *Crop*: It is a subsystem with uniform density of vegetation that absorbs and transmits solar and thermal radiation. Its thermal capacity can be considered negligible and uniform temperature throughout its volume is assumed.
- *Air*: It is considered homogeneous in terms of thermodynamic properties except in models that include forced ventilation.

- *Soil*: It is considered as a medium divided into a finite number of horizontal layers which are assumed homogeneous in their thermodynamic properties and chemical composition. Heat flux is generally considered unidirectional, regardless of the study of water movement.

2.1.1.2 First Principles Model Architecture and General Hypotheses

To model the distributed nature of the greenhouse, a partial differential equation (PDE) model should be used to account for both time and spatial evolution of the state variables of the system. Nevertheless, greenhouses are often equipped with few sensors and the actuators affect all the greenhouse volume, so that a typical assumption is to consider a perfect mixing behavior such that the greenhouse dynamics are defined by a system of ODEs given as

$$\frac{d\mathbf{X}}{dt} = f(\mathbf{X}, \mathbf{U}, \mathbf{D}_m, \mathbf{V}, \mathbf{C}, t) \text{ with } \mathbf{X}(t_i) = \mathbf{X}_i \qquad (2.3)$$

where $\mathbf{X} = \mathbf{X}(t)$ is a n-dimensional vector of state variables, $\mathbf{U} = \mathbf{U}(t)$ is a m-dimensional vector of input variables, $\mathbf{D}_m = \mathbf{D}_m(t)$ is an o-dimensional vector of measurable disturbances, $\mathbf{V} = \mathbf{V}(t)$ is a p-dimensional vector of system variables, $\mathbf{C}$ is a q-dimensional vector of system constants, t is the time, $\mathbf{X}_i$ is the known initial state at the initial time t_i and $f = f(t)$ is a nonlinear function based on mass and heat transfer balances.

The number of equations describing the system and their characteristics depend on the greenhouse elements, the installed control actuators, and the type of cultivation method. The model presented in this section corresponds to a typical greenhouse located in the Mediterranean area with a tomato crop. It has been developed assuming some general hypotheses:

- The greenhouse is divided into four elements (Fig. 2.2): Cover, internal air, soil surface, and one soil layer. The crop is not considered as an element as no measurements of the leaf temperature are usually available (the related sensors are not very accurate) and thus it is considered as a source of disturbance for the inside climate. As some of the physical processes require the crop temperature to be known (i.e., thermal radiation among the solid elements), it has been considered to be equal to the greenhouse air temperature.
- The state variables of the model are: The internal air temperature ($X_{T,a}$) and humidity (absolute $X_{H_a,a}$ and relative $X_{H_r,a}$), cover temperature ($X_{T,cv}$), soil surface temperature ($X_{T,ss}$), and first soil layer temperature ($X_{T,sl}$). The PAR radiation onto the canopy (output variable $X_{rp,a}$) is also modeled with an algebraic equation. The CO_2 concentration is measured.
- The exogenous and disturbance inputs acting on the system are the outside air temperature ($D_{T,e}$) and absolute humidity ($D_{H_a,e}$), wind speed ($D_{ws,e}$) and direction ($D_{wd,e}$), sky temperature ($D_{T,sky}$), calculated using the Swinbank formula [55],
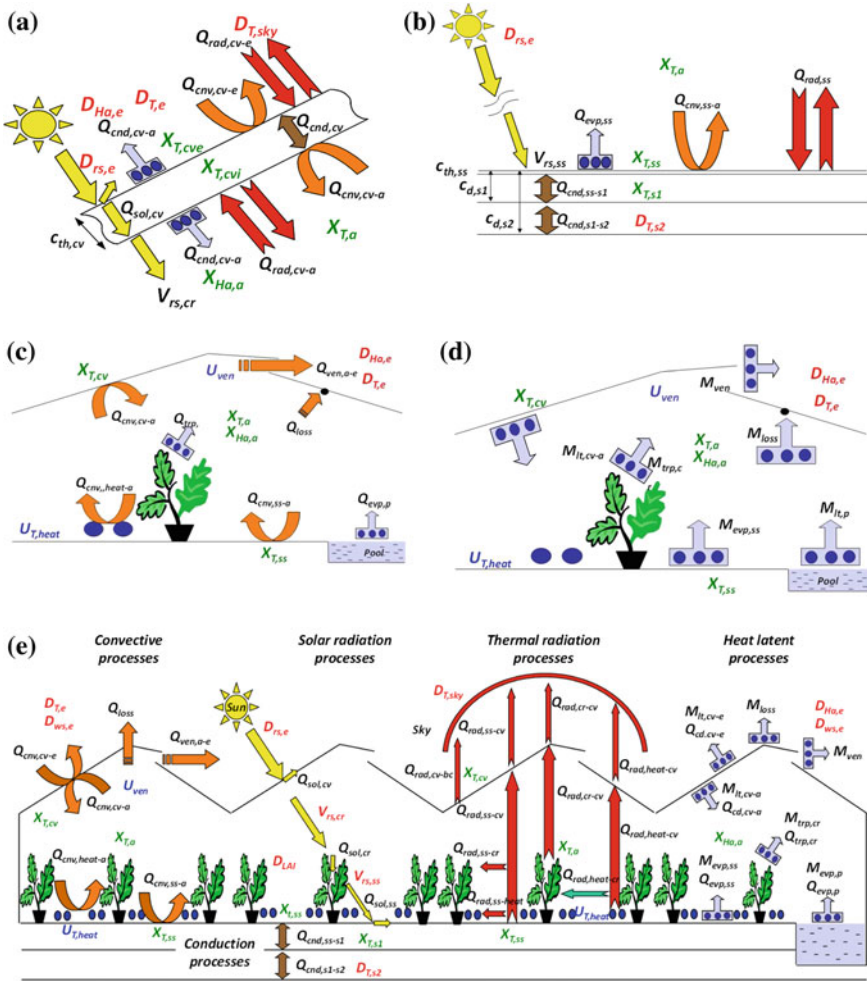
Fig. 2.2 Heat and mass transfer fluxes in a greenhouse. **a** Heat transfer fluxes in a cover. **b** Heat transfer fluxes in the soil layers. **c** Heat transfer fluxes with the internal air. **d** Mass transfer fluxes with the internal air. **e** Complete heat and mass transfer fluxes with the internal air

outside global solar radiation ($D_{rs,e}$), PAR radiation ($D_{rp,e}$), greenhouse whitening (D_{wh}) [26], the transpiration rate inside the greenhouse via the leaf area index (LAI, D_{LAI}) and the temperature of the deepest soil layer ($D_{T,s2}$) which can be calculated as the average of the external air temperature during one year or measured using dedicated sensors [55].

- The control inputs of the system are the position of the natural ventilation (U_{ven}), the position of the shade screen (U_{shd}) and the heating system control signal ($U_{T,heat}$, that is the temperature of the water of the pipes or the air heater status, depending on the type of heating system used, as commented in Sect. 3.1.2.2).

- The heat fluxes are one-dimensional. The model only considers the vertical dimension.
- The temperature models are based on a heat transfer balance where the following physical processes are included: Solar (sol) and thermal radiation (rad) absorption, heat convection (cnv) and conduction (cnd), crop transpiration (trp), condensation (cd), and evaporation (evp).
- In order to design the humidity model, a mass balance is used based on artificial water influxes, exchange with the outside, crop, condensation, and evaporation.
- The models of short and long wave radiation do not consider reflection, and the air is inert to these processes.
- The physical characteristics of the different elements (cover material, soil components, air, etc.), such as density or specific heat are considered constant in the temperature range the greenhouse evolves.
- The thickness of the cover is in microns, so the conductive heat flow is quantitatively negligible compared to other heat flows that appear in the cover temperature models. For this reason, it is accepted that the temperatures of both cover surfaces are similar.

In what follows, the models representing the heat transfer and mass balances in the four elements constituting the greenhouse are developed. The units of the different variables are indicated in the acronyms section.

2.1.1.3 Model of the PAR Radiation

The PAR radiation onto the canopy is modeled using an algebraic equation, because it is similar to the PAR radiation outside the greenhouse dimmed by the different physical elements that absorb the radiation (mainly cover material, cover whitening and shade screen). So it is modeled using Eq. (2.4).

$$X_{rp,a} = V_{tsw,g} D_{rp,e} \qquad (2.4)$$

where $V_{tsw,g}$ is the greenhouse short wave radiation transmission coefficient, described by:

$$V_{tsw,g} = \begin{cases} c_{tsw,cv} & \text{no shade, no whitening} \\ c_{tsw,cv}c_{tsw,wh} & \text{no shade, whitening} \\ c_{tsw,cv}c_{tsw,shd} & \text{shade, no whitening} \\ c_{tsw,cv}c_{tsw,wh}c_{tsw,shd} & \text{shade, whitening} \end{cases} \qquad (2.5)$$

where $c_{tsw,cv}$ is the cover solar transmission coefficient, $c_{tsw,shd}$ is the shade screen solar transmission coefficient and $c_{tsw,wh}$ is the whitening solar transmission. This last parameter is difficult to determine because it depends on the whitening concentration between 4 kg whitening/4 l water ($c_{tsw,wh} = 0.1$) and 0.7 kg whitening/4 l water ($c_{tsw,wh} = 0.65$) [278]. It is thus necessary to take measurements of global and PAR

radiation inside and outside the greenhouse to determine this coefficient. Another option is to search the value of this parameter in the modeling calibration phase. Note that Eq. (2.5) introduces a switch in the simulation process. As will be discussed later, the simulation packages used (both block-oriented ones as Simulink [268] and object-oriented ones as Modelica [117]) can cope with such behavior. The same happens with Eqs. (2.14), (2.19) and (2.22).

2.1.1.4 Heat Transfer Through the Cover

As Fig. 2.2a shows, the cover has two sides with different temperatures. Due to the fact that the cover is made using a single material (plastic film) and that its thickness is a few microns, the conduction heat flux, $Q_{,cv}$, is quantitatively not significant compared to the other fluxes appearing in the balance given by Eq. (2.6) [138]. So, the temperatures of the two sides are assumed to be similar and only one cover temperature is modeled ($X_{T,cv}$) using the heat transfer balance given by Eq. (2.6).

$$c_{sph,cv} c_{den,cv} \frac{c_{vol,cv}}{c_{area,ss}} \frac{dX_{T,cv}}{dt} = Q_{sol,cv} - Q_{cnv,cv-a} - Q_{cnv,cv-e} - Q_{cd,cv} + Q_{rad,cv}$$
(2.6)

where $Q_{sol,cv}$ is the solar radiation absorbed by the cover, $Q_{cnv,cv-a}$ is the convective hear transfer with the internal air, $Q_{cnv,cv-e}$ is the convective heat transfer with the outside air, $Q_{cd,cv}$ is the latent heat produced by condensation on both sides of the cover, $Q_{rad,cv}$ is the thermal radiation absorbed by the cover from the inside and outside of the greenhouse, $c_{sph,cv}$ is the specific heat of the cover material, $c_{den,cv}$ is the cover material density, $c_{vol,cv}$ is the cover volume and $c_{area,ss}$ is the greenhouse soil surface.

The solar radiation absorbed by the cover is determined by the short wave radiation cover material absorptivity, $c_{asw,cv}$, using the following equation:

$$Q_{sol,cv} = c_{asw,cv} D_{,e}$$
(2.7)

The convective heat transfer from inside air to cover is calculated based on the difference between the cover temperature, $X_{T,cv}$, and the greenhouse air temperature, $X_{T,a}$, using the typical model of this type of heat transfer:

$$Q_{cnv,cv-a} = V_{cnv,cv-a} \frac{c_{area,cv}}{c_{area,ss}} (X_{T,cv} - X_{T,a})$$
(2.8)

where $c_{area,cv}$ is the cover surface, $V_{cnv,cv-a}$ is the cover inside convective heat transfer coefficient based on the difference between the cover temperature and the internal air temperature, and the mean greenhouse air speed, $V_{ws,a}$:

$$V_{cnv,cv-a} = c_{cnv,cv-a1} |X_{T,cv} - X_{T,a}|^{c_{cnv,cv-a2}} + c_{cnv,cv-a3} (V_{ws,a})^{c_{cnv,cv-a4}}$$
(2.9)

where $c_{cnv,cv-ax}$ are empirical parameters that have to be estimated. This analysis uses the Nusselt, Prandtl, Grashof, and Reynolds numbers related to the climate variables involved in this process. There are tables with general cases, facilitating the calculations. The parameters $c_{cnv,cv-a1}$ and $c_{cnv,cv-a2}$ are different depending on the convection type (laminar or turbulent). In order to simplify the model, the approach proposed by Chalabi and Bailey [85] is used: If the internal air temperature is higher than the cover temperature, the heat transfer is turbulent; otherwise it is laminar. On the other hand, the parameters $c_{cnv,cv-a1}$ and $c_{cnv,cv-a3}$ vary with the position of the shade screen. When the screen is extended, the air is divided into two volumes, so it is necessary to include three new balance equations (air between the cover and the screen, upper and lower surfaces of the screen). Measurements of these surface temperatures are not usually available, so the effect of the shade screen on the convective coefficient is modeled by decreasing the value of this parameter. As will be seen in the next sections, good results are obtained under this simplification.

The measurement of the greenhouse air speed is a difficult task, because during long time intervals of the greenhouse operation the values are very low ($< 1\,\mathrm{ms}^{-1}$). So it is necessary to use special anemometers (like ultrasound or thermal effect based ones). As the installation of such sensors is not usual in Mediterranean greenhouses, it can be estimated using the studies in [477], which provide the following expression:

$$V_{ws,a} = \frac{V_{ven,flux}}{c_{ven,areap}} \tag{2.10}$$

where $c_{ven,areap}$ is the greenhouse section area perpendicular to the ventilation flux and $V_{ven,flux}$ is the volumetric flow rate (also known as ventilation rate). There are different theories to calculate this last variable. Models "M1" and "M4" proposed by Boulard and Baille [61] have been used because the type of greenhouse structures studied are similar to those treated in this book, equipped with long continuous roofs. Moreover, the five models proposed by Boulard and Baille [61] were tested and "M1" and "M4" fix better to the data. These models are based on the thermal buoyancy (depending on the temperature difference between inside and ourside air ($X_{T,a} - D_{T,e}$)) and wind forces (function of the outside wind speed $D_{ws,e}$), and are described by Eqs. (2.11) and (2.12),

$$V_{ven,flux_{M1}} = \frac{c_{ven,n}c_{ven,l}c_{ven,d}D_{T,e}}{3c_{gv}(X_{T,a} - D_{T,e})}\left[\left(V_{ven,hef}c_{gv}\frac{X_{T,a} - D_{T,e}}{D_{T,e}} + c_{ven,wd}D_{ws,e}^2\right)^{3/2}\right.$$
$$\left. -(c_{ven,wd}D_{ws,e}^2)^{3/2}\right] + V_{loss} \tag{2.11}$$

$$V_{ven,flux_{M4}} = \frac{c_{ven,n}c_{ven,l}c_{ven,d}V_{ven,hef}}{2}\left[\left(c_{gv}\frac{V_{ven,hef}}{2}\frac{X_{T,a} - D_{T,e}}{D_{T,e}}\right)^{0.5}\right.$$
$$\left. +(c_{ven,wd}^{0.5}D_{ws,e})\right] + V_{loss} \tag{2.12}$$

Fig. 2.3 Relationship between vents aperture and effective height of ventilation
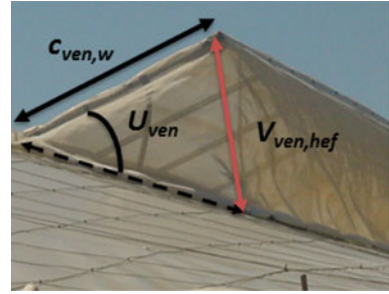
where $c_{ven,n}$ is the number of vents, $c_{ven,l}$ is the length of the vents, $c_{ven,d}$ is the discharge coefficient, c_{gv} is the gravity constant, $c_{ven,wd}$ is the wind effect coefficient, and $V_{ven,hef}$ is the cord joining the two extremities of the vent based on the position of the vent [rad, °], U_{ven}, using the following equation (see Fig. 2.3):

$$V_{ven,hef} = 2c_{ven,w} \sin (U_{ven}/2) \tag{2.13}$$

where $c_{ven,w}$ is the width of vent.

V_{loss} is the leakage when the vent is closed, based on the wind speed, which can be approximated by:

$$V_{loss} = \begin{cases} c_{loss,lw} & D_{ws,e} < c_{ws,lim} \\ c_{loss,hw} & D_{ws,e} \geq c_{ws,lim} \end{cases} \tag{2.14}$$

$c_{loss,lw}$ being the leakage with low wind speed, $c_{loss,hw}$ is the leakage with high wind speed and $c_{ws,lim}$ is the wind speed considered as the limit between high and low wind. In [61], the authors proved empirically that the discharge and wind effect coefficients are not really constant and their values depend on some variables as the wind speed, but in this work they are considered to be constant due to the difficulty involved in estimating these relations. After calibration of the model, the values obtained for these parameters were lower than those provided by the references due to the effect of insect-proof screens located on the vents [278]. A study was also performed to analyze the effect of wind direction modifying the structure of the model. The wind speed was modulated based on direction and orientation of vents and it was observed that the wind effect was low, dependent on wind direction. This result agrees with the conclusion drawn by Boulard and Baille [61]. In the case that the greenhouse has lateral and roof ventilation, the following expression can be used to estimate ventilation rate [219]:

$$V_{\text{ven,flux}} = c_{\text{ven,d}} \left[\left(\frac{V_{\text{ven,area-lat}} V_{\text{ven,area-roof}}}{\sqrt{V_{\text{ven,area-lat}}^2 + V_{\text{ven,area-roof}}^2}} \right)^2 \left(2c_g c_{\text{ven,h}} \frac{X_{\text{T,a}} - D_{\text{T,e}}}{D_{\text{T,e}}} \right) \right.$$
$$\left. + \left(\frac{V_{\text{ven,area-lat}} V_{\text{ven,area-roof}}}{2} \right)^2 c_{\text{ven,wd}} D_{\text{ws,e}}^2 \right]^{0.5} + V_{\text{loss}}$$

$$(2.15)$$

where $c_{\text{ven,h}}$ is the vertical distance between the midpoints of the lateral and roof vents, $V_{\text{ven,area-lat}}$ and $V_{\text{ven,area-roof}}$ are the areas of the roof and sidewall ventilation openings, given by the following equations based on U_{vent} expressed in %:

$$V_{\text{ven,area-lat}} = c_{\text{ven,l-lat}} c_{\text{ven,w-lat}} (U_{\text{ven}}/100) \qquad (2.16)$$

$$V_{\text{ven,area-roof}} = 2c_{\text{ven,l-roof}} c_{\text{ven,w-lat}} \sin\left(\frac{U_{\text{ven}}}{100} \frac{U_{\text{ven,max}}}{2} \right) \qquad (2.17)$$

where $c_{\text{ven,l-[lat,roof]}}$ and $c_{\text{ven,w-[lat-roof]}}$ are, respectively, the length and width of lateral or roof vents.

The convective heat transfer from outside air to cover is calculated in a similar way as the inside convective term using the formula:

$$Q_{\text{cnv,cv-e}} = V_{\text{cnv,cv-e}} \frac{c_{\text{area,cv}}}{c_{\text{area,ss}}} (X_{\text{T,cv}} - D_{\text{T,e}}) \qquad (2.18)$$

where $V_{\text{cnv,cv-e}}$ is the cover outside convective heat transfer coefficient based on the difference between the cover temperature and the external air temperature, $D_{\text{T,e}}$, and on the outside wind speed. In this case, the wind effect is predominant, so the temperature effect is neglected in the calculation of $V_{\text{cnv,cv-e}}$. Some authors [57] propose a linear relationship with the wind speed and others [21] propose an exponential one. Both approaches are tested in this work and the data fixed better using a mixed formula including a linear equation for low wind velocity and an exponential equation for high wind speed conditions. This formula is used by other authors as indicated by Boisson [55]:

$$V_{\text{cnv,cv-e}} = \begin{cases} c_{\text{cnv,cv-e1}} D_{\text{ws,e}}^{c_{\text{cnv,cv-e2}}} & D_{\text{ws,e}} > c_{\text{ws,lim}} \\ c_{\text{cnv,cv-e3}} D_{\text{ws,e}} + c_{\text{cnv,cv-e4}} & D_{\text{ws,e}} \leqslant c_{\text{ws,lim}} \end{cases} \qquad (2.19)$$

where $c_{\text{cnv,cv-ex}}$ are empirical parameters that have to be estimated.

The most important latent convective fluxes on the cover are produced by condensation on the inside surface. For this reason, some references [277, 447] do not consider the effect of the condensation on the outside surface. Indeed, some authors, van Henten and Tap et al. [177, 443], neglect the effect of condensation on both cover surfaces compared with the other heat processes.

Condensation takes place when water vapor concentration of the internal air, $X_{\text{H}_{\text{a,a}}}$, is greater than water concentration of the cover at saturation, $V_{\text{hsat,cv}}$, calculated based on the cover temperature. This flux can be written as:

$$Q_{cd,cv} = V_{lt,vap} M_{cd,cv} \qquad (2.20)$$

where $V_{lt,vap}$ is the latent heat of evaporation of water calculated at internal air temperature (in °C) using Eq. (2.21).

$$V_{lt,vap} = 4185.5(597 - 0.56 X_{T,a}) \qquad (2.21)$$

$M_{cd,cv}$ is the mass condensation flux from the cover calculated based on a convective term:

$$M_{cd,cv} = \begin{cases} 0 & X_{H_a,a} < V_{hsat,cv} \\ c_{den,a} \dfrac{V_{cnv,cv-a}}{c_{sph,a}} \dfrac{c_{area,cv}}{c_{area,ss}} \left(V_{hsat,cv} - X_{H_a,a} \right) & X_{H_a,a} \geq V_{hsat,cv} \end{cases} \qquad (2.22)$$

where $c_{sph,a}$ is the specific heat of air and $c_{den,a}$ is the air density.

The cover thermal radiation flux can be calculated using the Stefan–Boltzmann theory subtracting the thermal radiation emitted by the cover (two surfaces) and the thermal radiation emitted by the other solid elements of the greenhouse: Internal soil surface (ss), pipe heating (heat), crop (cr), and upper hemisphere (sky) that reach the cover surface. Related to the effect of the outside soil surface, some authors consider the temperature similar to the external air temperature [217]. In this proposal, this flux is neglected like other authors (e.g. [447]). The crop is a solid whose surface and volume are variables in time, so the thermal radiation processes between the rest of the solids and the crop are also variable. To model this effect, the long wave crop extinction coefficient, $c_{extlw,cr}$, and the LAI, D_{LAI}, are used to modulate the crop growth and its effect on thermal processes. The LAI can be measured online or modeled using, for example, Tomgro model developed in [211].

On the other hand, the thermal processes among the soil surface and pipe heating with the rest of the solids are influenced by the crop status because it is located between them, so these processes are modulated by the LAI, so that the heat transfer is smaller when the crop grows. So, this flux can be described by:

$$\begin{aligned} Q_{rad,cv} = {} & \frac{c_{area,cv}}{c_{area,ss}} c_{alw,cv} c_{sb} \left[\left(c_{vf,ss-cv} c_{elw,ss} X_{T,ss}^4 + c_{vf,heat-cv} c_{elw,heat} U_{T,heat}^4 \right) \right. \\ & \exp\left(-c_{extlw,cr} D_{LAI} \right) + c_{vf,sky-cv} D_{T,sky}^4 \\ & \left. + c_{vf,cr-cv} c_{elw,cr} \left(1 - c_{extlw,cr} D_{LAI} \right) X_{T,cr}^4 - 2 c_{elw,cv} X_{T,cv}^4 \right] \end{aligned} \qquad (2.23)$$

where $c_{alw,cv}$ is the long wave cover absorbance, c_{sb} is the Stefan–Boltzmann constant, $c_{elw,x}$ are the long wave emissivities of the solid elements, and $c_{vf,x-cv}$ are the view factors for radiation exchange between the different considered elements x (ss, heat, sky, crs) and the cover. These last parameters can be estimated using input/output data due to the difficulty involved in obtaining their exact values in this type of greenhouse with several surfaces forming the cover and the geometry of the plants elements. In the case that the heating system is based on air heaters, the flux due to this actuator can be ignored.

2.1.1.5 Heat Transfer Fluxes in the Soil Layers

The soil (greenhouse thermal mass) plays an important role in greenhouse climate. During diurnal time, the soil absorbs solar radiation on its surface, heating the deep soil layers. During night, the soil transfers heat to the greenhouse environment from these layers. So, the conductive fluxes are significant because this process is the source of the heat fluxes between them. As shown in Fig. 2.2b, a simple model of the soil is considered, divided into three layers (more layers could be taken into account): Surface, first layer, and a deep layer with a constant temperature. The conduction process is modeled solving the Fourier equation considering one-dimensional heat transfer along the deep axis, in steady state, the different soil layers as flat parallel planes, plus a delay in the process, obtaining acceptable results. This approach is considered because the computational cost decreases when compared with the solution obtained via diffusion equations while the results are similar (see Fig. 2.4).

Soil surface temperature model. Based on energy balance, the temperature of the soil surface (5 cm thickness) is represented by the following equation:
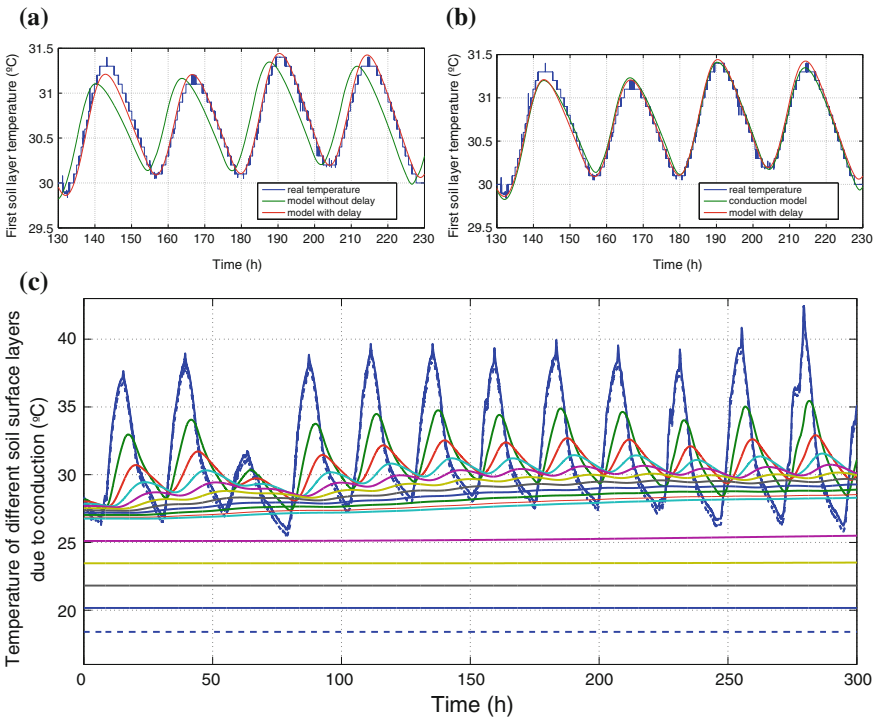

Fig. 2.4 First soil layer temperature model

$$c_{\text{sph,ss}} c_{\text{den,ss}} c_{\text{th,ss}} \frac{dX_{\text{T,ss}}}{dt} = Q_{\text{sol,ss}} - Q_{\text{cnv,ss}-a} - Q_{\text{cnd,ss}-s1} - Q_{\text{evp,ss}} + Q_{\text{rad,ss}}$$

(2.24)

where $Q_{\text{sol,ss}}$ is the solar radiation absorbed by the soil surface, $Q_{\text{cnv,ss}-a}$ is the convective flux with the internal air, $Q_{\text{cnd,s}-s1}$ is the conductive flux between the soil surface, and the first soil layer located at 30 cm depth, $Q_{\text{evp,ss}}$ is the latent heat produced by evaporation on the soil surface, $Q_{\text{rad,ss}}$ is the thermal radiation absorbed by the soil surface, $c_{\text{sph,ss}}$ is the specific heat of the soil surface material, $c_{\text{den,ss}}$ is the soil surface material density and $c_{\text{th,ss}}$ is the thickness of the soil surface.

The solar radiation absorbed by the soil surface is calculated based on the crop status (defined by LAI), using Eq. (2.25),

$$Q_{\text{sol,ss}} = c_{\text{asw,ss}} V_{\text{rs,cr}} \exp\left(-c_{\text{extsw,cr}} D_{\text{LAI}}\right)$$

(2.25)

where $c_{\text{asw,ss}}$ is the solar absorptivity of the soil surface material for short wave radiation, $c_{\text{extsw,cr}}$ is the canopy short wave extinction coefficient and $V_{\text{rs,cr}}$ is the solar radiation that reaches the top of the canopy based on the solar radiation absorption by the physical elements that the radiation crosses:

$$V_{\text{rs,cr}} = V_{\text{tsw,g}} D_{\text{rs,e}}$$

(2.26)

$V_{\text{tsw,g}}$ being the greenhouse short wave radiation transmission coefficient defined in Eq. (2.5).

The convective heat transfer from inside air to soil surface is calculated in the same way as cover convective fluxes using the following equation:

$$Q_{\text{cnv,ss}-a} = V_{\text{cnv,ss}-a}\left(X_{\text{T,ss}} - X_{\text{T,a}}\right)$$

(2.27)

where $V_{\text{cnv,ss}-a}$ is the inside soil surface convective heat transfer coefficient based on the difference between the soil surface temperature and the internal air temperature, and the mean greenhouse air speed on the soil surface. Using studies of [447], the mean greenhouse air speed proposed is calculated at crop level, so it is modulated based on LAI to obtain an estimation of the greenhouse air speed at soil surface level:

$$V_{\text{cnv,ss}-a} = c_{\text{cnv,ss}-a1}|X_{\text{T,ss}} - X_{\text{T,a}}|^{c_{\text{cnv,ss}-a2}} + c_{\text{cnv,ss}-a3}\left[V_{\text{ws,a}} \exp\left(c_{\text{cnv,ss}-a4} D_{\text{LAI}}\right)\right]^{c_{\text{cnv,ss}-a5}}$$

(2.28)

where $c_{\text{cnv,ss}-ax}$ are empirical parameters that have to be estimated and $V_{\text{ws,a}}$ can be measured or estimated using Eq. (2.10).

The conductive flux between the soil surface and the first soil layer is calculated based on the assumption that the heat flux is one-dimensional (Z axis)

$$Q_{\text{cnd,ss}-s1} = c_{\text{cnd,s1}} \frac{X_{\text{T,ss}} - X_{\text{T,s1}}}{c_{\text{d,s1}} - c_{\text{d,ss}}}$$

(2.29)

where $c_{\text{cnd,s1}}$ is the heat conductivity of the first soil layer, $c_{\text{d,ss}}$ is the soil surface deepness, and $c_{\text{d,s1}}$ is the first soil layer thickness.

The latent heat in the soil surface is mainly produced by evaporation, calculated as a convective flux using Eq. (2.30),

$$Q_{\text{evp,ss}} = V_{\text{lt,vap}} M_{\text{evp,ss}} \tag{2.30}$$

where $M_{\text{evp,ss}}$ is the mass evaporation flux from the soil surface, which can be obtained by:

$$M_{\text{evp,ss}} = c_{\text{den,a}} \frac{V_{\text{cnv,ss}-\text{a}}}{c_{\text{sph,a}}} \left(V_{\text{hsat,ss}} - X_{\text{H}_{\text{a,a}}} \right) \tag{2.31}$$

$V_{\text{hsat,ss}}$ being the water concentration of the soil surface at saturation, calculated based on the soil surface temperature. The diffusion effect to the soil surface of the water content in the internal soil layers is not considered. Some tests were performed to show that this term is negligible when compared with other fluxes due to the fact that the soil surface is mulched [421]. In such cases, evapotranspiration can be considered equal to crop transpiration ($M_{\text{trp,cr}} = V_{\text{ET}}$).

Similar to the cover thermal radiation flux, the Stefan–Boltzmann theory is used to calculate the soil surface thermal radiation flux, considering the effect of the crop growth between the soil surface and the cover and the sky and the effect of the cover long wave transmission, $c_{\text{tlw,cv}}$, in the radiation processes between the soil and the sky. So, the model of this process is as follows:

$$\begin{aligned} Q_{\text{rad,ss}} = c_{\text{alw,ss}} c_{\text{sb}} &\left[\left(c_{\text{vf,cv}-\text{ss}} c_{\text{elw,ss}} X_{\text{T,cv}}^4 + c_{\text{vf,sky}-\text{ss}} c_{\text{tlw,cv}} D_{\text{T,sky}}^4 \right) \right. \\ &\exp\left(-c_{\text{extlw,cr}} D_{\text{LAI}} \right) + c_{\text{vf,cr}-\text{ss}} c_{\text{elw,cr}} \left(1 - c_{\text{extlw,cr}} D_{\text{LAI}} \right) X_{\text{T,cr}}^4 \\ &\left. - c_{\text{elw,ss}} X_{\text{T,ss}}^4 \right] \end{aligned} \tag{2.32}$$

where $c_{\text{alw,ss}}$ is the long wave soil surface absorbance, and $c_{\text{vf,x}-\text{ss}}$ are the view factors for radiation exchange between the solid elements x and the soil surface and $X_{\text{T,cr}} = X_{\text{T,a}}$ following the hypothesis adopted when developing the model.

Heat transfer fluxes in the first soil layer. As can be seen in Figs. 2.1 and 2.2b, in the first soil layer, only the conductive fluxes are considered and so, the heat balance in this element is represented by Eq. (2.33),

$$c_{\text{sph,s1}} c_{\text{den,s1}} c_{\text{th,s1}} \frac{dX_{\text{T,s1}}}{dt} = Q_{\text{cnd,ss}-\text{s1}} - Q_{\text{cnd,s1}-\text{s2}} \tag{2.33}$$

where $c_{\text{sph,s1}}$ is the specific heat of the first soil layer material, $c_{\text{den,s1}}$ is the first soil layer material density and $c_{\text{th,s1}}$ is the thickness of this layer, $Q_{\text{cnd,ss}-\text{s1}}$ is the conductive flux between the soil surface and the first layer of the soil, $Q_{\text{cnd,s1}-\text{s2}}$

is the conductive flux between the first soil layer and the deep layer at constant temperature, $D_{T,s2}$, described as

$$Q_{cnd,s1-s2} = c_{cnd,s2} \frac{X_{T,s1} - D_{T,s2}}{c_{d,s2} - c_{d,s1}} \tag{2.34}$$

where $c_{cnd,s2}$ is the heat conductivity of the second soil layer, $c_{d,s2}$ is the second soil layer deep, and $c_{d,s1}$ is the first soil layer deep.

Note that these models are formulated using physical properties of the different materials constituting the soil, as the conductivity coefficient, specific heat, density, or solar absorptivity. As some of these parameters are unknown, they are estimated instead of using approximated values obtained from the literature.

It is interesting to show the behavior of the used simplified model of the soil layer temperature. As indicated, the conduction processes between the different soil layers were modeled considering steady-state regime to solve the Fourier equation. The temperature of the first soil layer was modeled using this approach because there are only conduction processes as energy fluxes. The dynamic response of a soil layer temperature is characterized by a time constant based on the density and specific heat of the material forming the layer and its thickness. Although this approach is commonly used in the literature on greenhouse climate, the model based on the diffusion equation is implemented and calibrated too, to compare the real first soil layer temperature with the temperature estimated by the simplified model (low computational cost) and that estimated by the diffusion model (high computational cost). Figure 2.4a shows that the amplitude of the real temperature is similar to the estimation of the simplified model without delay, although both curves are shifted in the time axis. The delay between the real and the simulated temperature is due to the consideration of the steady-state regime of the heat transfer between the soil layers. On the other hand, if the diffusion equation is solved using Dirichlet conditions in the soil surface and the second soil layer, the estimation of the model is similar in amplitude and delay to the real temperature of the first soil layer (Fig. 2.4b). The considered solution in this work is to use the simplified model including a delay, so that the estimation of the model is similar to the real values, as shown in Fig. 2.4, decreasing the computational cost.

2.1.1.6 Heat Transfer Fluxes with the Internal Air

Based on the processes shown in Fig. 2.2c, the greenhouse air temperature can be modeled using the following balance:

$$c_{sph,a} c_{den,a} \frac{c_{vol,g}}{c_{area,ss}} \frac{dX_{T,a}}{dt} = Q_{cnv,cv-a} + Q_{cnv,ss-a} + Q_{heat-a}$$
$$- Q_{ven} - Q_{trp,cr} - Q_{evp,p} \tag{2.35}$$

where $Q_{cnv,cv-a}$ is the convective flux with the cover described in Eq. (2.8), $Q_{cnv,ss-a}$ is the flux with the soil surface described in Eq. (2.27), Q_{heat-a} is the convective flux with the heating pipes, Q_{ven} is the heat lost by natural ventilation and the heat lost by infiltration losses, $Q_{trp,cr}$ is the latent heat effect of the crop transpiration, $Q_{evp,p}$ is the latent heat effect of evaporation in the pools (in those cases in which there are water reservoirs inside the greenhouse for the Nutrient Films Technique (NFT) irrigation system), and $c_{ter} = c_{sph,a}c_{den,a}(c_{vol,g}/c_{area,ss})$ is the product of specific heat of air, air density, and effective height of the greenhouse (greenhouse volume/soil surface area).

Heat fluxes with the heating systems. Based on the heating system facilities, the used model must be different. In the case of heating pipes, heat transfer is produced by heat convective fluxes with the pipes (see Sect. 3.1.2.2 for details). It is calculated considering that the hot water temperature is similar to the temperature of the external surface of the pipes, neglecting the effect of the convective flux between the hot water with the internal surface of the heating pipes and the conductive flux of the pipes. This term is given by the following equation:

$$Q_{cnv,heat-a} = V_{cnv,heat-a}\frac{c_{area,heat}}{c_{area,ss}}\left(U_{T,heat} - X_{T,a}\right) \tag{2.36}$$

where $c_{area,heat}$ is the heat pipe surface, $U_{T,heat}$ is the water temperature in the heating pipes and $V_{cnv,heat-a}$ is the heating convective heat transfer coefficient calculated in the same way as the rest of convective coefficients:

$$V_{cnv,heat-a} = c_{cnv,heat-a1}\left|\frac{U_{T,heat} - X_{T,a}}{c_{cl,heat}}\right|^{c_{cnv,heat-a2}} + \left[V_{ws,a}\exp\left(c_{cnv,heat-a4}D_{LAI}\right)\right]^{c_{cnv,heat-a5}} \tag{2.37}$$

$c_{cnv,heat-ax}$ being empirical parameters that have to be estimated and $c_{cl,heat}$ is the characteristic length of the heating system (in this case the diameter of the heating pipes).

On the other hand, if the energy is supplied by an air heating system supposing the heating system to be perfectly linear with respect to the control signal $U_{T,heat}$, it can be assumed that

$$Q_{cnv,heat-a} = Q_{heat,en}c_{heat,ef}U_{T,heat} \tag{2.38}$$

where $Q_{heat,en}$ is the nominal energy of the heating system, $c_{heat,ef}$ is its coefficient of efficiency, $Q_{max} = Q_{heat,en}c_{heat,ef}$ is the maximum energy that can be contributed by the system, and $U_{T,heat}$ is the heater's activation control signal (on/off).

Heat lost by natural ventilation. The heat lost by natural ventilation term is modeled according to ASAE standard EP406.3 (1998), [14]:

$$Q_{\text{ven}} = \frac{c_{\text{den,a}} c_{\text{sph,a}}}{c_{\text{area,ss}}} V_{\text{ven,flux}} \left(V_{\text{Texh,a}} - D_{\text{T,e}} \right) \qquad (2.39)$$

where $V_{\text{ven,flux}}$ is the volumetric flow rate described in Eqs. (2.12), (2.11) or (2.15) and $V_{\text{Texh,a}}$ is the exhaust air temperature, calculated as a linear combination of external and internal air temperature [379]:

$$V_{\text{Texh,a}} = V_{\text{ven,reg}} X_{\text{T,a}} + \left(1 - V_{\text{ven,reg}} \right) D_{\text{T,e}} \qquad (2.40)$$

where $V_{\text{ven,reg}}$ is the ventilation regime coefficient. $V_{\text{vent,reg}} = 1$ is a good approach for natural ventilation through windows (as the type of greenhouse modeled in this work), so Eq. (2.39) now becomes:

$$Q_{\text{ven}} = \frac{c_{\text{den,a}} c_{\text{sph,a}}}{c_{\text{area,ss}}} V_{\text{ven,flux}} \left(X_{\text{T,a}} - D_{\text{T,e}} \right) \qquad (2.41)$$

This term includes the heat lost by infiltration losses, as shown in the equation of the volumetric flow rate (2.12), (2.11) or (2.15).

Latent heat effect of crop transpiration. The crop affects the greenhouse air temperature. As no measurements of the leaf area are usually available online, it is not possible to use a convective factor in the heat balance equation using it as a boundary variable. One way to model the effect of the crop on the air temperature is based on the latent heat due to transpiration of the plants described by Eq. (2.42),

$$Q_{\text{trp,cr}} = V_{\text{lt,vap}} M_{\text{trp,cr}} \qquad (2.42)$$

where $M_{\text{trp,cr}}$ is the transpiration of the crop. Most transpiration estimators are based on the Penman–Monteith equation. In 1948, Penman derived an equation that combined the energy balance and the convective transport of vapor. Later, this model was adapted by Monteith to estimate actual evapotranspiration from plants [277]. This equation essentially combines the equation for heat transfer between the crop and the mass of the surrounding air. A simplified pseudo-physical transpiration model can be used based on two main variables: solar radiation (V_{rs}) arriving at a particular depth in the canopy plant, and vapor pressure deficit (VPD, V_{vpd}), [374]:

$$V_{\text{lt,vap}} M_{\text{trp,cr}} = \exp\left(-c_{\text{extsw,cr}} D_{\text{LAI}}\right) V_{\text{rs}} c_{\text{rs}} + V_{\text{vpd}} D_{\text{LAI}} c_{\text{vpd}} \qquad (2.43)$$

where $c_{\text{extsw,cr}}$ is the light extinction coefficient for crops (it is related to the leaf inclination angle and the leaf arrangement with regard to the LAI, and provides an indication of the plant's efficiency on intercepting solar radiation). The coefficient c_{rs} is constant with appropriate dimension dependent on the crop. To obtain more reliable results, the parameter c_{vpd} is obtained for diurnal (c_{vpd_d}) and nocturnal (c_{vpd_n}) periods through calibration.

On the other hand, various authors have obtained new formulations without satisfactory results for various crops. In the case treated in this book, the crop is tomato,

so a specific transpiration model for this crop can be used, like the proposal of Stanghellini [419] also based on the Penman–Monteith equation:

$$M_{trp,cr} = \frac{1}{V_{r,trp}} \left(V_{hsat,a} + \frac{1}{c_{den,a}} \frac{V_{ssvp}}{c_{psyco}} \frac{V_{r,bl}}{2D_{LAI}} \frac{V_{rn,cr}}{V_{lt,vap}} - X_{H_{a,a}} \right) \qquad (2.44)$$

where $V_{hsat,a}$ is the water concentration of the air at saturation (calculated at air temperature), c_{psyco} is the thermodynamic psychometric constant, V_{ssvp} is the slope of the saturated vapor pressure curve (calculated using the air temperature), $V_{rn,cr}$ is the net radiation available to the canopy (calculated on the basis of solar radiation), and $V_{r,trp}$ is a transpiration resistance described by Eq. (2.45),

$$V_{r,trp} = \frac{1}{2D_{LAI}} \left[\left(1 + \frac{V_{ssvp}}{c_{psyco}} \right) V_{r,bl} + V_{r,s} \right] \qquad (2.45)$$

where $V_{r,bl}$ is the boundary layer resistance and $V_{r,s}$ is the stomatal resistance. $V_{r,bl}$ depends on the aerodynamic regime that prevails in the greenhouse. In [63], the buoyancy effect is neglected when compared with the wind effect, so this resistance can be expressed with respect to the average inside air speed using Eq. (2.46),

$$V_{r,bl} = 220 \frac{c_{cl,cr}^{0.2}}{V_{ws,a}^{0.8}} \qquad (2.46)$$

where $c_{cl,cr}$ is the characteristic length of the crop leaf. $V_{r,s}$ depends on the global radiation on the crop, the greenhouse humidity, and the crop temperature [422]. For greenhouse tomato crops, the effect of the global radiation is the most important, so it can be calculated using the approach in [63]:

$$V_{r,s} = 200 \left(1 + \frac{1}{\exp(0.05 V_{rs,cr} - 50)} \right) \qquad (2.47)$$

Latent heat effect of the evaporation in the pools. This is not a typical process, but may appear if the cultivation method is NFT [151]. The greenhouse contains nonisolated pools to recycle the fertilized water to maintain the continuous water flow. The evaporation of the water of the pools affects the greenhouse climate. In the same way, the transpiration of the crop is included in the balances, a factor has been added to the latent heat term:

$$Q_{evp,p} = V_{lt,vap} M_{evp,p} \qquad (2.48)$$

where $M_{evp,p}$ is the evaporation flux from the pools. The evaporation from an open water surface is produced by two main factors: The energy to provide the vaporization latent heat (solar radiation) and the capacity to move the water vapor out of the evaporation surface due to wind speed and the air humidity on the surface. Evaporation

can be calculated by mixing the aerodynamic method based on the vapor pressure deficit and the energy method based on the energy balance [90]. This mixed method is adequate for small surfaces with known climate conditions and so, the following equation is used:

$$M_{\text{evp,p}} = \frac{V_{\text{ssvp}}}{V_{\text{ssvp}} + c_{\text{psyco}}} c_{\text{evp},1} V_{\text{rn,ss}} + \frac{c_{\text{psyco}}}{V_{\text{ssvp}} + c_{\text{psyco}}} c_{\text{evp},2} V_{\text{vpd,a}} \qquad (2.49)$$

where $c_{\text{evp},1}$ is a factor to calibrate the effect of the net radiation on the soil surface and $c_{\text{evp},2}$ is a factor to calibrate the effect of the air vapor pressure deficit, $V_{\text{vpd,a}}$ calculated as

$$V_{\text{vpd,a}} = V_{\text{vpsat,a}} \left(1 - \frac{X_{\text{H}_{\text{r}},\text{a}}}{100} \right) \qquad (2.50)$$

where $V_{\text{vpsat,a}}$ is the saturation vapor pressure calculated as an exponential function of the internal air temperature and $X_{\text{H}_{\text{r}},\text{a}}$ is the relative humidity calculated in the basis of the absolute humidity, $X_{\text{H}_{\text{a}},\text{a}}$ (see Eq. (2.52)), using the following expression:

$$X_{\text{H}_{\text{r}},\text{a}} = \frac{c_{\text{den,a}}}{0.00217} \left(\frac{X_{\text{H}_{\text{a}},\text{a}} X_{\text{T,a}}}{V_{\text{vpsat,a}}} \right) \qquad (2.51)$$

2.1.1.7 Water Mass Transfer Fluxes with the Internal Air

A model of absolute humidity (water vapor content of the greenhouse air) is based on a water vapor mass balance equation. As Fig. 2.2d shows the main sources of vapor in a greenhouse are crop transpiration, evaporation of the soil surface and pools, and water influx by fogging or cooling. The vapor outflow takes place through condensation on the internal side of the cover, ventilation, and vapor lost by infiltration losses. As artificial water influxes (cooling, fogging, etc.) are not installed in greenhouses in which the experiments were carried out, the mean water vapor content of the greenhouse air, $X_{\text{H}_{\text{a}},\text{a}}$, (absolute humidity) is modeled using the water mass balance equation given by Eq. (2.52),

$$\frac{c_{\text{vol,g}}}{c_{\text{area,s}}} c_{\text{den,a}} \frac{\text{d} X_{\text{H}_{\text{a}},\text{a}}}{\text{d}t} = M_{\text{trp,cr}} + M_{\text{evp,p}} + M_{\text{evp,ss}} - M_{\text{cd,cv}} - M_{\text{ven,a}-\text{e}} \qquad (2.52)$$

where $M_{\text{trp,cr}}$ is the crop transpiration flux described in Eq. (2.44), $M_{\text{evp,p}}$ is the evaporation flux from the reservoirs described in Eq. (2.49), $M_{\text{evp,ss}}$ is the mass evaporation flux from the soil surface described in Eq. (2.31), $M_{\text{cd,cv}}$ is the condensation flux from the cover described in Eq. (2.22) and $M_{\text{ven,a}-\text{e}}$ is the outflow by natural ventilation described by the following equation, where the volumetric flow rate, $V_{\text{ven,flux}}$, is described in Eqs. (2.12), (2.11) or (2.15):

$$M_{\text{ven,a}-\text{e}} = \frac{c_{\text{den,a}}}{c_{\text{area,ss}}} V_{\text{ven,flux}} \left(X_{\text{H}_\text{a},\text{a}} - D_{\text{H}_\text{a},\text{e}} \right) + M_{\text{loss,a}-\text{e}} \qquad (2.53)$$

where $M_{\text{loss,a}-\text{e}}$ are infiltration losses.

2.1.1.8 Model Implementation

The designed greenhouse climate model is composed of five ODEs related to the main greenhouse climate variables (temperature and humidity of internal air, cover temperature, soil surface temperature, and first soil layer temperature) and 49 algebraic equations including the PAR radiation onto the canopy. This model is divided hierarchically using a top-down approach from a high level that includes all the submodels to the lower level where each physical process is modeled [355]. The advantages of using this hierarchical division are:

- Each submodel can be studied independently, simplifying the problem of parameter calibration.
- A new state variable submodel can be easily added, such as the crop temperature or CO_2 concentration, programming the new balance equations and adding or eliminating physical effects in the determined submodels.
- A submodel can be added or eliminated depending on the installed actuators. If a new actuator is installed (e.g., cooling), it can be modeled and added to humidity and temperature submodels easily.
- A model of a physical process can be substituted when a better model is available by changing the corresponding submodel.
- A submodel can be substituted by its real measurements when these are available, thus reducing the uncertainties because the number of variables to estimate is smaller.
- Each submodel can act separately as a "soft sensor," providing an estimate of unmeasured state variables (e.g., cover temperature) based on other measured variables.

The input/output scheme of the model is shown in Fig. 2.5 and is divided into the following submodels:

A. Temperature submodel

   A.1. Cover temperature submodel
     A.1.1. Cover solar radiation absorption submodel
     A.1.2. Cover internal convective flux submodel
     A.1.3. Cover external convective flux submodel
     A.1.4. Cover condensation flux submodel
     A.1.5. Cover thermal radiation absorption submodel
   A.2. Soil Surface temperature submodel
     A.2.1. Soil surface solar radiation absorption submodel
     A.2.2. Soil surface convective flux submodel

DISTURBANCES

Outside air temperature
Outside wind speed
Outside wind direction
Outside air humidity
Sky temperature

Outside global radiation
Outside PAR radiation

INPUTS

Natural ventilation

Heating system

Shade screen

Crop
(Leaf area index)

2nd soil layer temperature

OUTPUTS

PAR radiation onto the canopy

Inside air temperature

Inside air humidity

Cover temperature

Soil surface temperature

1st soil layer temperature

Fig. 2.5 Input–output scheme

In order to implement the model, two paradigms can be used:

- A block-based modeling and simulation approach using Simulink [268] running on Matlab. Matlab is a high-performance language for technical computing. It integrates computation, visualization, and programming in an easy-to-use environment [267]. Simulink is an interactive system for modeling, simulating, and analyzing linear and nonlinear dynamical models (continuous, sampled, or hybrid systems). It is a graphical mouse-driven program that allows the user to model a system by drawing a block diagram on the screen and manipulating it dynamically. Simulink includes a comprehensive block library of sinks, sources, linear and nonlinear components, and connectors, so that the user can build the model using these blocks and connecting them adequately. It is possible to add new customized blocks. Each Simulink block is composed of an input vector and output vector, and a state vector relating inputs to outputs. The main advantage of this tool is that it is not necessary to write a program as happens with other simulations tools. The initialization of the model is performed by a designed Matlab program that loads in the workspace of Matlab the greenhouse structure data (surface, volume, etc.), the characteristic of the materials used in the greenhouse (cover, soil, etc.), the features of the actuator systems (length and width of the vents, diameter of the heating tubes, etc.), universal physical constants (psicometric constant, etc.), values of the coefficients involved in the physical processes (convective and conduction coefficients, etc.), crop data (density of plants, extinction coefficient, etc.), and the initial values of state, output, characteristic, and disturbance variables. Furthermore, it reads the values of the available external variables contained in data files (note that the model could also be used for online estimation of state variables as typical sampling time is enough for their calculation, which could be included, for instance, in predictive control schemes or production optimization arquitectures). The way in which the Matlab program has been developed simplifies the use of the developed model for new greenhouse structures or new external data inputs. The greenhouse climate model has been divided into several submodels hierarchically organized in five levels:

1. System level. It consists of two blocks (climate model and crop model). The inputs (control and disturbances) and the outputs are included, as well as the relations between the systems that constitute the compound model.
2. Variable type level. It corresponds to climate variables, consisting of three models: PAR radiation, temperature, and humidity.
3. Variable level. Some climate type variables can be defined by some variables. The temperature level is divided into four submodels: Cover, soil surface, first soil layer, and greenhouse air temperatures.
4. Process level. It is formed by the submodels of physical processes involved in the models of the variables.
5. Implementation level. It corresponds with Simulink code to implement the process models of the upper level.

On the other hand, the simulation of this model involves the numerical integration of five ordinary differential equations. Simulink provides a number of solvers for the integration of such equations. Due to the diversity of dynamic system behaviors, some solvers may be more efficient than others when solving a particular problem. In the case treated in this paper, the Gears methods are used, as the greenhouse climate is a stiff problem (the system has slow and fast dynamics and these at last reach a steady state).

- An object-oriented modeling proposal using Modelica as a declarative and equation-based language for modeling multidomain physical systems [116, 117]. One natural method for physical systems modeling is to decompose the whole system in subsystems interconnected by means of their interfaces. These subsystems could decompose themselves in other interconnected subsubsystems and so on. Each subsystem is modeled using conservation laws (energy, mass, momentum, etc.) and constitutive equations in terms of differential and algebraic equations (DAE). This methodology promotes greatly building reusable models. This paradigm is different from the block-oriented modeling, presenting some advantages as the causality management. To develop the model of the compound greenhouse climate model using Modelica, the OMT (Object Modeling Technique) methodology, proposed by Rumbaugh et al. [367], is used. This tech nique proposes a formal graph showing the relations (association, aggregation, and generalization) between the different objects that constitute the systems and their properties and attributes. Three general classes are defined [355, 363]:

`Crop_model` class. It represents the LAI (modeled or measured) of a tomato crop.

`Greenhouse_class`. This class describes the greenhouse where the simulation test is designed. Its attributes are the parameters of the different elements constituting the greenhouse. The main advantage of this design is the possibility of changing or adding a physical element (i.e., actuators) easily. These classes are described by their own name:

  `Structure`. Type and dimensions of the greenhouse structure.

  `Ventilation`. Type and dimensions of the ventilation.

  `Heating`. Type and parameters of the heating system.

  `Soil_surface`. Type of material of the soil surface.

  `First_layer_soil`. Type of material of the first layer soil.

  `Second_layer_soil`. Type of material of the second layer soil.

  `Cover`. Type of cover material.

`Greenhouse_model` class. It represents the different models that describe the greenhouse climate variables. It is related to the `Greenhouse_class` to obtain the parameters of the greenhouse where the simulation experiences are performed. Furthermore, this class is related with the `Crop_model` class to model the effects of the plants on the climate. It is constituted by an aggregation relation of the following classes:

  `Temperature_model`. Class of the different models of internal air temperature.

Humidity_model. Class of the different models of internal air humidity.
Cover_model. Class of the different models of cover temperature.
Soil_model. It is formed by two subclasses:
    Soil_surface_model. Class of the different models of soil surface temperature.
    Soil_layer_model. Class of the different models of the soil layer temperature.

The compound model is defined by five ordinary differential equations and 59 algebraic equations. This equation system is solved using the DASSL algorithm [65] because the simulation computational time was the smallest and it is very efficient to solve stiff systems.

The use of modeling environments as Simulink or Dymola/Modelica and systematic procedures for decomposing the complete model in submodels, which can be independently validated, has shown to facilitate the implementation of the compound model (as an integration of the single submodels) and its extension to other types of greenhouses. The choice of a simulation paradigm and implementation tool depends on the skill and ability of the user to implement the models and especially their preferences on the working methodology of each.

2.1.1.9 Model Calibration

Due to the large set of unknown parameters (more than 30), it is difficult to obtain their values using a unique search technique with the compound model. The solution consists in performing single experimental tests for each one of the involved processes to estimate their parameters in a similar way as the experiences carried out by Bot [57]. These experiments are not easy to perform, and some of them are expensive and present a long duration. On the other hand, the input/output meteorological and actuator status data are often at hand in a typical greenhouse installation, so it would be desirable to use only these data to calibrate the greenhouse climate model, without losing the physical meaning of the processes involved in the balance equations. This problem can be simplified considering the following facts:

- Data of the different climate variables to model, the disturbances and the actuators status are measured, so the problem has been divided into some submodels calibration processes (air humidity and cover, air, soil surface, and first soil layer temperature).
- Some of the involved physical processes in the balance equations are not coupled or they have no influence in determined time lapses of a day (e.g., the solar absorbance during the night or the crop presence), so all the parameters of a single submodel do not have to be estimated simultaneously.
- Some of the involved physical processes are modeled in different forms based on determined situations (as the convection process between the internal side of the cover and the greenhouse air in which the parameters of the convection

coefficient are different depending on laminar or turbulent regimes). So, the calibration process can be divided for each of these situations.

- In order to estimate the parameters related to the actuation systems, some guided test (mainly step response and impulse response ones) can be performed at the real greenhouse.

Based on these considerations, a methodology to calibrate the compound model was proposed by Rodríguez [355]. In what follows, the step sequence that has to be carried out to calibrate the implemented model for any greenhouse is briefly explained based on the typical measured data in a greenhouse. In each step, the number of the estimated parameters is indicated:

1. Calibration of the climate variables with an empty greenhouse (without crop)

    a. Climate variables calibration without the effects of the actuation systems (no heating, no ventilation)
        i. Calibration of the first soil layer temperature submodel [4 parameters]
        ii. Calibration during nocturnal time intervals (without solar radiation)
        iii. Calibration of cover temperature submodel
        iv. High wind speed [1 parameter]
        v. Low wind speed [3 parameters]
        vi. Calibration of soil surface submodel [6 parameters]
        vii. Calibration during diurnal time intervals (with solar radiation)
        viii. Calibration of cover temperature submodel [3 parameters]
        ix. Calibration of soil surface temperature submodel [3 parameters]
        x. Calibration of internal air humidity submodel [2 parameters]
    a. Calibration of the parameters related to natural ventilation (without heating) [2 parameters]
    b. Calibration of the parameters related to heating system (without vents) [2 parameters for pipe heating systems or 1 parameter for air heaters]

2. Calibration of the climate variables with crop

    a. Calibration of the long wave parameters in the cover temperature submodel [1 parameter]
    b. Calibration of the long wave parameters in the soil surface temperature submodel [2 parameters]
    c. Calibration of the parameters related with the crop transpiraton process [4 parameters]

3. Calibration of the PAR radiation model [1 parameter]

The largest number of parameters to estimate simultaneously is six in the processes of soil surface calibration in nocturnal time intervals with an empty greenhouse. The use of an adequate parameter search technique can help to solve this problem. In order to obtain the unknown parameters in the equations described in Sect. 2.1.1.2, a large set of input/output data obtained at the real greenhouses are used in such a

way that the values of the parameters are obtained by minimizing a least squares criterion:

$$J = \|\mathbf{X}_{\text{real}} - \mathbf{X}_{\text{sim}}\|^2 = \sum_{i=1}^{N}(X_{\text{real}}(i) - X_{\text{sim}}(i))^2 \qquad (2.54)$$

where $\mathbf{X}_{\text{real}} = (X_{\text{real}}(1), \ldots, X_{\text{real}}(N))$ is a set of N real measurements of the variables to estimate and $\mathbf{X}_{\text{sim}} = (X_{\text{sim}}(1), \ldots, X_{\text{sim}}(N))$ are the values of the variables calculated by the implemented model. The used parameter search technique is divided into two phases.

In a first phase, the submodels were calibrated independently using a direct sequential search [330], consisting in an iterative method incrementing the values of the parameters between upper and lower limits (wide margins) with a determined step until a n-tuple of parameters that minimizes the least square criterion is found. The initial upper and lower bounds were obtained from physical properties and from values found in the literature. The search can be improved by decreasing the limits and the sequential increment step. The main disadvantage of this type of techniques is the high computational cost because it must evaluate all the values of the search space. So, it is used to obtain only approximated values of the model parameters reducing the search space.

```
Begin;
time=0;
generate initial population, P0;
evaluate P0;
while not finish-condition do
    begin;
    time=time+1;
    select potential solutions Mtime from Ptime-1;
    alter Mtime using genetic operators;
    create new population Ptime from Mtime;
    evaluate Ptime;
end
End.
```
Algorithm 1: Parameter search technique.

In a second phase, genetic algorithms (GAs) were used as heuristic search technique to refine the obtained values of the model parameters in the first phase. GAs are globally oriented in searching and thus potentially useful in solving optimization problems in which the objective functions response contain multiple optima and other irregularities [172, 329, 463, 475]. Empirical studies have demonstrated that GAs have been successfully applied to several types of problems, including function optimization or model fitting [369]. GAs differ from the iterative search in that they search among a population of points and use probabilistic rather than deterministic transaction rules. These algorithms are formulated using a direct anal-

ogy with evolution processes observed in nature. GAs work simultaneously with a population of individuals (n-tuples of parameters) exploring a number of new areas in the search space in parallel, thus reducing the probability of being trapped in a local minimum [269]. As in nature, individuals in a population compete with each other for surviving, so that fitter individuals tend to progress into new generations, while the poor ones usually die out. This process is described in Algorithm 1.

The initial population is randomly generated within certain boundaries. The determination of these boundaries is a difficult problem. In the case treated in this section, these limits were determined by the study performed with the sequential search phase. In order to evaluate the population, the simulation is run for each individual (set of all model parameters to estimate), and a numerical value is assigned to each member of the population (possible set of model parameters) using the least squares criterion given in Eq. (2.54). All the individuals in the population are evaluated and their fitness are used as the basis of the selection. A common selection approach assigns a probability of selection, $P(j)$, to each individual j based on its fitness value. A series of N random numbers is generated and compared against the cumulative probability of the population:

$$C(i) = \sum_{j=1}^{i} P(j) \tag{2.55}$$

The appropriate individual, i, is selected to belong to the new population if $C(i-1) < U(0, 1) < C(i)$ where $U(0, 1)$ is a uniform distribution. In [190] different methods to assign probabilities to individuals are proposed, such as the roulette wheel and ranking methods. A normalized geometric ranking method has been used in this application. It assigns a probability $P(i)$ based on the rank of solution i when all solutions are sorted. The method defines $P(i)$ for each individual using the following equation:

$$P(i) = \frac{P_{\text{best}}}{1 - (1 - P_{\text{best}})^{P_s}} (1 - P_{\text{best}})^{\text{rank}(i)-1} \tag{2.56}$$

where P_{best} is the probability of selecting the best individual, P_s is the population size and rank(i) is the rank of the individual where 1 is the best. In order to alter the selected individuals to generate the new population, GAs used two basic types of operators:

- Crossover. This operator takes two individuals and produces two new individuals exchanging genetic information in pairs or larger group between the parents. There are some crossover operators and in this application, the real value simple crossover has been used. Let $\mathbf{X}$ and $\mathbf{Y}$ two m-dimensional row vectors of floats denoting individuals from the population. This operator generates a random number n from a uniform distribution $U(0, 1)$ and creates two new individuals $\acute{\mathbf{X}}$ and $\acute{\mathbf{Y}}$ based on the following equations:

$$\acute{\mathbf{X}} = n\mathbf{X} + (1 - n)\mathbf{Y}$$
$$\acute{\mathbf{Y}} = (1 - n)\mathbf{X} + n\mathbf{Y} \tag{2.57}$$

- Mutation. This operator alters one individual to produce a single new solution. A
  uniform mutation algorithm has been used that selects randomly one variable j,
  and sets it equal to a uniform random number $U(a_i, b_i)$ where $\underline{a}(i)$ and $\overline{a}(i)$ are
  the lower and upper limit of the interval of variation of the parameter at parent
  chromosome position, that is:

$$\acute{X}(i) = \begin{cases} U(\underline{a}(i), \overline{a}(i)) & \text{if } i = j \\ X(i) & \text{if } i \neq j \end{cases} \tag{2.58}$$

Table 2.1 and Fig. 2.6 (mean absolute error, maximum absolute error and standard
deviation) show that the estimation of the coefficients using GAs methods is better
than the iterative search for the complete model. Furthermore, this technique is more
efficient in time. Although it is necessary to indicate that the search space of the

Table 2.1 Comparison between real temperature (°C) and relative humidity (%) and the estimation
of the compound model using GAs (GA) and direct sequential search (Sec) during August 2000 in
Araba greenhouse

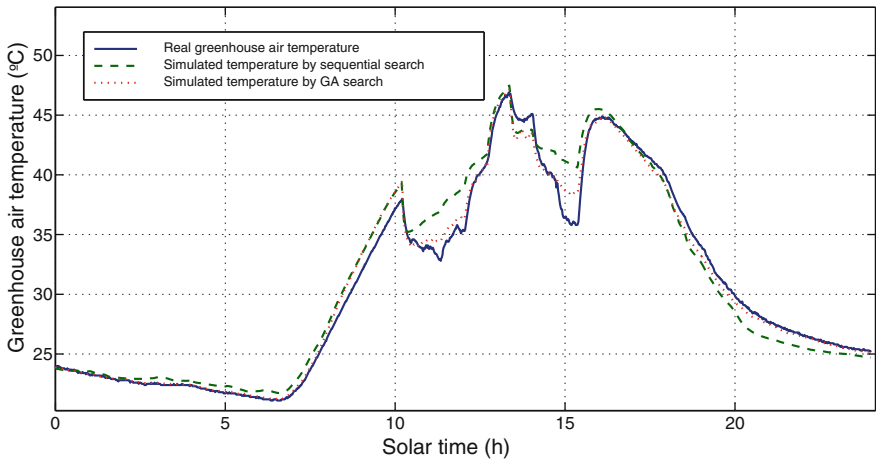|	Air temperature		Cover temperature		Soil surface temperature		First soil layer temperature		Air relative humidity	
	Sec	GA	Sec	GA	Sec	GA	Sec	GA	Sec	GA
Mean absolute error	1.13	0.93	0.89	0.79	0.74	0.64	0.34	0.32	4.29	3.92
Maximum absolute error	5.15	4.63	5.17	4.81	4.66	4.65	1.36	1.26	29.47	24.32
Standard deviation	0.88	0.65	0.79	0.64	0.63	0.50	0.28	0.26	3.76	3.69

Fig. 2.6 Comparison between real temperature and complete model simulated temperatures of
greenhouse air using GAs and sequential search

initial population was reduced because it was deduced of the study carried out with the sequential search of the simple submodels.

In order to calibrate the parameters of the greenhouse climate models, several tests were performed in the greenhouses: In summer season (without crop and with guided experiences using natural ventilation) from June to August, and others in winter season (with tomato crop and guided experiences using the heating system) from December to March. Data of 15 days with 1-min sample time (21,600 real measurements) were used in the calibration phase in each season. In order to calibrate the PAR radiation, modeled by an algebraic equation, data of a month without whitening were used (January) to verify the data provided by the manufacturers of the cover material and the shade screen. The values are slightly corrected because they lose the original properties along time. This variation of the parameters is not accounted for by the model because the chemical equations that describe the degradation of the physical characteristics are not known. In any case, the degradation process takes place slowly, so it is logical to suppose that these parameters are constant during a simulation experiment (during one season at the most). It is obviously necessary to calibrate these values along time. The used data calibrating the effect on the transmission coefficient of the cover when it is whitened correspond to May and June. The submodels are independently calibrated because all the needed input/output data are measured. The calibration process is similar for any greenhouse, so only the obtained results for Araba greenhouse (see Appen. A) are shown in this section for lack of space.

Some of the results of the calibration processes are shown in Fig. 2.7 and Table 2.2, where a comparison between real measurements and those obtained by separate simulations are shown using data of August for all the variables and data of January for air temperature and humidity (which are the main variables). These results are different depending on the models defined by the known state variables:

- Configuration 1. Simple submodel with full measurements of the other state and exogenous (external) variables. The model only estimates the air temperature.
- Configuration 2. Using real data of cover and soil temperatures and exogenous variables. The model estimates the air greenhouse temperature and humidity.
- Configuration 3. Using real data of soil temperatures and exogenous variables. The model has to estimate the greenhouse air temperature and humidity, and the cover temperature.
- Configuration 4. Using real data of humidity and exogenous variables. The model has to estimate the temperature of the first soil layer, the soil surface, the cover, and the greenhouse air.
- Configuration 5. Without supplying data of humidity, cover temperature, and soil temperatures (complete model). All the state variables are simulated and only external variables are supposed to be known.
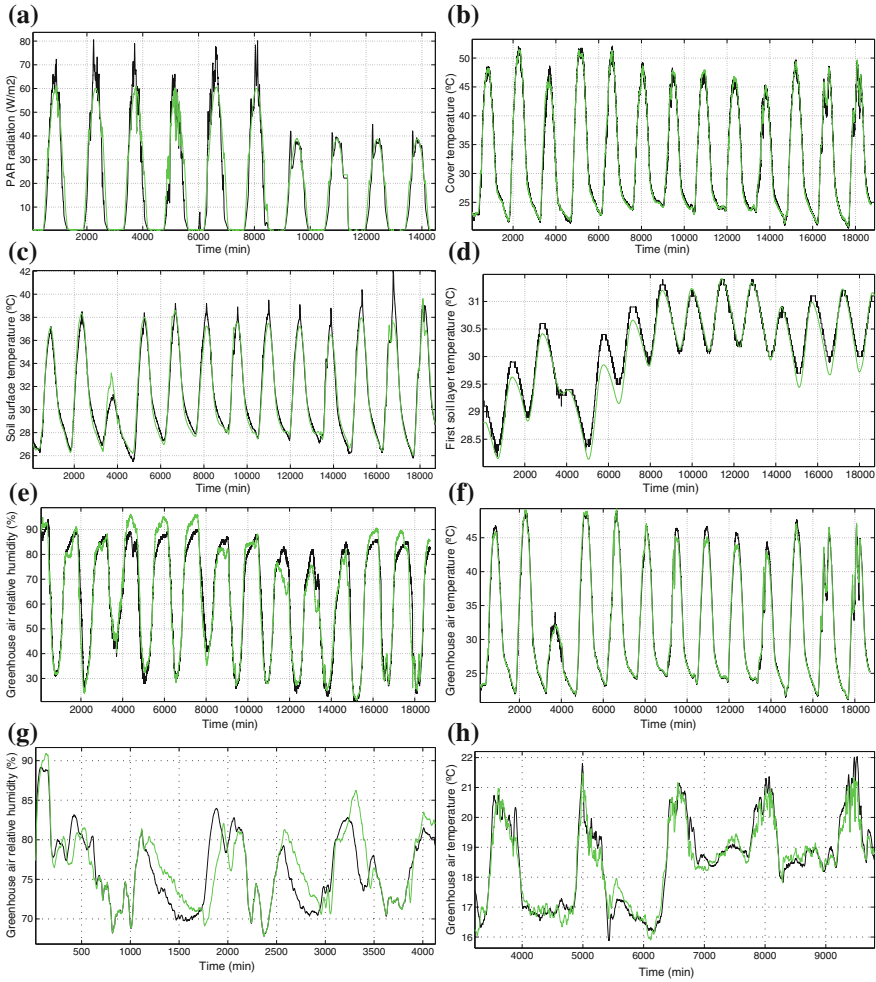
Fig. 2.7 Simulation results with the independent submodels in the calibration process. **a** PAR radiation submodel in spring. **b** Cover temperature submodel in summer. **c** Soil surface submodel in summer. **d** First soil layer submodel in summer. **e** Greenhouse humidity submodel in summer. **f** Greenhouse temperature submodel in summer. **g** Greenhouse humidity submodel in winter. **h** Greenhouse temperature submodel in winter

Table 2.3 provides the results of the temperature estimated by the five configurations, in terms of maximum, mean and standard deviation absolute errors when compared with real data. As more variables are required to be modeled, larger errors are obtained, as shown in Fig. 2.8. This is due to the fact that the uncertainties in the modeled processes increase the numerical errors, which are greater because it is necessary to solve a larger number of equations. This result was predictable, although the behavior of the model can be considered adequate in every configuration because

Table 2.2 Comparative results of the estimation of the different climate variables in the calibration process

	Summer				Winter		
	Air temp.	Air relative humidity	Cover temp.	Soil surface temp.	First soil layer temp.	Air temp.	Air relative humidity
Variation interval	21.1–49.0 (27.9 °C)	21–94 (73 %)	20.55–52.1 (31.55 °C)	25.5–42 (16.5 °C)	28.19–31.4 (5.9 °C)	11.5–25.5 (14 °C)	47.9–100 (50.3 %)
Mean	0.51	3.96	0.52	0.68	0.25	0.52	2.53
Maximum	2.81	24.32	3.38	4.12	0.79	2.06	17.19
Standard deviation	0.52	3.75	0.53	0.44	0.17	0.48	2.39

Table 2.3 Comparative results of the estimation of the greenhouse air temperature using different configurations

	Configuration 1	Configuration 2	Configuration 3	Configuration 4	Configuration 5
Mean	0.51	0.52	0.61	0.93	0.95
Maximum	2.81	2.83	3.12	4.63	4.73
Standard deviation	0.52	0.53	0.59	0.65	0.66

the mean of the absolute errors is not greater than 4 % within the variation interval of the greenhouse air temperature. As the results show, the model calibration process has been successfully performed.
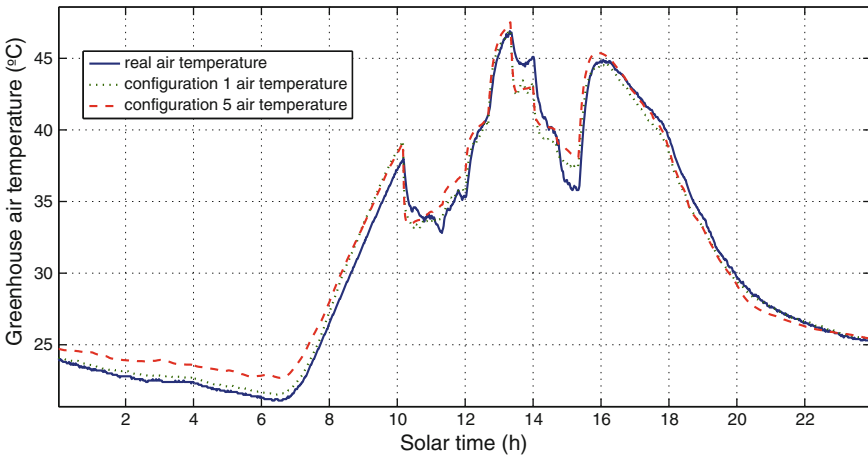

Fig. 2.8 Simulation results with the independent submodels in the calibration process

2.1.1.10 Sensitivity Analysis

A sensitivity analysis based on the variation of the optimal obtained parameters has been carried out to study the robustness of the model formulation. The numerical methods proposed by Cameron [75] have been used, consisting in the calculation of the cost function described in Eq. (2.54) for 21 values of each one of the model parameters, in a variation interval of $\pm 10\,\%$ with respect to their optimal values. As an example, Fig. 2.9 shows the greenhouse air temperature sensitivity analysis for summer time (without crop) and during winter time (with crop and heating system). A zoom of the obtained results shows that the curves corresponding to the variations of the cost function are not symmetrical with respect to the minimum. This is mainly due to the nonlinear dependence of the models with the parameters. Even so, it is observed that around $\pm 5\,\%$ of the parameters optimal value, the linearization hypothesis is valid and so the selection of a quadratic cost function can be considered correct. The conclusions of the sensitivity analysis of each submodels are the following:

- Air temperature submodel. As Fig. 2.9a shows, in the case of an empty greenhouse during summer time conditions, this model is more sensible to the parameters of the convection process between the cover and the greenhouse air. This fact can be explained because the greenhouse air temperature depends on the outside climate and the cover acts like a union among them. Therefore, a small variation in this process will cause a great difference between the real value and the model estimation. Also, there are two sets of parameters providing a same variation of the cost function (Fig. 2.9b shows with more detail these two groups). These are those related to the convection with the soil surface, because the soil acts as a climate regulator, providing energy during the nocturnal periods. Figure 2.9b also
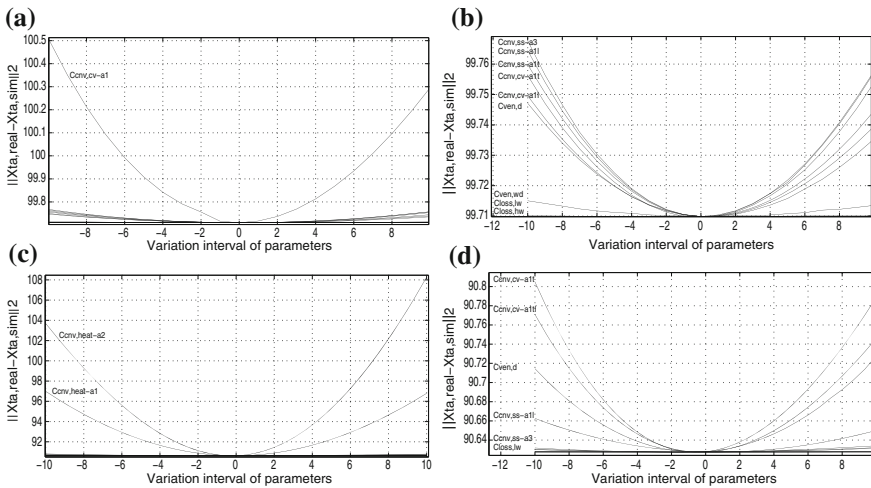

Fig. 2.9 Greenhouse air temperature sensitivity analysis. **a** Summer time complete analysis. **b** Summer time detail analysis. **c** Winter time complete analysis. **d** Winter time detail analysis

shows that the air temperature has low sensitivity to the parameters related to the ventilation process. This is not what was expected as the ventilation is the main cooling source. Some sensitivity analyses were performed for diurnal periods of 10 h where the ventilation was acting during a long time interval, observing that all the obtained results are similar. A possible cause of the obtained result is the low ventilation rate of the ventilation system installed in the analyzed greenhouse. This result should not be extrapolated to other greenhouse structures. In the case of a greenhouse with crop under winter conditions, the temperature of the air is more sensible to the convection process with the heating pipes parameters as Fig. 2.9c shows. Figure 2.9d shows a zoom of the influence of the rest of parameters. The results are similar to the previous analysis, where the model is sensible to cover convection parameters, moderately robust to changes in the parameters of soil convection and quite robust to the variation of the ventilation parameters.

- Cover temperature submodel. The cover temperature submodel is quite sensible to the parameters related to long wave radiation between the cover and the rest of the solids (soil, crop, and heating system) due to the fact that the temperature difference between the different elements is the source of the processes of heat transmission. The temperature of the heating system is very high compared with that of the other elements, reason of why its effect is larger. The heat transmission by thermal radiation depends on the temperature difference power to 4, reason of why its contribution is very important.
- First soil temperature submodel. This model is more sensible to the conduction coefficient with the soil surface as was to be expected. It is observed that the degree of sensitivity with respect to other parameters is of similar order, since the value of the cost function varies between 45 and 48, reason of why a special sensitivity to anyone of the parameters cannot be deduced.
- Soil surface temperature submodel. Some of the previous conclusions are extrapolated to the soil surface temperature submodel, which is more sensible to the variation of those parameters related to the processes of thermal radiation. In a second level, the model is more sensible to the conduction processes than to the convection processes with the inner air, due to the fact that the soil is a thermal buffer where the conduction processes are dominant.
- Humidity submodel. The sensitivity analysis of the humidity submodel has been divided into two stages. The first one corresponds to a period without crop under summer conditions, where the humidity model is more sensible to the parameters related to the evaporation process in the irrigation pools, mainly with the parameter related to the solar radiation. This is logical as under these conditions, this process is the main source of water contribution to the greenhouse air. On the other hand, it is less sensible to the parameters related to the natural ventilation as happened with the temperature submodel previously commented. In the second stage, a tomato crop with a middle-development state (LAI = 3) was considered, where the humidity model is more sensible to the parameters related to the processes of thermal radiation. This is due to the fact that, in this case, the main source of water contribution is the crop transpiration that directly depends on the net radiation

that reaches the canopy (related to the short wave and the thermal radiation). The sensitivity to the rest of parameters is similar to that of the first period.

2.1.1.11 Model Validation

As some state variables are not measured (cover and soil layers temperatures), only the configuration 5 of the compound climate model has been used to validate the greenhouse air temperature and humidity. Due to the fact that all the state variables are related, if two of them are validated, it can be expected that the behavior of the rest of them is adequate. In any case, the estimation of these variables provided by the model has been studied to confirm that their evolution is that expected. The experiences performed to validate the model are the following:

- Model validation with data of Araba greenhouse. After the calibration, the model for this greenhouse (described in the previous sections) with data of winter and summer seasons, the following tests were performed:

  – Evaluation of the model in the same seasons of another year: January and August.
  – Evaluation of the model in a different season of those used in the calibration process: Spring season.

  Figure 2.10 shows some results of these experiences. Analyzing these data, the validity of the developed model can be confirmed both from quantitative and qualitative viewpoints, because it follows the dynamics of the modeled variables and the errors are within acceptable intervals for this type of applications (the relative error of the absolute error average is less than 7 %). Obviously, this assertion is valid only for this greenhouse, so in order to generalize this conclusion, it was necessary to perform new validation experiences in other greenhouses with different structures, different actuators, and different control strategies as is commented in what follows.

- Model validation with data of Araba greenhouse number 3. This greenhouse is similar to Araba greenhouse except the position of the roof vents. So it was necessary to carry out the calibration of the ventilation parameters. The rest of the parameters are the same of the Araba greenhouse. In order to validate the model, some tests were carried out for three different seasons: Winter (January), spring (April), and summer (August). Table 2.4 shows some results of these experiences. The conclusions are similar to the another Araba greenhouse with a relative error of the absolute error average less than 8 %.
- Model validation with data of Inamed greenhouse. This is a hard test for the model structure as this greenhouse is different from the previous ones. After the estimation of the model parameters for Inamed structure (different to the Araba structure) using the data corresponding to the winter and summer seasons, three different experiences were performed to validate the climate model under different climate
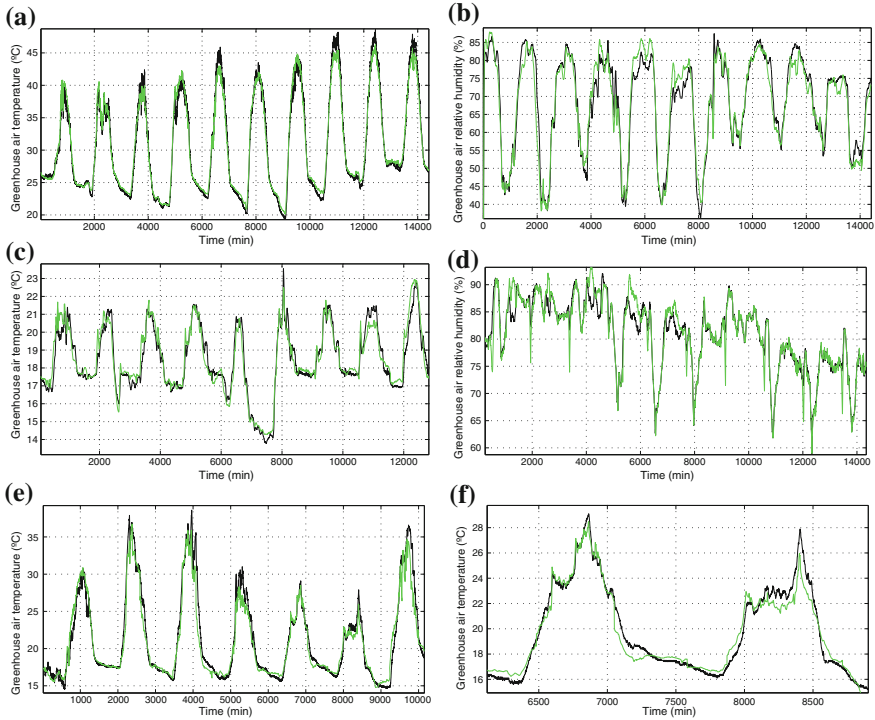
Fig. 2.10 Simulation results of Araba greenhouse in the validation process. **a** Greenhouse air temperature in summer. **b** Greenhouse air relative humidity in summer. **c** Greenhouse air temperature in winter. **d** Greenhouse air relative humidity in winter. **e** Greenhouse air temperature in spring. **f** Detail of greenhouse air temperature in spring

Table 2.4 Comparative results of the estimation of the different climate variables in Araba greenhouse number 3 in the validation process

	January		April		August	
	Temperature	Humidity	Temperature	Humidity	Temperature	Humidity
Variation interval	11.43–21.67 (10.24 °C)	45.4–99.1 (53.7 %)	11.3–27.3 (16.0 °C)	29.3–58.66 (59.36 %)	18.5–51.1 (32.6 °C)	31.42–92.21 (60.79 %)
Mean	0.56	4.11	0.58	4.54	1.12	3.62
Maximum	4.25	17.85	3.99	20.84	6.05	14.89
Standard deviation	0.52	3.99	0.58	4.09	0.94	3.43

conditions: Winter (January), spring (April), and summer (August). Figure 2.11 and Table 2.5 show some of the results, obtaining similar conclusions as those previously discussed.
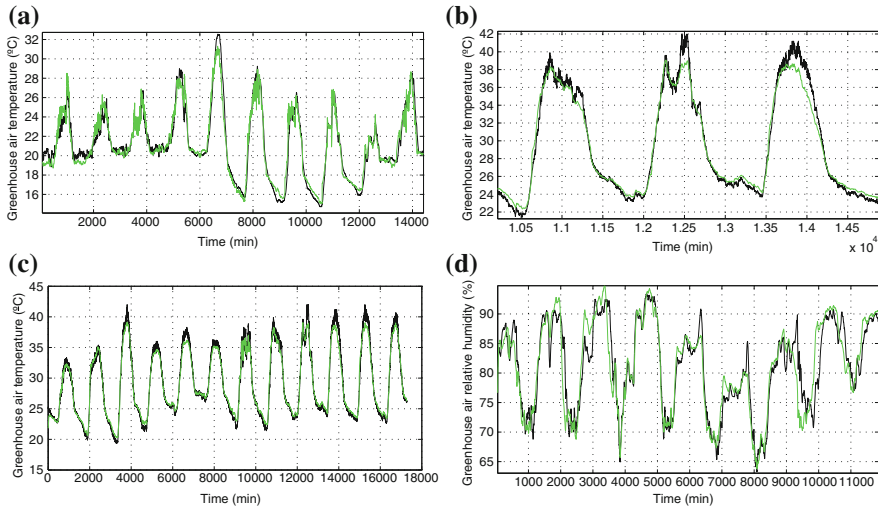
Fig. 2.11 Simulation results of Inamed greenhouse in the validation process. **a** Greenhouse air temperature in spring. **b** Detail of greenhouse air temperature in spring. **c** Greenhouse air temperature in summer. **d** Greenhouse air relative humidity in summer

Table 2.5 Comparative results of the estimation of the different climate variables in Inamed green-house in the validation process

	January		April		August	
	Temperature	Humidity	Temperature	Humidity	Temperature	Humidity
Variation interval	12.54–23.66 (11.12 °C)	59.4–100 (40.6 %)	14.72–32.53 (17.81 °C)	63.18–93.41 (30.23 %)	18.5–51.1 (32.6 °C)	31.42–92.21 (60.79 %)
Mean	0.48	3.26	0.63	2.11	1.12	4.01
Maximum	3.12	16.01	4.89	12.99	6.05	15.54
Standard deviation	0.43	3.17	0.55	2.19	0.94	3.97

- Model validation with data of Almería greenhouse. The same procedure was applied to this kind of greenhouse and the obtained results were similar to the Inamed case (not included for sake of space).

As it can be observed, simulations with a high degree of exigency were carried out to validate the compound model, using data of other seasons (different to those used in the calibration process) and with different greenhouse structures, obtaining adequate results that confirm the validity and performance of the model.

2.1.2 Pseudo-Physical Climate Models

2.1.2.1 General Considerations

As it has been analyzed in Sect. 2.1.1.2, the climate inside a greenhouse can be
described by a system of first-order ODE which characterize the dynamics of the air,
crop, soil and cover temperatures, air humidity, and CO_2 concentration. Such model
is very useful for simulation and optimization purposes, but for other applications,
such as climate control, simplified versions capturing the dominant dynamics of the
system can be used. Several authors have proposed simple models keeping some
physical sense [38, 177, 202, 384, 441, 448, 459, 460, 461]. To derive a simplified
version of the model developed in Sect. 2.1.1.2, the following simplifications have
to be done:

- The cover is not considered as a greenhouse element characterized by its tempera-
  ture, but an interface between the inside and outside air where energy is exchanged
  depending on the inside-outside temperature difference. Thus, models of convec-
  tion processes between the cover and the outside and inside air and the conduction
  process between its two surfaces are replaced.
- The crop is not considered an element and its effect on climate is modeled by tran-
  spiration and CO_2 supply or consumption due to photosynthesis and respiration.
  The modeling of these contributions can be done either using empirical relation-
  ships with climatic variables or detailed models developed by other authors.
- When modeling air temperature, the fundamental heat sources are the sun and the
  heating system, while ventilation and losses through the cover are the main heat
  losses. The effect on the temperature of the crop is usually taken into account,
  whereas the radiation through the cover is used both by the plants to perform
  transpiration and photosynthesis and to heat the air. The latent heat due to con-
  densation on the cover or the evaporation in the soil surface or pool are not taken
  into account.
- The model of water vapor content in the air has as fundamental contributions crop
  transpiration and humidification systems, and ventilation as the main cause of
  moisture loss by exchange with the outside.
- The model of CO_2 concentration has as main inputs the artificial CO_2 supply
  systems and the crop respiration, and ventilation and photosynthesis as the main
  losses.
- Some authors include the model of the soil surface temperature in which only
  the energy fluxes due to convection processes with greenhouse air and conduction
  ones with the first soil layer (boundary condition) are taken into account. The
  thermal radiation processes among physical elements of the greenhouses are not
  considered.
- Although air is inert to radiation, most simplified models of inside air temperature
  include a term depending on global radiation to model air warming due to the
  sun. It used to be a constant factor between 0 and 1 multiplying the solar radiation
  transmitted through the cover.

- Heat transfer coefficients with the soil or heating pipes are considered constant and not a function of the temperature difference between the solid and the fluid or the velocity of the latter.
- The model of several physical processes such as ventilation is simplified, often using empirical relationships or considering some energy fluxes in steady state (constant), such as those from the heating system.

2.1.2.2   General Hypotheses and Simplified Model Development

The simplified pseudo-physical climate model developed in this section for control purposes is developed under the following hypotheses:

1. The state variables of the system are the inside air temperature $X_{T,a}$ and humidity (absolute $X_{H_a,a}$ and relative $X_{H_r,a}$). The CO_2 concentration is not modeled because CO_2 enrichment systems are not available, but this variable is measured.
2. Three main external systems interact with the greenhouse: Outside air, soil surface, and crop.
3. The exogenous variables and disturbances acting on the system and considered as boundary conditions are the outside air temperature $D_{T,e}$ and absolute humidity $D_{H_a,e}$, wind speed $D_{ws,e}$ and direction $D_{wd,e}$, global radiation $D_{rs,e}$, soil surface temperature $D_{T,ss}$ and LAI as measurement of the state of the crop D_{LAI}.
4. The control inputs are the vents positions U_{ven}, the shade screen position U_{shd}, and the temperature of the water within the pipes of the heating system $U_{T,heat}$ (or the heater activation control signal in the case of air heating systems).
5. A uniform homogeneous distribution of variables is considered in the air volume.
6. With respect to the processes associated with solar radiation, the following assumptions are made: Air is not inert to radiation (it absorbs and transmits radiation). Reflection effects are not considered.
7. In the heating by hot water pipes installation, water temperature is measured 1 m downstream the mixing valve, but the convection with air is done by the external surface of the tubes. The assumption is to disregard the effects of convection between hot water and inner surface of the pipes and conduction between inside and outside of the tubes, so that it is considered that the temperature of the outer surface of the pipes is equal to that of the water flowing through them.
8. The physical properties of air, such as density or specific heat, are considered constant with respect to temperature and time.

2.1.2.3   Internal Air Temperature Model

The greenhouse air temperature can be modeled using the following balance:

$$c_{sph,a} c_{den,a} \frac{c_{vol,g}}{c_{area,ss}} \frac{dX_{T,a}}{dt} = Q_{sol,a} + Q_{cnv,ss-a} + Q_{heat-a} + Q_{cnv-cnd,a-e}$$
$$- Q_{ven,a-e} - Q_{loss,a-e} - Q_{trp,cr} \qquad (2.59)$$

where $Q_{sol,a}$ is the solar radiation absorbed by the air, $Q_{cnv,ss-a}$ is the convective flux with the soil surface, Q_{heat-a} is the flux with the heating pipes, $Q_{cnv-cnd,a-e}$ is the convective flux with the cover, Q_{ven} is the heat lost by natural ventilation, $Q_{loss,a-e}$ is the heat lost by infiltration losses, $Q_{trp,cr}$ is the latent heat effect of the crop transpiration, and $c_{ter} = c_{sph,a}c_{den,a}(c_{vol,g}/c_{area,ss})$ is the product of specific heat of air, air density and effective height of the greenhouse (greenhouse volume/soil surface area). These fluxes can be modeled in different ways. In the case treated in this book, the following paragraphs contain the terms used.

Solar radiation absorbed by the air. The solar radiation transmitted through the cover and reaching the crop $V_{rs,cr}$ is determined by:

$$V_{rs,cr} = V_{tsw,g}D_{rs,e} \tag{2.60}$$

where $V_{tsw,g}$ is the short wave heat transmission coefficient, which depends on the heat transmission coefficient of the cover, the whitening state, and the shading screen, as indicated by Eq. (2.5). The solar radiation absorbed by the air $Q_{sol,a}$ is given by:

$$Q_{sol,a} = c_{asw,a}V_{rs,cr} \tag{2.61}$$

where $c_{asw,a}$ is the short-wave absorption coefficient of the greenhouse air, although as the air is inert to solar radiation, it is mostly a parameter of thermal efficiency of solar energy. This coefficient must be estimated in the model calibration process.

Convective heat transfer between the soil surface and the inside air. The heat transfer between the soil surface and the inside air $Q_{cnv,ss-a}$ is a function of the temperature difference between soil surface temperature $X_{T,ss}$ and inside air temperature $X_{T,a}$, Eq. (2.62),

$$Q_{cnv,ss-a} = c_{cnv,ss-a}(X_{T,ss} - X_{T,a}) \tag{2.62}$$

where $c_{cnv,ss-a}$ is a convection coefficient considered constant and that has to be estimated.

Heat transfer by convection and conduction in the cover between the outside and the inside air. This process is considered proportional to the temperature difference between outside air temperature, $D_{T,e}$ and inside air temperature, $X_{T,a}$:

$$Q_{cnd-cnv,a-e} = c_{cnd-cnv,a-e}(X_{T,a} - D_{T,e}) \tag{2.63}$$

where $c_{cnd-cnv,a-e}$ is a thermal loss coefficient (considering convection and conduction processes) which is considered constant and is estimated empirically.

Heat transfer by the heating system. The same models described in previous sections can be used (Eqs. (2.36) and (2.38)).

Heat transfer to the outside air due to ventilation and infiltration. As mentioned above, both fluxes are modeled simultaneously as the infiltration losses process is included as a constant effect in the ventilation flux $V_{\text{ven,flux}}$, as evidenced by Eqs. (2.12), (2.11) and (2.15). Therefore, the following model is used to describe these processes:

$$Q_{\text{ven,a}-\text{e}} + Q_{\text{loss,a}-\text{e}} = \frac{c_{\text{den,a}}c_{\text{sph,a}}}{c_{\text{area,ss}}} V_{\text{ven,flux}}(X_{\text{T,a}} - D_{\text{T,e}}) \qquad (2.64)$$

The ventilation flux is described by Eqs. (2.12), (2.12) and (2.15). Another option is to consider a simplified volumetric flow rate using an exponential expression of the aperture control signal (this is usual in greenhouses of Almería type [325]):

$$V_{\text{ven,flux}} = c_{\text{ven,n}}c_{\text{ven,l}}c_{\text{ven,w}} D_{\text{ws,e}}(\alpha_v U_{\text{ven}}^{\beta_v}) + V_{\text{loss}} \qquad (2.65)$$

where U_{ven} in this case is the percentage or normalized aperture of the vents, $c_{\text{ven,n}}$ is the number of vents, $c_{\text{ven,l}}$ is the length of the vents, $c_{\text{ven,w}}$ is the width of the vents, and α_v and β_v are tuning parameters which, according to actual measurements, show subtle variations between leeward and windward ventilation, and V_{loss} is the leakage when the vent is closed. This is a very simplified expression as the effective opening surface should have to be used through variable $V_{\text{ven,hef}}$, as in Eqs. (2.12) and (2.11) (Eq. (2.15) if both roof and sidewall ventilation openings are considered—in that case Eq. (2.65) should include two terms accounting for both control signals), but it has demonstrated to be valid for the kind of greenhouses considered in this book [326].

Latent heat transfer by crop transpiration. The effect of crop transpiration on the inside air temperature can be modeled using Eq. (2.42), considering that the net radiation absorbed by the crop is equal to the solar radiation neglecting the effect of thermal or long-wave radiation and that the boundary layer resistance, $V_{\text{r,bl}}$, can be considered constant and equal to $200 \, \text{s} \, \text{m}^{-1}$ in the range of wind speeds inside the greenhouse [420].

2.1.2.4 Internal Air Humidity Model

The greenhouse air humidity can be modeled using the following equation:

$$c_{\text{den,a}}(c_{\text{vol,g}}/c_{\text{area,ss}})\frac{dX_{\text{H}_{\text{a,a}}}}{dt} = M_{\text{trp,cr}} - M_{\text{ven,a}-\text{e}} \qquad (2.66)$$

where the main source of water vapor is crop transpiration $M_{\text{trp,cr}}$, described in Eq. (2.44), while the primary source of loss of water vapor is produced by the
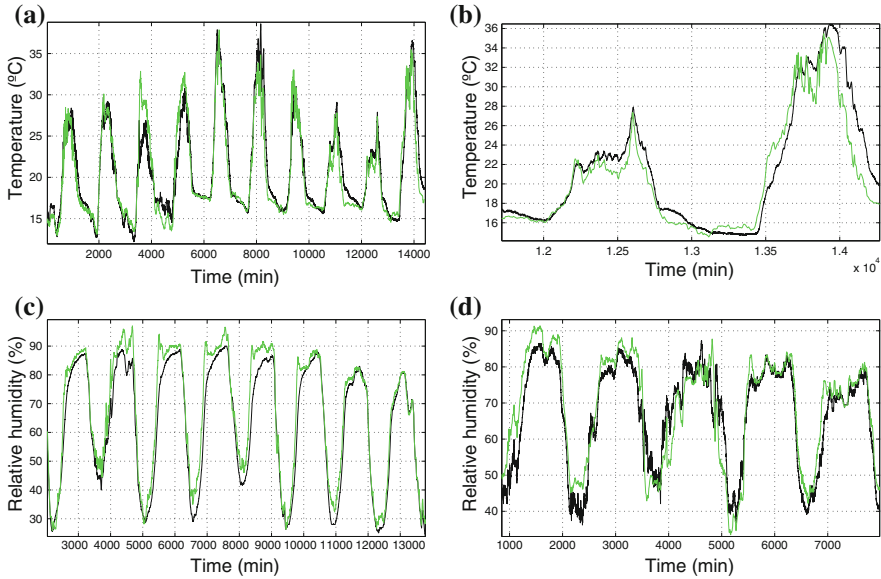
Fig. 2.12 Simulation results of Almería greenhouse with simplified physical models. **a** Temperature in April. **b** Detail of temperature. **c** Humidity in August. **d** Humidity in April

exchange of air with the outside through ventilation and the infiltration, $M_{\text{ven},a-e}$, computed using Eq. (2.53).

2.1.2.5 Implementation, Calibration and Validation of the Model

In order to implement and calibrate de model, the same techniques described in Sects. 2.1.1.8 and 2.1.1.9 were used.

After the identification of the model parameters for the different greenhouses structures using the data corresponding to winter and summer seasons, different experiences were performed to validate this simplified climate model under different climate conditions: Winter (January), spring (April), and summer (August). Figure 2.12 and Table 2.6 show some of the results of Almería greenhouse, obtaining similar results in the other greenhouses. As it can be observed, adequate results were obtained that confirm the validity and performance of the model.

2.1.3 Data-Driven Models

As has been demonstrated in the previous sections, in the design, implementation, calibration, and validation of nonlinear simulation models, the rigorous develop-

Table 2.6 Comparative results of the estimation of the different climate variables in Almería greenhouse in the validation process with simplified physical models

	January		April		August	
	Temperature	Humidity	Temperature	Humidity	Temperature	Humidity
Variation interval	13.76–23.55 (9.79 °C)	55.64–100 (44.36 %)	14.5–38.6 (24.1 °C)	36.2–87.7 (51.5 %)	19.4–48.6 (29.2 °C)	36.36–87.4 (51.11 %)
Mean	0.74	3.64	1.31	4.32	1.14	4.71
Maximum	3.67	17.10	6.71	20.02	5.32	22.01
Standard deviation	0.71	3.23	1.36	3.86	1.09	3.79

ment of dynamic models for simulating the production system in a greenhouse is a time-consuming task that requires a wide knowledge of the involved physical processes, both in the design phase and in the model validation stage. An alternative to models based on physical principles are those obtained from data, also known as black box ones, as they are described by dynamic equations (linear or nonlinear), which coefficients are obtained through an identification procedure, defined as the problem of building mathematical models of dynamic systems based on observed data [257]. Therefore, empirical models can be developed, so that a very flexible mathematical structure with modifiable parameters estimated from experimental data can be used regardless of any consideration of the governing physical principles. The identification process begins with the design and subsequent realization of experiments in the system (using signals exciting the desired bandwidth the model has to reproduce), acquiring the necessary input and output data from the system during a given period of time. Next, the nature, size, and parametric structure of the model is determined. Based on a predetermined criteria, the model is estimated, identifying the free parameters of the selected structure. To determine whether the model is acceptable, it is then validated using real data different that those used in the parameter estimation process. It is thus an iterative process, as if the model is not properly validated, the procedure is repeated changing decisions made in the previous stages. Obviously, these models are limited as they reproduce the dynamics of a system under particular operating conditions. However, they present a number of advantages, among which the relative simplicity of obtaining the model based on an appropriate methodology stands out. In the literature, there are many techniques for obtaining data-driven models, both based on linear and nonlinear structures. In this section, some of the most used black box model structures used within the greenhouse climate framework are described.

2.1.3.1 Linear Model Obtained with Reaction Curve Method

When considering small changes around an operating point, most industrial processes can be described by a linear model, usually of high order [72]. The reason for this is that most processes are comprised of many dynamic elements, typically first order,

so that the full model order is equal to the number of elements. If, as happens in many processes, one of the time constants is much greater than the others, the smaller time constants are joined to produce a delay that acts as a pure delay. It is therefore possible to approximate the dynamic model of a complex high-order system using a first order plus dead time (FOPDT) description. Hence, one of the most common practices in process control is the estimation of simplified models of stable overdamped dynamic systems (such as the greenhouse) from type tests, being the most widespread method called the *reaction curve*, by which the system in open loop undergoes a change in the input in the form of step and so that the output is modeled as a FOPDT system, described by three parameters: Static gain c_k, time constant c_τ and time delay c_{t_r}, so that the system output $Y(t)$ is described by a first-order differential equation as a function of the input $U(t)$, as described in all classical control textbooks [17]:

$$c_\tau \frac{\mathrm{d}Y(t)}{\mathrm{d}t} + Y(t) = c_k U(t - c_{t_r}) \tag{2.67}$$

The main advantage of this method is its simplicity, ease of understanding by staff with little mathematical background, generally short duration of the involved test (on the order of magnitude as the dominant system dynamics), and the existence of specific control methods for this type of systems [72]. It involves introducing a step input and study the behavior of the output until steady state is reached, yielding the model parameters in a graphical manner. In [295, 407, 408, 461] climate models are obtained by this method.

This section summarizes the development of a FOPDT model of the temperature of the greenhouse (state variable $X_{T,a}$, considered homogeneous) obtained using the reaction curve method. The exogenous variables and disturbances acting on the system considered for modeling purposes are the outside temperature ($D_{T,e}$), wind speed ($D_{ws,e}$), outside global radiation ($D_{rs,e}$), and LAI (D_{LAI}). The control inputs are the vents position (U_{ven}), shade screen position (U_{shd}), and the temperature of the water inside the pipes of the heating system ($U_{T,heat}$). The influence of crop on climate inside the greenhouse has been taken into account in the transfer function that relates temperature with radiation, since plants absorb part of this for their vital functions, including transpiration and thus influencing the state variable.

Analyzing the influence of each of the disturbances and control inputs on greenhouse air temperature, a series of simple models can be obtained. Different single-input single-output (SISO) models represented by transfer functions can be obtained, relating indoor air temperature with ventilation ($G_{ven}(s)$), heating ($G_{heat}(s)$), shade screen ($G_{shd}(s)$), outside radiation ($G_{rs,e}(s)$), outside temperature ($G_{T,e}(s)$) and wind speed ($G_{ws,e}(s)$), s being the complex variable used in Laplace transform. As transfer functions apply on linear systems, the superposition principle holds, so that the effect of each of the variables on temperature is independent and is added to produce the output (Fig. 2.13). The transfer functions are obtained by applying the Laplace transform to Eq. (2.67) with null initial conditions (defining deviation variables from a specified operating point) and have the form:

Fig. 2.13 Transfer functions
relating inputs and
disturbances to inside air
temperature
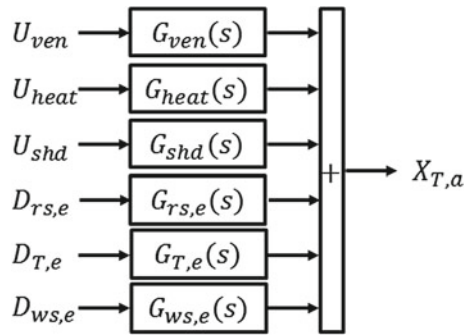
$$G(s) = \frac{c_{\mathrm{k}}}{(c_{\tau}s + 1)}e^{-c_{\mathrm{tr}}s} \qquad (2.68)$$

After the performed experiences, it has been observed that different parameters
are obtained when steps of different magnitude or sign are applied to the inputs
around a particular operating point, as was to be expected from the nonlinear nature
of the system. Arithmetic means of the obtained parameters can be applied. In the
Almería type greenhouse, the obtained results are summarized in Table 2.7. Notice
that in the manipulated inputs, it is easy to perform open-loop step tests, but in
the case of disturbances, the historical database has to be searched trying to find
situations in which abrupt changes occur (with approximated step shape), while the
rest of inputs and disturbances are in quasi-steady state. Thus, the obtaining of these
simple models is constrained by the profile of disturbances. Obviously, if a nonlinear
model has been previously developed, simple transfer functions can be obtained by
linearizing it around the desired operating point. Another possibility is to obtain the
parameters of the transfer functions by identifying them using, for instance, a least
squares (LS) identification algorithm [257], as commented in the next section. The
mean of the absolute errors obtained with these models is around 6.5 %.

Fig. 2.14 shows a graphical comparison between the real temperature for spring
and winter seasons (shown in dark and continuous line) and that obtained with the
simplified linear model based on the reaction curve (shown with a continuous line

Table 2.7 Parameters of the SISO FOPDT transfer functions relating air temperature with inputs
and disturbances

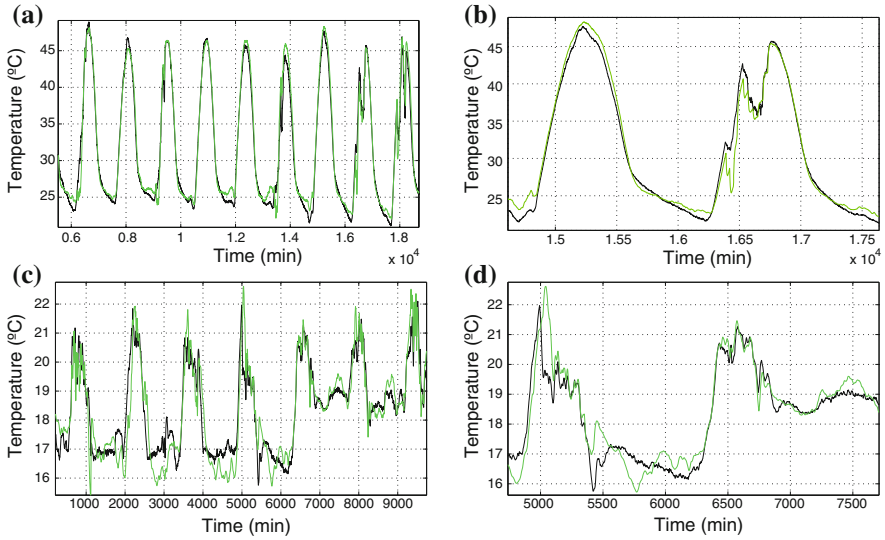|	Radiation	Wind speed	Outdoor temperature	Ventilation	Heating	Shadow net
Static gain c_{k}	0.015 $V_{\mathrm{tsw,g}}$ ($°C\ W^{-1}\ m^2$)	−0.1 ($°C\ m^{-1}\ s$)	1 ($°C\ °C^{-1}$)	−0.09 ($°C\ \%^{-1}$)	0.1 ($°C\ °C^{-1}$)	−0.023 ($°C\ \%^{-1}$)
Time constant c_{τ} (min)	42	3	30	3	25	6
Time delay c_{tr} (min)	1	1	1	1	10	1

Fig. 2.14 Greenhouse air temperature simulation using FOPDT models versus real temperature. **a** Greenhouse air temperature in summer (details on the *right*). **b** Greenhouse air temperature in winter (details on the *right*)

of light color). As can be seen, the model captures the dominant dynamics of the greenhouse air temperature in different situations as clear day or the effect of the actuator continued operation. In nocturnal periods, the model shows a significant deviation from the real temperature due mainly because the effect of the thermal mass of the ground during these periods of time has not been modeled.

In order to compare the obtained results with the simulation model (Sect. 2.1.1), Fig. 2.15 shows a comparison of the real measured temperature with that simulated using linear FOPDT models and the full first principles-based model. The simplified model has worse quantitative and qualitative results, but captures the main dynamics of the system, being able to confirm the validity of the linear model obtained by the method of the reaction curve for type of applications that need some simplified models and control algorithms.

2.1.3.2 Linear Models Obtained with Input-Output Data

As shown in the previous section, due to the existence of a well-established mathematical theory and the fact that many systems present a linear behavior around certain operating points, linear models are one of the most used tools in identification for control [11]. A linear system, time invariant and causal is completely characterized by its impulse response, so that the output of the system $Y(t)$ (considering the SISO
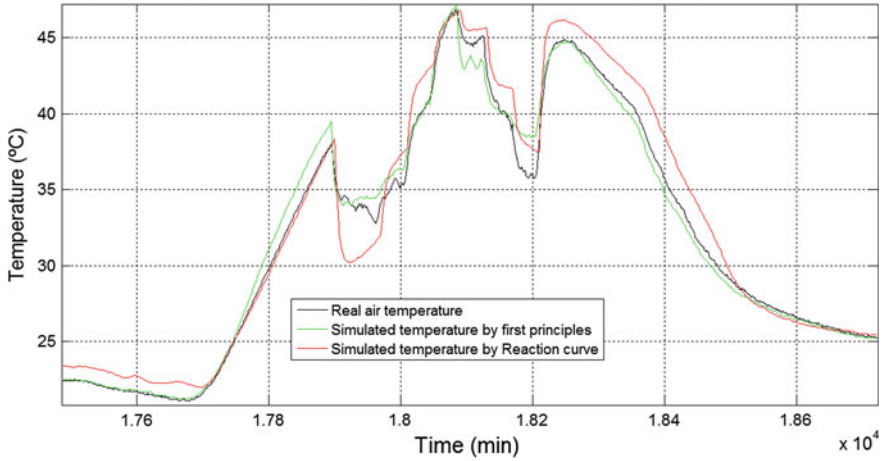
Fig. 2.15 Comparison of simulated air temperature by the complete model based on first principles versus linear model developed using the reaction curve method

case) in discrete time[1] t, is related to the input (measurable disturbance and control signal $U(t)$), through the general equation of convolution in discrete time:

$$Y(t) = \sum_{i=1}^{\infty} g(i)U(t-i) + \sum_{i=1}^{\infty} h(i)V(t-i) \qquad (2.69)$$

where $V(t)$ is a zero mean white noise representing a disturbance. By applying the backward shift operator z^{-1},

$$Y(t) = G(z^{-1})U(t) + H(z^{-1})V(t) \qquad (2.70)$$

where $G(z^{-1})$ is the transfer function associated to the input and $H(z^{-1})$ represents the transfer function relating the output to disturbance. Linear parametric models more widely used correspond to the following general structure:

$$A(z^{-1})Y(t) = \frac{B(z^{-1})}{F(z^{-1})}U(t) + \frac{C(z^{-1})}{D(z^{-1})}V(t) \qquad (2.71)$$

For a model of this type, the transfer functions associated with inputs and disturbances are given by:

$$G(z^{-1}) = \frac{B(z^{-1})}{A(z^{-1})F(z^{-1})} \qquad (2.72)$$

$$H(z^{-1}) = \frac{C(z^{-1})}{A(z^{-1})D(z^{-1})} \qquad (2.73)$$

---

[1] In this book, t is used both for continuous and discrete time, depending on the context.

Different model structures can be obtained as a function of the polynomials which are used, see Table 2.8.

Despite the fact that the AR and ARMA models do not considered the inputs, $B = 0$, the main difference among model structures lies in the consideration of disturbances. AR and ARX structures suppose that disturbances are a white noise, $C, D = 1$, meanwhile ARMA and ARMAX suppose that they present a certain temporal structure. Furthermore, while the transfer functions of the ARX and ARMAX structures share the denominator, that is, $D, F = 1$ for both kind of model structures, OE and BJ models are totally independent. Finally, ARX, ARMAX, and BJ models are used as prediction models, while OE are simulation models which do not include any hypothesis about the structure of the disturbances since $A, C, D = 1$, and in addition, they only model the transfer function associated with the inputs of the system [257].

In [49, 51–54, 60, 104, 296, 305, 408, 461, 482, 483] climate models are obtained using these methods and different structures. In the experiences shown in this section, the system is modeled as a multiple-inputs single-output one (MISO), where the output is the inside air temperature $X_{T,a}$, the disturbances are the outside temperature $D_{T,e}$, wind speed $D_{ws,e}$, solar radiation $D_{rs,e}$, soil temperature $D_{T,ss}$, and the inputs are the percentage of vents opening, one for roof ventilation $U_{ven,r}$ and another one for lateral ventilation $U_{ven,l}$. The models are valid in the operation around a particular operating condition, defined by the boundary conditions and state of the actuators and system. Thus, the linear models obtained by this way are only valid to operate around the particular conditions defining the data used for identification purposes.

Thus, these kind of models serve to determine seasons and stage of the crop. As an example, using data from the Almería greenhouse, the best structure fitting data using cross-validation and residual analysis was an ARX443 model of fourth order (Table 2.9), with 92.53 % fit and mean error in the order of the precision of the used temperature sensors. As an example, Fig. 2.16 shows the greenhouse air temperature predicted by this ARX model, comparing it with the real values measured in summer with a large range of variation. As can be seen, the behavior of the ARX model is reasonably closed to the data, with a mean deviation smaller than 1.5 °C. In [281, 355] there is an extensive analysis of this kind of models for both temperature and humidity identified with data obtained in different climatic conditions of the Southeast of Spain.

Table 2.8 Linear models structures

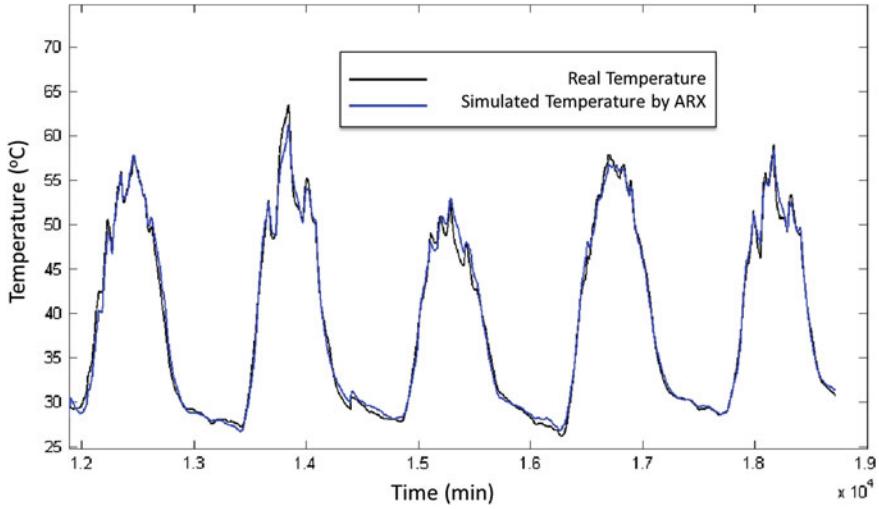| Used polynomials	Model
$B = 0, C = 1, D = 1$	Autoregressive (AR)
$B = 0, D = 1$	Autoregressive Moving Average (ARMA)
$C = 1, D = 1, F = 1$	Autoregressive with eXogeneous inputs (ARX)
$D = 1, F = 1$	Autoregressive Moving Average with eXogeneous inputs (ARMAX)
$A = 1, C = 1, D = 1$	Output Error (OE)
$A = 1$	Box-Jenkins (BJ)

Fig. 2.16   Validation of the ARX443 temperature model with data measured in the greenhouse

Main error sources inside a wrong system identification are known as constant systematic error (bias) and random error (variance) [257]. On the one hand, constant systematic errors can be originated by: (i) input signals without adequate frequency content, (ii) a wrong choice of the model structure or operation model, for example, trying to perform the system identification using a closed loop configuration instead of an open loop one. On the other hand, random errors are introduced through the

Table 2.9   Description of the ARX model

Number of outputs: 1 ($Y = X_{T,a}$)	
Number of inputs: 6 ($U_1 = U_{ven,r}$, $U_2 = U_{ven,l}$, $U_3 = D_{T,e}$, $U_4 = D_{ws,e}$, $U_5 = D_{T,ss}$, $U_6 = D_{rs,e}$)	
Order: 4	Fit: 91.53 %

A polynomial order $n_a = [4]$
B polynomials orders $n_b = [444444]$
delays [sample times] $n_{tr} = [330000]$

Model structure: $A(z^{-1})Y(t) = \sum_{i=1}^{6} B_i(z^{-1})U_i(t) + E(t)$
$A(z^{-1}) = 1 - 1.145z^{-1} - 0.1101z^{-2} + 0.07028z^{-3} + 0.19111z^{-4}$
$B_1(z^{-1}) = -9.354e^{-5}z^{-3} - 3.428e^{-5}z^{-4} + 2.642e^{-56}z^{-5} - 4.608e^{-5}z^{-6}$
$B_2(z^{-1}) = -0.0001363z^{-3} - 7.982e^{-5}z^{-4} - 6.114e^{-5}z^{-5} - 2.5e^{-5}z^{-6}$
$B_3(z^{-1}) = 0.05246 - 0.06033z^{-1} + 0.00823z^{-2} + 0.003358z^{-3}$
$B_4(z^{-1}) = -0.0001545 - 0.01797z^{-1} + 0.00133z^{-2} + 0.0134z^{-3}$
$B_5(z^{-1}) = 5.191e^{-5} + 3.447e^{-5}z^{-1} + .857e^{-6}z^{-2} - 1.977e^{-5}z^{-3}$
$B_6(z^{-1}) = 0.6663 - 0.4621z^{-1} - 0.2932z^{-2} + 0.0933z^{-3}$

Maximum absolute error $= 3.2\,°C$ Mean absolute error $= 0.7\,°C$ Standard deviation $= 0.5\,°C$

presence of noise in the data, which prevent that the model reproduce exactly the output of the system. In addition, models can also be affected by various factors just as: The number of parameters of the model, identification of experiment length, and the proportion between the noise/signal ratio [80].

Besides, the choice of an adequate set of input-output signals acceptable for the whole identification process is one of the most fragile points along the total procedure, since it permits a consistent estimation (free of constant systematic errors) of the parameters of the model. Within the framework of control theory, the reaction curve method is widespread used for obtaining models from data, as analyzed in the previous section. However, step or impulse signals are not always appropriate for a correct identification of industrial systems, since their frequency analysis only shows a low-frequency persistent excitation near to the stationary state. Hence, for a correct estimation of the parameters of a model, it is necessary to obtain the identification and validation data sets by means of an excitation signal with a wide frequency spectrum or within the range where the identification will be performed.

Furthermore, determining the model structure is another vital factor in order to obtain a system identification free of constant systematic errors. To do that, it is necessary to select a structure with an order high enough that helps to capture the real dynamics of the system but avoiding increasing the model order in excess. Information criteria such as the Akaike's Information Criterion (AIC) are used during the model selection stage to find a trade-off between performance and model order (between bias and variance) [257]. More information about the selection of input signals, identification data set and model structure can be found in [163, 164, 257, 350].

2.1.3.3 Linear Fuzzy Models

Fuzzy set theory uses linguistic concepts for representing quantitative values and can be used to describe the greenhouse climate based on the system identification approach [79, 148, 238, 258, 457]. Compared with traditional mathematical modeling, fuzzy modeling possesses some distinctive features, such as the reasoning mechanism in human understandable terms, the capacity of taking linguistic information from human experts and combining it with numerical data and the ability of approximating complex nonlinear functions with simple models. Several methods for fuzzy identification are proposed in the literature [239], many of which generate fuzzy rule relations from real input-output data. Generally, the resultant rule base of the fuzzy system contains a large set of rules and may make the interpretation of their consequences difficult. The Takagi–Sugeno (T-S) fuzzy model approach allows the nonlinear system to be represented under the form of a valid linear model on a restricted domain [435, 438]. This kind of models are described by rules representing the local relations of linear input-output relations in various operation points of a system. These local representations, called "submodels," make it possible to express in state space the dynamics of a system around particular operation points. Thus, the fuzzy formalism intervenes in the determination of the contribution of

each one of these submodels to the representation of the total system. That is, a nonlinear model can be represented by a set of linear models combined thorough fuzzy rules. Thus, each subsystem may contain information related to the nonlinear system. Consequently, a better resolution of the control problems is allowed.

Typically, the T-S fuzzy models represented in the discrete time state space are described by a set of N rules using membership functions μ_{li} and fuzzy variables $z_l(t)$ as follows:

Rule i : IF $z_1(t)$ is μ_{1i} and $z_l(t)$ is μ_{li}

$$THEN = \begin{cases} \mathbf{X}(t+1) = \mathbf{A}_i\mathbf{X}(t) + \mathbf{B}_i\mathbf{U}(t) + \mathbf{D}_i\mathbf{V}(t) \\ \mathbf{Y}(t) = \mathbf{C}_i\mathbf{X}(t) \end{cases} \quad (2.74)$$

where $\mathbf{A}_i$, $\mathbf{B}_i$, $\mathbf{D}_i$ and $\mathbf{C}_i$ are constant matrices of appropriate size, $\mathbf{X}(\cdot) \in \mathbb{R}^n$ is the state vector, $\mathbf{U}(\cdot) \in \mathbb{R}^m$ is the control signal vector, $\mathbf{V}(\cdot) \in \mathbb{R}^s$ is the disturbance vector and $\mathbf{Y}(\cdot) \in \mathbb{R}^p$ is the output vector. The overall global model can be structured as follows:

$$\begin{cases} \mathbf{X}(t+1) = \sum_{i=1}^{N} h_i(t)(\mathbf{A}_i\mathbf{X}(t) + \mathbf{B}_i\mathbf{U}(t) + \mathbf{D}_i\mathbf{V}(t)) \\ \mathbf{Y}(t) = \sum_{i=1}^{N} h_i(t)\mathbf{C}_i X(t) \end{cases} \quad (2.75)$$

where $h_i(t)$ are the so-called normalized activation function in relation with submodel ith such that:

$$h_i(t) = \frac{\Pi_{j=1}^{l}\mu_{ji}(z_j(t))}{\sum_{i=1}^{N}\Pi_{j=1}^{l}\mu_{ji}(z_j(t))}, h_i(t) \geq 0 \quad (2.76)$$

In [288, 290, 292], a climate model for greenhouses, expressed using fuzzy logic is presented. In particular, a T-S model is derived from a standard nonlinear model representing energy and water vapor balances (from the pseudo-physical climate models showed in Sect. 2.1.2), giving a set of linear models related through fuzzy logic. This makes it possible to derive a greenhouse climate model based on linear models. The variables considered for modeling purposes are:

- Output: Inside air temperature ($X_{T,a}$) and humidity ($X_{H_{a,a}}$).
- Input: Aperture of the roof ($U_{ven,r}$) and lateral ($U_{ven,l}$) ventilations and heating system ($U_{T,heat}$).
- Disturbances: Outside temperature ($D_{T,e}$), wind speed ($D_{ws,e}$), soil surface temperature ($D_{T,ss}$), outside global solar radiation ($D_{rs,e}$) and LAI (D_{LAI}).

The model was validated with data of winter and summer from quantitative and qualitative viewpoints, because it follows the dynamics of the modeled variables (see [292]) and the errors are within acceptable intervals for this type of applications (the estimation root mean square error, RMSE, of the temperature is $1.24\,^\circ\text{C}$ whereas for humidity is $10.6\,\%$). As an example, Fig. 2.17 shows the interior temperature predicted by the T-S model, compared with the real values measured in early spring

(the first eight days shown) and late autumn (the last four days) [291]. The T-S model is reasonably close to the data taken in the different climatic conditions, with a mean deviation smaller than $1\,^{\circ}C$.

It can be seen that during some nights the fuzzy model can not exactly approximate the air temperature inside the greenhouse. This drawback often attributed to T-S approximation method is in reality a problem of the mathematical model which is used to extract the T-S fuzzy model.

2.1.3.4 Nonlinear Volterra Models

Before using nonlinear models, it is always advisable to explore all possibilities of simplicity. After linear models, the next step in complexity are those models with concentrated nonlinearities such as Volterra, Hammerstein or Wiener ones [114]. These models are unions of linear dynamic and static nonlinear blocks. Specifically, Volterra models were used to generically exhibit a good behavior and their structure can be exploited in the design of controllers, especially in the case of second-order models with the truncation of terms (truncation orders N_1 and N_2), which can be defined as:

$$Y(t) = h_0 + \sum_{i=1}^{N_1} a(i)U(t-i) + \sum_{i=1}^{N_2}\sum_{j=1}^{N_2} b(i,j)U(t-i)U(t-j) \qquad (2.77)$$

which corresponds to a linear convolution model with a nonlinearity as additional and additive term, as described in [156]. In that model, $Y(t)$ and $U(t)$ represent the last measured output and input to the system, respectively (t is the actual sampling instant). The offset is denoted with h_0 and the linear and nonlinear term parameters are given by $a(i)$ and $b(i,j)$, respectively. Notice that Volterra models are frequently used to model bilinear systems in such a way that it seems to be a good idea to use this formulation for modeling greenhouse temperature dynamics, including the disturbances in the nominal formulation of second-order Volterra models.
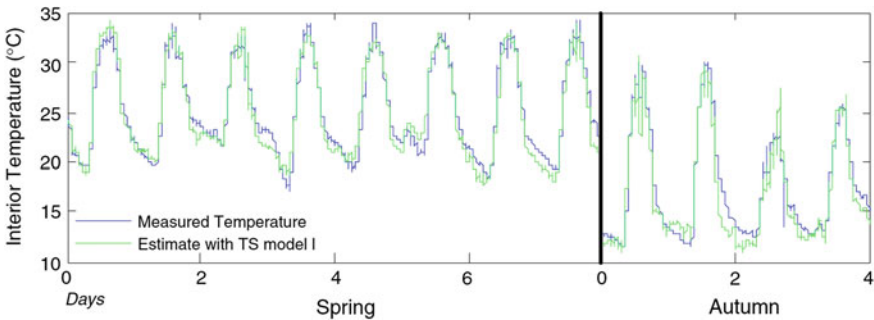

Fig. 2.17 Validation of the TS model with data measured in the greenhouse. As a courtesy of the authors [291]

A preliminary Volterra model was developed to model the inside temperature of an empty greenhouse (without crop) in order to evaluate the behavior of this modeling technique for this kind of systems [155]. Several pseudo random multilevel sequence (PRMS) [350] tests were performed using natural ventilation to obtain adequate data for identification purposes, because typical PRBS (pseudo random binary sequence) and RBS (random binary sequence) tests do not sufficiently excite nonlinear systems. The resulting model adequately fitted the real data but the number of parameters was excessively high. Furthermore, the crop has an important effect on the greenhouse temperature and thus it is a key factor to be included in the system model. In [156], two Volterra models (AR and Non-AR) are developed in order to account for the main dynamics describing changes in inside air temperature to outside weather using only natural ventilation. The influence of the crop is taken into account as a disturbance to the greenhouse temperature by means of the LAI. Thus, the main variables considered for modeling purposes are:

- Output: Inside air temperature ($X_{T,a}$).
- Input: Aperture of the roof ($U_{ven,r}$) and lateral ($U_{ven,l}$) ventilations.
- Disturbances: Outside temperature ($D_{T,e}$), wind speed ($D_{ws,e}$), soil surface temperature ($D_{T,ss}$), outside global solar radiation ($D_{rs,e}$) and LAI (D_{LAI}).

The main interest is to see how these models cope with the nonlinear behavior inherent in the relationship between temperature and vents aperture, through the ventilation rate, which is one of the most difficult dynamics to be modeled in the greenhouse.

A second-order Volterra series model of the greenhouse temperature was identified. In the model validation, carried out with the second data set containing the period from September 2008 to June 2009, a mean square error in the temperature of 0.93 was obtained. As a representative result, a comparison of the greenhouse temperature and the output of the identified model is given in Figs. 2.18 and 2.19, both for the autumn (10–19 January 2009) and spring conditions (15–24 May 2009), respectively. As can be seen in the results, the model output shows a promising fit with the measured greenhouse temperature. In autumn conditions, the model presents a mean value of the absolute error of 0.6 °C, a standard deviation of 0.5 °C, a mean relative error less than 4 %, and a maximum error of 2.1 °C in a range of 11.1–26.4 °C. In spring conditions, similar results were obtained, resulting in a mean value of the absolute error of 0.68 °C, a standard deviation of 0:63 °C, a mean relative error less than 4 %, and a maximum error of 2.5 °C in a range of 15.4–31.4 °C.

2.1.3.5 Nonlinear Neural Networks Models

Artificial neural networks (ANN) are computational elements inspired by networks of neurons in the nervous system of living beings. They consist of elements (neurons or nodes) connected in parallel, whose collective action is able to reproduce complex functions. In addition, the connections between nodes are customizable so that the overall function of the network can be modified [11]. These characteristics can be used to solve problems of identification of dynamical systems like climate
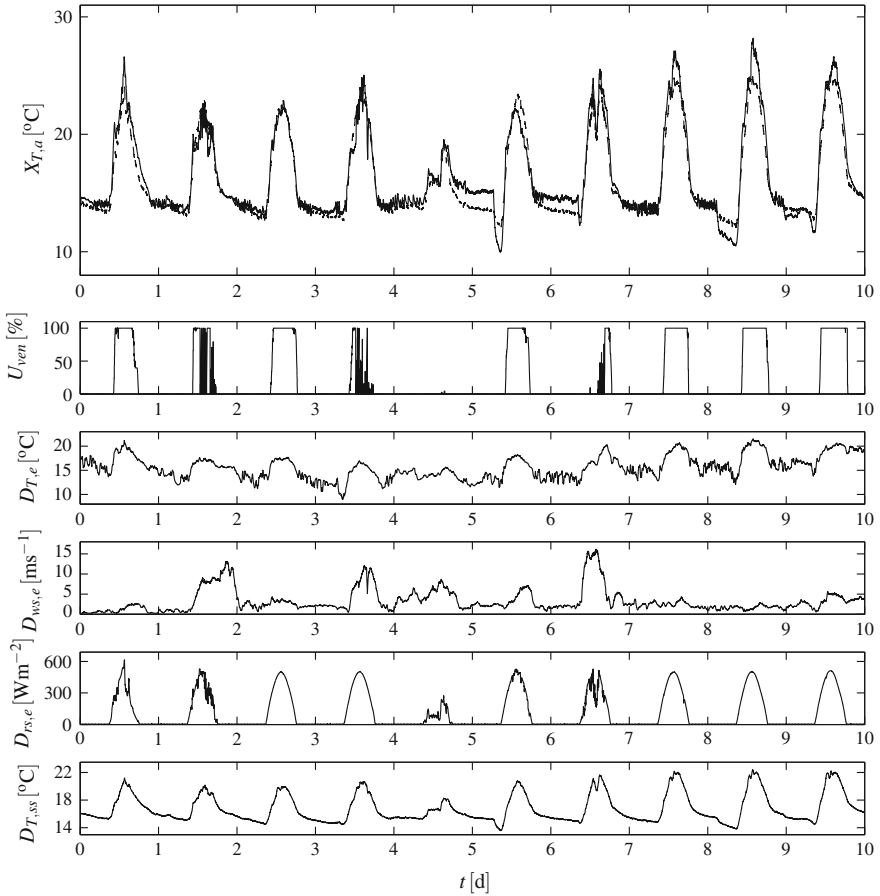
Fig. 2.18 Data set used for the model validation with the greenhouse temperature $X_{T,a}$ (*solid line*) and the model output (*dashed line*) for autumn conditions (10–19 January 2009), the input U_{ven} (aperture of the roof and lateral windows) and the disturbances $D_{T,e}$ (outside temperature), $D_{ws,e}$ (outside wind speed), $D_{rs,e}$ (outside global solar radiation), and $D_{T,ss}$ (soil surface temperature). As a courtesy of the authors [156]

that is generated inside a greenhouse, finding numerous references in the literature emphasizing specialized work [8, 128, 129, 131, 254, 255, 312, 380, 381, 440, 453, 471].

The reasons for using neural networks as identification systems is due to its fast response (parallel processing), their ability to interpolate, their flexibility to describe nonlinear functions and the ability to work with spaces of large dimension. Different neural models for the identification of dynamic systems exist, most of them are extensions to the nonlinear case of linear parametric models, although the NARX model (nonlinear autoregressive model with exogenous inputs) provides great flexibility and allows it to be adjusted with simple algorithms [11]. The output of the
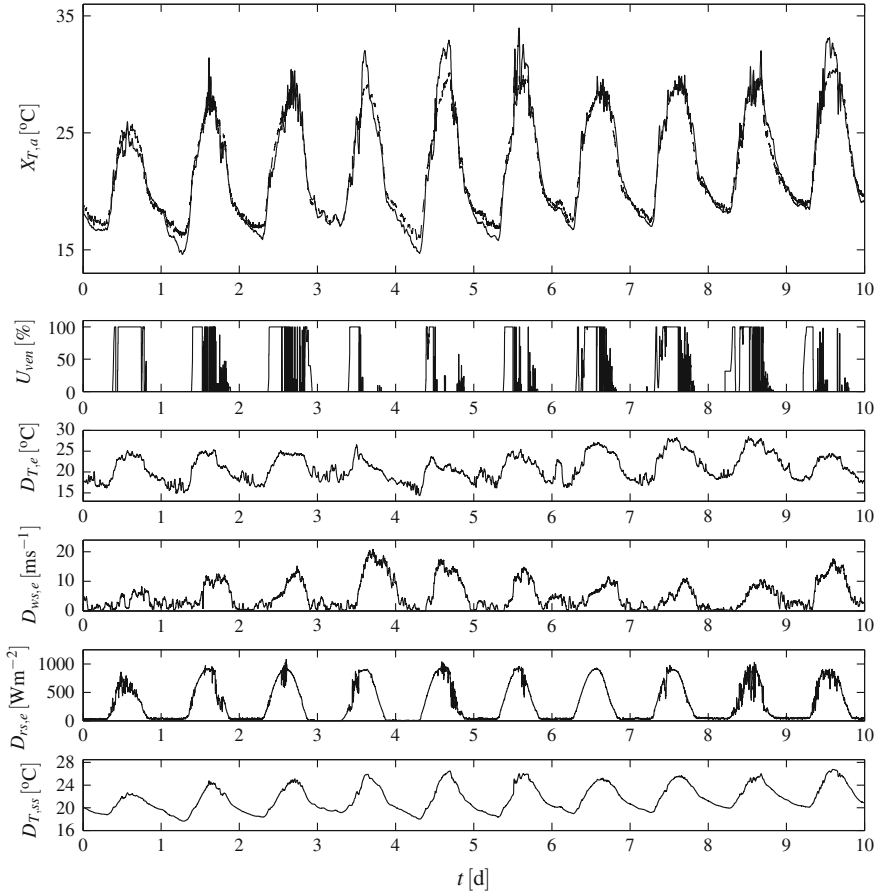
Fig. 2.19 Data set used for the model validation with the greenhouse temperature $X_{T,a}$ (*solid line*) and the model output (*dashed line*) for spring conditions (15–24 May 2009), the input U_{ven} (aperture of the roof and lateral windows) and the disturbances $D_{T,e}$ (outside temperature), $D_{ws,e}$ (outside wind speed), $D_{rs,e}$ (outside global solar radiation), and $D_{T,ss}$ (soil surface temperature). As a courtesy of the authors [156]

NARX model requires past values of input and outputs, so that tapped delay lines (TDL) are used in the implementation. Mathematically the prediction model is given by the following expression [356]:

$$\mathbf{Y}(t+1) = h[\mathbf{Y}(t), \ldots, \mathbf{Y}(t-l), \mathbf{U}(t), \ldots, \mathbf{U}(t-m), \mathbf{D}(t), \ldots, \mathbf{D}_m(t-n)] \quad (2.78)$$

where $\mathbf{U}(t)$ is the input vector of the system at discrete time instant t, which includes the values of ventilation, heating and shade screen, $\mathbf{Y}(t)$ is the output vector at time instant t, which includes the values of temperature and relative humidity, $\mathbf{D}_m(t)$ is the vector of measurable disturbances at time t, which includes the values of outside

Table 2.10 Past values of the inputs of the ANN

Variable	Past values
Temperature	3
Humidity	3
Outside temperature	4
Solar radiation	2
Wind speed	9
Ventilation	5
Heating	10
Shade screens	2

temperature, humidity, radiation, wind speed and direction. The orders l, m and n of the output, input and disturbance vectors are known only in some situations, but generally are obtained by observations made on the system. The NARX model shown in Eq. (2.78) can be implemented by neural networks using as input vector of a historic values of the measured variables [356].

The time domain has been considered trying the past values of the variables as different inputs to the system that feed a static neural network by means of TDL. The number of past values used, as a rule, is unknown and difficult to determine. For a higher number of past values, the stronger the prediction, but at the same time, the model may be inefficient due to the high number of entries required. Moreover, a lower number will cause the model could not accurately predict future outputs. There are a number of methods for selection of input variables for nonlinear models, having used a model based on the estimated gradient as a ratio of distances between points in the enclosed space entries, combined with the use of the information obtained from linear methods using ARX type models, so that the past values of input and output feedback linear models are used as indicative values for the neuronal nonlinear models [356]. For example, the last values used to obtain a model of the temperature and humidity inside the greenhouse Araba number 2 in a given instant t, are shown in Table 2.10 [355, 356]. The selected ANN structure is a multilayer perceptron (MLP), with an input layer with 38 nodes, one hidden layer with 8 nodes and nonlinear activation, and an output layer with 2 nodes. The weights are set as connections to nodes with constant values. The number of nodes is determined by training the different networks and determining, by the method of cross-validation, their approximation and generalization ability. This process was carried out using two disjoint sets of data: One for training the network and one for validation. The training of the implemented neural network has been performed using the method of supervised learning with back propagation, so that the least squares criterion is minimized, as a function of the square of the difference between the measures of real variables acquired in greenhouses and the values estimated by the model, as has been done in the calibration of other models developed in previous sections.

In order to validate the ANN model of temperature and relative humidity using MLP as a network representation, data from Araba number 2 greenhouse and from
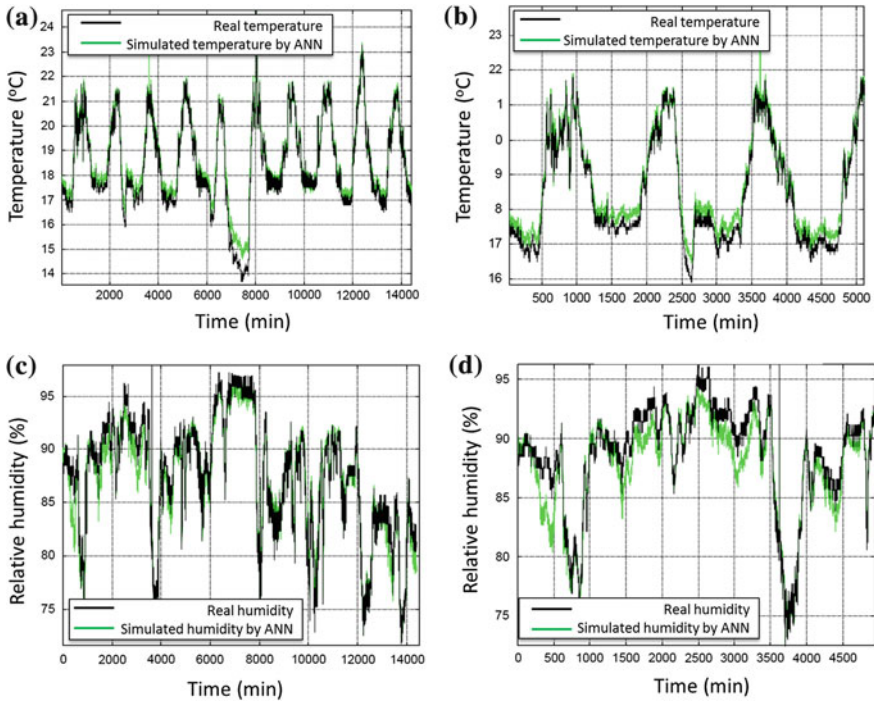
Fig. 2.20 Comparison between real temperature and ANN model estimation. **a** Temperature evolution during 10 days. **b** Zoom of the evolution. **c** Relative humidity evolution during 10 days. **d** Zoom of the evolution

the same season in which the model is calibrated (winter) were used. The results obtained for the temperature are shown in Fig. 2.20 in which the real measurements are represented by a dark solid line and the estimated by the models by a light solid line color.

As can be seen, the temperature in summer is overestimated mainly because the greenhouse roof is whitened which affects the final result. Table 2.11 shows the statistical of the residues in absolute value of the real temperature and relative humidity and the estimated by the neural model. The temperature relative error is 2.4 % in winter, while rises above 6 % for the summer. It is due to the fact that the neural network has been trained with data of winter, so the best results are obtained with conditions an data located near the area of the input/output data used in the identification processed. The extrapolation to distant points from the training space may not produce the desired results [11], as seen in the results for summer whose outside disturbance are different to the training space formed by the corresponding disturbances to winter. However, the relative humidity model behaves correctly in all tests performed at different season of the year, with a constant error for all of them, not being more than 5 % in the range of variation of this variable. Even so, the results are acceptable for use in model-based control algorithms.

Table 2.11 Results with the ANN model

	Temperature			Relative humidity		
	January	August	August	January	August	August
Variation	13.76–.55	19.4–48.6	21.1–49	55.64–100	36.36–87–47	21–94
interval	[9.79 °C]	[29.2 °C]	[27.9 °C]	[44.36 %]	[51.11 %]	[73 %]
Mean error	0.24	1.75	1.62	1.96	2.46	3.24
Maximum error	2.59	3.72	3.27	1.12	2.09	2.51
Standard deviation	0.21	1.12	1.02	1.12	2.09	2.51

Another possibility is to use finite impulse response (FIR) discrete time nonlinear models with integrated variables for greenhouse indoor temperature simulation in order to reduce the number of past values needed as inputs [12]. In this case, the interest is in obtaining a discrete time model for simulation where the actual output of the system $Y(t)$ is not known at any time (except perhaps at the beginning of the simulation $t = 0$). A model that uses past values of Y (i.e., an autoregressive model) must then use its own output $\hat{Y}$ as an estimation of the true output and use it recursively during the entire simulation time. This can cause a built-up of the simulation error producing errors that are larger as the simulation horizon increases. A model that uses just past values of the input signal belongs to the family of FIR models. The output of a FIR model is obtained as a linear combination of past values of the system's input. Since the real output of the system is not needed, this kind of models produces simulation errors that are independent of the simulation horizon. Also, any FIR model obtained by identification is stable, in the bounded input—bounded output (BIBO) sense, since the output of the model is obtained as a combination of past input values. Due to the nonlinear behavior of the greenhouse temperature, NFIR (nonlinear counterpart of the FIR family) was used. The input variables used are the same, but in the first case, the function that combines them is a nonlinear mapping produced in this section by an artificial neural network. As a result, the input vector for the ANN at sample time t is computed as:

$$\mathbf{U}(t) = [U_1(t - d_1 - 1), \ldots, U_1(t - d_1 - n_1), \ldots, U_{nv}(t - d_{nv} - n_{nv})] \quad (2.79)$$

where all variables included (U_1 to U_{nv}) are control actions or disturbances. The values d_j $j = 1, \ldots, nv$ are the dead time for variable j. Model orders are the number of lagged values n_j of each variable from $j = 1$ to $j = nv$. The dimension of the input vector is thus $\dim \mathbf{U} = \sum_{j=1}^{nv} n_j$.

The output variable is assumed to be a nonlinear function of the input vector plus a white noise signal n.

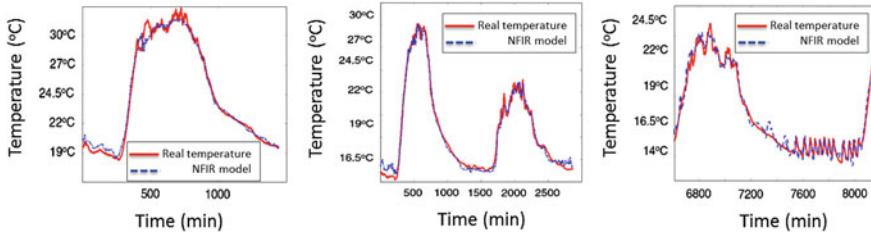$$\mathbf{Y}(t) = f(\mathbf{U}(t)) + n(t) \quad (2.80)$$

Fig. 2.21 Comparison between real temperature and ANN model estimation. As a courtesy of the authors [12]

A variation of NFIR models consists of including integrated values of some variables. Then, instead of using $U(t - d - i)$ for $i = 1, 2, \ldots, n$ it is possible to accumulate the effect in just m sums with $m < n$ being the new variables

$$w(t, j) = \sum_{i=s_j}^{i=f_j} U(t - d - i) \tag{2.81}$$

for $j = 1$ to $j = m$. Obviously the initial and final index for the sums must verify: $s_1 = 1, s_{p+1} = f_p + 1$ for all $p = 1, \ldots, m - 1$ and $f_m = n$. The initial (s) and final (f) index define a time window in which the integration of variable U takes place to yield the integrated variable W. Using the integrated variables, the input vector for a neural NFIR model at sample time t is computed as:

$$\mathbf{U}(t) = [w_1(t, 1), \ldots, w_1(t, n_1), \ldots, w_5(t, 1), \ldots, w_5(t, n_5)] \tag{2.82}$$

The adjustable parameters of the models are obtained minimizing a quadratic criterion of the simulation error. For NFIR12314 model structure (the root mean squared error was the lowest), a neural network was constructed of 20 hidden nodes, obtained better results than the complete first principles model [12]. Figure 2.21 shows a simulation example. The real temperature is plot in solid line, while the simulated one obtained by model NFIR12314 is plot in dashed line. The simulation corresponds to: a. clear day, b. vents opening, c. heating during the night.

2.2 Crop Growth Models

2.2.1 Tomato Growth and Development Models

Growth can be defined as an increment in biomass or an increment in the dimensions of the plant, that are quantitative aspects [87]; growth can also be defined as an increment in weight or height of the organs of the plant [149]. Development is a

concept that indicates a change or organized process (not always) towards a superior state, more organized or more complex [45]. Development implies qualitative aspects that are not only phase transitions as the change from juvenile to adult state, but also the formation of new organs, the senescence of the organs [87] or the start of the establishment of fruits (fruit setting), or tuber filling, changes in appearance of the plant that can occur even if there is no weight increment [149]. Development is an irreversible process of change in the state of an organism, which generally progresses according to a pattern more or less fixed and specific for the species [149]. In [272] there is a very detailed numeric system which allows the description of the states of phenologic development through a uniform code in plant species; this system is known as the BBCH scale (Biologische Bundesanstalt, Bundessortenamt and Chemical).

To study growth and development of the crops, it is necessary to understand the physiological processes behind them, as far as the current knowledge allows it. The basic physiological processes in plants are: Photosynthesis, respiration, metabolic activities, nutrients and water uptake, nutrients and water transport, transpiration and the generation of reproductive structures. Many of these processes have their limits genetically determined, but microclimate, substrate, nutrition regime, and some specific enzymes play an important role [276].

Because of its importance, microclimate has been extensively studied in the modeling of growth and development of greenhouse crops. Microclimate includes main elements that affect the physiological processes of the plant: Solar radiation, CO_2 concentration and temperature. The considered radiation is the one that has the range utilized by plants which is the PAR. There are other limiting elements that play a role as relative humidity. Some authors give different weight to the elements mentioned before, for example, for Challa and coworkers [87], the most important climatic factors within the greenhouse are: CO_2 concentration, air temperature, and vapor pressure of water. Radiation can be considered as a surrounding condition due to the fact that it is imposed by the exterior climate.

2.2.1.1 Importance and Classification of Growth Models

Models as an abstraction of reality are a tool that humans have developed in many disciplines and also, with some delay, in the food production field. Is in the industry where models have had a huge development, specially compared with agriculture. At the beginning of the 1970s of the last century, the perception of the development of models in agriculture can be summarized as follows: "A chemical engineer would not design a chemical plant, nor its control processes, without first having a model of the chemical process to be done by such plant as the foundation for the design. However, the agricultural engineer, who is in charge of the design of environmental systems for the biggest chemical factory in the world (the transformation of the energy from the light and other chemical processes to food), does not have a proper model of the system with which he or she works" [101].

This situation has changed as it is explained below; however, agriculture is still a field where the time between the generation and the application of a new technology is greater than that in the services industry [338].

In agriculture, there are several families of models: Descriptive, teleonomic, process based and functional-structural. The descriptive models include the statistical regression and the empirical or black box ones. As has been treated in previous sections, they are direct descriptions of data and they indicate the relationship between variables of a system, but do not give any explanation about mechanisms for those relationships.

The models based on processes, also called explanatory or mechanistic, contain submodels with at least one hierarchical level of greater depth than the described response [243]. In a physiological model, every additional depth level increases the explanatory power of the model. The mechanistic modeling follows the reductionist traditional method, which has been successfully applied in the Physical Sciences, Molecular Biology and Biochemistry [451].

The empirical models are direct descriptions of observed data, which can be of great utility in certain circumstances [451]. In an empirical model, any proposed mathematical relationship is not restricted by physical laws such as the conservation of energy or the laws of thermodynamic or by biological information, or by any knowledge of the structure of the system [451].

Another approach to modeling are the teleonomic models, which are clearly formulated in terms of goals [451]. Even though this view has been questioned, some authors claim the importance of these models to model the processes in live organisms, and they indicate that processes oriented with an objective are intrinsic to life itself, and not to nonliving things [332]; therefore, these types of models can be useful as a link between empirical models and explanatory models [451], and they have been applied in many aspects, among them the distribution of dry matter between root and shoot [470] and to cellular level modeling [208].

Another approach are the functional-structural models, these models are oriented to merge geometrical models of plant visualization with process based models. In this approach, the goal is to control the whole plant development in its organogenesis and photosynthesis; the organs play the true roles as sources and sinks and have interaction between the architecture and the functioning during the plant development [344], this approach has emerged relatively recently and represents one of the key challenges for plant modeling [445].

Most of the explanatory models are based on photosynthesis. The main components of the models based on photosynthesis are: Development of leaf area, light interception, photosynthesis, and respiration [265].

Models in crops have several applications. It is possible to utilize them in help systems for decision-making in agricultural production, in scientific research, in the definition of politics for agricultural development, in agricultural teaching [137], and also in the climatic control of greenhouses [360, 430, 441].

2.2.1.2 Growth Models for Tomato in Greenhouses

In the tomato crop, the most important growth and development models are of the explanatory type, they are based on physiological processes; besides, these models have been validated in different degrees and varied conditions of the crop. Despite the improvement of this type of models, there is still a lot to be done, and the most important weaknesses of the explanatory models are: The simulation of the development of leaf area, the maintenance respiration, organ abortion, the content of dry matter and the quality of the product [185, 265]. In [185], it is pointed out that quality modeling in dry matter is a very important parameter. The models are described in the next paragraphs.

Tomgro is a physiological model of development and yield for the tomato crop, in which a series of differential equations represents the changes in number and weight of leaves, fruits, segments of stem, leaf area as well as initiation of new organs, their age, senescence, or those that are pruned. The model utilizes an approximation source–sink for the distribution of carbohydrates for the growth of different organs [211].

This model is schematic and it is also modular, which means that it can be easily adapted and its subprograms can be replaced by others and it can be combined with more understandable greenhouse models, and it can also be utilized in procedures of economical optimization [105]. This model was calibrated and validated with data acquired in controlled conditions for varieties of "indeterminate" growth type [106, 211].

Tomgro has been modified to include the simulation of the growth and development of individual organs, providing good simulations of number and weight of fruits per cluster [211]. This model has also interface adjustments that permit the establishment of initial parameters and conditions before the simulation [136]. In the most complete version, *Tomgro* can have 574 state variables and simulates with great detail the development of fruits due to the fact that every fruit has a specific position within the cluster, and in relation to the number of clusters [216]. With the aim of adapting *Tomgro* for the climatic control of greenhouses, the model has been reduced to five state variables, trying to preserve its main elements that allow it to be an explanatory model [212].

De Koning [227] developed a model to predict the distribution of dry matter in tomato, which can have 300 state variables. The number of organs is evaluated through the prediction of initiation, abortion and harvest of individual organs. The model calculates the sink strength of each organ through the potential growth. It is capable of predicting in a reasonable way the formation of clusters, time frame for the growth of the fruit and the distribution of dry matter, although the prediction of number of fruits per cluster does not give very acceptable results.

Tomsim is another model developed for tomato of the explanatory type with modular structure, which simulates growth and development [181–184]. The production of dry matter in this system is predicted by a general growth model for greenhouse crops, which has as a foundation the estimation of photosynthesis proposed by Gijzen [146]

that was validated by Heuvelink [184]. The functions of fruit development were adapted from the model developed by de Koning [227].

The *Tomsim* model of production of dry matter and its distribution to leaves, stems, and fruits was validated with different transplant dates and plant density, and the model was completed with data sets from commercial greenhouses, which is important to the fact that the tomato crop covers a complete season, whereas the experiments are evaluated only until 100 days after transplant. Besides, the model helps to perform analyses for the tomato crop and it can be a significant contribution as a decision support system in the crops management [182].

The *Tompousse* model is aimed to simulate the weekly production of greenhouse tomato taking into consideration the information available according to the production conditions. The key stages for the making of yield are the average transmission of radiation for the cover of the greenhouse, the interception of radiation by the canopy (dependant on LAI), the conversion of radiation to dry matter (in particular dependant on the amount of CO_2 and also on the distribution of a fraction of dry matter to the fruits). The model allows the user a good simulation of the production curves in changing climates as that in the French Brittany and in the Mediterranean region [135].

In [468], a simulation model for tomato crop was calibrated and validated using data from Spain and Netherlands in order to use this model in a model-based method to design greenhouses.

In what follows, the units of variables are not included in the paragraphs for the sake of space, but can be found in the acronyms section and in the tables included in the following sections.

2.2.1.3 The Simplified *Tomgro* Model

The simplified *Tomgro* model emerges as an option to eliminate the complexity of the complete *Tomgro* model [211] and to give the possibility of using the model in control systems on line preserving its physiologic characteristics [212]. The state variables in this model are: Number of nodes (X_N), leaf area index (X_{LAI}), total dry weight (X_W), dry matter of fruits (X_F), and dry mater of mature fruits (X_{MF}). For more details about the simplified *Tomgro* model refer to [212].

The number of nodes is the result of the speed of nodes formation and this is a function in sections of the variable temperature of the greenhouse microclimate, modulated by an empirical coefficient. The maximum speed in the nodes appearance is established under temperature conditions between 12 and 28 °C and it is considered that a temperature lower than 9 °C or greater than 50 °C stops the nodes appearance. This state variable is calculated in the same way in all *Tomgro* versions [212].

The LAI considers daily average temperature, empirical coefficients, and plant density. When all the leaves within the plant reach their maximum, they will be pruned or will enter the state of senescence which is also considered in the model.

The total dry matter is a function of the growth rate of the plant. This growth is a function of photosynthesis rate minus respiration multiplied by a conversion

coefficient from carbohydrates to dry matter and multiplied also by a function of distribution of dry matter to roots, which depends on the number of nodes. When the maximum LAI is reached, a coefficient of lost of dry matter is applied. Photosynthesis is calculated with the variables: Temperature, photosynthetically active radiation, carbon dioxide, and LAI. Respiration is a function of temperature and total dry matter.

Dry matter of fruits starts from the amount of nodes in which appears the first fruit. Parameters of allocation to fruits and transition from vegetative to reproductive growth are included. It is also included a function that calculates the effect of the daily average temperature on the distribution between vegetative and reproductive growth. Finally, it is considered a critical temperature for warm days, above such temperature the allocation to fruits decreases.

Regarding dry matter of mature fruits, the dynamic of mature fruits is based on the effect of temperature over fruit ripening through a linear function in sections that is activated at certain amount of nodes, that indicates the period from the appearance to the ripening of the first fruit. The assumption in the model is that mature fruits are harvested immediately.

With data from greenhouses located Southeast of Spain, a region with mild climate conditions with a minimum temperature of $12\,°C$, without addition of carbon dioxide and for a fall-winter season, a process of parameter adjustment was performed using the LS method with data sampled every minute.

The main equations of the *Tomgro* model [211, 212, 341] (some parameters that have to be calibrated with their units are explained in Table 2.12) are given by:

$$\frac{dX_N}{dt} = N_m f_N(X_{T,a}) \tag{2.83}$$

where $f_N(X_{T,a})$ is a piecewise linear function that depends on temperature [212]. The dynamic evolution of LAI is given by:

$$\frac{dX_{LAI}}{dt} = \begin{cases} \rho \delta_l f_{LAI}(\bar{X}_{Td,a}) \frac{\exp(\beta_l(X_N - N_b))}{1 + \exp(\beta_l(X_N - N_b))} \frac{dX_N}{dt} & \text{if } X_{LAI} < c_{LAI,max} \\ 0 & \text{if } X_{LAI} \geq c_{LAI,max} \end{cases} \tag{2.84}$$

where ρ is the plants density, and $c_{LAI,max}$ is defined as the LAI when the set of leaves of the plant reaches its maximum (it will be pruned or will inter into state of senescence) and unitless function $f_{LAI}(\bar{X}_{Td,a})$ depending on average daily temperature reduces the rate of leaf area expansion.

The total dry weight is described by:

$$\frac{dX_W}{dt} = GR_n - p_1 \rho \left(\frac{dX_N}{dt}\right) \tag{2.85}$$

where p_1 is a parameter describing loss of leaf dry weight per node after reaching $c_{LAI,max}$ and GR_n is a function modeling net aboveground growth rate, defined as

$$GR_n = c_E(V_{fot} - V_{res})(1 - f_R(X_N)) \tag{2.86}$$

Table 2.12 Estimated parameters for *Tomgro* reduced model

Parameter	Description	Value	Units	Variable
c_E	Coefficient of dry matter conversion	0.12	$(g_{dry\ weight}\ g_{CH_2O}^{-1})$	X_W
c_{extlw}	Light extinction coefficient	0.61	–	X_W
N_m	Maximum rate of nodes appearance	0.57	$(node\ d^{-1})$	X_N
N_b	Parameter in expolinear equation	7	$(node)$	X_{LAI}
T_{crit}	Mean daytime temperature above which fruit abortion starts	26	$(°C)$	X_F
V_{max}	Maximum increase in vegetative tissue per node	6	$(g_{dry\ weight}\ node^{-1})$	X_{LAI}
α_F	Maximum partitioning of new growth to fruit	95	$(fraction\ d^{-1})$	X_F
α_l	Light efficiency	0.09	$\left(\mu mol_{CO_2}\ \mu mol_{absorbed\ photon}^{-1}\right)$	X_W
β_l	Coefficient in expolinear equation	0.5	$(node^{-1})$	X_{LAI}
δ_l	Maximum leaf area expansion per node	0.062	$(m^2\ node_{leaf}^{-1})$	X_{LAI}
ν	Vegetative-fruit transition coefficient	0.38		X_F
τ_c	Carbon dioxide efficiency	0.12	$(g_{dry\ weight}\ node^{-1})$	X_W

where V_{fot} is photosynthesis, V_{res} is respiration, c_E is the growth efficiency, a parameter that expresses the conversion of carbohydrates to dry matter and $f_R(X_N)$ is the fraction of distributed growth to roots and it is considered as a function of the number of nodes.

Photosynthesis is given by the following equation:

$$V_{phot} = \frac{c_{cnv,phot}\, F_{max}\, f_{T,phot}(X_{T,a})}{c_{extlw}} \ln \left[\frac{(1-c_m)F_{max} + \alpha_e c_{extlw} V_{PAR}}{(1-c_m)F_{max} + \alpha_e c_{extlw} V_{PAR} \exp(-c_{extlw} X_{LAI})} \right]$$

$$(2.87)$$

where c_m is the light transmission coefficient through leaves, c_{extlw} is the light extinction coefficient, α_e is the light efficiency, $c_{cnv,phot}$ is a units conversion coefficient, $f_{T,phot}$ is a piecewise linear function that modifies photosynthesis to suboptimal temperatures throughout the day and F_{max} computes the effect of CO_2 as $F_{max} = \tau_{CO_2} V_{CO_2}$.

Respiration is described by:

$$V_{res} = \int_{t_i}^{t_e} Q_{10}^{(X_{T,a}-20)/10}\, r_m (X_W - X_{FM})\mathrm{d}t \qquad (2.88)$$

where Q_{10} is the sensitivity of respiration to temperature and r_m is a maintenance respiration coefficient, t_i is the initial time and t_f is the final time. Breathing is calculated updating in time the matter that has become ripe fruit, this means that once a fruit has reached maturity is immediately harvested.

The dry matter of fruits (X_F), is described by

$$\frac{dX_F}{dt} = GR_n\alpha_F f_F(\bar{X}_{\text{Td,a}})\,(1 - \exp(-\nu(X_N - N_{\text{FF}})))\,g(X_{\text{T,day}}) \quad \text{if}\, X_N > N_{\text{FF}} \quad (2.89)$$

where ν is the vegetative-fruit transition coefficient, α_F is the maximum partitioning of new growth to fruit, N_{FF} is the number of nodes per plant when first fruit appears, function $f_F(\bar{X}_{\text{Td,a}})$ computes the effect of average daily temperature on the distribution between vegetative and reproductive growth under low temperatures, while function $g(X_{\text{T,day}})$ modifies the distribution of fruits in very hot days [211, 212, 339], where $X_{\text{T,day}}$ is the average temperature of the daylight hours during the day.

The dry mater of mature fruits (X_{MF}) is given by:

$$\frac{dX_{\text{MF}}}{dt} = D_F(\bar{X}_{\text{Td,a}})(X_F - X_{\text{MF}}) \quad \text{if} \quad X_N > (N_{f1} + K_F) \qquad (2.90)$$

where K_F indicates the number of nodes since the first fruit appears until it matures, N_{f1} indicates the number of nodes when the first fruit appears and $D_F(\bar{X}_{\text{Td,a}})$ is a piecewise linear function of average daily temperature [211, 212, 339].

Figure 2.22 shows the behavior of the state variables for the *Tomgro* model when data from the spring season was used. Regarding the dynamic of the state variables, it can be observed an acceptable behavior of the model. In [339], the average absolute error is included, which has the following ranges of values: 0.5 and 1.9 for number of nodes, 0.11 and 0.24 $\text{m}_{\text{leaf}}^{-2}\,\text{m}_{\text{soil}}^{-2}$ for leaf area index (X_{LAI}), 23.9 and 44.4 g m^{-2} for total dry matter (X_W), 19.9 and 42.1 gm^{-2} for dry matter of the fruits (X_F), and 37.1 and 44.9 for dry matter of mature fruits (X_{MF}) when the *Tomgro* model was applied using data from the spring–summer and the fall-winter season, one of which was performed with data from a commercial operation.

2.2.1.4 The Tomsim Model

The *Tomsim* model [182–184] is oriented towards the knowledge of the tomato dynamic beginning at the flowering stage; it is considered no restriction of water and nutrients and an optimum control of pests and diseases. This is a model based on photosynthesis and it allows the user to know with great detail the clusters appearance, the growth of the vegetative segment between two consecutive clusters (called vegetative unit), and the growth of every cluster. Distribution of dry matter is regulated by the sink organs and it is independent from dry matter production [182, 183]. It is required to have data for the 24 h: Temperature, light intensity, and carbon dioxide concentration. Partition of photoassimilates among sink organs occurs every day according to the relative strength of the sink, calculated considering the sum of all the sinks [182–184]. This model utilizes previous work [146] for the simulation of photosynthesis and production of dry matter. The photosynthesis equation used
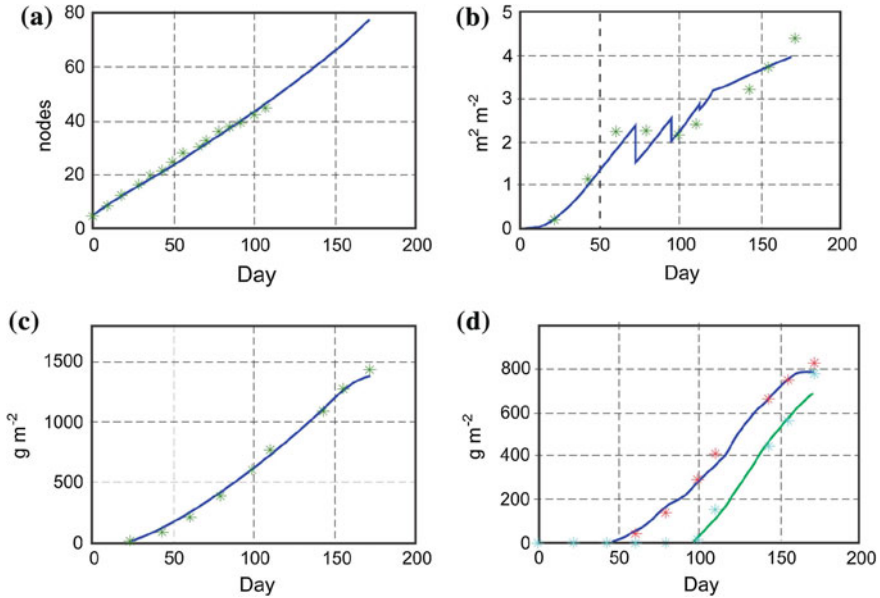
Fig. 2.22 *Tomgro*: Simulation (*solid line*) and observed data (*asterisks*) during a spring season. **a** Number of nodes. **b** LAI. **c** Total dry weight. **d** Dry weight of fruits and mature fruits. Day = day after planting

was validated in different experiments with different ranges of CO_2 concentration and PAR radiation [184].

Photosynthesis in this model is based on the *Sukam* model [146], which considers photosynthesis for leaves and extrapolates the results to the whole canopy. The model includes the calculation of absorption of photosynthetic radiation for the layers of the canopy, the diffused and the direct photosynthetically active radiation that reaches every layer of leaves, and it is calculated in function of temperature, carbon dioxide, and photosynthetically active radiation. The model takes into consideration dark respiration, which is function of temperature, and also maintenance respiration which considers the state of the different organs (leaves, stem, roots, and fruits).

Flowering estimation is described by state X_{NT} describing number of trusses. The function of clusters appearance per day in *Tomsim* has been developed with data from different experiments [184, 227] and it is an empirical function that considers temperature as an essential variable. Number of fruits is not modeled and it is an entry from the user.

Trusses are harvested after a growth period from anthesis to ripening of fruits. This growth period decreases with temperature, but the degree of this reduction is different according to the fruit development [184]. Every day the model estimates the stage of development of the fruit, which has values between 0 and 1. When the development stage of the fruit reaches the value of one, it is ripe and must be harvested.

The potential growth of every cluster is the maximum growth achieved under optimum conditions. This is modeled from different parameters obtained in an empirical way. The vegetative unit is formed by the stem section and three leaves between two clusters, although the number of leaves before the first cluster is between 9 and 12, and therefore the first vegetative unit is assumed to be 2.5 times bigger than the other [182, 184].

This model considers the detailed growth of the vegetative part of the crop, and it measures the growth using vegetative units. The potential growth of the vegetative units is a function of the daily average temperature and the potential growth of one fruit in the cluster of reference. A vegetative unit starts its growth approximately 3 weeks before the corresponding cluster.

The allocation of dry matter is regulated by the sinks or destination of assimilates, and these sinks are the clusters and the vegetative units. The available assimilates (g of CH_2O per plant) are distributed among the total number of sinks per plant according to the strength of every sink, which is the potential growth of clusters and vegetative units. The sink strength for roots is established in 15 % of the vegetative sink strength. The distribution within the vegetative part of the plant is 7:3:1.5 for leaves, stem, and roots, respectively [183]. If the amount of available photoassimilates is equal or greater than the sum of the sinks, every organ will grow to its potential and the unused photoassimilates will be sent to storage. The next day these reserves are added to the newly formed photoassimilates [182, 184].

LAI is simulated based on the estimated dry matter of the leaf area X_{LDW} and the specific leaf area (SLA). The model considers that leaves are eliminated when their corresponding cluster reaches a development stage of 0.9 [183]. Specific leaf area (SLA) expressed in $cm^{-2} g^{-1}$ is modeled by *Tomsim* with a function of day of the year.

Figure 2.23 shows the simulations and the observed data for a spring-summer season applying *Tomsim*. With the exception of the regression coefficient for the exponential equation that relates relative growth rate and maintenance respiration which value is 10, and the extinction coefficient for diffuse radiation which value is 0.712 [339], the values of the utilized parameters are in [182] and [184]. This model was applied with data from different spring-summer and fall-winter seasons, and the average errors in relation to the observed data were the following: 0.41–0.59 on number of trusses (X_{NT}), 21.6–52.3 gm^{-2} on total dry matter (X_W), 9.9–28.3 gm^{-2} on dry weight of fruits (X_F), 1.53–3.21 gm^{-2} on the first cluster, 2.07–4.75 gm^{-2} on the second cluster, 1.57–2.73 gm^{-2} on the third cluster, 2.61–6.24 gm^{-2} on the fourth cluster, and 1.68–6.46 gm^{-2} on the fifth cluster [339, 341]. Equations of the model and values of parameters are not included for the sake of space, but can be found in [182, 184, 339, 341].
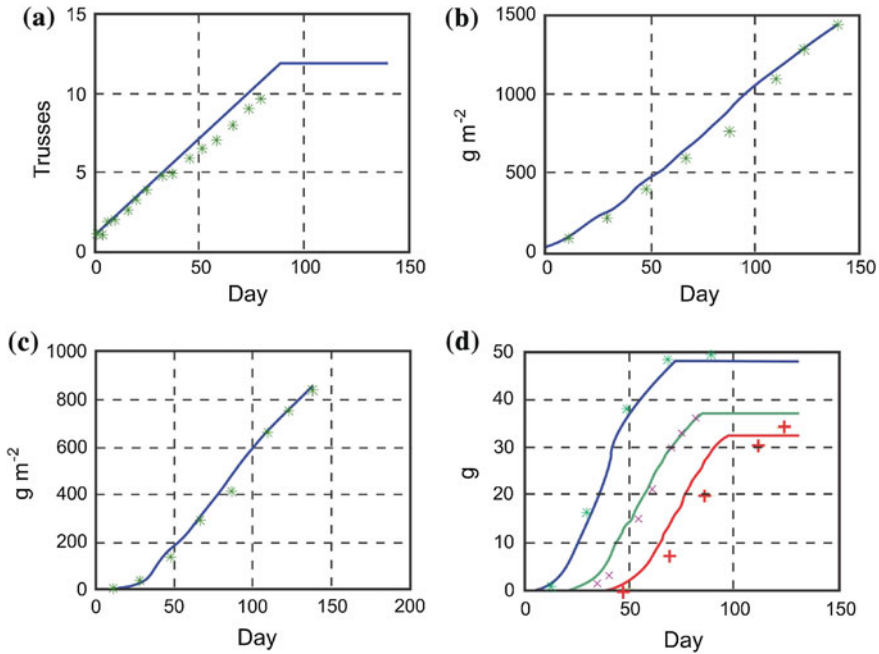
Fig. 2.23 *Tomsim*: Simulation (*solid line*) and observed data (*asterisks*) during a spring season crop. **a** Amount of clusters. **b** Total dry weight. **c** Dry weight of fruits. **d** Dry weight of clusters 1, 3 and 5

2.2.2 Effect of Salinity, Water Deficit and Vapor Pressure Deficit in Yield

2.2.2.1 Salinity

The growth models of crops are oriented to the evaluation of the production of dry matter; however, the product that growers take to the market is a fresh product, with water content between 93 and 95 % [186]. Simulation models allow the users to estimate fresh yield by knowing the relationship dry weight/fresh weight of fruits. According to some reports, the content of dry matter for tomato mature fruits is 5 % in fall and 5.6 % in spring for the southeast of Spain [33, 339].

It is known that salinity in the root media causes a yield reduction of the commercial fresh weight of fruit vegetables [92, 120, 250, 411, 413, 414, 418]. Table 2.13 indicates the magnitude of the decrease of yield for different salinity degrees, expressed as electrical conductivity (EC [mS cm^{-1}], represented by state variable X_{EC}) of the nutrient solution. In some conditions there was no effect, for example in [411] it is indicated that a beefsteak variety grown in the fall had a solution that lasted 90 days and had EC of 2.9. EC was then increased to 5.0 for one treatment and to 6.8 for another, and these values were applied from day 91 to day 130; as a result, there

Table 2.13 EC indicated by different authors and related to yield of tomato fruits

Crop	Length of the season (months)	Threshold value (mS cm^{-1})	Decrease of commercial yield (% per unit of X_{EC})	Min and max X_{EC} in experimental trial (mS cm^{-1})	Reference
Estafette	4 (autumn)	2.5	2.3	2.5–5.2	[413]
Turbo	8 (spring–summer)	2.9	7.2	2.5–5.2	
Abunda,	4 (autumn)	2.4	5.2	2.4–4.6	[411]
Calypso,	4 (spring)	2.6	7.0	2.6–3.5	
Angela					
Rambo,	5 (winter–spring)	2.7	9.8	2.7–13.0	[415]
Daniela,					
Moneymaker					
Daniela	5 (spring)	3.79	8.7	2.72–7.84	[261]
Chaser	5 (spring VPD=0.49)	2.0	5.1	2.2–9.3	[250]
	5 (spring VPD=0.30)	2.0	3.4	2.2–9.0	
nd	8 (autumn–winter –spring)	3.4	4.4	3.4–5.7	[418]
Gokce F1	4 (spring)	1.9	8.3	2.8–6.2	[120]
FA 361	6 (autumn)	1.9	9.1	2.3–5.8	
Counter	3 (spring)	3.0	5.7	1.0–11.0*	[92]
	3 (autumn)	3.0	1.5	1.0–11.0*	
Capello	6 (autumn)	2.5	3.7	2.5–5.5	[479]
L1	4 (spring)	1.8	9.5	1.9–9.1	[346]

Done with information from the cited sources

were no significant differences in yield when compared with 2.9 during the whole season treatment. By contrast, when the increase in EC was done at day 60 there was a decrease of 3.1 % for every mS cm^{-1} increased.

It has been also reported that under poor conditions of light and during early stages of growth, high salinity values did not affect yield in the long run [411]. The same was observed when high values of salinity and poor light conditions were applied in the reproductive stage. In some experiments where EC ranged from 2.0 to 5.6 dS m^{-1} there was no yield reduction in commercial fruits developed under 100 μmol m^{-2} s^{-1} of artificial light, a CO_2 concentration of 800 ± 200 ppm and temperatures between 17 and 21 °C [112].

When the concentration of nutrients in the nutrient solution is lower than crop requirements the yield decreases [411]. Figure 2.24 describes the relationship between EC in the rhizosphere and relative yield; if the EC is below a minimum or above a maximum there is a decrease in yield [411]. The maximum value above which yield decreases is estimated at 2.55 mS cm^{-1} and it is the average of the values in Table 2.13. The average reduction in yield is 6.1 % per mS cm^{-1}. Figure 2.24
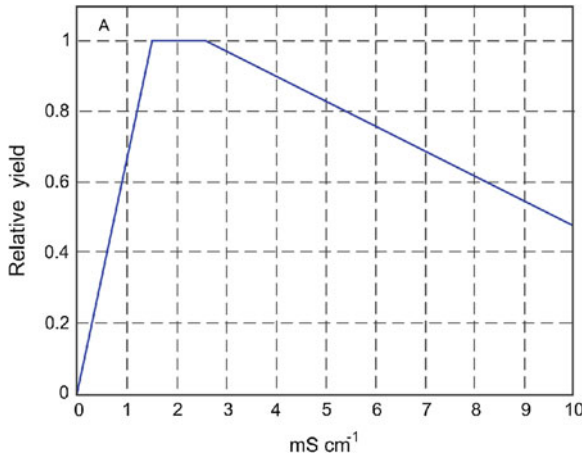
Fig. 2.24 Effect of salinity on tomato yield, relative yield respect to EC in the nutrient solution (mS cm^{-1})

indicates the relationship between relative yield and salinity or nutrients deficiency, which can be indicated as a function in sections.

From the information in Table 2.13, it is possible to formulate a function of yield or fresh weight of fruits which is valid when EC of the nutrient solution is above the threshold of yield:

$$X_{\mathrm{FF}} = \frac{X_{\mathrm{MF}}}{D_{\mathrm{mc}}}[1 - R_y(X_{\mathrm{EC}} - S_t)] \qquad (2.91)$$

where X_{FF} is fresh matter of fruits, X_{MF} is dry matter of mature fruits, D_{mc} is the content of dry matter in mature fruits, R_y is the reduction in yield per unit of EC of the nutrient solution X_{EC}, and S_t is the threshold of electric conductivity above which there is a yield decrease.

It should be noted that there is an effect in the decrease of yield when the ionic concentration in the nutrient solution expressed as X_{EC} is below the threshold. Also, it should be noted that yield decrease is greater when data from the experimental trials in Spain are considered, compared to average results dealing with salinity.

2.2.2.2 Water Deficit

The effect of poor supply of water on yield of crops has been extensively studied with the main goal of developing irrigation recommendations [109]. The equation of Stewart, which relates yield with water supply, was evaluated in different crops and is as follows:

$$1 - \frac{V_R}{V_{\text{Rmax}}} = c_{ky}\left(1 - \frac{V_{ET}}{V_{ET_{\text{max}}}}\right) \tag{2.92}$$

where V_R is yield obtained with limited irrigation, estimated in function of actual evapotranspiration (V_{ET}), V_{Rmax} is the yield obtained in non-limited irrigation conditions, equivalent to the maximum evapotranspiration ($V_{ET_{\text{max}}}$), and c_{ky} is a sensitivity to evapotranspiration deficit factor or a crop response factor [109]. The value of c_{ky} is determined at 0.68 [218] for greenhouse tomato grown in soil with insufficient irrigation. Reference [109] provides values of 1.0 and 1.1 for c_{ky}.

Applying a deficit irrigation, a linear equation for fresh fruit yield is developed for greenhouse tomato, in which yield is function of irrigation applied as function of evapotranspiration [37].

$$V_R = 0.99 V_{\text{Rmax}}\left(\frac{V_{ET}}{V_{ET_{\text{max}}}}\right) - 0.14 \tag{2.93}$$

Considering the references mentioned above, and assuming in the growth models the crop is well irrigated with maximum evapotranspiration, it is possible to develop simulation models to show the effect of less amount of water than the required.

2.2.2.3 Vapor Pressure Deficit

Vapor pressure deficit (VPD) also has effect on yield, which is important during the winter months in poor ventilated greenhouses or during the hottest months of the year. When studying the effect of high VPD, [44] compared 2.2 kPa and 1.6 kPa calculated during the six driest hours of the day and found a decrease of 16 % in tomato yield with high pressure deficit. At the other extreme, a yield decrease of approximately 30 % was reported when the treatments of 0.5 kPa (control) and 0.1 kPa (high humidity) were compared and estimation was done considering the average of the 24 h of the day [286]. A piecewise linear function was created with the mentioned data, as shown in Fig. 2.25.

2.3 Water Models in Artificial Substrates

2.3.1 Water Dynamics

Water is important for plants; it is a constituent of vegetable tissues, a solvent, a reagent, keeps cellular turgor [233, 276], and is an excellent medium for temperature regulation [276]. Between 80 and 90 % of fresh weight of plants is water. A decrease in water content is accompanied with a loss of turgor and wilting, cellular elongation halt, stomatal closure, reduction of the photosynthetic activity, and malfunctioning of
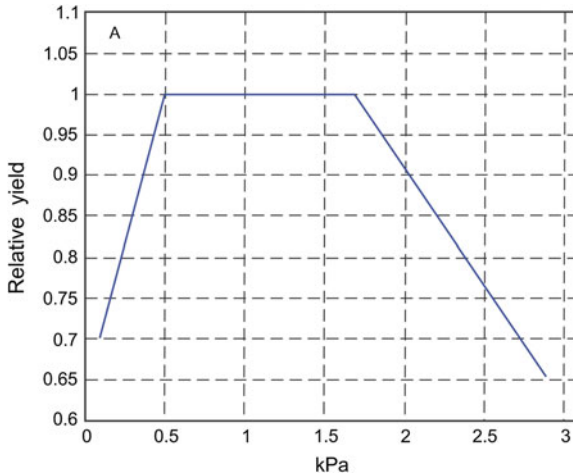
Fig. 2.25 Relative yield respect VPD [kPa]

many other basic metabolic processes [233, 434]. A nonadequate supply of water to maintain turgor results in immediate reduction of vegetative growth [233, 276, 434].

It is important to analyze the hydric balance in a crop because this analysis helps to understand the medium-plant-atmosphere continuum dynamics and makes it possible to efficiently manage water. This analysis can be done considering: Water in the substrate, water uptake, transport from root to leaves, and movement from leaves to the atmosphere. Since there is a close relationship between the processes mentioned above, this division is only for analysis purposes.

2.3.1.1 Dynamics of Water in the Substrate

Movement of water is studied and explained in function of the energetic state of water, describing the flux through a substrate [68] or the soil [233]. In this type of flux it is considered that inertia in the movement of water is small, and what is important is the potential energy [68].

It is possible to define a function for hydric potential that takes values in all the points of the substrate, in which the flux of water at every point goes from greater to smaller potentials and the direction is determined by the maximum variation of the potential [68], although [233] indicates that there are situations where this tendency is not followed. The speed of water is proportional to the gradient of such potential [68], and the proportionality constant is a specific characteristic for the substrate utilized. In other words, the same gradient of potential will generate a different flux in different substrates [68].

The potential energy per unit of mass (or volume) of water is the hydric potential, and at any point of the substrate it receives various contributions due to several factors as gravity field, influence of dissolved ions, and local pressure [68, 233].

Therefore, the hydric potential of the substrate ψ_{hs} is the sum of potentials that can be measured in an independent way [68] and can be expressed as

$$\psi_{hs} = \psi_{pr} + \psi_g + \psi_{os} \tag{2.94}$$

where ψ_{pr} is the potential of pressure, ψ_g is the gravitational potential and ψ_{os} is the osmotic potential. The potential of pressure is composed of the matric potential ψ_m, the pneumatic potential ψ_n and the enclosing potential ψ_e [68]. The gravitational potential can be expressed in terms of height differences between the considered and the reference point:

$$\psi_g = c_{\text{den,w}} c_g c_z \tag{2.95}$$

where $c_{\text{den,w}}$ is density of water, c_g is acceleration of gravity and c_z is the level in relation to the reference point. The osmotic potential is given by osmotic pressure of the substrate solution, and it can be determined with the equation of the state of the perfect gases:

$$\psi_{os} = -c_{\text{csol}} c_R T_s \tag{2.96}$$

where c_{csol} is the solutes concentration, c_R is the universal constant for gases, and T_s is the absolute temperature. The potential of pressure depends on the local content of water and for practical purposes the matric potential is considered as the only component of the potential of pressure [68]. The matric potential can be understood as the suction force applied by the plant to extract the water retained by the substrate [10, 223].

On the other hand, and from the point of view of substrate characterization, one important aspect is the capacity for water retention in function of its physic characteristics, porosity, structure, size, and distribution of size of particles [10, 68]. Substrates with particles between 1 and 10 mm have little variation in the amount of retained water, and the capacity of water retention increases when particles are smaller than 1 mm [10]. The maximum content of water of a substrate is known as container capacity and it is a function of the substrate characteristics and height of the container [10, 68].

Water retained by the substrate expressed as its humidity content follows a nonlinear relationship with the matric potential and shows a hysteresis phenomena; in other words, the humidity content is different if the substrate is getting dry than if is getting wet [68]. The knowledge of this relationship has been the object of many studies [68, 409] and is useful to formulate models of hydric balance.

2.3.2 Water Uptake by the Plant

2.3.2.1 Water Flow Towards the Root

The most important structures in the root system are epidermis and root hairs because they make direct contact with the soil and are the surfaces through which most water and minerals enter the root. A root generally has access to all the available water in a ratio of approximately 6 mm. When the soil (substrate) dries off due to the effect of the matric forces, the movement of water slows down [241].

Water uptake occurs because of potential gradients from the substrate to the roots; there are two uptake mechanisms, active and passive. The first mechanism, also called osmotic uptake, occurs in plants with slow transpiration where the roots behave as osmometers [233], and not as resistances, so in absence of transpiration the uptake of ions to the xylem produces a flow of osmotic nature and therefore it produces a pressure at the root level [426]. Passive uptake in plants happens when transpiration is high and water is suctioned toward the roots [233]. There is evidence that forces involved in the uptake of water to roots (passive process) are caused by a tension created by transpiration of the canopy, which expands to the root xylem [241, 426], although some authors recognize that the relationship between time of response and transpiration strategy of plants is not clear [121].

By definition, and for modeling purposes, the hydraulic properties of roots have two parameters: The minimum gradient of hydric potential to induce a flow, and the hydric conductivity [347]. The flow of the soil solution from soil to root and from root to canopy occurs through a complex structure with variable hydraulic resistances, some of which can be considered serially (in different tissues of the root cylinder) or in parallel (different cellular ways for water) [427].

2.3.2.2 Water Potential in Root and Leaves

In a similar way as the hydric potential in the substrate, in vegetable cells there is a hydric potential determined by the potential of pressure, the osmotic pressure due to solutes and the matric potential, although the matric potential is very small [451]. Measurement of hydric potential in roots is difficult and the commonly used methods are not completely appropriate because they utilize cut roots and the conditions are different from the conditions in roots of intact plants [491]. Different studies of hydric potential in roots indicate that this is influenced by climatic factors and by the plant itself. Hydric potential in roots, specifically the osmotic potential of sap in roots, decreases with flood treatments and the cause is osmolality [204]. This additional osmotic force explains a greater speed of the flow of the sap through the tomato roots of flooded plants, compared with well-drained plants in similar experimental conditions of pressure applied [204].

When severe hydric deficit was applied it was observed a decrease in the hydric potential in leaves, reaching values of -2.5 MPa, although this hydric poten-

tial was partially reestablished when the deficit stopped ($-1.8\,\text{MPa}$) in Populus seedlings [398]; in tomato the hydric potential was -1.65 and $-0.40\,\text{MPa}$ for the maximum hydric stress and when irrigation was restored, respectively [456].

Salinity induces a decrease of hydric potential within the plant (usually measured in the leaves) [78, 266, 364, 375], and the response is different according to the species and the salinity degree.

The minimum gradient of hydric potential for a flow to happen within the roots is in the range of 0.08 and 0.49 MPa. These values were determined in intact plants; the gradient is associated to the presence of exodermis in the root, and it is not correlated to the cortex thickness or with the root diameter [374].

2.3.2.3 Hydraulic Conductivity in the Roots

Hydraulic conductivity is a property of roots and expresses the relationship between water flow and the hydric potential gradient [347]. Hydraulic conductance or resistance in roots has a different magnitude if it is a radial flow through the root cylinder or an axial flow along the xylem, and the axial conductance is smaller [427]. The behavior of conductance or resistance depends on the age of the root and can be different according to the external conditions (salinity or water deficit) or internal factors (nutrition or water needs of the plant) [426].

According to some authors hydraulic resistance in the plant is independent of the flow of water for transpiration, and there is a linear relationship between transpiration and gradients of hydric potential of the nutrient solution in relation to stem, and also of the stem in relation to the leaves [248].

Hydraulic conductivity increases as transpiration speed increases [210, 427], whereas such conductivity decreases when plants are flooded at the beginning of the morning when daylight starts, and this could be originated by the decrease of O_2 in the root zone [108].

2.3.3 Transpiration

Transpiration has been described in Sect. 2.1.1.6, Eqs. (2.42)–(2.47), following the approaches based in the Penman-Monteith equation [241, 301, 419, 451]. Transpiration causes a decrease in the leaf cells hydric potential, and it originates water demand toward the evaporation surfaces. This flow continues as long as there are gradients, which are established step-by-step through the soil–plant system, and they define the flow speed of the water to the leaf [233, 491].

The elements to simulate the movement of water dynamics from the soil or the substrate to the atmosphere, passing by the plant, are: Hydric potentials, resistance of the substrate to water movement, resistance of the roots, resistance of the transfer elements, resistance for the water to leave toward the atmosphere and the architecture of the root system.

2.3.4 Integrated Water Model

In this section a generic model that considers water balance from an integral point
of view is presented as a submodel to make connection with an explanatory growth
model for the crop and the ecosystem. It is dynamic, explanatory and simple. It
considers the amount of water in the substrate, the root and the shoot (leaves, stems
and fruits). The model of water balance is combined to a growth model in which the
dry matter is divided into structural biomass and nonstructural biomass (storage),
whereas the soil or substrate has only one layer. The state variables are mass of
water in the substrate, mass of water in root, and mass of water in shoot; it has
30 parameters, 6 of which can be changed [452] to adjust the model to different
conditions.

The main dynamics of the state variables, that are mass of water in the shoot (X_{wc})
and root (X_{wr}), are defined by the next equations.

$$\frac{dX_{wc}}{dt} = F_{w_{r-c}} - V_{ET} \tag{2.97}$$

$$\frac{dX_{wr}}{dt} = F_{w_{s-r}} - F_{w_{r-c}} \tag{2.98}$$

where $F_{w_{r-c}}$ is the water flow from root to shoot, V_{ET} is the flow from shoot to
atmosphere, and $F_{w_{s-r}}$ from substrate or soil to root.

When the relative water content in the substrate (θ_r) is greater or equal to field
capacity or container capacity (θ_{mx}) the water flow is an excess flow or drainage
($F_{w_{dr}}$) and therefore the mass of water in the soil (X_{wss}) does not change; in other
cases it happens that:

$$\frac{dX_{wss}}{dt} = F_{w_s} \tag{2.99}$$

where F_{w_s} is the water flow in the soil or substrate. Flows of water are determined
according to:

$$F_{w_s} = F_r - F_{w_{s-r}} \tag{2.100}$$

$$F_{w_{s-r}} = \frac{\psi_{hs} - \psi_{hr}}{r_{wsr}} \tag{2.101}$$

$$F_{w_{r-c}} = g_{wrc} \left(\psi_{hr} - \psi_{hc} \right) \tag{2.102}$$

$$F_{w_{dr}} = F_{w_s} \tag{2.103}$$

where F_r is the irrigation supplied, ψ_{hs}, ψ_{hr} and ψ_{hc} are water potentials of soil,
root and canopy, respectively; r_{wsr} is the resistance to the flow from soil to root, and
g_{wrc} is conductivity of the flow from root to shoot.

The model is oriented toward the application in intensive crops which have low volume of substrate and the height of the container is less than 15 cm. Under these conditions the hydric potential of the substrate considers Eq. (2.94), in which the gravity potential is negligible because of low height of container. It is also considered that the matric potential (ψ_m) is the most important component of the pressure potential, therefore the hydric potential of the substrate can be estimated with the following equation:

$$\psi_{hs} = (\psi_{os} + \psi_m) \tag{2.104}$$

Taking into consideration the relationship between the matric potential and the characteristic curve for water retention, the expression proposed by van Genutchen [141] is used:

$$S_e = \frac{1}{(1 + |c_{w1}\psi_m|^{c_{w2}})^{c_{w3}}} \tag{2.105}$$

where S_e is the effective water content of the substrate or effective saturation, c_{w1}, c_{w2} and c_{w3} are parameters of shape from the water retention curve. Hydraulic conductivity of the substrate is calculated according to equation [285]:

$$K_{rSe} = S_e^{0.5}\left(1 - \left(1 - S_e^{\frac{1}{c_{w3}}}\right)^{c_{w3}}\right)^2 \tag{2.106}$$

where K_{rSe} is the relative hydraulic conductivity, $K_{rSe} = K_{Se}/K_s$, where K_s is the hydraulic conductivity at saturation.

The potentials in root (ψ_{hr}) and canopy (ψ_{hc}) are defined by the osmotic potential (ψ_{osr} and ψ_{osc}) and the pressure potential (ψ_{prr}, ψ_{prc}) in each, according to the following equations:

$$\psi_{hr} = \psi_{osr} + \psi_{prr} \tag{2.107}$$

$$\psi_{hc} = \psi_{osc} + \psi_{prc} \tag{2.108}$$

$$\psi_{osr} = -\frac{c_R(X_{T,a} + 273.15)f_{neor}M_{ner}}{\mu_S X_{wr}} \tag{2.109}$$

$$\psi_{prr} = \frac{c_\varepsilon\left(\frac{c_{prr}X_{wr}}{M_{er}} - 1\right)}{c_{den,w}} \tag{2.110}$$

where c_R is the universal constant of gases, M_{ner} is the nonstructural root dry matter, M_{er} is the structural root dry matter, X_{wr} is the mass of water in roots, $X_{T,a}$ is the air temperature, f_{neor} is the osmotically active storage fraction of the root, μ_S is the molal mass of storage, c_{prr} is a parameter that affects the pressure component of the hydric potential within the root, c_ε is the parameter of rigidity of the cell wall and

$c_{den,w}$ is water density. In a similar fashion are defined the osmotic potential and the pressure potential for the canopy.

The resistance to the passage of water from the soil to the root (r_{wsr}) and hydraulic conductivity (g_{wrc}) from the root to the canopy, are defined as

$$r_{wsr} = \frac{c_{sor} V_{den,r}}{K_{so} M_{er}} + \frac{c_{rsr}}{V_{den,r}} \left(\frac{M_{er} + c_{kwrs}}{M_{er}} \right) \tag{2.111}$$

$$g_{wrc} = c_{nw} \frac{X_{wr} X_{wc}}{X_{wr} + X_{wc}} \tag{2.112}$$

where c_{sor}, c_{rsr}, c_{nw}, and c_{kwrs} are parameters affecting the resistance between soil and root, K_{so} is the soil hydraulic conductivity and $V_{den,r}$ is the density of roots.

It is known that root hydraulic resistance is variable, and that with high transpiration amounts such resistance lowers leading to a quick uptake of water [365, 427]. A coefficient is included (c_{khr}) [-] in which the resistance to water flux from soil to root is modified (r_{wsrm}) as an effect of transpiration through an exponential function:

$$r_{wsrm} = r_{wsr} (\exp(-c_{khr} V_{ET})) \tag{2.113}$$

With the aim of adapting the model, some parameters can be considered as just one. The parameters are the nonstructural osmotically active fraction of dry matter for root and canopy (f_{neor}, f_{neoc}) and the molal storage mass (μ_S). The relationship between these parameters is indicated by the following expressions: $c_{far} = f_{neor}/\mu_S$ and $c_{fac} = f_{neoc}/\mu_S$.

The model was adapted to the *Tomgro* model mentioned before, which has been adjusted to estimate structural and nonstructural dry matter utilizing the results of [331] for the tomato crop.

Figure 2.26 shows the dynamic of the water potential in the substrate, root and canopy during 4 days with data of the integrated water model. In the middle of the day the plants have the most negative water potential, therefore it is the period when the crop is more susceptible to stress in the case of having insufficient supply of water in the substrate. By contrast, the less negative water potentials are at dawn, in this moment the water in the system substrate-root-canopy can be in equilibrium.

Figure 2.27 shows the behavior for the water content in the substrate, the dynamic of the simulated and measured data can be seen in this graph.

2.4 Disturbance Forecast

Automatic weather forecasts are important to devise control strategies for greenhouses, being necessary to perform long-term (days) and short-term (min) predictions which help the user to obtain optimal trajectories for the controlled variables
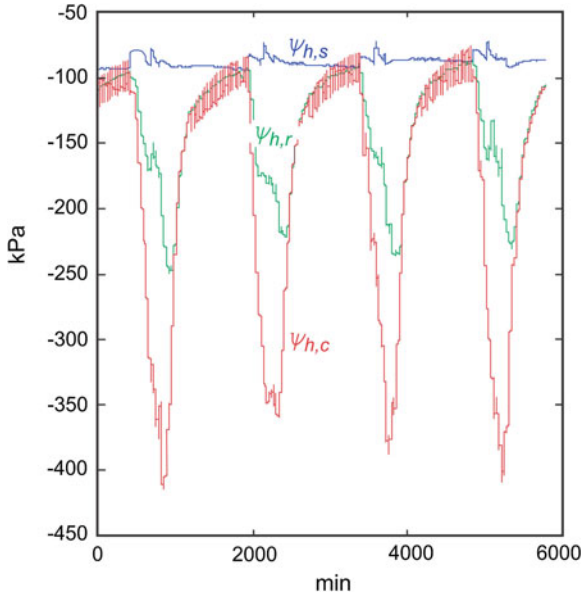
Fig. 2.26 Water potentials in: Substrate (ψ_{hs}), root (ψ_{hr}) and canopy (ψ_{hc})
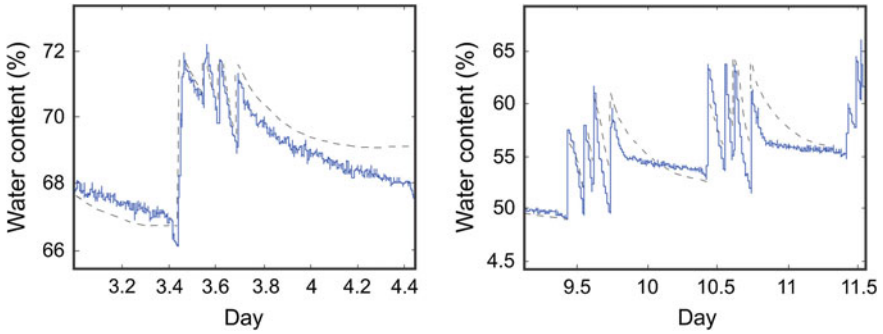

Fig. 2.27 Water content simulated (*continuous*) or measured (*dashed*) in the rock wool substrate

taking the desired objectives into account [71, 343]. There are several methods to perform weather forecasts, and can be classified as a function of:

1. Prediction horizon: Long-term [270] or short-term [345] predictions.
2. Used methodology: There exist in literature different methodologies which can be used to estimate disturbances [307, 345, 484]. In this section, three different methods are summarized: (i) Pattern search models, (ii) Time-series models and, (iii) Artificial Neural Networks (ANN).

2.4.1 Pattern Search Based on the Information Provided by the AEMET

The AEMET which depends on the Agriculture, Food and Environment Spanish Ministry is the reference organism regarding weather forecasts in Spain. These forecasts are obtained through the execution of a limited area numeric prediction model (HIRLAM) based on the environmental conditions provided by the model of the European Centre of Weather Forecasting Medium Range (ECWFM). Therefore, the weather forecasts daily updated (from 05:45—UTC) are published in the Web of the AEMET (http://www.aemet.es/es/portada) and they offer a prediction horizon equal to 7 days for each city of Spain, and equal to 4 days for each province and autonomous community. In Fig. 2.28 a snapshot of the information provided by AEMET by city is shown. More specifically, this information mainly comprises sky state (sunny, cloudy, rainy, etc.), the probability of precipitation, maximum and

Fig. 2.28 Weather forecast by city. *Source* http://www.aemet.es/es/portada

minimum expected temperature, thermal sensation and relative humidity, wind velocity and direction, and the maximum ultraviolet index.

Moreover, as environmental variables usually repeat each year certain behavior patterns, it is possible to use historic data series as weather forecast. In [303] a predictor module, whose main architecture can be observed in Fig. 2.29a, which provides accurate short/long-term weather forecasts of these outdoor variables which affect the indoor climate of a closed environment is shown. More specifically, the predictor module is able to integrate the information provided by AEMET with data series obtained since 1994, and look for the best pattern equivalent to the forecasts performed by AEMET. For this, the predictor module follows the general algorithm which is shown in Fig. 2.29b. Therefore, it is able to interpret the predictions provided by AEMET, and perform a pattern search within the historic database with the main objective of obtaining a set of patterns with characteristics similar to the predictions of AEMET. Then, each one of the patterns are analyzed as a function of several constraints, as the length of the prediction horizon and the maximum error allowed, and finally, the best pattern is selected from that ones which fulfill the established constraints. If any of the patterns satisfies these constraints, they are relaxed, and the pattern search process starts again.

In order to test the performance of the proposed methodology, to obtain short- and long-term predictions of two important environmental variables, outdoor irradiance and temperature, have been used. On the one hand, for short-term predictions a prediction horizon equal to one day is fixed and, on the other hand, for long-term predictions the prediction horizon is between 60 and 90 days. As can be observed in Figs. 2.30 and 2.31, this methodology provides acceptable results for both long-term and short-term predictions.

2.4.2 Time-Series Models

In general, weather disturbances are represented as time-series structures since they present stochastic behavior. Therefore, a prediction of weather disturbances can be obtained through time-series models. Such models are based on the assumption that the modeled data is autocorrelated and characterized by trends and seasonal variations [323]. Hence, the main objectives derived from time-series methods are: modeling, prediction, and characterization. More specifically, prediction by means of time-series methods require, first, to identify the pattern observed in the data, and second, to propagate it in time with obtained trends and integrate with other data. To do that, in [323] four different well-known time-series methods are analyzed and compared: Discrete Kalman Filter (DKF) [377], discrete Kalman Filter with Data Fusion (DKFDF) [300], Exponentially Weighted Moving Average (EWMA) [464], and Double Exponential Smoothing (DES) [297]. More specifically, they are used to estimate short-term forecasts of solar radiation from real data of a meteorological station placed in the Almería type greenhouse. Nevertheless, the proposed methods and methodology can be easily extrapolated to any location with an appropriate
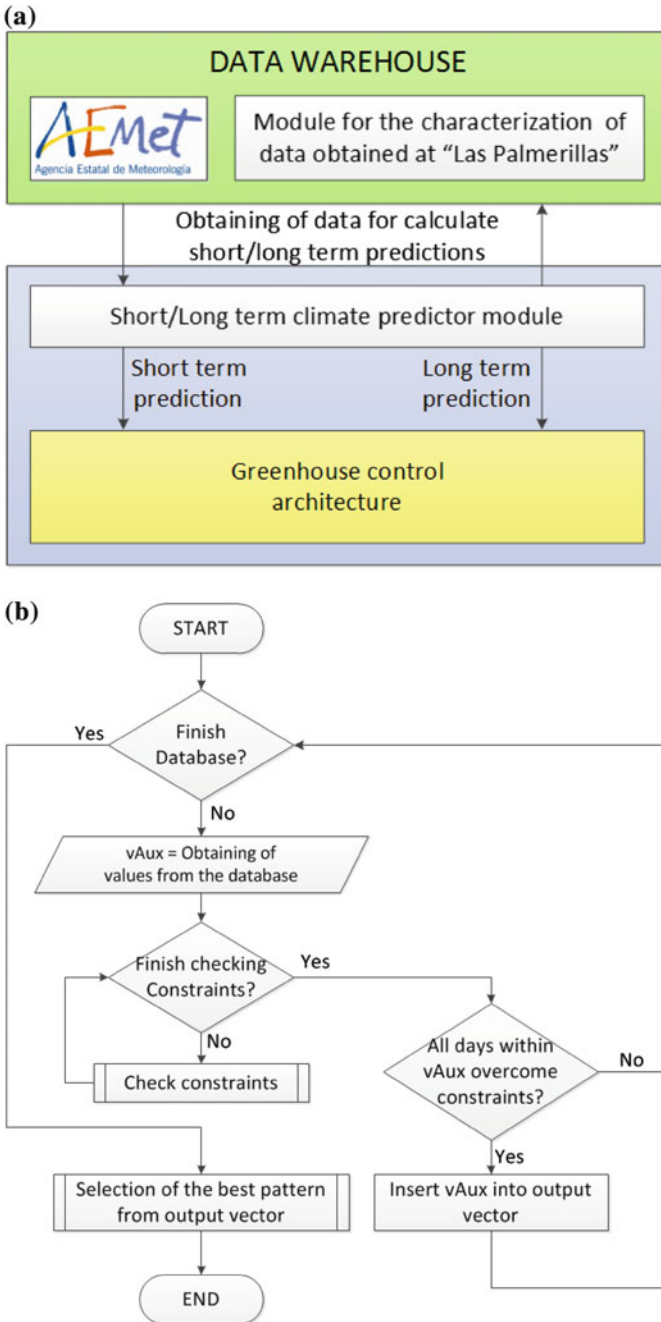
Fig. 2.29 Pattern Search based on the Information provided by the AEMET [303]. **a** Main scheme. **b** General algorithm for the short/long-term climate predictor module
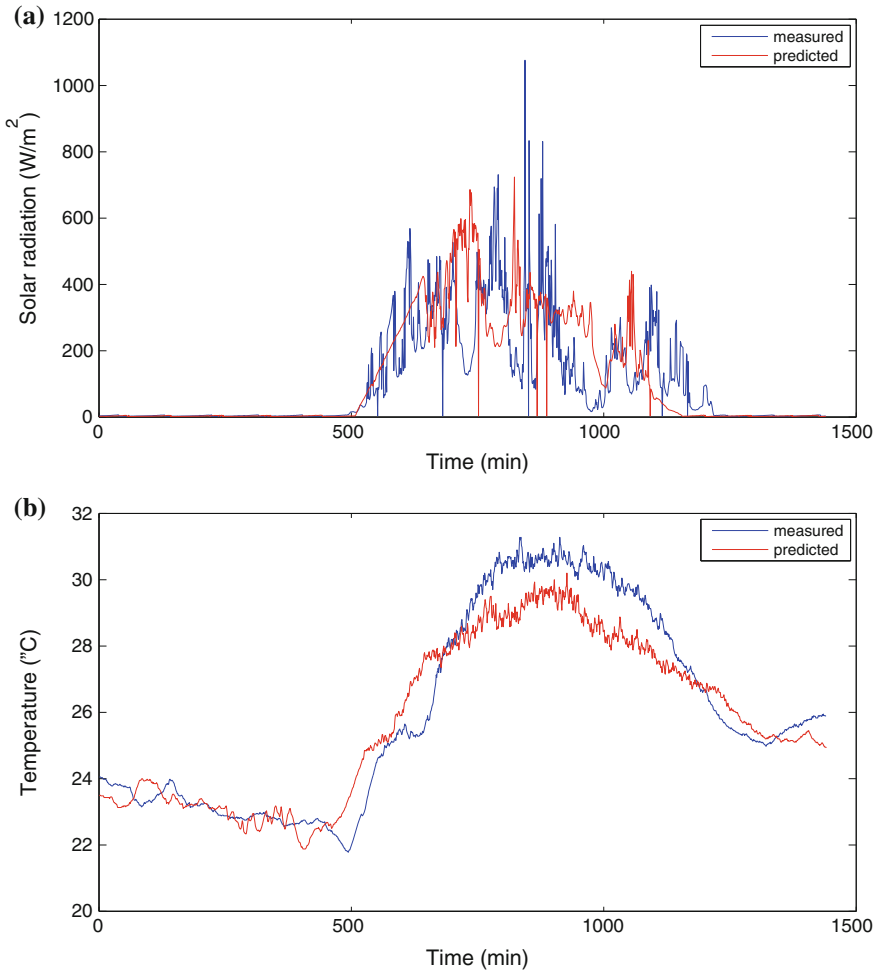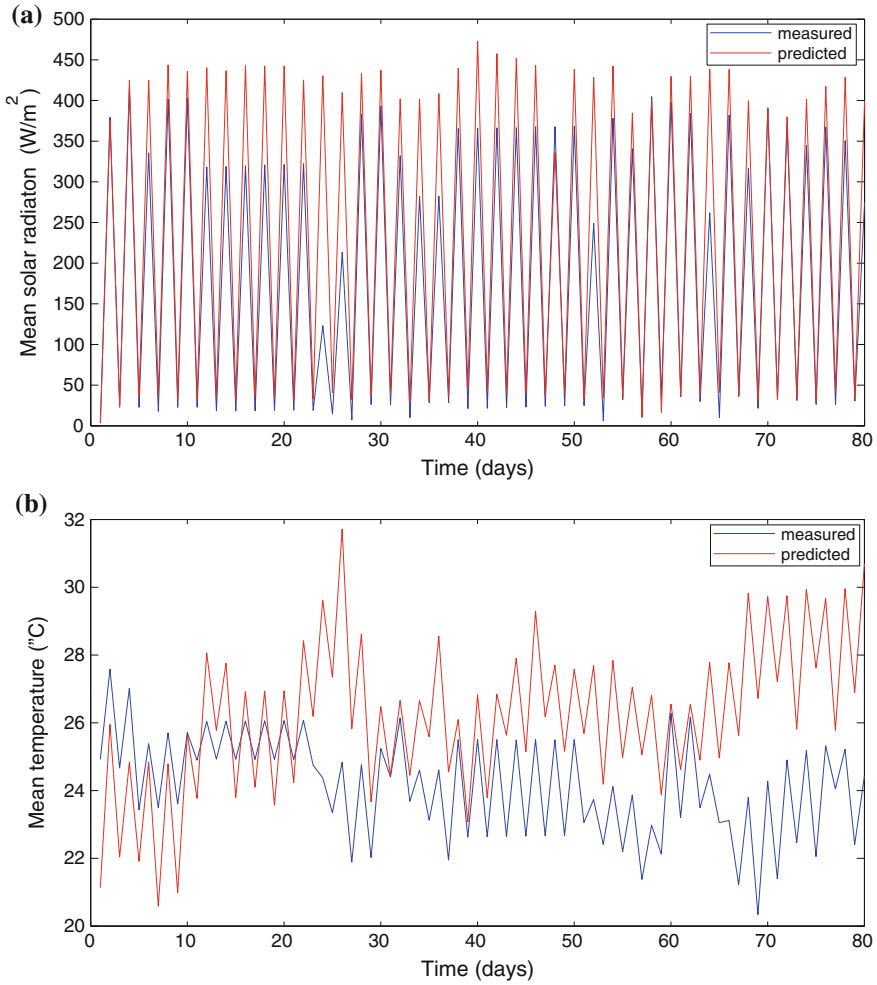
Fig. 2.30 Short-term prediction. *Source* As courtesy of the authors [303]. **a** Short-term prediction of outdoor irradiance. **b** Short-term prediction of outdoor temperature

meteorologic station. A complete description of each of these methods can be found in [323].

To validate the application of the previous forecast methods, one year of meteorological data collected with a sample time, $t_s = 1$ [min] have been used. Figure 2.32 shows the results obtained for each of the time-series methods mentioned previously and for the prediction of solar radiation under different conditions, a clear day and a day with passing clouds. In addition, a short-term horizon equal to 15 samples, that is, 15 min has been used. The obtained results [323] are good since a precise approximation is obtained with all the analyzed methods.

Fig. 2.31 Long-term prediction. *Source* As a courtesy of the authors [303]. **a** Long-term prediction of outdoor irradiance. **b** Long-term prediction of outdoor temperature

2.4.3 Artificial Neural Networks

Finally, ANN can be also used to obtain disturbance models since, as mentioned previously within the climate ANN approximation, their design is based on training and it is not necessary to perform any statistical assumption for the training dataset. As example of the application of this method to estimate disturbance models, two different approximations to obtain solar radiation and outdoor air temperature short-term predictions have been developed. For this, the methodology commented in Sect. 2.1.3.5 of this chapter has been used. More specifically, in this case, two
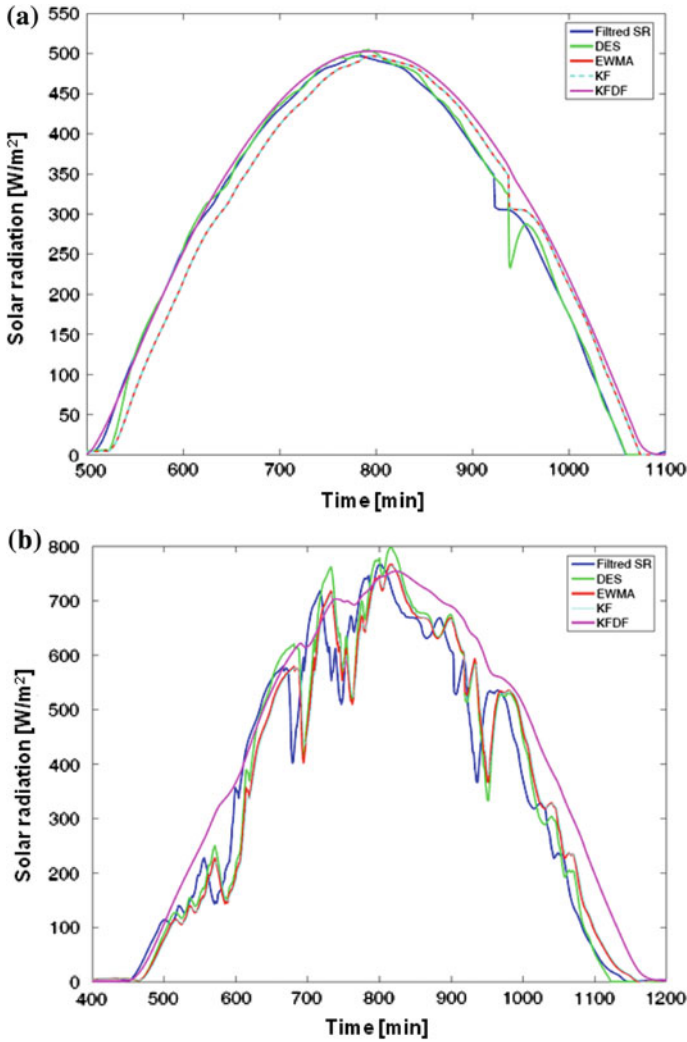
Fig. 2.32 Example of the solar radiation time-series model model under different conditions. *Source* Courtesy of the authors of [323]. **a** Clear day with a 15-sample horizon (15 min). **b** Day with passing clouds and a 15-sample horizon

different NARX ANN have been calculated. The structure of the selected ANN is similar for both, and consists of a NARX configuration with 1 node in the input, a hidden layer with 10 nodes, and a node in the output layer, the solar radiation or the outdoor air temperature prediction. In addition, TDL blocks to take into account past values of the inputs have been included in the ANN architecture. More specifically, a number of past values equal to 4 for each one of the inputs have been used. Besides, different approximation by varying the prediction horizons have been
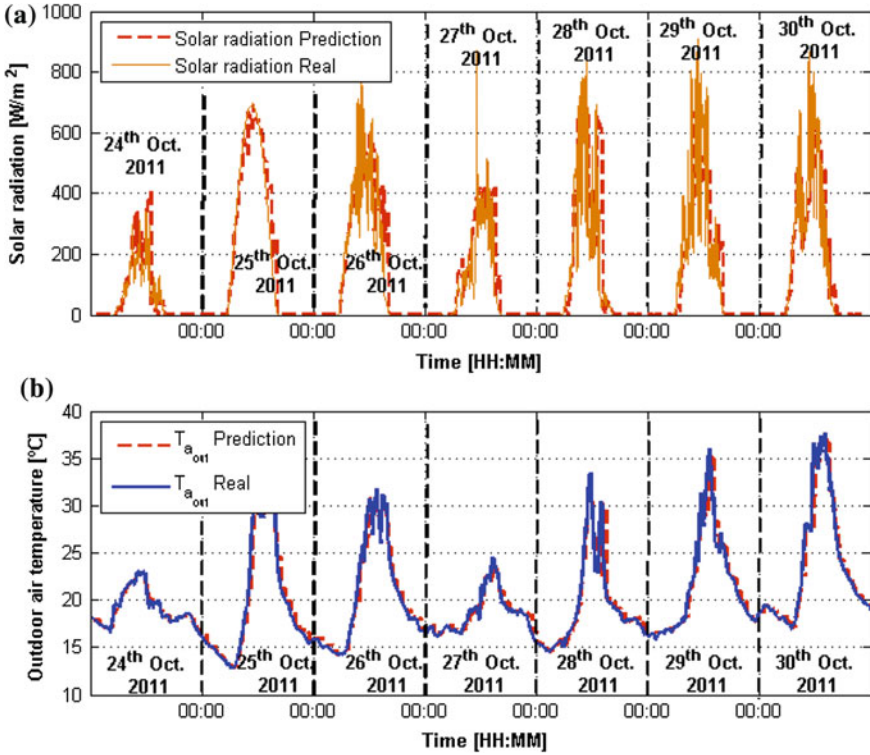
Fig. 2.33 Example of solar radiation and outdoor air temperature ANN short-term prediction models. **a** Solar radiation with a prediction horizon equal to 60 min. **b** Outdoor air temperature with a prediction horizon equal to 60 min

used, $N = [5, 10, 15, 60]$ (min). The training process has been performed using a variable-step gradient descent process, namely the Matlab's implementation of the Levenberg-Marquardt algorithm [282]. Furthermore, as training dataset different fragments within the period from 1st September 2010 to 29th February 2012 and a sample time of $t_s = 60$ (s) has been used. Finally, the different models were validated using a real dataset from the meteorologic station. More specifically, the selected dataset has a total duration of a week, from 24 to 30th October 2011, and a sample time of $t_s = 60$ (s). The results obtained for the solar radiation and outdoor air temperature with a prediction horizon equal to 60 min can be observed in Fig. 2.33a, b respectively.

2.5 Conclusions

A complex nonlinear dynamical model of the greenhouse climate has been developed for the particular conditions of the Southeast of Spain, where the largest concentration of greenhouses in the world is located [355]. These greenhouses are characterized by low-cost structures of medium yield, normally passive or with a low-level of automation and made of plastic cover, taking advantage of favorable outside climatic conditions. In Sect. 2.1.1.2, a description of the dynamic model of the industrial greenhouse climate is formulated. It is composed of six submodels describing the cover temperature, soil surface temperature, first soil layer temperature, inside air temperature and humidity, and PAR radiation onto the canopy. The model implementation is described in detail. It was hierarchically implemented using top-down and bottom-up approaches to provide insight into how the model is organized and how its parts interact. Two different modeling paradigms, block-oriented modeling and object-oriented modeling, were used. The methodology proposed to estimate the unknown parameters of the model is explained based on the fact that the involved physical processes are not coupled. A combination of sequential iterative search and genetic algorithms techniques is used to search the values of the parameters of the model obtaining acceptable results. A sensitivity analysis of the model with respect to the parameters is also included. The model validation process is also explained with different greenhouse structures in winter, spring, and summer seasons, comparing real data measured in greenhouses with data estimated by the model.

The same approach is used for semiphysical models development, aimed at finding simplified models that retain the main nonlinear characteristics of the system but can be used for control purposes. The chapter also includes different structures data-driven models, from linear (based on reaction curve tests or identification), Volterra, and ANN ones.

The second part of the chapter is devoted to develop models for tomato growth for climate conditions of the Southeast of Spain. The tomato crop growth models *Tomsim* and *Tomgro* were calibrated and validated for total dry matter production and calibrated for fruit dry mater production. The parameter estimation was carried out in such a way that the models can be used to simulate the main dynamics of tomato crop growth with differences less than 10 % in total dry matter estimation in both models. The dynamics of tomato crop growth are represented by both models in an acceptable way.

Moreover, water management models are described for soilless systems to supply the adequate quantities without yield reduction but with saving of lixiviates emitted to the environment.

Prediction models for disturbances are also introduced. They play an important role in the hierarchical control architecture where climate setpoints are generated based on the models described in this paper and on predictions of weather and market forecasts.

Chapter 3
Climate and Irrigation Control

3.1 Basic Automatic Control Algorithms for Climate and Irrigation

3.1.1 Introduction

This chapter deals with climate and irrigation control strategies aimed at maintaining ideal conditions for crop growth inside greenhouses. The controlled variables are usually PAR radiation, temperature, relative humidity and CO_2 concentration. The usual actuators are natural ventilation, shading screen, heating, CO_2 injection and fogging. Fertigation control systems are also required to provide the required quantity of different fertilizers, taking into account the pH and electrical conductivity of the drain and reference nutritive solutions. The disturbances affecting the system are outside ones like temperature, relative humidity, solar irradiance, wind speed and direction, sky temperature and rain. Also crop transpiration can be considered as a disturbance, as well as a set of variables describing other elements of the greenhouse like cover and soil temperature. Although the algorithms presented in this book are of general nature, the results focus on Mediterranean greenhouses in which the control problem is mainly refrigeration and irrigation. Anyway, some control strategies for heating are also included. For a more extensive analysis of the heating problem, the book of van Straten et al. [431] is strongly recommended. For tropical climates, recent surveys have been published [391], while the general case is treated in Duarte-Galvan et al. [115].

A greenhouse is a closed environment where some climate variables can be manipulated to control the development and growth of the crop. The Horticulture Science proposes reference values of the climate and fertigation variables, which can be also obtained through the optimization of a given objective function involving costs, incomes, and other aspects, as will be shown in Chap. 4. So, control engineering practice allows the engineers designing and implementing automatic control systems to

help tracking these reference values in spite of disturbances acting on the system, thus obtaining the optimal performance of the crop [357, 358].

Greenhouse environmental control involves four fields of study [215]:

- *Physics*. Knowledge of climatic factors: Light/radiation, temperature, air humidity, CO_2, air circulation, and the relationships among these factors.
- *Physiology*. Knowledge of the influence the greenhouse environment has on plant growth. The basic processes for growth are photosynthesis and transpiration and both can be optimized to adequate environmental control.
- *Technology*. Availability of environment control equipment, such as heating, ventilation, screens, lighting, misting, CO_2 enrichment, and so on, as well as sensors of the outside and inside environmental variables.
- *Control technology*. As the way to optimize inside greenhouse climate based on measured variables and acting on greenhouse equipment.

The main objective of greenhouses crop production is to increment the economic benefits of the farmer by means of finding a trade-off between the improvement of the quality of the horticultural products and the cost of obtaining adequate climatic conditions using new greenhouse structures and automatic control strategies. As a basic requirement, climate control helps to avoid extreme conditions (high temperature or humidity levels), which can cause damage to the crop and to achieve adequate temperature integrals that can accelerate the crop development and its quality while reducing pollution and energy consumption [1, 69, 194, 226, 349].

As has been mentioned previously, the dynamic behavior of the microclimate is a combination of physical processes involving energy transfer (radiation and heat) and mass balance (water vapor fluxes and CO_2 concentration). These processes depend on the outside environmental conditions, structure of the greenhouse, type and state of the crop, and on the effect of the control actuators [57]. The main ways of controlling the greenhouse climate are by using ventilation and heating in order to modify inside temperature and humidity conditions, shading and artificial light to change internal radiation, CO_2 injection to influence photosynthesis, and fogging/misting for humidity enrichment. Fertigation control systems are also required to provide the required quantity of different fertilizers, taking into account the pH and electrical conductivity of the drain and reference nutritive solutions [41].

The main variables affecting plant growth in Mediterranean greenhouses have been shown in Fig. 2.5 of Chap. 2. Variations to such list can be considered by including as state variables CO_2 concentration and light intensity at plant level, fogging/misting systems [2] and CO_2 enrichment as control variables (although these systems have not an extensive use) and outside CO_2 concentration and leaf area of the plants (evapotranspiration rate inside the greenhouse) as disturbances.

Disturbance variables have a dominant role and coherent action onto the formation of the greenhouse environment. As has been pointed out in [408], solar radiation has a strong immediate effect on the internal conditions and produces frequent oscillations (i.e., under passing clouds) in the controlled variables. In practice, a time running average filter can be used when the measurements of this variable are used for control purposes. Outside temperature and humidity suffer slow variations and

their measurements can be directly used for disturbance attenuation. Wind velocity includes a steady component, corresponding to the mean wind speed, and a transient component, corresponding to the gusting of the wind about the mean value. Mean wind velocity affects the air exchanges of the greenhouse or else the heat balance and can be also used for control purposes. Two crop properties that can influence the inside environment are its albedo and canopy resistance [381]. In well-irrigated crops, both properties are likely to be well correlated with the LAI, which can be included as a measurable disturbance, as in this case, the growth and development of the plants are considered to be measured/estimated.

This chapter briefly describes the elements of the greenhouse climate control systems and different algorithms to control greenhouse climate. The main actuators considered are natural ventilation, heating, and shading screen. A review of cooling and heating technologies can be found in Sethi and Sharma [386] and [387, 388], respectively. An overview of control algorithms for shading screen can be found in [32] and references therein. The chapter is mainly devoted to explain the control of greenhouse climate conditions, that is the bottom level (fast time scale-seconds/minutes) of the hierarchical control system explained in Chap. 1, Fig. 1.2. Traditionally, this regulatory layer implements classical [215] or feedback-feedforward control (FF), sometimes involving adaptive control (AC) algorithms and online estimation of simple model parameters. The problem of optimal control of greenhouse crop growth has been treated in an excellent way in the book by van Straten et al. [431]. Other recent approaches include Model Predictive Control (MPC), Nonlinear Control (NC), Robust Control (RC), Event-Based Control (EBC) or Fuzzy Logic Control (FLC). Some of these approaches are explained in this chapter. Tables 3.1 and 3.2 overview different approaches used within climate control framework.

3.1.2 Climate Control

The climate control problem has the main following features (some of them treated in Chap. 2):

- The system (greenhouse climate) is subject to strong disturbances, both measurable and nonmeasurable (including errors and noise in the sensors). The characteristics of disturbances impose fundamental limits to the system.
- There is a high correlation degree between several variables, like temperature and humidity, and the same actuators are used to control them.
- It is a time-varying system in which the characteristic parameters associated to the actuators (generally of convective nature) are affected by disturbances, so that the same state of actuators may produce different effects.
- There exist constraints in inputs of amplitude, slew rate, and quantization type. The saturation limits sometimes are time dependent (for instance, in tube-based heating systems). There are also constraints in the states and outputs (operative and security ones) of the system. The greenhouse temperature must evolve between a minimum and a maximum value to promote growth and avoid stress or damage to plants. In

Table 3.1 Different approaches in greenhouse climate control (I)

Controlled variable	Control variable	Control technique	References
Temperature	Natural vents Heating	Proportional control PI + antiwindup	[49, 103, 461, 462, 478]
Temperature	Heating	PI (cascaded)	[104]
Temperature, humidity, CO_2	Natural vents, spraying, CO_2 enrichment	PID control (multiobjective)	[192]
Temperature	Heating	PIP control	[482, 483]
Temperature, humidity	Vents, heating, humidifiers, shading	PDF control	[6, 389, 390]
Temperature	Heating	Feedforward control	[361, 439, 440]
Temperature, humidity, PAR radiation, CO_2	Natural vents, heating, shading, CO_2 enrichment	Gain scheduling on/off	[41, 215]
Temperature	Natural vents	Adaptive control (multirate)	[13, 43, 362, 407]
Temperature	Vents, heating	GPC control	[49, 342, 354]
Temperature	Heating	GPC control	[296]
Temperature, humidity, CO_2	Heating, vents spraying, CO_2 enrichment	Nonlinear adaptive PID control based on RBFN	[485]
Temperature, humidity,	Natural vents, humidifiers	Multivariable MPC	[384]
Temperature, CO_2	Vents, heating, shading, CO_2 enrichment	Multivariable MPC	[50]
Temperature	Heating	Decentralized MPC	[119]
Temperature	Heating, refrigeration	Dynamic Matrix Control DMC	[480]
Temperature	Heating	MPC, feedback linearization	[327]
Temperature	Vents, heating	MPC (genetic and particle swarm optimization)	[94, 95]
Temperature, humidity	Heating, fogging, natural vents	Nonlinear MPC	[48, 153, 154, 492]
Temperature	Heating, CO_2 enrichment	Nonlinear neural network MPC (expert systems)	[471]
Temperature CO_2	Natural vents, heating, CO_2 enrichment	Receding horizon MPC Optimal control (Pontryagin), feedforward	[132, 177, 428, 430, 432, 441, 442, 443]
Temperature CO_2	Heating, natural vents	Optimal control, feedforward neural network control	[7]
CO_2	Vents, CO_2 enrichment	Optimal control	[255]
Temperature	Heating	Optimal control (Pontryagin)	[447]
Temperature	Heating, natural vents	Optimal control (linear programming, Pontryagin)	[159, 200]

Table 3.2 Different approaches in greenhouse climate control (II)

Controlled variable	Control variable	Control technique	References
Temperature, CO_2	Natural vents, CO_2 enrichment	Optimal control (Pontryagin), feedforward	[202]
Temperature, humidity, CO_2	Heating, vents fogging	Backstepping, optimal control	[34]
Temperature, humidity	Heating, vents, fogging	Feedback-feedforward linearization, extended Kalman Filter	[169, 395]
Temperature, humidity	Vents, fogging	Feedback-feedforward linearization, decoupling and feedforward	[42, 158]
Temperature, humidity	Natural vents, heating	Exact linearization	[158]
Temperature CO_2	Natural vents, heating, CO_2 enrichment	Robust QFT control	[253, 284]
Temperature	Heating	H_∞ PI control	[406]
Temperature, humidity	Heating, roofing, shading, moistening	H_2 robust control	[38]
Temperature	Vents	Neural network control	[20]
Temperature, humidity, CO_2	Heating, shutter, sprayer, shading, natural vents	Neural network control	[130, 260, 371, 481]
Humidity	Humidifiers	Neural network control	[399, 402, 403, 404]
Temperature, humidity	Natural vents, heating shading, misting	Hybrid control	[165, 259, 280, 336, 337, 362]
Temperature	Heating	Hybrid predictive control	[242, 280]
Temperature	Natural vents, heating	Event-based control	[127, 313, 314, 316, 317, 318, 319, 320, 321, 322]
Temperature, humidity	Heating, natural vents, shading, fogging	Model-free control	[240]
Temperature, humidity	Heating, humidifiers	Fuzzy logic control	[203]
Temperature, humidity	Natural vents, heating, humidifiers	Fuzzy logic control	[238]
Temperature	Vents, heating	Fuzzy logic control	[139]
Temperature, humidity, CO_2, illuminance	Natural vents, heating, CO_2 enrichment, shading, artificial lighting, fogging	Fuzzy logic control	[76, 77, 79, 89, 122, 123, 139, 148, 168, 195, 205, 209, 225, 238, 247, 258, 274, 288, 290, 291, 292, 298, 334, 372, 396, 417, 457, 490]

some cases [401], constraints on temperature integrals can be also imposed [228]. Furthermore, humidity has lower and upper bounds on the achievable values, to avoid reaching saturation water vapor and condensation on the cover or in the plants, as this may cause the appearance of fungal diseases such as *Mildium* or *Botrytis* [29, 207]. Moreover, high relative humidity is not desirable, since it reduces transpiration and correct pollination. Low relative humidity leads to closing stomata and thus reducing photosynthesis. In Mediterranean areas, it is also usual to control the photoperiod of the crop including a time-varying constraint on the maximum solar irradiance. As mentioned above, the constraints values are time-varying, since the crop evolves in different phases (sowing, transplant, fruit set, and harvesting) requiring different climatic conditions. In addition, in certain situations, such as potential disease problems, certain weather conditions are needed to minimize their adverse effects. Moreover, there are different types of crop cycles (long, autumn short, and spring short), which obviously have different climatic disturbances that result in diverse bounds.

- Greenhouse climate is a complex process that cannot be completely described by linear models (used for control purposes), as there are unmodeled dynamics and parameter estimation errors which cannot be handled by using linear time-invariant models. In order to properly control the system, information on possible sources of uncertainty (parametric or structural) is required, assessing their effect on the behavior of the whole system.
- Most control approaches consider perfect mixing (homogeneous thermodynamical properties of air), but there always exist spatial gradients. As a few amount of sensors are usually placed inside greenhouses, it is considered that the greenhouse climate is represented by these local measurements, not considering the distributed nature of the system. Moreover, most actuators do not allow the user to perform a distributed control of this kind of installations.

The following sections will focus on the temperature (and humidity) control problem, as PAR radiation is usually managed by on/off controllers. Some ideas on irrigation control are also included.

Temperature is the climate variable that directly influences on crop growth, and that is traditionally controlled inside greenhouses. The plants grow only under the influence of light, that is, when photosynthesize, thus requiring a relatively high temperature. During the night crop is not active (there is not growth), so it is not necessary to keep it at a high temperature. It is, therefore, desirable to have a higher temperature during the day than at night, so that different temperature set points are defined for these periods. In those areas with favorable weather conditions (like Mediterranean ones), during daytime periods, the energy required to reach the optimum temperature is provided by the sun. The contribution of additional energy is not necessary except in extreme situations.

The problem of controlling the daytime temperature is to avoid the temperature is above this optimum, since its effect is detrimental to the crop. Natural ventilation is used for this purpose. If the temperature is less than the set point, the vents are closed and the heating should be used to achieve the desired reference value, but

this option is usually rejected because the associated cost does not compensate the obtained benefit (although, as will be commented on in Chap. 4, this is not always true and many growers are nowadays changing their idea about the use of the heating systems). During the night periods, as it is not necessary to maintain a high growth temperature, lower set points are determined but keeping adequate conditions for the plants. While the temperature remains above the set point value, the heating system does not operate. If the temperature surpasses the lower limit, the heating system must be switched on.

The daytime temperature set point is the one from which it starts to open the vent. There exists a temperature interval in which no control action is required (the actuators do not work), as the daytime set point must be greater than the night one. The size of this dead zone varies with the greenhouse performance, common values being from 0.5 to 6 °C [215]. The objective of this zone is to avoid frequent switching between ventilation and heating. Moreover, abrupt or sudden changes in temperature are not desirable because they can lead to condensation of water vapor in the air onto leaves and fruits or the cover, producing water falling onto the plants that may lead to some kind of cryptogamic diseases [207].

Figure 3.1 shows an example of control of greenhouse air temperature for 2 days, in which the main features of set point changes are commented on.
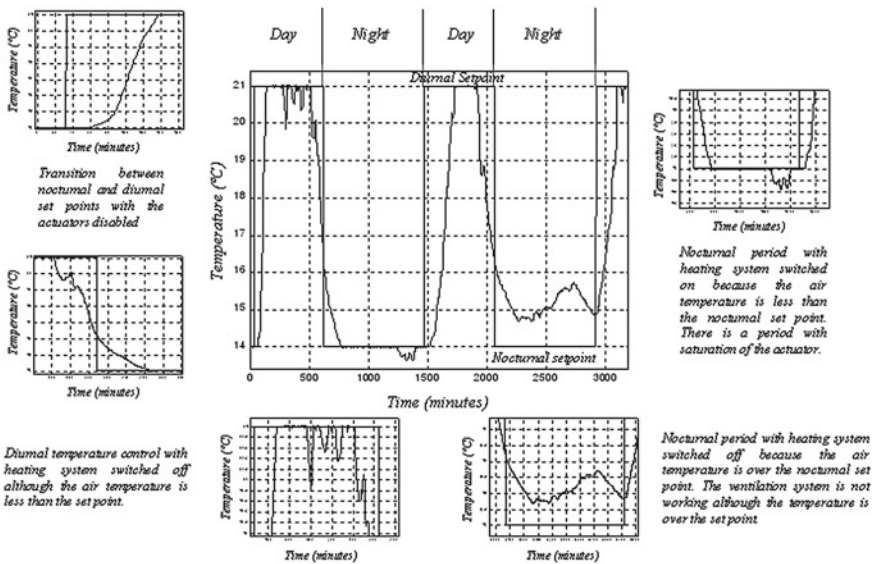
Fig. 3.1 Example of temperature control where the main characteristics of set point changes are commented on

3.1.2.1 Temperature Control Using Natural Ventilation

Natural ventilation provides air exchange between the inside and outside of the greenhouse. As the outside air is generally cooler than the indoor air, it tends to fill the lower layers of the air volume and hot air rises to the upper layers coming out through the open vents. In this way, the inside air temperature is diminished. The controller should calculate the vents opening required to reach the desired set point. The daytime temperature control problem using natural ventilation has the following features:

- The actuation system has two main structural limits:
  - Saturation: The vent may be opened between 0 and 100 % (or corresponding angular aperture).
  - Output resolution: Although it is a continuous actuation system, the window positioning is performed using a rack whose teeth permit minimal movement of 5 % (approximately depending on the facilities).

- The temperature response of indoor air to ventilation steps typically behaves like a FOPDT system, where the describing parameters (time constant, static gain, and dead-time) vary depending on the amplitude of the input step and also when changing from one operating point to another. This is logical as the system is nonlinear (smooth).
- Outside conditions significantly influence on the effect of ventilation on the temperature. When opening the vents, hot air inside the greenhouse is replaced by colder outside air. The air removal speed mainly depends on the size of the vents (greenhouse design constant) and on the difference between indoor and outdoor temperature and wind speed, so that the controller should have to take into account the outdoor weather conditions to compute the ventilation opening. The representative static gain, time constant, and dead-time values vary with wind speed and outside temperature.

Considering all these features, different techniques can be used to address this control problem, some of which are developed in this chapter.

3.1.2.2 Temperature Control Using Heating

Temperature control in greenhouses is a practical problem of considerable interest and economic significance since the primary objective of greenhouses is to produce agricultural products outside the cultivation season, representing the fuel-based heating costs and 30 % of the overall operational costs in the greenhouse industry. Generally, greenhouses are heated by hot water that circulates in pipes or by hot air that is distributed by ducts. In [24], six types of heating systems were presented and discussed: (1) heat exchangers in the soil, (2) heat exchangers laid directly on the ground, (3) aerial pipes near the ground or benches, (4) fan heater units, (5) roof heating systems, and (6) a combination of two of these. In Sethi et al. [387, 388], a review and evaluation of all the available heating technologies for worldwide agricul-

tural greenhouses is discussed. The influence of the heating method on greenhouse climate and energy consumption if treated in Bartzanas et al. [31].

Regulating air temperature in the greenhouse is important for both vegetative growth and fruiting. To determine heating requirements, it is essential to know the minimum temperature requirements for the crop, the lowest outdoor temperature that might be expected, and the surface area of the greenhouse. Heat lost will be also affected by wind and site exposure. Due to the favorable weather conditions in the Mediterranean areas, the required energy to provide adequate temperature integrals to the crop during daylight is provided by the sun. Moreover, during the day the problem is to avoid large values of the temperature and thus natural and forced ventilation are used. During the night, the temperature set points are lower and while the temperature remains over these the heating is not used. The most widely used heating systems in Mediterranean greenhouses are based on hot air, distributed in the greenhouse via perforated polyethylene ducts [449] or hot-water PVC pipe systems in new greenhouses:

- *Heating by aerial pipes.* The pipes heated by hot water circulating through them transmit heat to the air by convection, producing an increase in the greenhouse inside temperature. Then, the control problem consists in calculating the required temperature of the water within the pipes to meet inside air set point requirements. In order to perform this task, the system has one three-way valve to mix the water of the boiler (constant temperature) with the water returning from the greenhouse in a cascade structure (Fig. 3.2), where the temperature measurement is acquired near the boiler. The actuators have constraints as the water temperature through
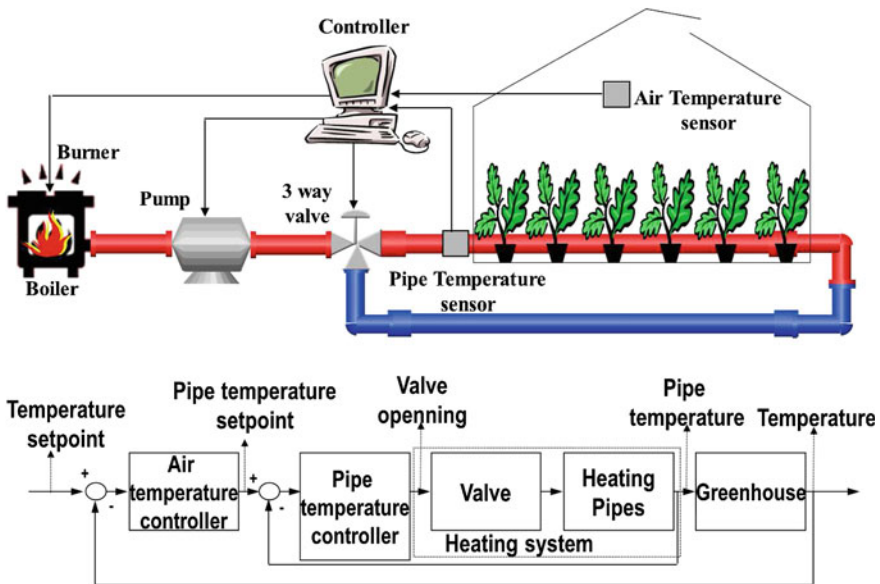

Fig. 3.2 Schematic diagram of the aerial pipes heating system and control blocks
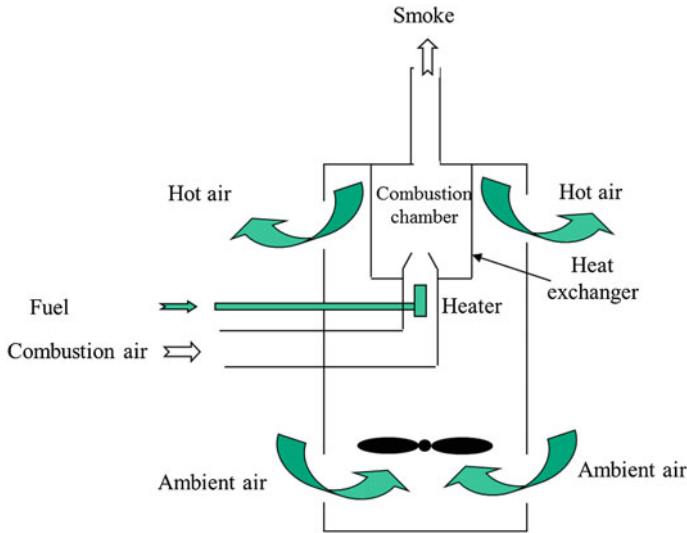
Fig. 3.3 Schematic diagram of the air heating system

the pipes is lower than the water temperature in the boiler and higher than that of
the greenhouse air.

- *Heating by forced-air heaters.* In this kind of systems, the equipment is composed
  by an indirect combustion hot air generator using a heat exchanger to separate
  exhaust gases from hot air that is introduced in the greenhouse (Fig. 3.3). The
  system incorporates three units: A combustion chamber supplied with fuel oil, the
  heat exchanger, and a fan to extract the exhaust gases throughout a chimney. The
  efficiency is between 80 and 90 %.

  The main features of the heating control system are:

- All actuators have limited resolution and saturation limits, that may vary with time
  depending on the inside temperature.
- The dynamical response to stepwise changes in the actuator can be modeled as
  a FOPDT system, which descriptive parameters vary with input signal amplitude
  and operating point.
- Outside disturbances (mainly outside temperature and wind speed) influence the
  heating temperature set points.

These features must be taken into account by the control strategies used to control
greenhouse temperature and humidity.

There are several examples in the literature of the application of various tem-
perature control techniques using heating systems (see Tables 3.1 and 3.2). For
instance, [461, 462] evaluated several PI control structures, comparing them with
AC strategies, which showed a good behavior in stationary state but with greatly
excessive oscillations. The authors of [104] used a PI control in cascade, which gave
better results. Concentrating on greenhouses in a Mediterranean climate, in [200]

different techniques in Israel are developed using linear programming, and the Pontryagin Principle, to minimize the heating costs. In Spain, [355] and [342] carried out the integration of a heating system within a hierarchical control scheme by making use of different control techniques, such as cascade control (CC) and GPC. They obtained acceptable results with a 15 % saving in fuel.

3.1.2.3 Humidity Control

The content of water vapor in the air inside the greenhouse, measured for example by the relative humidity, is not one of the climatic variables that directly affect crop growth, although its control is of particular interest. As described in Chap. 2, the emergence and development of fungal diseases is favored with high relative humidities, thus decreasing transpiration, reducing the absorption of water and nutrients, which can result in deficit of elements such as calcium. However, with low relative humidities, the transpiration rate increases which can lead to water stress, the closure of the stomata, and therefore reducing photosynthesis [81]. Based on these facts, it is necessary to maintain the relative humidity within a certain range, which for tomato crop can be set between 60 and 80 %. Controlling the relative humidity of air inside the greenhouse has two major drawbacks:

- Air temperature and relative humidity are highly inversely correlated.
- Both temperature and humidity share the same actuation systems.

As the main variable is air temperature, as it affects crop growth, it is considered as the controlled variable, so that climate controllers should try to keep humidity within a desired range, modifying temperature-based control action accordingly. The general actions that are usually performed when the relative humidity has a value outside the defined range are:

- *Low relative humidity*. This problem is usually associated with excessive temperature and the solution is to provide water to the greenhouse through nebulizers, humidifiers, or cooling pads, but installing such systems is not widespread in the area.
- *High relative humidity*. Generally, this situation occurs in closed greenhouses under cold weather or first/last night hours. The solution should be to combine the action of heating and ventilation, so that greenhouse warm and humid air is replaced with cold outside air that raises the temperature and reduces relative humidity.

It is interesting to analyze the effect of ventilation and heating on relative humidity to better understand the control algorithms used for controlling it. Absolute humidity is defined as the ratio of the mass of water vapor with respect to the mass of dry air that contains (kg_{water}/kg_{air}). Greenhouse air can hold a maximum amount of water vapor depending on the temperature (air is saturated). Relative humidity provides a measure between the amount of water vapor contained in the air and that obtained when saturated at the same temperature.

When heating is activated, the greenhouse vents are usually closed, so that no water vapor exchange with the outside exists and if transpiration is not considered, relative humidity should remain constant. An increase in air temperature causes a reduction in relative humidity. This reduction in moisture will be partially compensated by an increase in crop transpiration.

When using ventilation, the mixing of indoor and outdoor air produces two effects. On one hand, the inside temperature decreases as the outside temperature is lower, and on the other hand, the absolute humidity is also reduced, since, generally, the amount of water vapor inside the greenhouse is higher than that contained by the outside air. These two facts cause a decrease in relative humidity.

The daytime control of inside air temperature is performed using natural ventilation. Two situations may arise:

- High internal temperature and too low relative humidity. If vents are opened, temperature will reach the set point, but humidity will also decrease as outside humidity is lower. If vents keep closed, no water vapor is removed, although temperature stays too high.
- Low indoor temperature and high relative humidity. This case is the opposite. If vents are opened, humidity would decrease, but also temperature. If vents keep closed, temperature would reach a better value, but water vapor content should remain high (above soil evaporation and crop transpiration).

The solution adopted is to change the temperature set point within an interval depending on the relative humidity. The reference governor uses a predefined relative humidity. If relative humidity surpasses that value, the temperature set point is reduced to produce vent opening helping to evacuate water vapor. If relative humidity is quite low, temperature set point is increased to avoid vents opening.

During the night the heating system is used to raise the temperature (reducing the relative humidity) so that when used, there is usually no problem of excess water vapor, except at sunrise by condensation. During spring, summer, and autumn, when demand for warmth at night is minimal or absent, the temperature of water in the pipes (in the case of aerial pipes heating system) is kept at a minimum value determined for the air that is not saturated with water vapor (100 % relative humidity).

3.1.2.4 PID-Type Controllers

As in other industrial processes, PID control has been widely used for greenhouse climate control purposes [6, 49, 103, 104, 192, 389, 390, 461, 462, 478, 482, 483]. Most PID tuning techniques are based on simplified transfer function models obtained from reaction curve tests or linearization of nonlinear models around the desired operating point. Due to the significant variations in the dynamic characteristics of greenhouses, it is difficult to obtain a satisfactory performance over the total operation range with a fixed parameter controller, mainly if well damped and fast responses are required. As the system response for both ventilation and heating is of FOPDT

type, the use of PID controllers with fixed parameters is anyway a very good option for greenhouse climate control tuned for disturbance compensation purposes.

The classical implementation of the PID controller is the noninteractive scheme, where the control signal is given by:

$$U(t) = c_{K_p} \left(E(t) + \frac{1}{c_{T_i}} \int_0^t E(\eta) \, d\eta + c_{T_d} \frac{dE(t)}{dt} \right) \tag{3.1}$$

where $U(t)$ is the control signal (for instance, percentage of vents opening in daytime climate control), $E(t)$ is the error signal, computed as the difference between the set point and the measured variable (e.g., difference between temperature reference T_{ref} and measured inside air temperature $X_{T,a}$), c_{K_p} is the proportional gain, c_{T_i} the integral time and c_{T_d} the derivative time. These last three parameters represent the degrees of freedom the designer has to achieve the requested performance (generally in terms of well damped response, adequate disturbance rejection capabilities and so on). Figure 3.4 shows the implementation selected in the examples shown in this text, where $1/s$ stands for an integrator in Laplace transform. The typical tuning methods are those based on step responses or analytical methods: Ziegler–Nichols (ZN), Chien, Hrones and Reswich, Cohen-Coon, AMIGO, λ method, SIMC, pole cancelation, pole placement, … [17]. The implementation should be done using antiwindup (AW) action (to account for actuator saturation effects, with descriptive parameter tracking time constant $c_{T_{aw}}$ [17]), two degrees of freedom setting and/or set point weighting (to design both for disturbance rejection and set point tracking purposes), derivative filtering (to reduce the effect of sensor noise in the control action), and bumpless transfer (to transfer from manual to automatic control mode or tolet changing the active controller in gain-scheduling or switching control schemes). Excellent references to these methods can be found in [17, 152, 299, 469] and references therein.

PID control is often used in combination with other control schemes, as those explained in the following sections. Its parameters are changed according to outside conditions or it is usually combined with a feedforward term in the control loop to account for the effect of measurable disturbances.
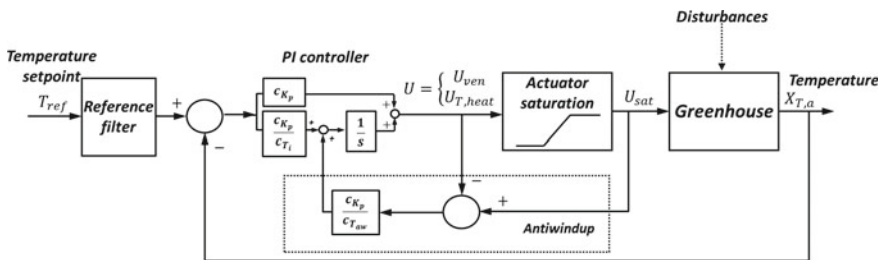

Fig. 3.4 PID control structure including antiwindup action

3.1.2.5 Gain-Scheduling Controllers

PI controllers are usually implemented in greenhouse climate control within a gain-scheduling (GS) strategy to explicitly take into account disturbances acting on the system. A typical implementation consists in using a PI controller based on inside temperature feedback to reduce sensitivity of the system with respect to disturbances and smooth nonlinearities. The nonlinear nature of the system prescribes an adaptive implementation of the PI controller, or an alternative like a GS controller [18]. Although not strictly considered an AC scheme in some classifications, GS can be used when there is a direct relationship (or through auxiliary variables) of disturbances with the main system dynamics. The controller parameters are modified from a table or function previously calculated for different operating points in terms of these auxiliary variables. It can be considered as a system with a closed loop controller where its gain is adjusted by a feedforward compensation. Actually, it is an open loop adjustment since there is no feedback to compensate for the wrong choice of parameters [18].

A drawback of this type of algorithm is the construction and design of the table or function relating the parameters of the controller with the variables measured, because lots of operating conditions have to be tested and the proper operation of the system has to be analyzed under numerous simulations. Moreover, in general there are no results on the robustness, performance, or stability of the controlled complete system, existing studies for cases where the access variable to the table is the reference or the output of the system. However, it has the advantage that the controller can be changed very quickly, depending on how the scheduling variable is able to capture the possible changes in the dynamics of the process.

When dealing with the ventilation problem (one of which objectives is to remove excess heat), the GS control approach takes into account outside conditions by implementing a control structure like the one shown in Fig. 3.5. The way in which proportional control gain is modified as a function of outside temperature and wind speed is shown in Fig. 3.6 [215] for the case treated in this book. For a constant set point, it can be seen how the proportional gain c_{K_p} increases when outside temperature rises to try to maintain the same rate of inside hot air removal. When outside wind velocity increases, vents opening should be smaller for a constant set point. The wind velocity signal has to be filtered before entering in the GS control computation to avoid noisy control signals.

Instead of using a table, the controller implementation must take into account the kind of installed vents, the desired inside temperature and the typical climate of the area. Six parameters have to be determined from tests in different operating conditions (units and typical values are shown in Fig. 3.6 and Table 3.3). Notice that this can be a time-consuming task and that may depend on the season the greenhouse is operated.

Only the controller proportional gain is modified in this way. The integral part of the controller avoids situations in which steady-state error may arise, being necessary to tune c_{T_i} parameter in a conservative way. Commercial control systems implement
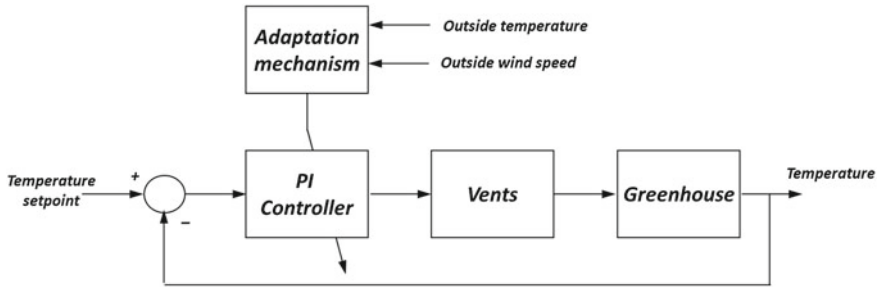
Fig. 3.5 Gain-scheduling control structure for temperature control using ventilation
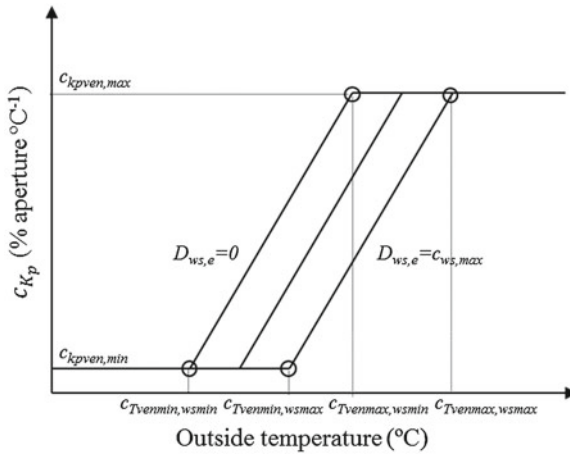

Fig. 3.6 Relationship between PI controller proportional gain c_{K_p} and outside conditions and characteristic parameters used to obtain it

Table 3.3 Descriptive parameters of the ventilation gain-scheduling controller

Parameter	Description	Typical value
$c_{Kpven,max}$	Maximum value of the proportional gain	20
$c_{Kpven,min}$	Minimum value of the proportional gain	5
$c_{Tvenmin,wsmin}$	Minimum outside temperature for vents opening without wind $(D_{ws,e} = 0 \text{ m s}^{-1})$	10
$c_{Tvenmin,wsmax}$	Minimum outside temperature for vents opening with maximum allowed wind speed $(D_{ws,e} = c_{ws,max} = 15 \text{ m s}^{-1})$	20
$c_{Tvenmax,wsmin}$	Outside temperature for maximum vents opening without wind $(D_{ws,e} = 0 \text{ m s}^{-1})$	25
$c_{Tvenmax,wsmax}$	Outside temperature for maximum vents opening with maximum allowed wind speed $(D_{ws,e} = c_{ws,max} = 15 \text{ m s}^{-1})$	35
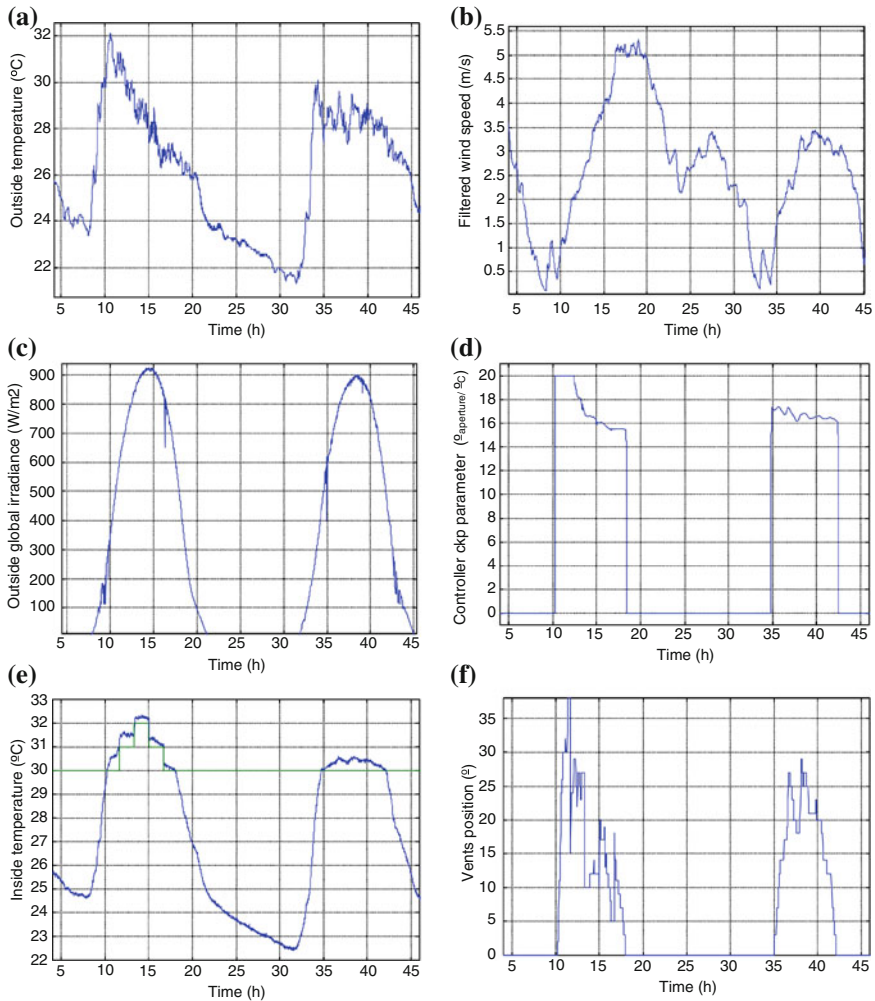
Fig. 3.7 Real test in summer conditions: gain-scheduling temperature control using ventilation. **a** Outside temperature (°C). **b** Filtered outside wind speed (ms^{-1}). **c** Outside global irradiance (Wm^{-2}). **d** Controller c_{k_p} parameter (° aperture °C^{-1}). **e** Inside temperature controlled during the day (°C). **f** Vents position (°)

the integral action in a stepwise version, opening or closing the vents at a determined amount depending on the steady-state error.

As an illustrative example of the performance achievable with this kind of controller, Fig. 3.7 shows results with the Araba greenhouse during August 2000 with the shading screen completely extended. The outside conditions are typical in summer time, with high values of irradiance and temperature and variable wind speed. The

proportional gain is sensible to the wind speed. Under high temperature and low wind conditions, the actuators are prone to saturation.

3.1.2.6 Feedforward Control

This section presents the development of feedforward (FF) controllers for greenhouse climate control. These controllers are mainly based on physical laws and measured data and are discussed in terms of their suitability for disturbances compensation and potential use for AC purposes [361]. As has been mentioned, crop growth control is characterized by both fast and slow dynamics [444], the first associated with the greenhouse climate and the second with crop growth. As a first approximation, seasonal optimization can treat the physical climate as immediately realizable through the control. In nowadays greenhouse climate control, the emphasis is on achieving a temperature integral for crop growing and development purposes. However, when disturbances due to environmental variables are subjected to large changes (solar radiation, wind speed and direction changes, etc.), greenhouse climate dynamics seriously affects the net profit [444], even leading to dangerous situations (e.g., condensation) as a consequence of the surpassing of temperature or humidity limits. Due to this reason, it is important to minimize the effect of disturbances in the inside conditions of the greenhouse by using adequate FF controllers, based on the measurement of disturbances and trying to compensate for their effects before they have created control errors. This control paradigm can be used for both linear and nonlinear systems and requires a mathematical model of the process [16]. Black box models or models based on heat balances may be used for FF control. Both should be updated by online parameter estimation and can be static or dynamic. Using conventional feedback control in combination with FF control has several advantages [74, 440]: The improvement of closed loop stability properties, the reduction of the control effort, and the avoiding of oscillatory behavior as the control system can react earlier on changes of outdoor weather conditions.

Using models relating the controlled variable and the inputs to the system, the control variable can be computed to cancel the effect of the disturbances on the system output. The set point tracking error resulting from modeling errors can be compensated for by adding a feedback controller. Without FF action, the feedback controller is used to track all load changes that occur in the process. However, when using also FF compensation, the feedback controller only has to compensate for those errors the FF controller cannot handle. There are mainly two basic ways of implementing FF: Parallel and series configurations [74]. In both cases, the measurable disturbances are used to maintain the inside air temperature of the gases at the desired level. Combined feedforward-feedback design is a research field very active nowadays [161, 162, 173, 352, 353].

The series implementation is presented in this section, as shown in Fig. 3.8, so that the reference temperature to the FF controller can be used as control action and thus the system has a static gain near unity and it can be treated as a SISO one as the disturbances are intrinsically compensated by the FF term. The output of the FF
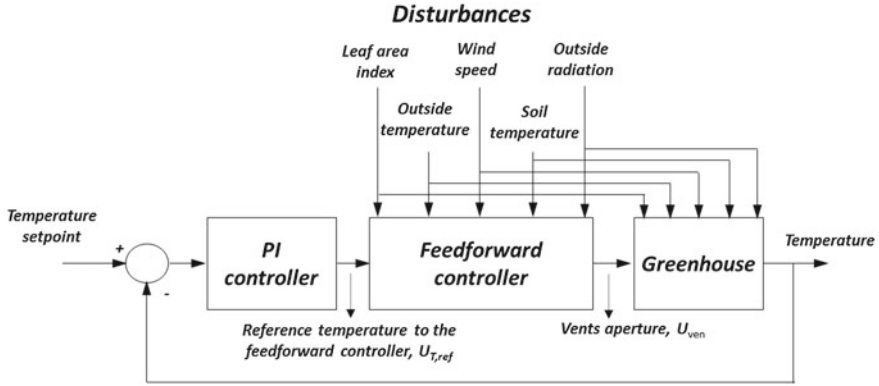
Fig. 3.8 Series feedforward controller for greenhouse temperature control using ventilation

controller is thus the vents opening. This configuration is of special interest when using AC techniques.

The production process in greenhouses can be described by a dynamic model represented in a general form by the expressions included in Chap. 2, Eq. (2.3). That kind of model is not suitable for control purposes due to its complexity (although it can be used within an optimization framework). A control model should account for the relevant environmental factors with their interactions (coupling) and be linearized and reduced, generating model inaccuracies. Important nonlinearities, such as product modulation of parameters (i.e., windows aspect with wind speed) can be accounted for by input variable transformation before entering the linearized model. Such separate FF actions and submodels are recommended due to the complexity of the greenhouse operation [408]. An approximation introduced in [74] and successfully used in [39, 71] for designing FF controllers for solar plants can be used in the greenhouse climate control framework, as the main sources of disturbances in the case of solar plants and greenhouses are of similar nature. Taking into account the most relevant terms in Eq. (2.3) and by performing several simplifications and assumptions, a relationship can be obtained relating inside temperature with control variables and disturbances (as done by other authors such as [253, 408]), given by Eq. (2.59). Considering some of the coefficient constants (calculated in regime operating conditions), the following simplified expression can be obtained:

$$
c_{\text{ter,a}} \frac{dX_{T,\text{a}}}{dt} = c_{\text{rs,a}} D_{\text{rs,e}} + c_{\text{cnv,ss-a}}(D_{T,\text{ss}} - X_{T,\text{a}}) + c_{\text{heat}} U_{T,\text{heat}}
$$

$$
+ c_{\text{cnd-cnv,a-e}}(X_{T,\text{a}} - D_{T,\text{e}}) - \frac{c_{\text{ter,a}}}{c_{\text{vol,g}}} V_{\text{ven,flux}}(X_{T,\text{a}} - D_{T,\text{e}}) - V_{\text{lt,vap}} M_{\text{trp,cr}}
$$

$$
(3.2)
$$

where $X_{T,\text{a}}$ is the greenhouse inside air temperature, $D_{\text{rs,e}}$ is the solar irradiance, $D_{T,\text{e}}$ is the outside temperature, $D_{T,\text{ss}}$ is the temperature of the soil (considered as a measurable disturbance for control purposes), $U_{T,\text{heat}}$ is the control signal of the air

heating system (usually on/off) described by Eq. (2.38),[1] $M_{trp,cr}$ is the transpiration of the crop, $c_{ter,a} = c_{sph,a}c_{den,a}(c_{vol,g}/c_{area,ss})$ is the product of specific heat of air, air density, and effective height of the greenhouse, $c_{rs,a}$ is a solar heating efficiency, $c_{cnv,ss-a}$ is the heat transfer coefficient from soil to inside air, c_{heat} is the heat power per soil surface unit, $c_{cnd-cnv,a-e}$ is the heat transfer coefficient (convection and conduction) from inside of the greenhouse out (assumed positive), $c_{vol,g}$ is the greenhouse volume, $V_{lt,vap}$ is the vaporization energy of water (temperature dependent), and $V_{ven,flux}$ is the ventilation flux, described by Eq. (2.11) (or by any of the models shown in [61], as done in [361]):

$$V_{ven,flux} = \frac{c_{ven,n}c_{ven,l}c_{ven,d}D_{T,e}}{3c_{gv}(X_{T,a} - D_{T,e})} \left[\left(V_{ven,hef}c_{gv}\frac{(X_{T,a} - D_{T,e})}{D_{T,e}} + c_{ven,wd}D_{ws,e}^2 \right)^{3/2} - (c_{ven,wd}D_{ws,e}^2)^{3/2} \right] + V_{loss} \tag{3.3}$$

with
$V_{ven,hef} = 2c_{ven,w} \sin(U_{ven}/2)$

where V_{loss} is the leakage when the vent is closed, given by Eq. (2.14), $c_{ven,n}$ is the number of vents, $c_{ven,l}$ is the length of the vents, $c_{ven,d}$ is the discharge coefficient, c_{gv} is the gravity constant, $c_{ven,wd}$ is the wind effect coefficient, and U_{ven} is the position of the vent (control signal, expressed here in angular aperture units). This model is characterized by the discharge coefficient and the wind coefficient, which have to be estimated (and another parameters explained in Eqs. (2.12)–(2.15)). The discharge coefficient depends on environmental factors, but it has been considered to be constant in the obtaining of a simple FF controller. Another option is to consider a simplified ventilation rate as that described by [326] for Almería-type greenhouses using an exponential expression of the combined aperture control signal:

$$V_{ven,flux} = c_{ven,\mathbf{n}}c_{ven,l}c_{ven,\mathbf{w}}D_{ws,e}(\alpha_v U_{ven}^{\beta_v}) + V_{loss} \tag{3.4}$$

where U_{ven} in this case is the percentage or normalized aperture of the vents, $c_{ven,\mathbf{w}}$ is the width of the vents, and α_v and β_v are tuning parameters which, according to actual measurements, show subtle variations between leeward and windward ventilation. This is a very simplified expression as the opening surface should have to be used through variable $V_{ven,hef}$, but it has demonstrated to be valid for the kind of greenhouses considered in this book, as will be shown in Sect. 3.2.3.

The value of the coefficients in Eqs. (3.2)–(3.4) have been obtained using input/ output data obtained at the greenhouse and by iterative search in the range of values given by different authors using genetic algorithms, as explained in Chap. 2. Figure 3.9 shows a comparison of the real temperature and the simulated tem-

---

[1] Notice that if heating pipes are used, the heat transfer by the heating system should be given by Eqs. (2.36) and (2.37) in this balance.
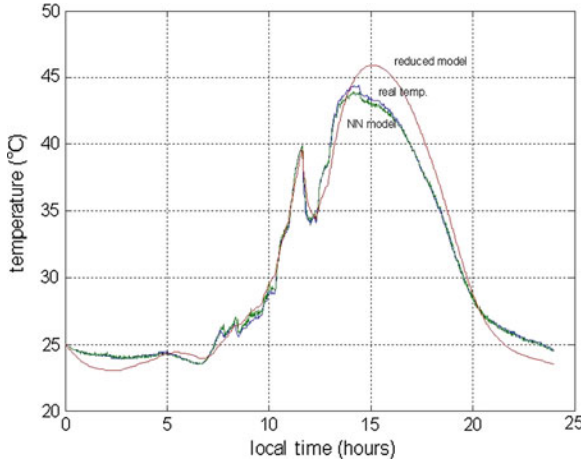
Fig. 3.9 Comparison of real and simulated temperatures

peratures obtained by using the nonlinear neural networks model developed in Sect. 2.1.3.5 [356] and the simplified model given by Eq. (3.2). Differences at night are due to the fixing of the coefficient $c_{cnd-cnv,a-e}$, which was estimated for winds of about $6\,\mathrm{m\,s}^{-1}$. At night wind speed decreases in the area and modeling errors due to this coefficient are evidenced.

By using the simplified representation of the heat balance given in Eq. (3.2) and considering a steady state balance $(dX_{T,a}/dt = 0)$ and $V_{loss} = 0$, it is possible to derive a correlation for the input variables (ventilation and heating) as function of the environmental conditions and the inside temperature. As will be explained below, the resulting expression can be used as a FF action in the control system. The input to the series FF controller is a reference temperature $(U_{T,ref})$ provided by a feedback controller. As a first approximation, as there is one output variable (temperature $X_{T,a}$) and two control variables (ventilation U_{ven} and heating $U_{T,heat}$), these are considered to be exclusive control actions when controlling temperature in order to save energy [200]. Then, using the mentioned static balance in Eq. (3.2), the series FF controller is obtained by substituting the air temperature $X_{T,a}$ by the desired temperature $U_{T,ref}$. Thus, for each sampling instant the following calculations have to be performed:

Day. If $U_{T,ref} > D_{T,e}$ and $D_{T,e} > 0$

1. $V_{ven,flux} = \dfrac{c_{vol,g}}{c_{ter,a}} \dfrac{(c_{rs,a}D_{rs,e}+c_{cnv,ss-a}(D_{T,ss}-U_{T,ref})+c_{cnd-cnv,a-e}(U_{T,ref}-D_{T,e})-V_{lt,vap}M_{trp,cr})}{(U_{T,ref}-D_{T,e})}$

2. $V_{ven,hef} = \dfrac{D_{T,e}}{c_{gv}(U_{T,ref}-D_{T,e})}\left[\left(\dfrac{3c_{gv}(U_{T,ref}-D_{T,e})V_{ven,flux}}{c_{ven,n}c_{ven,l}c_{ven,d}D_{T,e}} + (c_{ven,wd}D_{ws,e}^2)^{3/2}\right)^{2/3}\right.$

$$\left. -c_{ven,wd}D_{ws,e}^2\right]$$

3. $U_{\text{ven}} = 2\arcsin\left(\frac{V_{\text{ven,hef}}}{2c_{\text{ven,w}}}\right)$

Night.

$U_{T,\text{heat}} = \frac{1}{c_{\text{heat}}}\left(c_{\text{cnv,ss-a}}(U_{T,\text{ref}} - D_{T,\text{ss}}) + c_{\text{cnd-cnv,a-e}}(D_{T,\text{e}} - U_{T,\text{ref}}) + V_{\text{lt,vap}}M_{\text{trp,cr}}\right)$

where a low-pass filter is applied to solar irradiance and wind speed disturbances to avoid sudden changes in the control signals and conversions to normalized angular units are used in U_{ven}. Notice that the term accounting for latent heat in the experiments shown in this section is negligible, due to the fact that the crop was in the early stages of its development. In other cases, it has to be measured or estimated using Eq. (2.44). Feedforward controllers are usually calculated by using the ratio between the transfer function of the measured disturbance to the system output and the process transfer function (fully dynamic forward compensation) [161, 174]. The FF term developed based directly on the steady state energy balance relationship provides a trade-off between complexity and performance. Only filtering of the fast disturbances before entering the calculations is required. When humidity bounds are taken into account due to condensation, a reduced dynamic equation of humidity could be used in such a way that a system of two equations and two variables can be solved on line, providing the values of the desired heating and ventilation signals. These values should be implemented only when the humidity surpasses its limits. In other cases, the value given by the FF term obtained by using Eqs. (3.2) and (3.3) will be used. In the parallel FF case, the inside greenhouse temperature $X_{T,\text{a}}$ in the static balance is substituted by the set point temperature, and a similar development to that performed in the series FF case can be carried out.

Notice that the feedback controller must incorporate integral action to avoid steady-state errors. Feedforward tends to provide high values in the control action to compensate for disturbances and set point changes, what produces saturation in the control signal. To avoid integral windup [17], and AW compensation scheme is recommended. The way it has been implemented is shown in Fig. 3.10, where the inverse of the static FF term is used to map physical constraints into constraints in the reference temperature of the FF controller (control signal of the feedback controller).
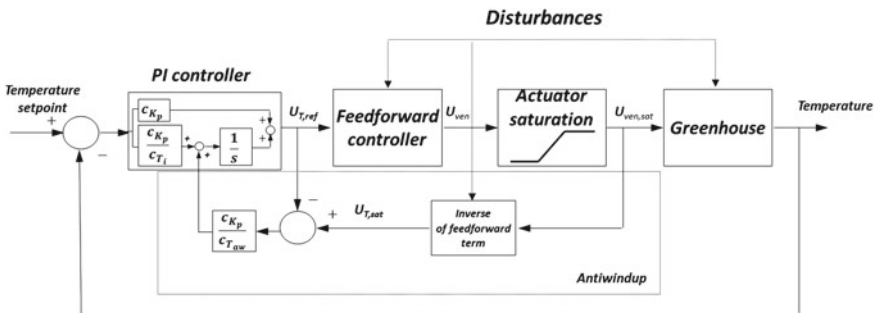

Fig. 3.10 Implementation of feedback PI control including series feedforward with antiwindup mechanism in temperature control using ventilation

In the classical approach, both the vents aperture demanded by the control system and that provided by the saturation block or actuator should fed the antiwindup block. The problem that arises in this application is that the control signal provided by the feedback controller is the reference temperature for the FF controller, which provides the vents aperture depending on the measurements of environmental variables. So, the first input point to the AW block has been displaced to the output of the feedback controller. Fortunately, when saturation occurs in the vents aperture, the corresponding reference temperature of the FF controller can be online calculated taking into account the actual value of disturbances (the FF term is invertible as inside temperature is higher than outside temperature when vents are used), in such a way that the scheme reproduces the classical one.

Figure 3.11 shows the results obtained when controlling ARABA-type greenhouse during summer. Both set point tracking and disturbance compensation results are quite acceptable under clear-day conditions with outside temperatures around 29 °C and variable wind speed. The series FF can be used for AC purposes using simplified linear models of the greenhouse [408]. In this case, the inclusion of a series FF term presents advantages, as the reference temperature to the FF term ($U_{T,\mathrm{ref}}$) can be used as the input signal to the identifier, instead of the aperture of the vents. As the FF compensates for variations in disturbances, the dynamic variations in the inside temperature will be mainly related to the control signal from the estimation and AC point of view [74]. If the feedback controller incorporates integral action, then the inside temperature should be close to the set point temperature in steady state and, and also the set point temperature to the FF term ($U_{T,\mathrm{ref}}$) and the model employed in the self-tuning algorithm will always have steady-state gain of approximately unity and the static nonlinearities will be canceled. This strategy will be explained in more detail in Sect. 3.2.2.

3.1.3 Irrigation Control

The importance of water in plants has been described in previous chapter. In this section, the main methods used for irrigation water supply in greenhouses are summarized. Whereas the field of knowledge is vast, only some representative works of each method are described. In soil-less systems it is important to precisely define the time and volume associated to water supply, as they are low capacity containers requiring high frequency of watering. Irrigation control is addressed from the perspective of water supply, regardless of the nutritional element that has its own dynamics for an adequate supply of nutrients required by plants.

The supply of water and nutrients to crops, called fertigation, has the following objectives: To provide the suitable amount of each nutrient, ensuring proper nutritional balance to promote plant growth, to provide good aeration to allow roots respiration in perfect condition, to keep the temperature levels within interval defined for each specie, to maintain the advisable amounts of readily available water (low retention stress), to facilitate the uptake of water, and to maintain uniformity of the above objectives across the volume of the container where the roots develop.
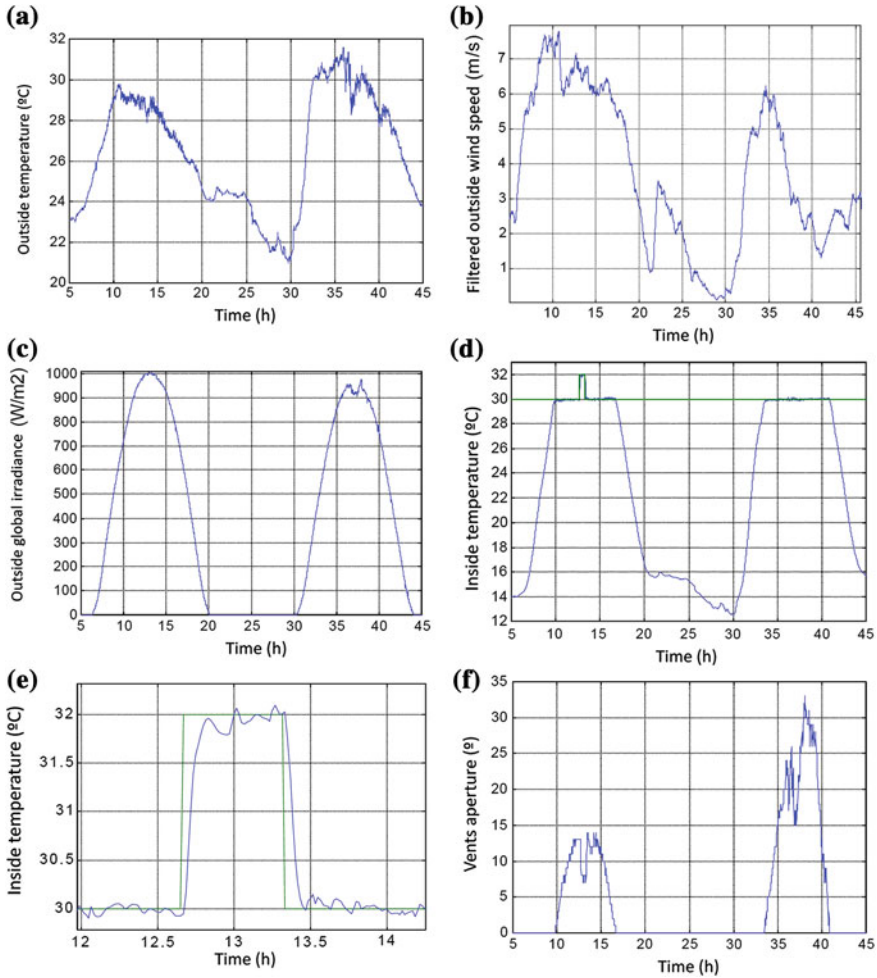
Fig. 3.11 Representative results of feedforward control **a** Outside temperature (°C). **b** Filtered outside wind speed (m s^{-1}). **c** Outside global radiance (W m^{-2}). **d** Inside temperature (°C). **e** Zoom of temperature set point tracking performance (°C). **f** Vents aperture (°)

The methods for the management of water supply in soilless systems seek predicting plant uptake under different approaches [220]:

- Adding the amount of water that forecasts indicate to be absorbed by the plants (amount criterion).
- Control of the humidity and nutrient concentration in the root environment (concentration criterion).
- Control of the water content and nutrients concentration of plant tissues ("speaking plant approach", [171, 214]).

In soilless systems a relevant aspect is the low reserve capacity of water and nutrients in the root zone. With a substrate volume between 0.014 (rockwool) and 0.025 (perlite) $[m^3 m_{surface}^{-2}]$, the water content in the root zone is comprised between 0.010 and 0.012 $m^3 m^{-2}$ for rockwool and perlite, respectively [220]. This indicates the importance of an adequate supply of water, both in time and frequency.

Nowadays, the control of water supply is carried out based on different specific criteria associated with: Moisture content of the soil or substrate, the estimated crop evapotranspiration, measures of the plant, the irrigation system and the integration of the plant–substrate–climate system.

3.1.3.1 Irrigation Based on the Moisture Content of the Soil or Substrate

It is based on measuring the volumetric water content or matric potential of soil or substrate [245]. In intensive crops grown in soilless systems, rhizosphere is a highly saline medium and therefore its osmotic potential contributes significantly to the total water potential of the substrate, which must be taken into account in determining this indicator. The determination of the starting time for irrigation is done by knowing the desired volumetric water content in the substrate or the hydric potential corresponding to the water capacity reserve of it.

The sensors used in determining the moisture content are based on the measurement of the dielectric constant of the matrix of the substrate, either Time Domain Reflectometry (TDR) or Frequency Domain Reflectometry (FDR). The first ones are based on the transmission time of an electromagnetic signal along a metallic tube inserted into the substrate, while the latter ones use the capacitance to measure the dielectric constant [64, 100].

Tensiometers determine the matric potential of the substrate, so that the irrigation set point is determined based on this measurement. The matric potential for soilless crop shows negative values lower than -10 kPa. In tomato crop the typical values for switching on the irrigation are -10 kPa for the first 139 days and -4 kPa from 140 to 221 days after transplantation [180]. The recommendation for pepper crop is a threshold to start irrigation of -8 kPa [309].

The electrical resistance based sensors consist of two electrodes, so that the dissolution of the substrate maintains an equilibrium with a sensor array. The electrical resistance between the electrodes is a function of moisture content. These kind of sensors require calibration, but are simple and easy to install [450].

The load cells are a type of lysimeter whereby the moisture content in the substrate is estimated [111]. Several weight platforms hold plants and a specific correlation among the crop, its age and the moisture content is established. The system sends the signal to the irrigation controller that activates irrigation when reaching the limit set by the user.

In a comparative study of different methods for measuring volumetric water content (TDR, tensiometers and load cells) in the substrate with physiological indicators of the plant (photosynthesis and stomatal conductance), it was pointed out the

limited predictive ability of load cells to manage water content in rockwool substrate and pure sawdust [111]. Load cells and TDR correlated with stomatal conductivity and sap flow in the substrate mixed with sawdust plus 30 % of wood fiber [111].

An important aspect to consider with this type of measurement is the variation of moisture content or water potential in the soil, since there is no uniformity in their distribution. In studies with rockwool, it is determined that more humidity is present in the lower level of the substrate located near the bottom of the container and lower on the top of it [66, 348]. The differences in the moisture content of rockwool substrate or due to the layered structure of the blocks and polyethylene bag containing it. There is also a gradient relative to the longitudinal and horizontal direction from the emitter; the furthest points of the dropper have less water [66, 348].

3.1.3.2   Irrigation Based on Evapotranspiration

Several works on estimation of evapotranspiration have been described in Chap. 2. One way to calculate water demand by the plants is using the estimation of water loss by the plants. Estimation of evapotranspiration in different species grown in greenhouse were developed: In ornamental plants [25], in tomato [206, 419, 422], in geranium [279, 374], and in cucumber [271], among others.

Irrigation management should be done with the information coming from the climate sensors and that provided by the user, from which evapotranspiration can be estimated.

An important point in this strategy is the estimation of LAI, which may be obtained from the user (measured offline) or by using some model. Other parameters are the dose of irrigation and desirable drainage level. The controller calculates the transpiration rate, the accumulated amount of water lost by evapotranspiration since the last irrigation, compare it to the previously set dose and when the transpiration integral equals the fixed dose activates irrigation. This type of strategy has been used in NFT [170] in tomato crop in which the model underestimated the amount of water required by the crop by 10–31 %. It was also used in rockwool substrate and the model underestimated the water required by up to 21 % [170]. The application of irrigation control using a transpiration model is reported in [150], which seeks the minimum cucumber crop transpiration.

3.1.3.3   Irrigation Based on Measurements

One option in this type of approach is the log of micrometer diameter variations of the plant, through dendrometers, depending on the hydric status of the plant. It is possible to use this kind of measurements after treatment of the data as the diameter variations can also be caused by growth. Such sensors have been used in experimental tests in tomato [67, 157, 246, 466], ornamental plants [27], melon [466], and pepper [97, 466].

The leaf temperature has also been used to measure the water status of the plant that determines a water stress index, which is feasible to be used for irrigation scheduling. This technique has the problem of being a late indicator of hydric stress because the temperature rise happens when partial stomatal closure occurs, taking place subsequently to the reduction of other more sensitive processes such as growth by leaf expansion [133]. In [423] the index of water stress for a kind of grass (*Lolium perenne*) was determined using infrared thermometry, while in [294] it was determined for *Impatiens* crop in order to set a threshold for irrigation activation, using limits allowing the users to detect hydric stress 1 or 2 days in advance regarding the visual symptoms.

The thickness of the leaves has also been used in irrigation scheduling [393]. The sensor continuously measures the thickness of the leaf with an accuracy of ± 1 micron. It is based on the principle that the thickness of the leaf is correlated with the potential of turgidity and leaf, and the fact that if the plant is subject to water stress its turgor decreases. It has been tested in fruit to turn irrigation systems in response to variations in the thickness of the leaf, producing high frequency and low volume irrigation, leading to water savings of 30 % in citrus tests for 6 years, avocado for 3 years, and cotton during a season [393].

The named sap flow technique obtains direct measurement of flow through the plant. The sensor is attached to the stem and may restrict growth or cause infections in heat-based sensors [118]. Some applications to woody plants have been developed to control irrigation using this technique [126, 311].

Another example of such devices is the development of an integrated system for measuring physiological conditions of the plant, which is linked to software that presents information in physiological and agronomic terms, so that the farmer can be alerted about possible problems in the crop [455]. It allows him to measure climate (solar radiation, temperature and relative humidity), sap flow, stem diameter, fruit diameter, leaf temperature, moisture, and soil temperature. With this system it is possible to define climate and irrigation set points using trial and error tests, and also helps in decision making [454].

3.1.3.4 Irrigation Based on Solar Irradiance

A method widely used in irrigation systems involves the application of irrigation empirical methods for estimating water demand based on solar radiation. An irrigation threshold is established based on the cumulative radiation. In [309] it is indicated that irrigation was applied when a threshold of 7 MJ m^{-2} is reached for pepper crop. In gerbera crop, the threshold was set in 2 MJ m^{-2} for irrigation start [236].

3.1.3.5 Irrigation Based on Drainage

The volume of drainage accumulated in a container determines the activation of irrigation trying to supply the water consumed by the plants. It is widely used in soilless systems [370].

Another approach is to measure the EC of drainage, activating irrigation based on maximum and minimum limits on this variable [46]. A method is described in [144] where drainage flow and ions are measured using ion-selective sensors, helping in the determination of volume of water and nutrients concentration to apply.

3.1.3.6 Irrigation Based on Integrated Methods

Irrigation based on integrated methods using models requires knowing the interactions of the water in the plant [210]. The application of integrated methods is based on models at three levels: Water absorption, water transport in plants, and water loss to the atmosphere. The models of these processes are essential to enable predicting accurate dynamics of plant water status and the development of practical irrigation management systems [210].

The development of a two-dimensional model of water flow on the substrate is described in [176], where the absorption of nutrients coupled to a model of lettuce growing in sand substrate is modeled. The supply of water and nutrients is carried out by estimating the demand by the plant. In [176] absorption of water and nutrients is described from tomato growth modeling and water flow and nutrients models in rockwool.

An integrated application was also developed from models of photosynthesis, transpiration, and nutrient demand; the required amount of water and nutrients by the plants was calculated based on the greenhouse climate and from that the set points of irrigation and nutrients were fixed. This procedure was applied to tomato and pepper crops [222–224].

Another example is *Hortimed*, which is a decision support system for the management of hydroponic systems [9]. It consists of two parts: Online and offline management. The online system operates as the supervisor of other irrigation control systems and implements the best management based on crop conditions, irrigation water, climatic conditions, and characteristics of irrigation equipment. The offline module considers climate inputs, installed equipment, crop production, and salinity tolerance and water resources available to assist in the decision about potential investments relating to hydroponic systems, so that the farmer can manage several scenarios.

3.2 Advanced Control Algorithms

3.2.1 Introduction

3.2.2 Adaptive Control of Daytime Temperature

This section presents the development of mixed feedforward-adaptive controllers (FF-AC) for greenhouse climate control [43]. This type of control strategy is adequate to control greenhouse temperature and humidity as the dynamics are nonlinear

(e.g., the relation between natural ventilation and temperature) and time-varying due to several factors such as crop growth, wearing down of constitutive elements, etc. Previous works in this field [408] used multiple-input multiple-output (MIMO) linear models for online parameter estimation purposes, requiring the estimation a large number of parameters (36). The identification in this case is possible if a sufficient number of variables is monitored and under conditions of persistent excitation. Important nonlinearities such as product modulation of parameters (i.e., windows aspect with wind speed) can be accounted for by input variable transformation before entering the linearized model. As discussed in Sect. 3.1.2.6, such FF actions and submodels are recommended due to the complexity of the greenhouse operation.

In the approach presented in this section, the combination of FF and adaptive feedback schemes and the accounting for humidity control by online set point modification simplifies the estimation stage of the control algorithm as only two parameters have to be identified. The system should continuously update the model parameters as the greenhouse properties drift due to physical changes, and also to account for nonlinearities and model structure inaccuracies. As it is also pointed out in [408], supervisory mechanisms seem to be necessary for practical purposes. The daytime climate control will be studied in this section (using natural ventilation as control input), although results shown are easily applicable to night operation (using heating system as control input).

During the daytime operation, the changes in vents aperture produce large variations in the dynamics of the system (the relationship between vents aperture and inside temperature is not linear), justifying the inclusion of AC schemes. It is even more interesting to compensate for changes in system dynamics due to crop growth and plastic cover deterioration, which require the modification of parameters in fixed parameters control schemes. In fact, many commercial solutions include heuristically tuned GS controllers to cope with both fast and slow changing dynamics. As an alternative, AC performs self-tuning of control parameters in the face of changing dynamics. As has been previously mentioned, a feature of this type of system is that it is convenient to include a FF term, like that explained in Sect. 3.1.2.6 within the control scheme to compensate for disturbances acting on the system. In this case, it can be used even to cancel nonlinearities, in such a way that if the FF controller is placed in series with the greenhouse, and the variations in inside temperature would be mainly dependent on vents aperture changes. This is a feature of systems using solar radiation as the main energy source [71, 74]. The system composed by the series FF controller plus the plant can then be modeled as a FOPDT system. Figure 3.12 shows the control scheme mixing the FF controller with an adaptive one. It consists of a self-tuning regulator [18] in which the plant to be identified is composed by the FF controller in series with the system, such that the feedback AC calculates the reference temperature for the FF term, that also generates the vents aperture to achieve the desired set point temperature. As the vents are physically constrained, an antiwindup scheme has to be included (see Fig. 3.10), as has been explained in Sect. 3.1.2.6.
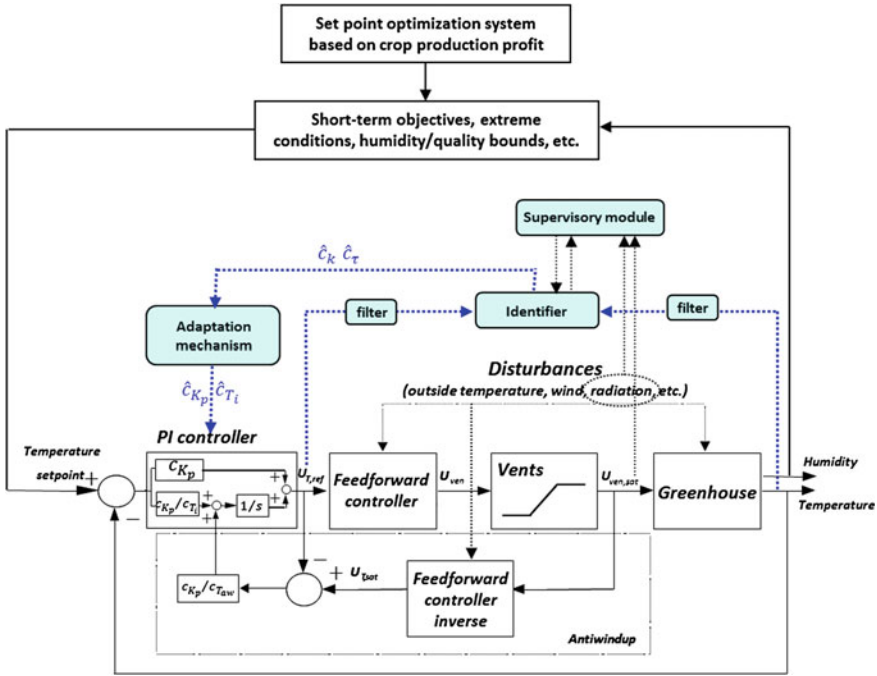
Fig. 3.12 AC architecture. *Source* As a courtesy of the authors [43]

In each sampling time, the AC:

1. Estimates the parameters of the linear model using filtered input (reference temperature for the FF controller) and output (inside temperature) signals. The identification algorithms used is described in [70] and is based on recursive least squares (RLS) identification with UDU factorization and variable forgetting factor in order to reduce the identifier memory and to avoid the identifier gain reaching zero. A supervisory module has been included to check conditions under which identification has to be stopped (saturation of the control signal, poor dynamic excitation, etc.) and to avoid the use of wrong estimated parameters.
2. Adapts controller parameters. The design of the PI controller in discrete time $(G_{\text{PI}}(z^{-1}) = (q_0 + q_1 z^{-1})/(1 - z^{-1}))$ has been performed by pole cancelation. The system between the reference temperature to the FF ($U_{T,\text{ref}}$) and the inside temperature can be modeled as a FOPDT system $G(z^{-1}) = bz^{-2}/(1 - az^{-1})$ with a delay of one sampling time, in such a way that only two parameters have to be identified (static gain and time constant). If the zero of the PI controller cancels the system pole ($q_1/q_0 = -a$, integral time equal the time constant), and, for instance, it is imposed that the closed loop system should have two real poles at the same location, the relationship $q_0 = 1/4b$ is obtained, in such a way that the adaptation mechanism is given by $q_0 = 1/(4\hat{b}))$ and $q_1 = -\hat{a}q_0$, where

$\hat{a}$ and $\hat{b}$ are online estimated by the RLS algorithm (related to static gain c_k and time constant c_τ).
3. Calculation of the control signal by the PI controller.
4. Supervision of the correct control behavior.

Regarding humidity control, the adopted solution has been to modify temperature set points as a function of the relative humidity (Fig. 3.12), that is, when humidity surpasses predefined bounds, the set point temperature is changed to help humidity evolve inside the operational band. More comments on this issue will be done in Sect. 3.2.9 devoted to switching control strategies.

The combined adaptive-feedforward scheme has been implemented and tested in simulation to analyze both short-term and long-term performance. On one way, the behavior of the control scheme has been analyzed during daily operation (fast time scale) to compensate for changing dynamics induced by operating point changes and disturbance cycles. The inclusion of a series FF controller serves both to compensate for disturbances and to perform a pseudolinearization of the nonlinear structure of the system. Unmodeled dynamics can then be compensated by the action of the feedback controller. If the FF term perfectly accounted for changes in disturbances, the inside temperature changes observed would be caused solely by changes in the control input signal. Although obviously exact elimination cannot be achieved, a compensation element based on steady state considerations considerably reduces the major problems inherent in the single input model and permits the successful estimation of the system parameters. Thus, the FF term serves to preserve the validity of the assumed system models in the control scheme that uses a SISO description of the plant [70]. The improvement achieved is not quite high and there are some risks related to the coupling of system dynamics with adaptation dynamics. Nevertheless, the inclusion of filters in data entering the identifier and supervisory mechanisms helps to avoid or diminish these undesirable effects.

On the other side, as the greenhouse dynamics vary during the whole crop cycle (from 90 to 180 days) as a consequence of crop growth (characterized by changes in LAI) and deterioration of plastic cover and even whitening, the inclusion of adaptation in this slow time scale provides clear benefits, as in other case the parameters of fixed PI controllers should be manually changed accordingly to drifts in system dynamics.

The behavior of the control system in the fast time scale (10 days) in which the crop state (represented by the LAI) can be considered constant, can be observed in Fig. 3.13, which shows the evolution of the representative parameters of a tests with data of August 2000. The daytime temperature set point was 40 °C (quite high due to extreme outside conditions and closing of the shade screen the second day) to avoid actuator saturation. The controller was working during the night also to see how the AW block adequately works even under extreme conditions in which vents are completely closed during more than 8 h. This figure also shows environmental conditions during this test. All the filters and supervisory mechanisms were implemented. The evolution of the estimated parameters is also shown. Figure 3.14 displays the evolution of the inside temperature during a test performed with data of spring 1998.

The daytime set point temperature was 30 °C. As can be seen, the effect of passing clouds and high wind speed values produced saturation during several parts of the operation.

The response of the adaptive PI control scheme is acceptable for all the considered seasons and for both slow and fast time scales (as the behavior is pseudolinearized by the action of the FF term). Adaptation has the advantage that the change of control parameters is done in an automatic way (GS being another possibility). Notice that even in the long-term scale, the LAI of the plants is an input for the FF controller and thus the adaptation to crop growth can be performed in part by this term. It is also interesting to comment that the identification mechanism of the self-tuning controller tends to identify a system with time constants higher than those expected from step response tests. One possible justification is that one of the supervisory mechanism activates identification when the control signal (vents aperture) is greater than zero (to avoid identification windup). This usually occurs when solar radiation is rising. Although the effect of solar radiation should be compensated by the FF term, unmodeled dynamics from solar radiation lead to the identification of a slower system (as the greenhouse integrates solar radiation). Another possible cause of the drift in the identified parameters may be the selection of the filters of signals entering
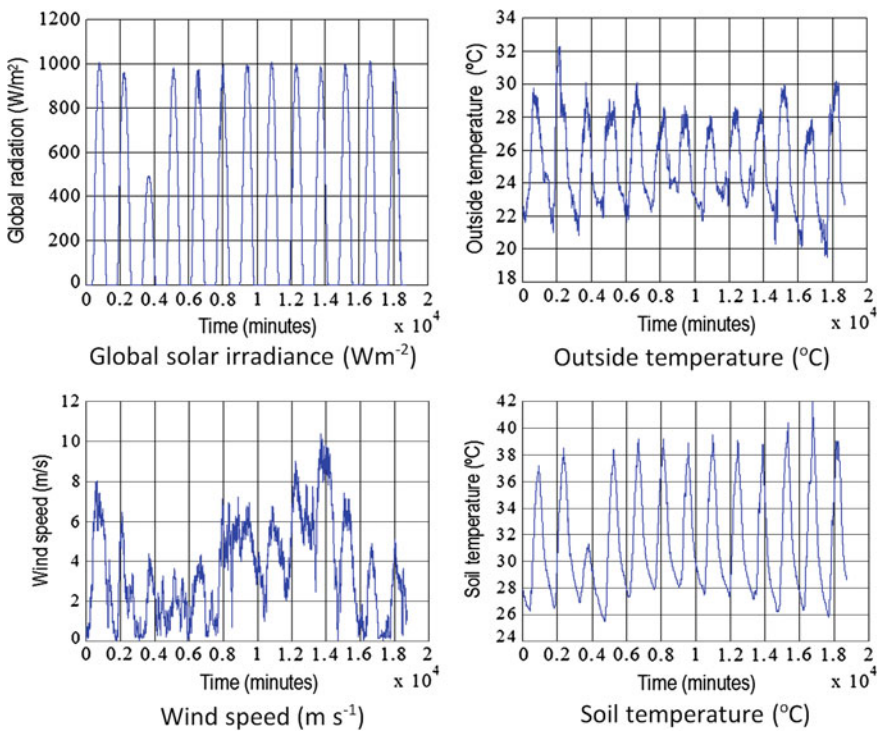

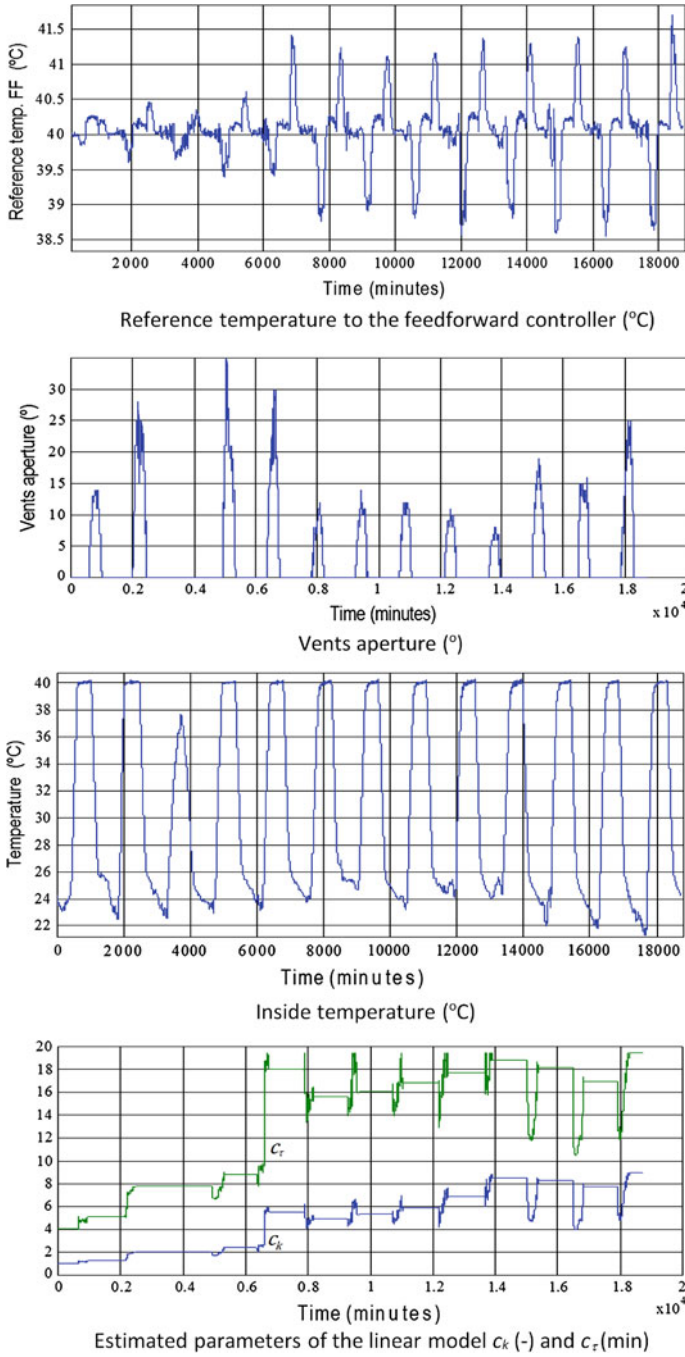**Fig. 3.13** Summer tests with the adaptive controller. As a courtesy of the authors [43]

Reference temperature to the feedforward controller (°C)

Vents aperture (°)

Inside temperature (°C)

Estimated parameters of the linear model c_k (-) and c_τ (min)
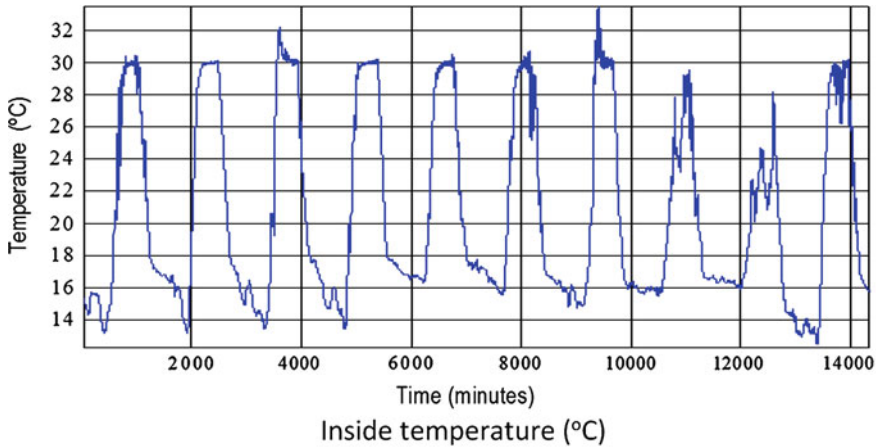
Fig. 3.13 (continued)

Fig. 3.14 Spring tests with the adaptive controller. As a courtesy of the authors [43]

the identifier. Nevertheless, the identification of a slower system increases the integral time of the PI controller leading to a more conservative behavior, which is secure from the operational point of view.

3.2.3 Feedback Linearization Control of Daytime Temperature

As has been studied in Sect. 3.1.2.6, the complexity of the obtained FF controller is high due to the implementation of Eq. (3.3) and the use of a static version of the algorithm tends to provide aggressive control actions. Taking these considerations into account, a feedback linearization (FL) control strategy can be developed to cope with the daytime temperature control problem, so that, the full dynamic simplified model given by Eq. (3.2) is used for control purposes and also a simpler description of $V_{ven,flux}$ given by Eq. (3.4) is implemented to obtain a less complex controller. Other examples of the application of FL control of temperature and humidity can be found in [158, 486].

The ventilation rate model used in this section is given by Eq. (3.4), which is a simplified version of that used for feedforward purposes. In [326] it is demonstrated that this simplified model fits well physical-based approaches proposed by other authors [219]. Figure 3.15 shows a plot of the results obtained with this simplified model when compared with that of [219].

The FL method is an approach to NC design methods where the main idea is to transform a nonlinear system into a linear one, and thus obtaining a closed loop dynamics in linear form, so that any linear control method can be applied. The final approach combines a linear controller with a nonlinear term obtained from the transformation. Several authors have used this control approach within the field of
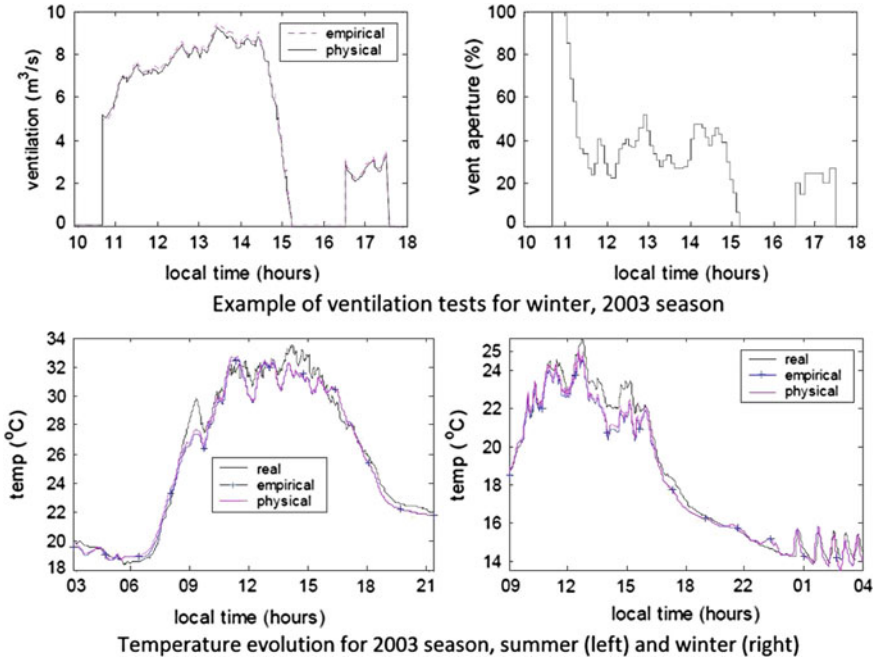
Fig. 3.15 Comparison of empirical and physical models of ventilation rate

greenhouse climate control (e.g. [6, 310]) with different types of models. In this section, input–output linearization is used to control the greenhouse daytime temperature using the dynamical model shown in Eq. (3.2). In order to analyze the controllability of the plant, the system in Eq. (3.2) has a relative degree equal to one, the same as the order of the system [410]. For systems that can be represented in the form $\dot{X} = f(X) + g(X) U$, a nonlinear mapping can be used to transform the system into a linear one:

$$U = \frac{\tilde{U} - f(X)}{g(X)} \tag{3.5}$$

with the condition that $g(X)$ cannot be equal to zero. A typical choice when using FL (see Fig. 3.16) consists in selecting:

$$\tilde{U}_{\text{ven}} = \frac{1}{c_{\text{ter,a}}} \Big(c_{\text{rs,a}} D_{\text{rs,e}} + c_{\text{cnv,ss-a}}(D_{T,\text{ss}} - X_{T,\text{a}}) + c_{\text{cnd-cnv,a-e}}(X_{T,\text{a}} - D_{T,\text{e}})$$
$$- \frac{c_{\text{ter,a}}}{c_{\text{vol,g}}} V_{\text{ven,flux}}(X_{T,\text{a}} - D_{T,\text{e}}) - V_{\text{lt,vap}} M_{\text{trp,cr}} \Big) \tag{3.6}$$

so that the resulting linear input–output relationship is represented by a simple integrator. Nevertheless, sometimes it is useful to include in the map only the nonlinear terms from the right hand side of Eq. (3.2), mainly in the face of unmodeled dynamics, disturbances affecting the system output and amplitude constraints in the actuators.
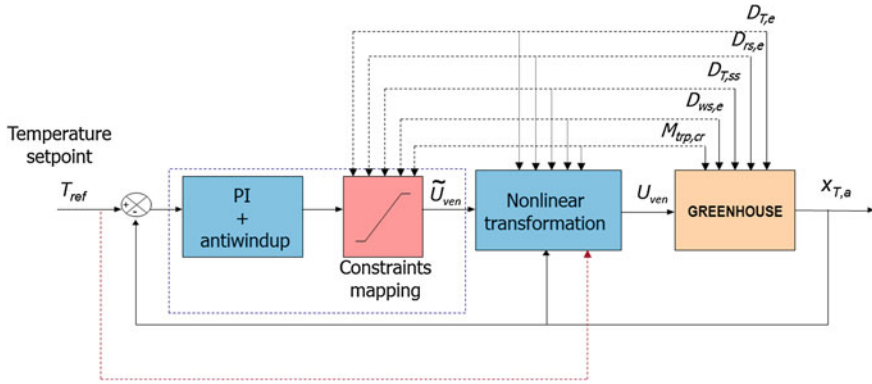
Fig. 3.16 Feedback linearization controller

In this case, the following selection is made:

$$\tilde{U}_{\text{ven}} = \frac{c_{ter,a}}{c_{\text{vol,g}}} V_{\text{ven, flux}}(X_{T,a} - D_{T,e}) + V_{\text{lt, vap}} M_{\text{trp,cr}} \tag{3.7}$$

$$= \frac{c_{ter,a}}{c_{\text{vol,g}}} \left(c_{\text{ven,n}} c_{\text{ven,l}} c_{ven,\mathbf{w}} D_{\text{ws,e}}(\alpha_{\text{v}} U_{\text{ven}}^{\beta_{\text{v}}}) + V_{\text{loss}} \right)(X_{T,a} - D_{T,e}) + V_{\text{lt, vap}} M_{\text{trp,cr}}$$

so that the resulting linear system (considering constant values of the coefficients) is given by:

$$c_{ter,a} \frac{\mathrm{d}X_{T,a}}{\mathrm{d}t} = c_{\text{rs,a}} D_{\text{rs,e}} + c_{\text{cnv,ss-a}}(D_{T,\text{ss}} - X_{T,a}) + c_{\text{cnd-cnv,a-e}}(X_{T,a} - D_{T,e}) - \tilde{U}_{\text{ven}} \tag{3.8}$$

Thus, it is possible to use any linear control method in order to obtain the virtual signal $\tilde{U}_{\text{ven}}$, and then the transform given by (3.7) can be applied to obtain the real control signal U_{ven}.

$$U_{\text{ven}} = \left[\frac{1}{c_{\text{ven,n}} c_{ven,l} c_{\text{ven,w}} D_{\text{ws,e}} \alpha_{\text{v}}} \left(\frac{c_{\text{vol,g}}}{c_{ter,a}} \frac{(\tilde{U}_{\text{ven}} - V_{\text{lt, vap}} M_{\text{trp,cr}})}{(X_{T,a} - D_{T,e})} - V_{\text{loss}} \right) \right]^{\frac{1}{\beta_{\text{v}}}} \tag{3.9}$$

Notice that input–output linearization can be practically achieved in all those cases in which the outlet and inlet temperatures are different, which covers all the operation regimes. Only the plant start-up has to be supervised to avoid numerical problems, or those cases in which wind speed ($D_{\text{ws,e}}$) is near zero (where the approximation given by (3.7) is not good, this being the main drawback of this approach). In the latter, the values of the vents aperture can be either held to the immediately previous or closed. In order to control the linearized system, a basic PI control structure with AW mechanism and disturbance compensation using FF control can be used. The FF part is composed by the terms in Eq. (3.8) including measurable disturbances.

A first set of parameters for the PI controller were obtained by using the greenhouse simulator explained in Sect. 2.1.1.8. A diagram of the final control structure is shown in Fig. 3.16. A sampling time of 1 min was chosen. During the start-up stage, the outside temperature may be higher than the inside one. This fact may cause that the temperature difference in (3.9) be negative. For this reason, during this period the same control structure is used, but the feedback signal used in the nonlinear mapping is the reference temperature instead of the inside temperature (dashed line in Fig. 3.16), which has many advantages in this phase. Once the outlet temperature reaches the reference, the control scheme is switched to nominal state. The control scheme shown in Fig. 3.16 resembles that of the FF controller analyzed in Sect. 3.1.2.6 [361], that were also based on a simplified physical model of the system, but considering steady-state conditions and a more complex expression of $Q_{\text{ven,a-e}}$. Thus, the main difference with the scheme presented in this section is that now an internal feedback is included both for linearizing and disturbance compensation purposes, providing smother control actions. An AW strategy has also been included to account for possible saturation of the control signal. The physical limits in the vents aperture can be dynamically mapped each sampling time into limits of the virtual control signal $\tilde{U}_{\text{ven}}$ using again the nonlinear mapping represented by Eq. (3.7). As can be seen, the physical limits of the real control signal are transformed into variable constraints of the virtual control signal that depend on the operating conditions. This mechanism has provided very useful results, mainly, during the start-up stage of the operation. All the disturbances (solar radiation, wind speed and outside temperature) are adequately filtered before entering the FL mechanism, to avoid sudden changes in the control signal.

Figure 3.17 shows a representative simulation result when applying the explained technique. As can be seen, the tracking and disturbance compensation properties of the control scheme are acceptable and disturbances, modeling uncertainties, and constraints in the actuator are adequately handled by this control technique through FF action, feedback, and AW, respectively. Notice that using this technique, the controller design can be done using linear techniques. Thus, in this case, the PI controller parameters can be tuned to achieve different control objectives. As pointed out, the main drawback of the scheme is the numerical sensitivity inherent to Eq. (3.9) and the control effort characteristic of FL, being necessary to include a supervisory level to avoid the evaluation of such expression when wind speed is below a threshold or when the outside temperature surpasses the inside one. Crop transpiration parameters were estimated by a physical model based on growth and transpiration models (Eq. (2.44)).

3.2.4 Robust Control of Daytime Temperature

This section deals with the development and implementation of RC techniques based on the quantitative feedback theory (QFT) aimed at achieving desired values of inside greenhouse temperature in spite of uncertainties and disturbances acting on
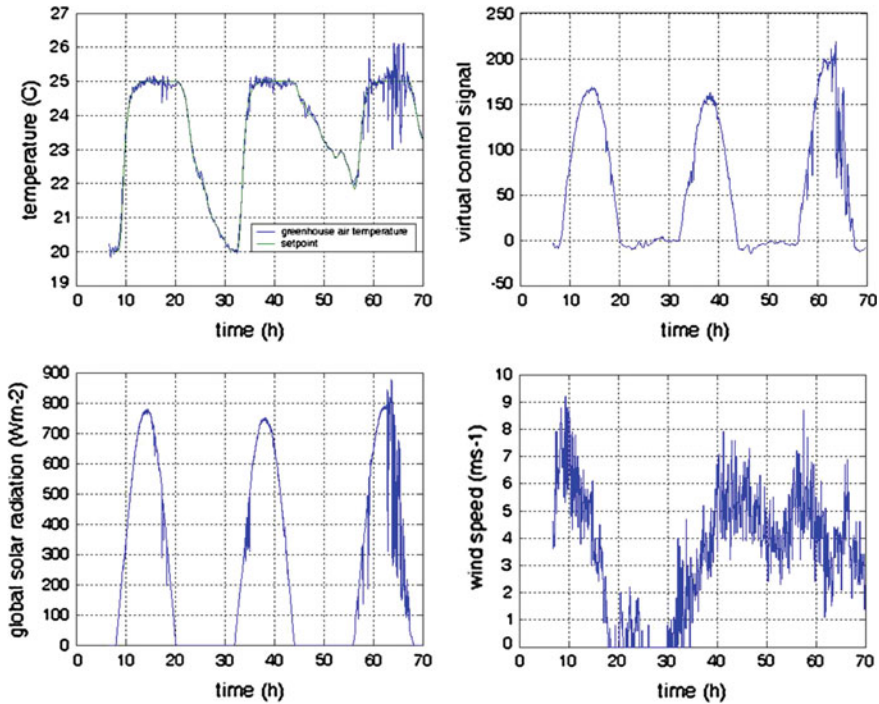
Fig. 3.17 Simulation results with the feedback linearization controller

the system [284]. From the system dynamics point of view, the greenhouse can be considered a smooth dynamical system which dynamics are operating point dependent. The classical approach in QFT method is to include the effect of disturbances as unmodeled dynamics or to formulate the problem as a disturbance rejection one. In the case of greenhouse climate, the disturbances have the important role of being the main energy source in the system and thus, they should be exploited to minimize the energy consumption and to help to achieve the desired set points. A modification to the standard formulation has been performed to include a FF controller previously described in Sect. 3.1.2.6 and AW action in combination with the RC to exploit the effect of measurable disturbances.

Quantitative Feedback Theory (QFT) is a RC design method [189] that uses a two degrees of freedom (2DoF) feedback scheme (Fig. 3.18), where it is assumed that the uncertain system is represented by a transfer function $P(s)$ belonging to a set of plants $\wp$, while $C(s)$ and $F(s)$ are, respectively, the compensator and precompensator to be synthesized in order to meet robust stability and performance specifications.

In QFT, closed loop specifications are given in the frequency domain, in terms of admissible bounds on closed loop transfer functions. Then, specifications are combined with the uncertainty of the system (given in the form of templates) to
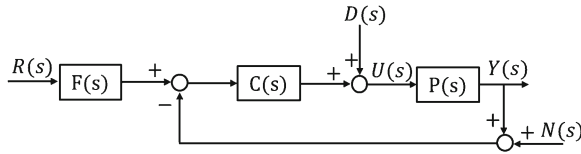
Fig. 3.18 A 2DoF feedback system

obtain limits or boundaries on the frequency shape of the compensator $C(s)$. In addition, nominal specifications are used to shape the precompensator $F(s)$.

The inclusion of the FF term described in Sect. 3.1.2.6 in series with the plant (Fig. 3.10, adding a prefilter F in the reference) helps to explicitly take into account the measured value of the disturbances in such a way that the control signal provided by the feedback controller is the reference temperature to the FF term. Notice that if the model used by the FF term was an exact one, the system constituted by the FF term in series with the plant should have a steady state gain near unity. Unfortunately, the simplicity of the models (fixed coefficients) in comparison with a large complex simulation model of the real system (in which several coefficients change depend on operating conditions) and the uncertainty in the system (it is impossible to exactly model the greenhouse dynamics) advices the use of RC techniques to account for the mentioned sources of uncertainties. To demonstrate this, Fig. 3.19 shows the results obtained when implementing only the FF term in open loop (without feedback controller). As can be seen, due to model mismatches the real behavior presents a different behavior, including offset.

Another feature of the system is that it suffers from frequent saturations of the input signal (vents) due to disturbances and operating point changes and deficient sizing of vents (often occurs), strongly limiting the control bandwidth. Due to this fact, as the controller must include integral action to track the set point temperature, the use of an AW scheme is of advice. In the classical approach, both the vents aperture demanded by the control system and that provided by the saturation block or actuator should feed the AW block. As has been mentioned in the case of FF and
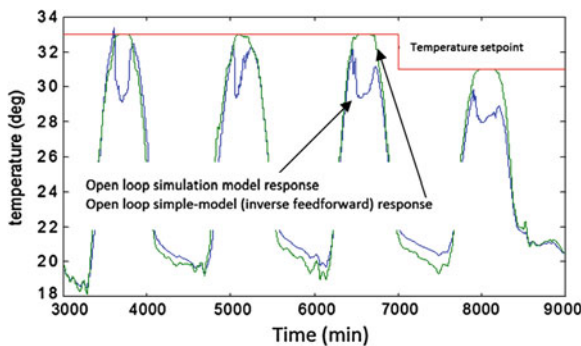

Fig. 3.19 Open loop effect of feedforward action. As a courtesy of the authors [284]

FL approaches, the problem that arises in this application is that the control signal provided by the RC is the reference temperature of the FF controller (Fig. 3.10), which provides the vents aperture depending on the measurements of environmental variables. So, the first input point to the AW block has been displaced to the output of the feedback controller. The drawback of this approach when compared to the classical one is that no conditions can be imposed to guarantee robust stability in the face of saturations, but the performance can be strongly improved, as it is shown in the results.

In order to design the RC a relationship between the FF term input and the greenhouse output has been found. The input–output description of the system constituted by the FF term in series with the plant consists of an uncertain first-order system:

$$P(s) = \frac{c_k}{c_\tau s + 1} \tag{3.10}$$

with $c_k \in [0.3, 10]$ and $c_\tau \in [360, 1{,}080]$ seconds (the delay of 60 s has not been taken into account as it is smaller than the characteristic time constant).

Due to the uncertainty in the system, RC can be used, and Horowitz's method is chosen. The first step in this method is to choose performance and stability specifications. Figure 3.20 shows the performance specifications.

In order to ensure stability of the closed loop, a gain margin of GM = 5 [dB] and phase margin of PM = 45 [°] are desired (ω being frequency in rad s^{-1}):

$$\left| \frac{C(j\omega)P(j\omega)}{1 + C(j\omega)P(j\omega)} \right| \le 2.3 \text{ dB}, \forall P \in \wp, \forall \omega > 0, \tag{3.11}$$

with $\wp = \left\{ \frac{c_k}{c_\tau s + 1} : c_k \in [0.3, 10], c_\tau \in [360, 1080] \right\}$.
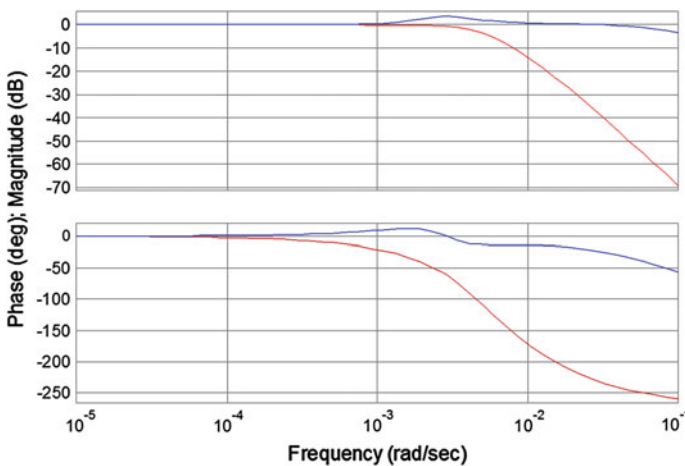

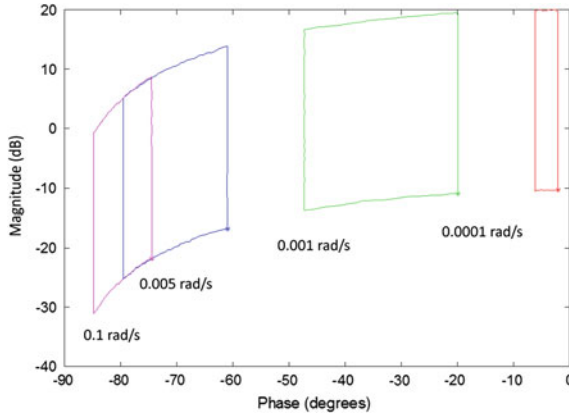**Fig. 3.20** Frequency domain specifications. As a courtesy of the authors [284]

Fig. 3.21 System value sets. As a courtesy of the authors [284]

A controller F, C is designed in order to enclose the closed loop transfer function T from reference to output between envelopes in Fig. 3.20, and the stability specification in Eq. (3.11) is achieved, with

$$T \in \Im = \left\{ F(s) \frac{C(s)P(s)}{1 + C(s)P(s)} : P \in \wp \right\}. \qquad (3.12)$$

In order to proceed with the design of the controller, the value sets [30], which describe the system uncertainty in the Nichols chart, are computed (Fig. 3.21).

Taking into account the typical time constants involved in this problem and specifications, this is a low-frequency problem and so, the selected frequency points [rad s^{-1}] for the design are $W = [0.0001, 0.001, 0.005, 0.01]$, leading to values of $\Delta|T(j\omega)| = [0.0063, 0.6777, 5.5564, 14.7622]$, respectively.

Using the algorithm in [283], the performance and stability boundaries are computed, and the nominal open-loop transfer function (Fig. 3.22) using computer tools [56].

The resulting controller C is given by equation:

$$C(s) = \left(10 + \frac{0.028}{s} \right) \left(\frac{0.021}{s + 0.021} \right) \qquad (3.13)$$

Finally, the precompensator F to achieve the nominal specification is:

$$F(s) = \left(\frac{0.017}{s + 0.0017} \right) \qquad (3.14)$$

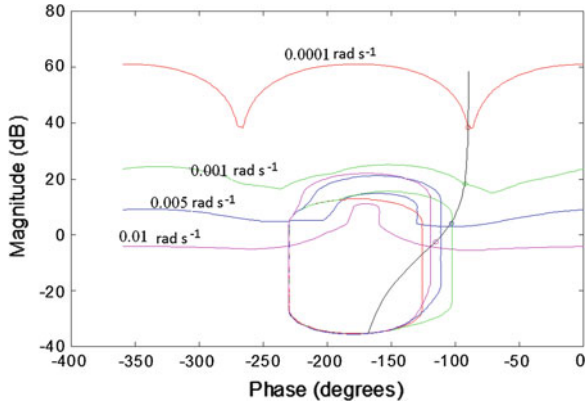Figure 3.23 shows the final result of the design for the considered set of plants $\wp$.

Fig. 3.22 Nominal open loop and bounds at design frequencies in W. As a courtesy of the authors [284]
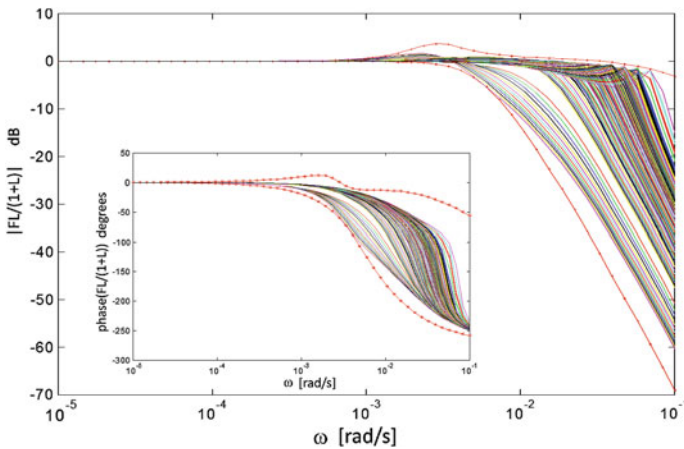

Fig. 3.23 Closed loop specifications (*dashdot*) and frequency responses (*solid*) of the controlled system. As a courtesy of the authors [284]

Some illustrative results of the proposed approach are shown in Fig. 3.24, which represents the evolution of a test covering 13 complete days in summer time with a fixed set point and a shading screen covering the greenhouse. Although the control scheme has been developed for operation during sun-shining conditions, it has not been turned off during the night to show the performance of the AW block even in such strongly adverse situation (the vents are completely closed during the night and so, large feedback errors feed the controller). The evolution of the outside solar radiation corresponds to clear-day conditions, except during the fifth and sixth day in which drops of more than 100 W m^{-2} occurs. Outside temperature conditions are also varying and wind velocity experiments quite large variations during all the
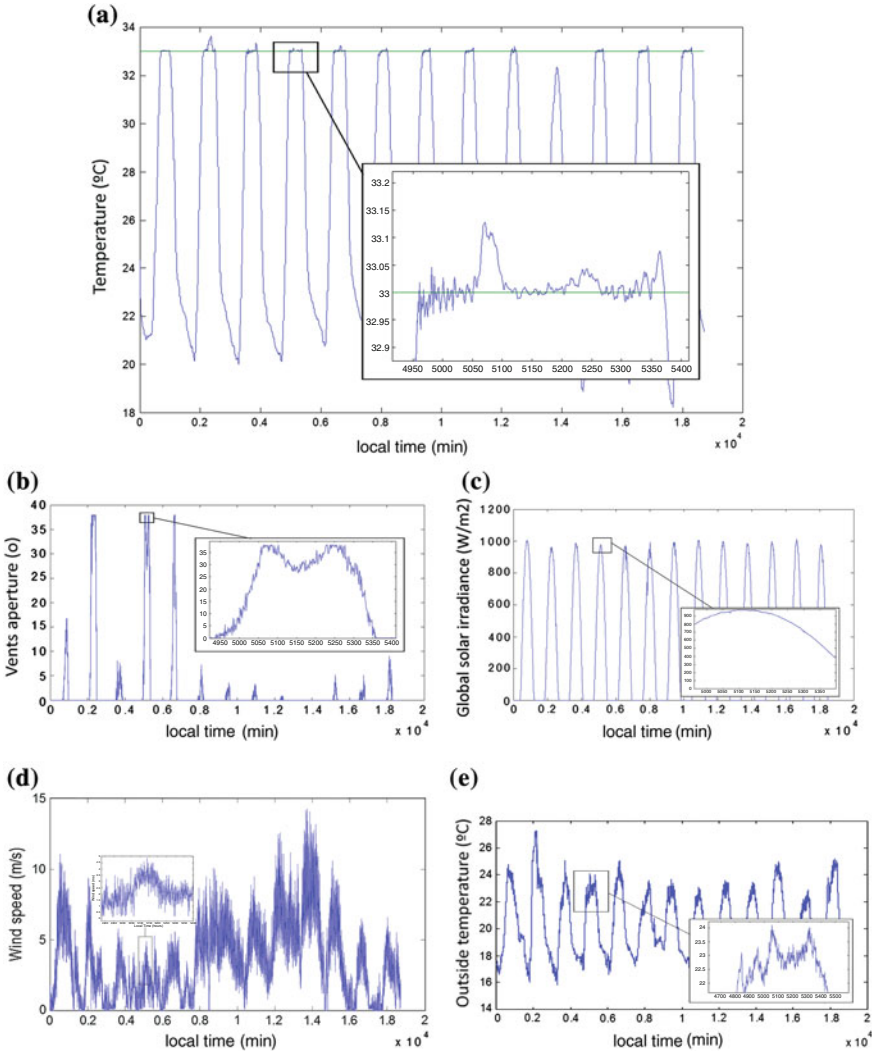
Fig. 3.24 QFT control: Complete 13 days simulation. As a courtesy of the authors [284]. **a** Set point and inside air temperature (°C). **b** Vents aperture (°). **c** Global solar irradiance (W m^{-2}). **d** Outside wind speed (m s^{-1}). **e** Outside temperature (°C)

days, covering values from 0 to 12 m s^{-1} which largely influence the system behavior when vents are opened. Due to the size of the figures, a zoom of a region has been included.

As can be seen, the tracking and disturbance rejection capabilities are adequate in those cases in which the vents are not saturated. When saturation occurs, no degrees of freedom are available to control the temperature. After saturation, the performance
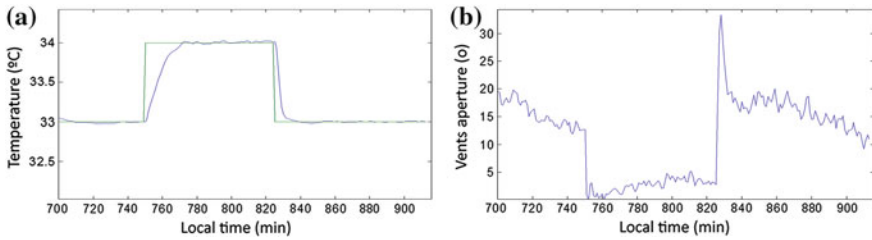
Fig. 3.25 QFT control: Response to set point changes. As a courtesy of the authors [284]. **a** Set point and inside air temperatures (°C). **b** Vents aperture (°)

of the system is quite good, as is expected due to the use of the AW scheme. As can be seen in Fig. 3.24b, the control signal suffers from large excursions covering the whole control range. This figure reflects the main drawback of the approach used in this section: As the controller tends to quickly react to changes in disturbances (mainly due to the structure of the FF term), the control system is prone to overactuate, thus increasing electricity costs associated to the motors moving the vents (even when filtering the disturbances before entering the FF term). The design can be improved by finding a trade-off between fast tracking and associated costs (by including stronger filters within the FF term or by including design restrictions in the control effort).

Figure 3.25 shows typical responses to set point changes and Fig. 3.26 shows the disturbance rejection capabilities of the system. Figure 3.25 corresponds to wind speed conditions of 7 m s^{-1} and clear-day solar radiation between 900 and 1,000 W m^{-2}. Set point changes of ± 2 °C have been performed around 33 °C. Due to the nonlinear nature of the system, different closed-loop time constants are obtained, but lying inside the specifications, even in the case in which the model used to develop the FF term is not a good approximation of the real system. Figure 3.26 shows the response under passing clouds and varying low wind speed conditions. It can be seen how the control system quickly reacts to changes in solar radiation in order to compensate for the temperature drop following a cloud (tracking error less than 0.5 °C).

3.2.5 Optimal Control

The problem of optimal control of greenhouse crop growth has been treated in an excellent way in the book by van Straten et al. [431] using the theory of optimal greenhouse climate control [22, 132], so this approach is not treated in this book, where the models and control approaches are different to tackle the greenhouse crop growth control problem from a hierarchical point of view. Some comments on this will be given in Chap. 4.
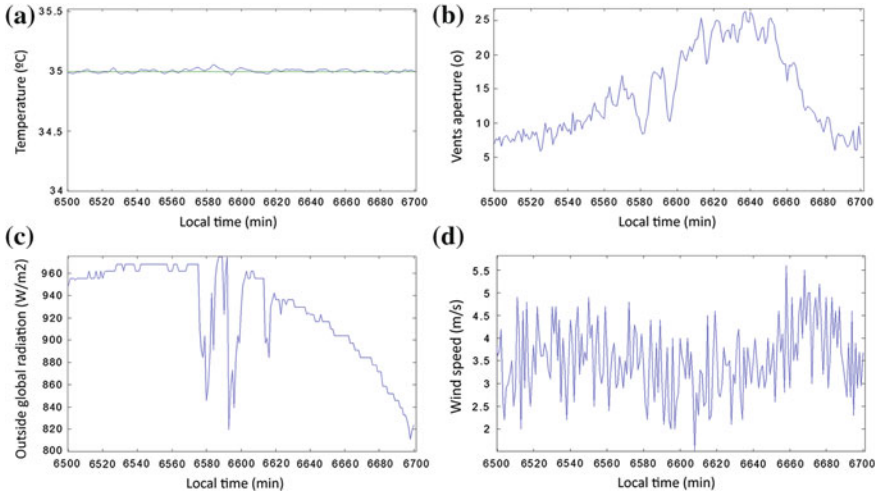
Fig. 3.26 QFT control: Disturbance response capabilities. As a courtesy of the authors [284]. **a** Set point and inside air temperature (°C). **b** Vents aperture (°). **c** Outside global solar radiance ($\mathrm{W\,m^{-2}}$). **d** Wind speed ($\mathrm{m\,s^{-1}}$)

The book [431] treats physical modeling of greenhouse climate in response to heating, ventilation, and other control variables with the biological modeling of variables such as plant evapotranspiration and growth. It includes the design of integrated optimal controllers that exploit rather than mitigate outside weather conditions, especially sunlight, given widely different time scales. The book reviews classical rule-based and multivariable feedback controllers in comparison with the optimal hierarchical control paradigm. Relevant references are: [7, 34, 132, 159, 177, 200, 202, 255, 428, 430, 432, 441, 442, 443, 447] and recent developments in that field can be found in [147].

3.2.6 Model Predictive Control of Daytime Temperature

In this section, several MPC approaches are presented to handle both daytime and nighttime temperature control of greenhouses. The daytime temperature is controlled using natural ventilation, while nighttime temperature control is performed using heating systems.

3.2.6.1 Daytime Temperature Control Using Generalized Predictive Control

As has been pointed out in previous sections, the climatic control problem in greenhouses is characterized by frequent actuator saturation, due to energy source and greenhouse structure layout characteristics. An MPC combined with a FF compensator is used in this section to face both disturbance and actuators saturation. As has been commented in the previous sections, the treatment of input constraints is usually addressed by means of AW techniques. Taking care about control signal constraints is very important when dealing with greenhouses climate control problems, because actuators suffer saturation continuously during daily operation. Therefore, this section is focused on the development of a predictive control algorithm (Generalized Predictive Control GPC is used in this case [73, 91]) in series with the FF controller developed in Sect. 3.1.2.6 to regulate the greenhouse inside temperature during the daytime period. The proposed control scheme helps to compensate process disturbances and adequately manage the input constraints [354]. Since the predictive control algorithm has not direct access to the control signal, because of the feedforwad is placed in series, a constraint mapping strategy [234, 351] is applied to translate the real input constraints to restrictions in the FF input along the control horizon, which can be managed by the predictive control algorithm. Figure 3.27 shows the combination of both systems. In this case, GPC internal model will be obtained taking into account the whole system shown above (Fig. 3.27). Moreover, as mentioned previously, adding FF controller to greenhouse in series makes it possible to obtain whole system linear models with nearly unitary gain and uncertainties that will be compensated by feedback controller.

GPC uses a model of the process and at each sampling instant, the future outputs are predicted for a given horizon ($\hat{Y}(t + j|t)$, $j = 1 \dots N$, t being the current sampling instant) and substituted within an objective function to compute the future controls ($U(t + j|t)$, $j = 0 \dots N - 1$), while taking process constraints into account. Following the receding horizon approach, the first control signal calculated is implemented and then the horizon is moved ahead and the procedure is repeated in the
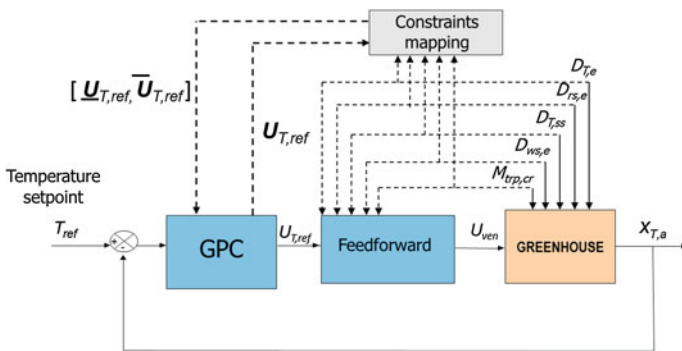

Fig. 3.27 Greenhouse control scheme using constrains mapping

next sampling instant as the new output is known (all the sequences are updated). A Controlled Autoregressive Integrated Moving Average (CARIMA) model [91] has been used obtained from transfer functions relating greenhouse temperature ($Y(t) = X_{T,a}(t)$) to changes in reference temperature of FF term ($U(t) = U_{T,\text{ref}}(t)$) and disturbances when operating around a particular set point. Both empirical transfer functions obtained by linearization of the full nonlinear climate model developed in Chap. 2 [355] have been used and integrated in the CARIMA model:

$$A(z^{-1})Y(t) = B(z^{-1})U(t-1) + D(z^{-1})D_m(t) + \frac{e(t)}{\Delta} \qquad (3.15)$$

where the variable $D_m(t)$ is the measured disturbance at discrete time t, $e(t)$ is a zero mean white noise, A, B, and D are adequate polynomials in the backward shift operator z^{-1}, and $\Delta = 1 - z^{-1}$.

The classical GPC cost function has been implemented and constraints have been taken into account [160].

$$J = \sum_{j=N_1}^{N_2} \delta(j)(\hat{Y}(t+j|t) - W(t+j))^2 + \sum_{j=1}^{N_u} \lambda(j)\Delta U(t+j-1)^2 \qquad (3.16)$$

In this cost function, $\hat{Y}(t+j|t)$ is an optimal system output prediction sequence performed with data known up to instant t, $\Delta U(t+j-1)$ is a sequence of future control increments, obtained from cost function minimization, N_1 and N_2 are the minimum and maximum prediction horizons, N_u is the control horizon, and $\lambda(j)$ and $\delta(j)$ are weighting sequences that penalize the future tracking and control efforts, respectively, along the horizons (in the applications shown in this book δ equals 1 and λ is a user-chosen constant). The reference trajectory $W(t+j)$ can be the set point itself or a smooth approximation from the present value of output $Y(t)$ to the set point, usually implemented as a first-order filter. If no constraints are taken into account, as the model is linear and the optimization criterion is quadratic, an explicit solution can be found. Otherwise, a quadratic programming (QP) optimization algorithm is used [73].

In the daytime greenhouse climate control problem, the main constraint is the vents aperture:

$$\underline{U}_{\text{ven}} = 0\,\% \le U_{\text{ven}} \le 100\,\% = \overline{U}_{\text{ven}} \qquad (3.17)$$

As well known, predictive control provides a clear constrains management, as it is possible to include systematic constraint handling during the design phase. The GPC algorithm described in the paragraph above is used for this purpose. Nevertheless, in this case the predictive algorithm uses the reference temperature of the FF controller as the control input, $U_{T,\text{ref}}$, which has to be mapped into the real control signal (the vents aperture). This method implies that, although the output constraints do not vary, the control signal (U_{ven}) constraints must be mapped into virtual signal ($U_{T,\text{ref}}$) constrains, as done in the case of the FL controller. This idea is shown in Fig. 3.27,

where the GPC algorithm provides a vector, $\mathbf{U}_{T,\text{ref}}$, with the future predictions of the reference temperature to the FF controller, which along with the current state and disturbances, are used to recalculate the mapped constraints, $[\underline{\mathbf{U}}_{T,\text{ref}}, \overline{\mathbf{U}}_{T,\text{ref}}]$, at each sampling time [351].

Before addressing the mapping algorithm, it is necessary to obtain the inverse function providing a mapping between real saturation signals into FF input saturation signals. Using the same approach followed in the development of the FF controller in Sect. 3.1.2.6 but using the simplified model of ventilation rate given by Eq. (3.4), already used in the FL control, the following expression can be obtained relating the vents aperture with the reference temperature to the FF term ($U_{\text{ven}} = \Phi(U_{T,\text{ref}}, \underbrace{D_{\text{rs,e}}, X_{T,\text{ss}}, D_{T,\text{e}}, D_{\text{ws,e}}}_{D_m})$):

$$\Phi^{-1}(U_{\text{ven}}, D_m) = U_{T,\text{ref}} = \frac{n_{\text{ref}}}{d_{\text{ref}}} \qquad (3.18)$$

$$n_{\text{ref}} = c_{\text{rs,a}} D_{\text{rs,e}} + c_{\text{cnv,ss-a}} D_{T,\text{ss}} - c_{\text{cnd-cnv,a-e}} D_{T,\text{e}}$$
$$+ \frac{c_{ter,\text{a}}}{c_{\text{vol,g}}} (c_{\text{ven,n}} c_{ven,1} c_{\text{ven,w}} D_{\text{ws,e}} (\alpha_{\text{v}} U_{\text{ven}}^{\beta_{\text{v}}}) + V_{\text{loss}}) D_{T,\text{e}} - V_{\text{lt,vap}} M_{\text{trp,cr}}$$
$$d_{\text{ref}} = c_{\text{cnv,ss-a}} - c_{\text{cnd-cnv,a-e}} + c_{\text{ven,n}} c_{ven,1} c_{\text{ven,w}} D_{\text{ws,e}} (\alpha_{\text{v}} U_{\text{ven}}^{\beta_{\text{v}}}) + V_{\text{loss}}$$

There are different ways to solve the mapping problem of combining predictive and feeforward control techniques considering input constraints. A simple solution would be to place a conservative limit on the range of the virtual control signal so the system never reaches saturation. This choice could be applied when FF input to the real control signal mapping varies within a narrow range, that is, low disturbances variability:

$$\underline{U}_{T,\text{ref}} = \Phi^{-1}(\overline{U}_{\text{ven}}, D_m)$$
$$\overline{U}_{T,\text{ref}} = \Phi^{-1}(\underline{U}_{\text{ven}}, D_m) \qquad (3.19)$$

However, if the FF input signal limits are not properly chosen, the control may be too conservative or too aggressive. Second, alternative lays on obtaining, for each instant in the control horizon, a pair of virtual saturation limit values using GPC future control signals to get future narrowest constraint bands. Assuming GPC algorithm is developed using a linear system, the objective lays on finding future constraints over $U_{T,\text{ref}}$ (see Fig. 3.27) along control horizon, the control signal sequence generated by GPC at $t - 1$ can be described as [234, 351]:

$$\mathbf{U}_{T,\text{ref}}(t-1|t-1) = [U_{T,\text{ref}}(t-1|t-1), U_{T,\text{ref}}(t|t-1), \ldots, U_{T,\text{ref}}(t+N_u-2|t-1)] \qquad (3.20)$$

whereas the first element in sequence $U_{T,\text{ref}}(t - 1|t - 1)$ is used to evaluate the control signal $U_{\text{ven}}(t - 1)$ by means of Φ transformation, the following elements may be used to make estimations of the future state variables (using an estimation of

future disturbances, usually considering them equal to the last measured value) from the discretized version of the linear system describing system dynamics, as shown in [351]. Therefore, each constraint band value can be obtained as a solution of the optimization problem described in [351] and considering the different disturbances constant along the control horizon. This solution can be represented as:

$$
\begin{aligned}
\underline{\mathbf{U}}_{T,\text{ref}} &= \Phi^{-1}(\max{(\overline{U}_{\text{ven}}, \Phi(\mathbf{U}_{T,\text{ref}}))}) \\
\overline{\mathbf{U}}_{T,\text{ref}} &= \Phi^{-1}(\min{(\underline{U}_{\text{ven}}, \Phi(\mathbf{U}_{T,\text{ref}}))})
\end{aligned}
\tag{3.21}
$$

After performing several tests in open loop, the GPC internal model was approximated as a FOPDT system representing the FF controller in series with the real plant. GPC parameters were obtained by testing and resulted in $N_1 = 2$, $N_2 = 8$, $N_u = 6$, $\delta = 1$, and $\lambda = 1$, with a sampling period of 1 min. In order to show the advantages of the control solution, the results are compared to the case where conservative constraints are considered along the horizon. For this study, the chosen simulation disturbances correspond to data recorded on April 6, 2009, where disturbances for 2 full days are evaluated. Figure 3.28 shows the control results for these 2 days using both strategies, GPC + FF with constant constrains mapping using conservative limits in the GPC control signal, and on the other hand, GPC + FF with online constrains mapping. As it can be seen from the figure, both control strategies work properly reaching the reference signal despite of the changing disturbances. The main difference between both cases can be observed at the beginning of the steps. The case with constant mapping is lower saturated because of the conservative limits. However, the GPC + FF using online mapping reaches the reference softly without going into saturation, since the saturation limits are changing depending on the inner temperature and disturbances values. Real results of the application of this approach can be found in [354].

The previous control strategy can be modified to try to better account for measurable disturbances in the prediction horizon. This GPC control architecture can be extended using DES (see Sect. 2.4.2) technique to perform future disturbance estimation [322]. In what follows, the disturbance models are obtained, validated, and embedded within a GPC controller to compensate for future disturbances. The proposed system is compared with a typical GPC without FF action, the GPC with FF considering constant disturbances in the future explained in the previous paragraphs, and a GPC with FF taking the original real data in the future. The proposed control scheme is tested by simulation of a greenhouse inside temperature control. The obtained results show that the GPC with disturbance forecasting provide improved behavior that standard techniques.

As has been mentioned in Sect. 2.4.2, there are many methods to estimate disturbances and they can be characterized by the prediction horizon length and the selected methodology. The prediction horizon can vary depending on the application and it can be considered as short-term for prediction up to 60 min [345], or long-term forecast for hourly, daily, and monthly prediction values [270]. On the other hand, the disturbance variables are usually represented as time-series structures due mainly to
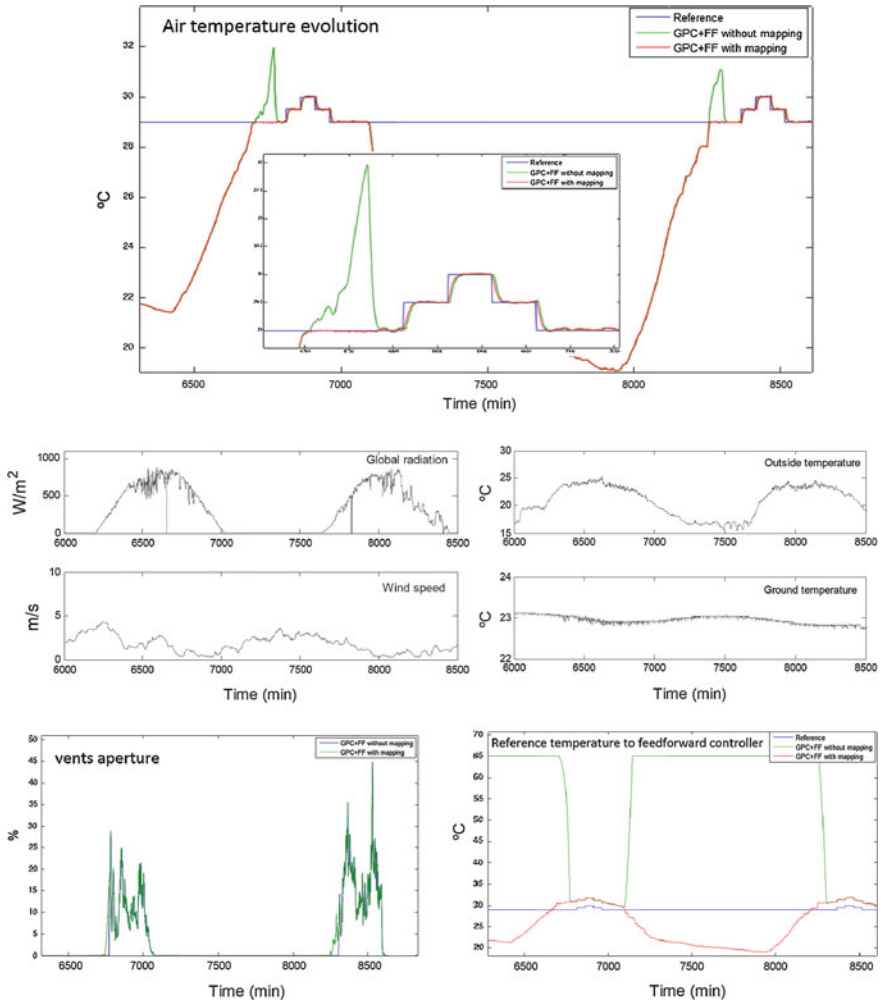
Fig. 3.28 Simulation results with GPC control. As a courtesy of the authors [354]

their stochastic behavior. Time-series models are one of the ways to estimate future values of disturbances. These models are obtained using past data and are used to estimate the future behavior along a prediction horizon [345]. Time-series models are based on the assumption that the modeled data are autocorrelated and characterized by trends and seasonal variations. Thus, well-known autocorrelated models (ARMA, ARIMA, ARMAX, ARIMAX) could be also used for disturbance estimation [345]. Furthermore, ANN also provides a good solution to perform estimations because its design is based on training and no statistical assumptions are needed for the source data.

The DES technique explained in [323] is used here for short-term disturbance estimation and it is described by the following equations [297]:

$$S(t) = \alpha_d D_m(t) + (1 - \alpha_d)(S(t-1) + M(t-1)) \tag{3.22}$$

$$M(t) = \gamma_d(S(t) - S(t-1)) + (1 - \gamma_d)M(t-1) \tag{3.23}$$

where $D_m(t)$ is actual disturbance signal value, $S(t)$ is the unadjusted forecast, $M(t)$ is the estimated trend, α_d is the smoothing parameter for data, and γ_d is the smoothing parameter for trend. Note that the current value of the series is used to calculate its smoothed value replacement in DES. The one-period-ahead forecast is given by:

$$\hat{D}_m(t+1) = S(t) + M(t) \tag{3.24}$$

and the j-periods-ahead forecast is given by:

$$\hat{D}_m(t+j) = S(t) + jM(t) \tag{3.25}$$

There are a variety of schemes to set initial values for $S(t)$ and $M(t)$ in double smoothing, but for this section $S(t_0) = D_m(1)$ and $M(t_0) = (D_m(1) + D_m(2) + xD_m(3))/3$ have been chosen as suggested in [297]. The first smoothing equation adjusts $S(t)$ directly for the trend of the previous period, $M(t-1)$, by adding it to the last smoothed value, $S(t-1)$. This helps to eliminate the lag and brings $S(t)$ to the appropriated base of the current value. Then, the second smoothing equation updates the trend, which is expressed as the difference between the last two values. The equation is similar to the basic form of single smoothing, but here it is applied to the updating of the trend. The values for α_d and $\gamma_d \in (0, 1)$ can be obtained via optimization techniques as described in [297].

The GPC approach has been the same described by cost function (3.16) and CARIMA model (3.15). When using this model to obtain a prediction of the system output in the prediction horizon, the second term of the right hand of Eq. (3.15) will include the effect of future measurable disturbances. In some cases, when related to the process load, future disturbance are known. In other cases, they can be predicted using trends or other means. If this is the case, the term corresponding to future deterministic disturbance can be computed. If the future load disturbances are supported to be constant and equal to the last measured value (i.e., $D_m(t+j) = D_m(t)$), then $\Delta D_m(t+j) = 0$ and the second term of this equation vanishes. Notice that this is not the case of the work presented in this section, since future behavior of the disturbances will be estimated using the DES technique.

Consider a set of N ahead predictions [73] with different prediction ($N = N_2$), control (N_u), and disturbance estimation (N_d) horizons [322]:

$$
\underbrace{\begin{bmatrix} \hat{Y}(t+1|t) \\ \hat{Y}(t+2|t) \\ \vdots \\ \hat{Y}(t+j|t) \\ \vdots \\ \hat{Y}(t+N|t) \end{bmatrix}}_{\mathbf{Y}} = \underbrace{\begin{bmatrix} g_0 & 0 & \cdots & 0 \\ g_1 & g_0 & \cdots & 0 \\ \vdots & \vdots & \ddots & \vdots \\ g_{j-1} & g_{j-2} & \cdots & g_0 \\ \vdots & \vdots & \vdots & \vdots \\ g_{N-1} & g_{N-2} & \cdots & g_{N-N_u} \end{bmatrix}}_{\mathbf{G}} \underbrace{\begin{bmatrix} \Delta U(t) \\ \Delta U(t+1) \\ \vdots \\ \Delta U(t+j-1) \\ \vdots \\ \Delta U(t+N_u-1) \end{bmatrix}}_{\Delta \mathbf{U}}
$$

$$
+ \underbrace{\begin{bmatrix} h_0 & 0 & \cdots & 0 \\ h_1 & h_0 & \cdots & 0 \\ \vdots & \vdots & \ddots & \vdots \\ h_{j-1} & \cdots & h_1 & h_0 \\ \vdots & \vdots & \vdots & \ddots \\ h_{N-1} & \cdots & \cdots & h_{N-N_d} \end{bmatrix}}_{\mathbf{H}} \underbrace{\begin{bmatrix} \Delta D_m(t+1) \\ \Delta D_m(t+2) \\ \vdots \\ \Delta D_m(t+j) \\ \vdots \\ \Delta D_m(t+N_d) \end{bmatrix}}_{\Delta \mathbf{D}_m} + \underbrace{\begin{bmatrix} f_1 \\ f_2 \\ \vdots \\ f_j \\ \vdots \\ f_N \end{bmatrix}}_{\mathbf{F}} \tag{3.26}
$$

$g_0 \ldots g_{N-1}$ being the step response coefficients of the system, $h_0 \ldots h_{N-N_1}$ the coefficients of the system step response to the disturbance, and $f_1 \ldots f_N$ the free response coefficients of the system.

If future disturbances are known or can be estimated, by making $\mathbf{F}' = \mathbf{H} \Delta \mathbf{D}_m + \mathbf{F}$, the prediction equation is now:

$$
\mathbf{Y} = \mathbf{G} \Delta \mathbf{U} + \mathbf{F}' \tag{3.27}
$$

which has the same shape as the general prediction equation used in the disturbance-free case. The future control signal can be found in the same way simply using as free response the process response due to initial condition (including external disturbances) and future "known" disturbances [73].

In order to implement this technique, the inside temperature greenhouse process is considered as MISO (Multi Input Single Output) system, where soil temperature ($D_{m1}(t) = D_{T,\text{ss}}(t)$), solar radiation ($D_{m2}(t) = D_{\text{rs,e}}(t)$), wind velocity ($D_{m3}(t) = D_{\text{ws,e}}(t)$), outside temperature ($D_{m4}(t) = D_{T,\text{e}}(t)$), and vents opening percentage ($U(t) = U_{\text{ven}}(t)$) are the input variables and the inside temperature ($Y(t) = X_{T,\text{a}}(t)$) is the output variable (see Fig. 3.29). In this case, only vents opening variable can be controlled and the rest of variables are considered measurable disturbances. Notice that wind velocity is characterized by fast changes in its dynamics, solar radiation is a combination of smooth dynamics (solar cycle) and fast dynamics (caused by passing clouds). Soil temperature and outside temperature are characterized by slow changes. As was presented in previous section, GPC scheme can consider measurable disturbances, but to take the full advantage of this feature is necessary to "know" the future disturbances.
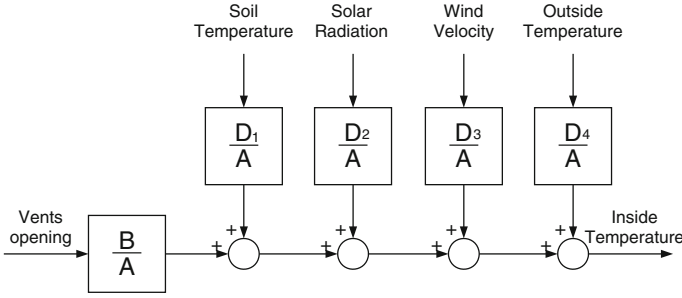
Fig. 3.29 Greenhouse's process model with disturbances for daytime temperature control. As a courtesy of the authors [322]

Considering all mentioned process properties, the CARIMA model can be expressed as follows:

$$A(z^{-1})Y(t) = B(z^{-1})U(t-1) + \sum_{i=1}^{4} D_i(z^{-1})D_{mi}(t) + \frac{e(t)}{\Delta} \tag{3.28}$$

Many experiments have been carried out through several days where a combination of PRBS and step-based input signals were applied at different operating points. It was observed that the ARX model using AIC as information criterion (see Sect. 2.1.3.2) presents better adjustment to the dynamic behavior of the real system. This fact is confirmed by cross-correlation and residuals analysis, obtaining best-fit model of 92.53 %. The following discrete-time polynomials were obtained as the results of estimation around 25 °C (see Fig. 3.29):

$$
\begin{aligned}
A(z^{-1}) &= 1 - 0.3682z^{-1} \\
B(z^{-1}) &= -0.0402z^{-2} - 0.0027z^{-3} \\
D_1(z^{-1}) &= 0.1989z^{-2} + 0.0924z^{-3} + 0.1614z^{-4} \\
D_2(z^{-1}) &= 0.0001z^{-1} + 0.0067z^{-2} + 0.0002z^{-3} \\
D_3(z^{-1}) &= -0.0002z^{-1} - 0.3618z^{-2} + 0.0175z^{-3} \\
D_4(z^{-1}) &= 0.0525z^{-1} + 0.3306z^{-2} + 0.0058z^{-3}
\end{aligned}
$$

Forecasting results: To perform the forecasts, the DES technique is used. This method has been implemented to estimate the future N_d values for each measurable disturbance. This action is repeated every sampling period for each disturbance variable obtaining the corresponding future forecast vectors $D_{m1} \ldots D_{m4}$. The matrices $\mathbf{H}_1 \ldots \mathbf{H}_4$ are calculated containing the coefficients of the system step response to the disturbances. Then, these matrices are included in the calculation of the free response $\mathbf{F}' = \mathbf{H} + \mathbf{F}$, where $\mathbf{H} = \mathbf{H}_1 \Delta \mathbf{D}_{m1} + \mathbf{H}_2 \Delta \mathbf{D}_{m2} + \mathbf{H}_3 \Delta \mathbf{D}_{m3} + \mathbf{H}_4 \Delta \mathbf{D}_{m4}$.
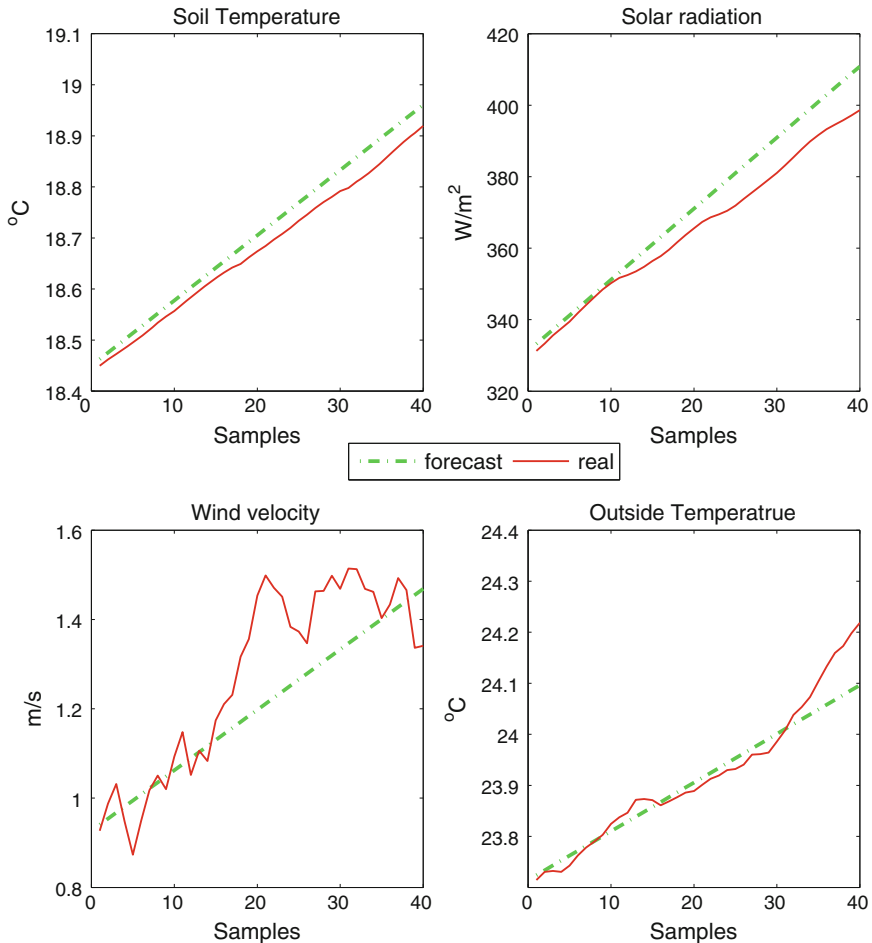
Fig. 3.30 Example of online prediction with the DES technique. As a courtesy of the authors [322]

Figure 3.30 shows the online prediction performed every sampling period for the different disturbances. Notice that a low-pass filter is used to filter all the real measurement before the DES processing due to noisy measurements. As it can be observed, variables with lower changing dynamics have been predicted with better accuracy. Wind velocity signal is characterized by a very noisy dynamics, and its prediction performance is worst but still acceptable [323]. It can be observed that future prediction (green line) acts as a filtered version of the real signal and approximates properly the future evaluation for each measurable disturbance (red line).

Control simulation results: To show the benefits of GPC control scheme with consideration of measurable disturbances, four control architectures have been simulated

in order to compare the results and observe the advantages of the proposed control scheme:

- "GPC"—generic GPC algorithm without consideration of measurable disturbances.
- "GPC + const."—GPC controller with disturbance models (implicit FF action) and the disturbance is kept constant along the prediction horizon.
- "GPC + real"—the real future values of the inputs variables (taken from the acquired data at the greenhouse) are provided in order to obtain optimal predictions (implicit FF action).
- "GPC + DES"—the GPC controller with disturbance models (implicit FF action) where the disturbances are estimated with the DES technique.

The simulations have been performed for 19 days from winter season with different disturbance profiles. Temperature set point was set to 25 °C for daytime period. The controller parameters were set to $N_1 = 1$, $N = N_d = 40$, $N_u = 10$, $\lambda = 1$, and $\delta = 1$. The GPC parameters have been selected after different simulations to provide good performance and the prediction horizon $N = 40$ to cover a time window in which disturbances may vary significantly. The DES technique parameters were $\alpha_d = 0.99$ and $\gamma_d = 0.1$. Due to physical limitation of actuators, GPC control scheme was implemented with constrains on control signal: $0 < U(t) < 100 \%$ $\forall t$ using QP optimization.

Figure 3.31 presents the control results for the 14 day. This day is characterized by a moderate wind speed and a clear sky. For this day, as expected, "GPC" scheme obtains the worst performance. "GPC + const." slightly improves the results from generic GPC, but the best performance is obtained for the controllers considering future knowledge of the disturbances. Analyzing the control signals, it can be observed that the controllers using information about the future behavior of disturbances react in advance to those without using future disturbance information.

Figure 3.32 shows the control results for 18th day, during this day the solar radiation was highly altered by passing clouds, what had direct influence on greenhouse inside temperature. As in the previously analyzed day the controllers with the future disturbance information obtains better results than "GPC" and "GPC + const". Passing clouds produce control signal change, and as can be observed "GPC + DES" reacts faster than other controllers. Also for this simulation day, "GPC + DES" controller shows that disturbance rejection can be improved by the estimation of future disturbances.

The control performance along the nineteen simulation days is summarized in Table 3.4, where the Integrated Absolute Error (IAE) is used as performance index. In this study, the prediction horizon $N = N_d$ has been modified in order to observe how this modification affects to the future disturbances estimations and system performance. Notice that as the prediction horizon increases, better performance is obtained for those techniques considering future knowledge of the disturbances. Table 3.4 shows that "GPC + DES" presents the best result even outperforming "GPC + real". This somewhat surprising fact may be related with the future degrees of freedom
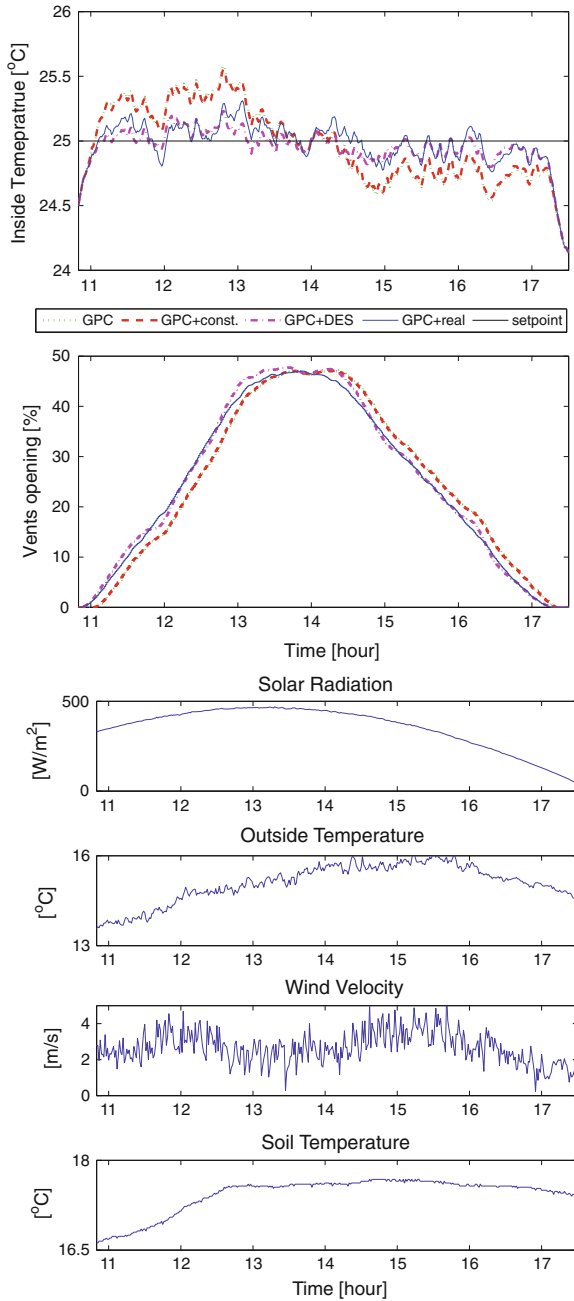
Fig. 3.31 Details of control performance for the 14 day. As a courtesy of the authors [322]
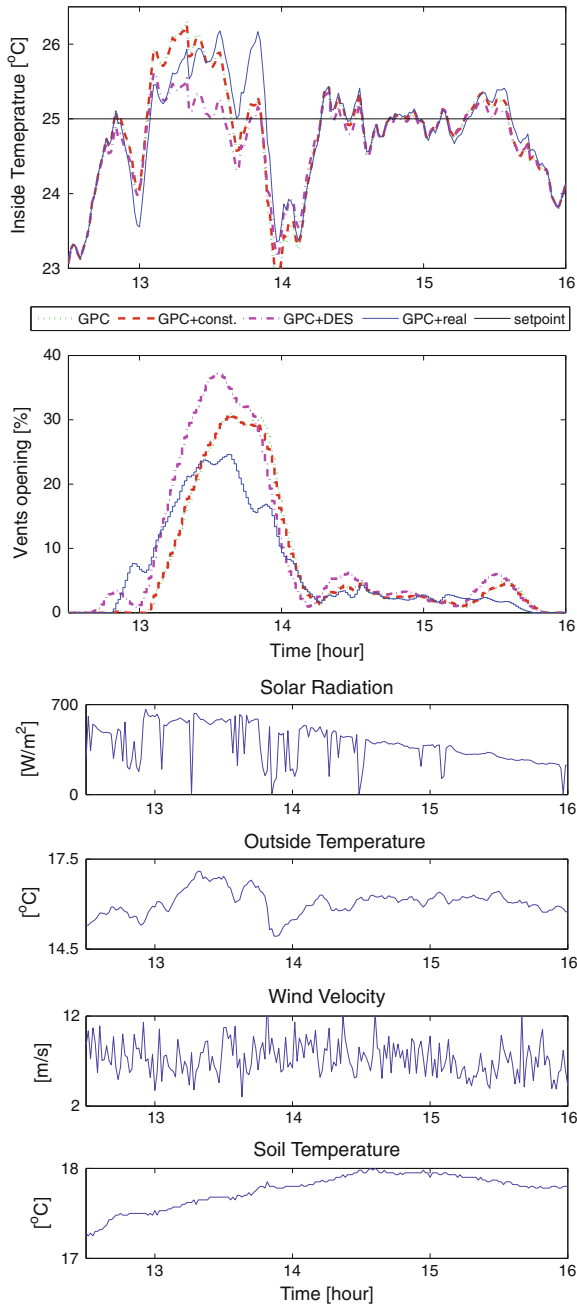
Fig. 3.32 Details of control performance for the 18th day. As a courtesy of the authors [322]

Table 3.4 Performance comparison using the IAE index for the 19th simulation days with $N_u = 10$

Prediction horizon	GPC	GPC + constant	GPC + real	GPC + DES
10	2275.0	2198.9	1931.1	1915.7
15	1971.1	1887.1	1472.3	1420.1
20	1848.1	1760.7	1260.0	1149.7
25	1794.4	1705.4	1163.3	992.0
30	1770.1	1680.4	1121.3	899.5
35	1759.0	1669.0	1103.4	844.5
40	1753.9	1663.7	1096.6	812.8

(control moves) required to account for changes in future values of the fourth disturbances. The filtering effect introduced by the DES technique helps to reduce control variability (the real disturbance signals contain local variations along the prediction horizon requiring more control effort). In Table 3.4 it can be observed that when N decreases, the performance of GPC + real and GPC + DES converge. For $N_u = N_d = N = 40$, GPC + real provides a value of the IAE index of 1,068, while GPC + DES provides 737. The comparison of both techniques depends on the values of the tuning knobs used in the GPC algorithm.

The previous results can be even improved by taking into consideration the approach presented in [317], where first, it is analyzed how the unconstrained GPC algorithm with implicit disturbance compensation can be interpreted as a typical feedback plus FF control scheme, where the main feature is that the FF action includes future estimations of the measurable disturbances. Then, it is shown that classical GPC cannot always eliminate the effect of measurable disturbances even using perfect disturbance models and having exact disturbance estimations along the prediction horizon. To overcome this problem, a particular GPC-tuning condition is proposed, which allows the improved GPC controller to eliminate the disturbance effect even in those cases where causality and instability problems can appear in the relation between the dynamics of the load disturbance and the process output with the dynamics of the control signal and the process output. Since the new tuning condition for disturbance compensation in GPC leads to a high bandwidth in the feedback loop, a two degrees of freedom control scheme within the Filtered Smith Predictor (FSP)-based GPC framework can be implemented to improve the robustness capabilities of the control law. In [317], results in greenhouse climate control problem are provided.

3.2.6.2 Daytime Temperature Control Using Nonlinear MPC Based on a Volterra Series

This section summarizes the design of a nonlinear model predictive control (NMPC) strategy for greenhouse temperature control using natural ventilation. The NMPC

strategy is based on a second-order Volterra series model (Sect. 2.1.3.4) identified from experimental input/output data of a greenhouse in [154].

The use of a nonlinear model changes the predictive control problem from a convex quadratic program to a nonconvex nonlinear problem, which is much more difficult to solve. Furthermore, in this situation there is no guarantee that the global optimum can be found, especially in real-time control, when the optimum has to be obtained in a prescribed time. The solution of this problem requires the consideration (and at least a partial solution) of a nonconvex, nonlinear problem (NLP), which gives rise to computational difficulties related to the expense and reliability of solving the NLP online. Nevertheless, when the process is described by a Volterra series model, efficient solutions for the MPC problem can be found [114, 252, 263]. This solution makes use of the particular structure of the model, giving an online feasible solution. The main advantage about the use of Volterra series models relies on the fact that being a natural extension of linear convolution models, they are quite straight-forward to obtain from input/output data without any prior consideration about the process-model structure. Being linear in the parameters, Volterra series models can be identified using the LS method. Hence, in this section the ability to capture non-linear dynamics of the process by a Volterra series model and its use in NMPC of the greenhouse temperature are shown. Preliminary versions of this work presented a Volterra series model of the greenhouse climate only for autumn seasons [156], which was used to design an NMPC strategy being validated by simulations for this same period [153].

A SISO second-order Volterra series model, with the truncation of terms (truncation orders N_1 and N_2), is defined by Eq. (2.77). Analogously, a second-order Volterra series model with 1 input and n measurable disturbances can be given by:

$$Y(t) = h_0 + \sum_{i=1}^{N_{1,u}} a_u(i) U(t-i) + \sum_{i=1}^{N_{2,u}} \sum_{j=i}^{N_{2,u}} b_u(i,j) U(t-i) U(t-j) \qquad (3.29)$$

$$+ \sum_{m=1}^{n} \sum_{i=1}^{N_{1,d_m}} a_{d_m}(i) D_m(t-i) + \sum_{m=1}^{n} \sum_{i=1}^{N_{2,d_m}} \sum_{j=i}^{N_{2,d_m}} b_{d_m}(i,j) D_m(t-i) D_m(t-j)$$

where D_m represents the measurable disturbances, and N_{1,d_m} and N_{2,d_m} denote the corresponding truncation orders. The linear and nonlinear truncation orders with respect to the input U are denoted with $N_{1,u}$ and $N_{2,u}$, respectively. The linear and nonlinear input term parameters are denoted with $a_u(i)$ and $b_u(i,j)$, respectively. In the same way, the parameters $a_{d_m}(i)$ and $b_{d_m}(i,j)$ are used in the linear and nonlinear terms depending on the disturbances D_m.

In this application, the Almería-type greenhouse has been used and thus the opening of the roof and lateral windows has been regarded as a combined variable. The main variables considered for modeling purposes are the greenhouse temperature, input aperture of the roof and lateral windows, outside temperature, outside wind speed, soil surface temperature, and outside global solar radiation. The model (3.29) has been defined with one input and $n = 4$ disturbances. The wind direction

has not been considered here as measurable disturbance because the greenhouse used in this work only has roof vents oriented to the West with high-density anti-insect screens, what decreases the wind effect on the ventilation process and thus the wind direction influence is despicable.

In order to identify the parameters of the Volterra series model of the greenhouse temperature, experimental data of autumn (from August to February) and spring (from March to June) seasons from 2007 and 2008 have been used [154]. A second set of experimental data of a long season from September 2008 to June 2009 has been used for validation purposes. The used sets for identification and validation have rich input signals, necessary for the identification of a second-order Volterra series model. The sample time for both sets was 1 min and the data of the wind speed and the global solar radiation were filtered through a first-order filter with a time constant of 5 min before using them for calibration purposes. The data used for identification and validation were normalized to the interval [0, 1]. To identify the parameters of the Volterra series model, both LS methods and constrained nonlinear optimization using sequential quadratic programming (SQP) have been used. The procedure followed to select the truncation orders is explained in [154], where simulation results are also shown.

The future output of the identified nonlinear model (3.29) with the prediction horizon N, the control horizon N_u and the truncation order N_t can be calculated in matrix form as:

$$\mathbf{Y} = \mathbf{G}_u\mathbf{U} + \mathbf{F}_u + \mathbf{c} \tag{3.30}$$

where here $\mathbf{U}$ is the future input sequence in this case $\mathbf{Y}$ the predicted output vector (both of length N) and the term $\mathbf{c}$ contains only terms which do not depend on the current or future inputs, as usual in the MPC formulation. The term $\mathbf{G}_u\mathbf{U}$ represents the linear part depending on the future input. Analogously, the vector $\mathbf{F}_u$ contains the future–future cross terms depending on the input sequence $\mathbf{U}$. For the future values of the disturbances, constant values are assumed in this application (equal to the last measured value).

For the design of a MPC strategy based on the identified second-order Volterra series model (3.29), the following general MPC optimization problem is considered:

$$\mathbf{U}^* = \arg \min_{\mathbf{U}} J, \ \text{s.t.} \ \mathbf{R}\mathbf{U} \leq \mathbf{r} \tag{3.31}$$

where the variable to be optimized is the future input sequence $\mathbf{U}$ and general linear inequality constraints are considered described by matrix $\mathbf{R}$ and vector $\mathbf{r}$ which dimension equals the number of constraints [160]. J is the typical cost function defined in Eq. (3.16). With the prediction model (3.30) based on a second-order Volterra series model and the cost function (3.16), an iterative approach to calculate the control action has been chosen. This approach, originally presented in [114, 263], represents an unconstrained NMPC. This approach has been modified in [154] to consider constraints in the input sequence to be optimized as well as a weighting for the control increments. For more details about this method see [154].

The proposed controller was implemented in Matlab/Simulink and used with a sampling time of $t_s = 1\,\text{min}$, corresponding to the sampling time used during the identification. The prediction and control horizons were chosen in such a way that the length of the considered dynamic behavior corresponds to the time constant of the identified model. Finally, based on the used truncation orders of the Volterra series model, values of $N = 9$ for the prediction horizon and $N_u = 9$ for the control horizon were chosen, respectively. The weighting factor used in the control strategy was set to a value of $\lambda = 0.01$ and constraints both in the control signal and its increments were considered:

$$
\begin{aligned}
0\,\% &\leq U(t+i|t) \leq 100\,\%, & i = 0, \ldots, N_u - 1 \\
-25\,\% &\leq \Delta U(t+i|t) \leq 25\,\%, & i = 0, \ldots, N_u - 1
\end{aligned}
\tag{3.32}
$$

The constraints in the control signal and its increments have been chosen according to the physical limitations of the actuators. The lower and upper bounds of the control signal represent completely closed or opened windows. The constraints in the control increments were necessary as the windows need time to completely open or close. Furthermore, the following hysteresis

$$
U(t|t) = \begin{cases} U^*(t|t) & \text{if } |U^*(t|t) - U(t-1)| \geq \varepsilon \\ U(t-1) & \text{if } |U^*(t|t) - U(t-1)| < \varepsilon \end{cases}
\tag{3.33}
$$

for the control signal has been used reducing the number of control changes in order to preserve the electric motors of the roof and lateral windows. With the given hysteresis, the control signal calculated by the controller is applied only if the difference to the last applied control signal is greater or equal than ε. Otherwise, the control signal applied in the previous sampling period will be applied again in the current sampling period. Based on the range of the input signal (from 0 % to 100 %) and the experience with the real system, a value of $\varepsilon = 3\,\%$ has been used.

After validation the proposed control algorithm in simulation [154], several tests were carried out in autumn and winter yielding promising results. Figure 3.33 shows the control results and the main system disturbances for the test performed in the period of 19–24 January 2010. It is important to mention that the presented results have been obtained with a tomato crop inside the greenhouse. During the shown experiment, the set point was set to 24 °C for most of the days and it was changed to 22 °C between days 2 and 3 in order to evaluate the reaction of the control algorithm. As it can be observed from the figure, the control algorithm properly follows the set point despite of system disturbances. Notice that most of the experiments are under cloudy days and with important variations in the wind speed. In the first day, the control system is not able to reach the set point. The reason is because it is a very cloudy day and thus there is not enough energy source to increase the inside temperature. Notice also how the control algorithm closes the windows in order to try increasing the controlled variable. On the other hand, during the third day, the inside temperature is slightly over the set point for all the day. The control algorithm fully opens the windows in order to decrease the inside temperature and the control
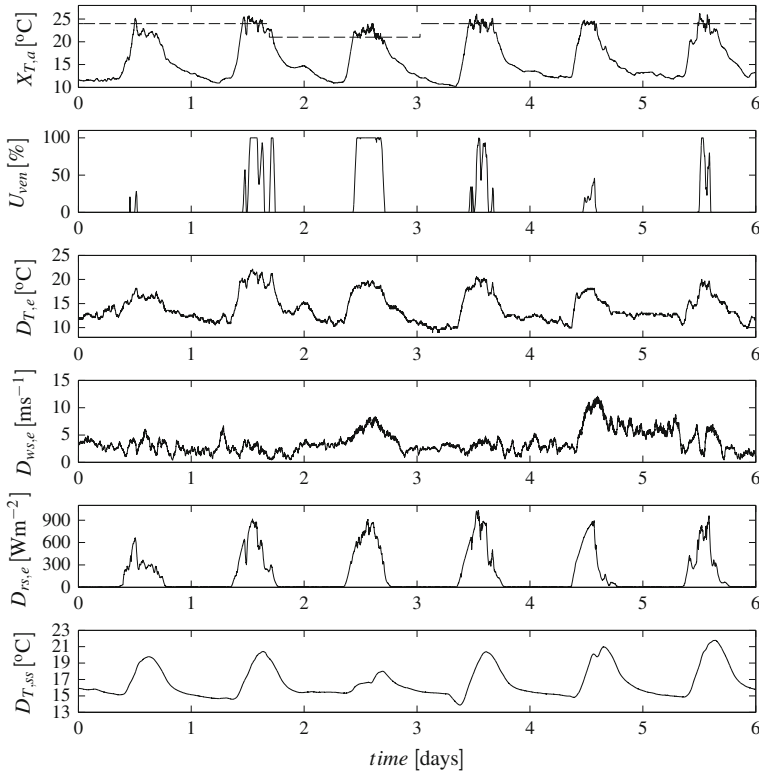
Fig. 3.33 Experimental results of the proposed controller for the period of 19–24 January 2010. From *top* to *bottom*: Output $X_{T,a}$ (greenhouse temperature) and desired reference, input U_{ven} (aperture of the roof and lateral windows) and disturbances $D_{T,e}$ (outside temperature), $D_{ws,e}$ (outside wind speed), $D_{rs,e}$ (outside global solar radiation), and $D_{T,ss}$ (soil surface temperature). Courtesy of the authors [154]

signal is saturated all the time. However, there is nothing to do since it is a warm day and the air exchange through the windows is not enough to decrease the inside temperature below the desired set point.

3.2.7 Model Predictive Control of Nighttime Temperature

3.2.7.1 Nighttime Temperature Control Using Generalized Predictive Control

This section presents the application of MPC strategies to two types of heating systems: Aerial pipes near the ground or benches and fan heater units. Results in the Almería-type greenhouse are provided. Several authors have used different greenhouse heating climate control strategies (mainly by aerial pipes). In [461, 462],

several PI control structures were tested and compared to model reference AC in a Venlo greenhouse with tomato crop, showing good steady-state behavior but large overshoots without optimizing efficiency. In [104], a cascaded PI control is introduced and tested in a Venlo greenhouse improving the results obtained with classical PI control. In [482], a PIP control scheme is used with a model of a Venlo greenhouse, while Tantau and co-workers [439, 440, 119] used FF controllers and extended linearized predictive controllers obtaining also acceptable results. In [49, 93] both PID and GPC controllers were used in a tunnel greenhouse in Portugal, obtaining better results with the GPC approach, accordingly with the results of [296] in cold climates. The most relevant experiences with receding horizon optimal controllers have been reported by van Straten and co-workers [428, 429, 430, 432, 441, 442, 443], demonstrating the feasibility and features of this kind of control technique in a Venlo greenhouse in the Netherlands. Seginer and co-workers [159, 200] studied different techniques using linear programming and Pontryagin's principle to minimize heating costs. In [215] the integration of heating within a hierarchical crop production control scheme is treated. Many authors only report results in simulation. Gain-scheduling control algorithms are explained in [215], without providing experimental results. Decentralized MPC controllers have been tested under simulation by [235], while [327] used several MPC control schemes, including embedded FL and RC. In [7] neural network based predictive controllers and optimal controllers are used to cope with the temperature control problems.

As seen before, many authors have selected MPC techniques for heating control purposes. There are some reasons which may justify the use of a MPC scheme when controlling greenhouse heating, as the problem is not only related with a classical regulatory control loop, but also to the costs associated to the control actions (fuel consumption). In this sense, the use of a cost function as that used by MPC algorithms helps the costs associated to the control actions to be taken into account. Although the delay time in this kind of applications is lower or of the same order of the dominant time constant of the system, it influences the consumption. Moreover, although many control strategies can cope with the disturbance rejection problem (mainly changes in outside temperature and wind speed), MPC approaches offer a natural way to deal with FF control. System constraints can be taken into account in the design and optimization process.

Commercial hot-water heating systems are usually controlled by proportional or cascaded PI + parallel FF controllers to cope with outlet disturbances like those shown in Fig. 3.2, while on/off control with dead zone is used in forced-air heaters. Commercially available control algorithms have been described in horticultural engineering textbooks (e.g., [215]). Although this system is nonlinear [355], it can be linearized when operating around a set point for control purposes, as a FOPDT system. The same conclusions can be obtained when linearizing a model of the system obtained from physical principles [355]. Notice that disturbances affect the heating performance. During the night, the greenhouse looses heat through the cover (conduction-convection), depending on the outside temperature and wind speed. Thus, ideally the controller must take into account the outside climatic conditions to calculate the water temperature in the pipes. Transfer functions can also be found
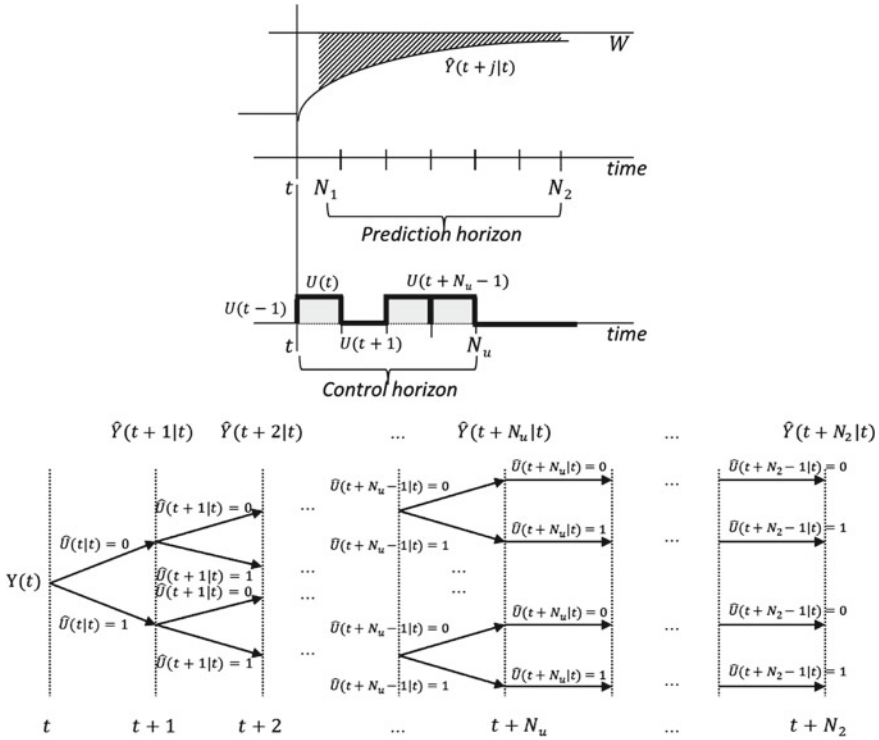
Fig. 3.34 Branch-and-bound GPC. As a courtesy of the authors [342]

relating these disturbances to changes in inside air temperature, to be used for FF control purposes. In other cases, a FF term based on first principles models can also be used [361].

In order to control heating systems based on aerial pipes, both a classical cascade control and a classical GPC control approach [91] defined by cost function (3.16) has been used including constraints in the actuators. For controlling the forced-air heaters, due to the discrete nature of the actuator, two possible ways of implementation have been considered, providing very similar results: A branch and bound strategy previously used by the authors within the control of photobioreactors framework [40] and a PWM (pulse width modulation) approximation in which the activation of the actuator is done between 4 min (1 %) and 10 min (100 %) using a control time of 1 min. When the tracking error is negative the control is switched off. Figure 3.34 shows the basic MPC strategy taking into account the discrete nature of the control signal in this problem. The predictions along the prediction horizon using possible input values in the control horizon are used to evaluate the following objective function:

$$J = \sum_{N_1}^{N_2} (\hat{Y}(t+j|t) - W(t+j))^2 + \sum_{j=1}^{N_u} \lambda(j)U(t+j-1)^2 \qquad (3.34)$$
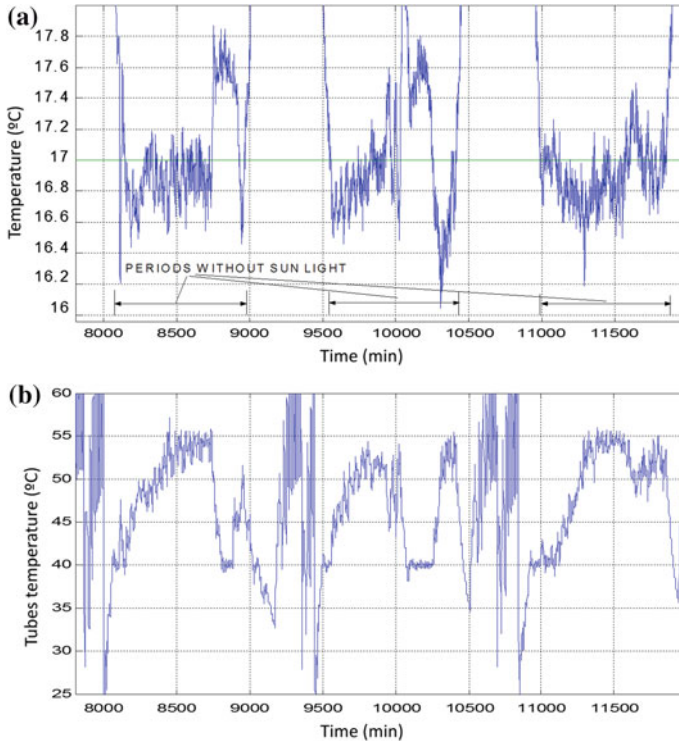
Fig. 3.35 Results under heating pipes cascade control. As a courtesy of the authors [342]. **a** Inside air temperature evolution. **b** Pipes temperature evolution

$\underline{Y} \leq \hat{Y}(\cdot) \leq \overline{Y}$, $U(\cdot) \in \{\underline{U}, \overline{U}\} = \{0, 1\}$, $\Delta U(\cdot) \in \{\Delta\underline{U}, \Delta\overline{U}\} = \{0, 1\}$, $\{0, 1\} : \{$off, on$\}$. Those future input values (and associated predictions) minimizing the cost function are selected and only $U(t)$ is implemented at the current sampling time. In this case, the values of the control actions have been used (weighted by the control effort weighting factor λ) as they are related with the costs associated to fuel consumption. Figure 3.34 illustrates the basic idea of this technique for the control space discretized into two alternatives (on/off control) and lower prediction horizon $N_1 = 2$.

Illustrative results of heating with aerial pipes: Figure 3.35 shows the results when controlling the greenhouse using the control scheme in Fig. 3.2, saturating the pipes temperatures at a maximum of 55 °C during three nights. Two kind of linearized models have been used to design the controllers: A first-order linear model relating inside temperature with heating has been obtained for an operating point defined by heating status (set point) and outside disturbances (temperature and wind speed levels), thus no explicit models of the disturbances have been considered. In a second stage, approximated linear models of how disturbances affect the inside temperature have been obtained using LS identification over a set of data. In both cases

acceptable results have been obtained when the linearized models have been used to design the controllers. The tuning of the master controller has been done using open loop Ziegler–Nichols rules around an operating point of 17°C, with a mean wind speed of $6\,\mathrm{m\,s^{-1}}$ and with an outlet mean temperature of 11°C (typical in the area from December to February). A proportional gain of 12.8 and an integral time of 300 min have been obtained. The same procedure has been used to tune the slave controller. As seen in the figure, the results are quite acceptable as in this case the actuator is continuous and the control scheme is appropriate for this kind of application, although it should be desirable to diminish the variance of the temperature signal. A classical constrained GPC strategy has been also implemented to calculate the desired temperature of the water pumped through the pipes using the same linear models. The parameters of the GPC are: $N_1 = 11$, $N_2 = 30$, $N_u = 30$, $\delta = 1$ and $\lambda = 0.001$. The sampling time is 1 min and the control signal has been saturated
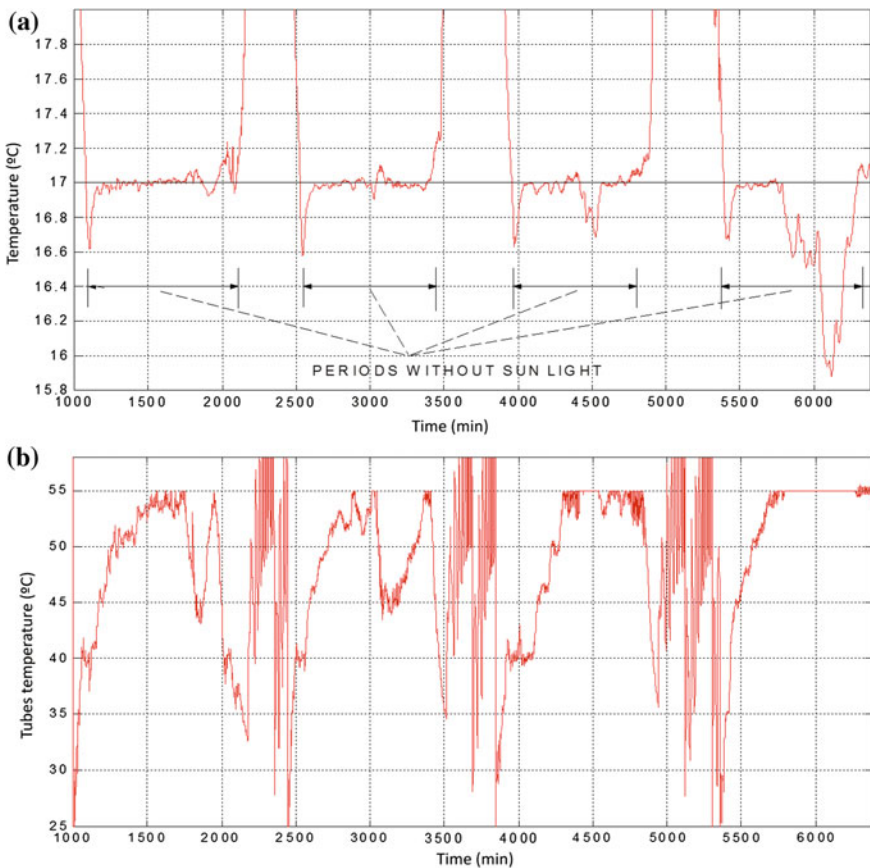

Fig. 3.36 Results under heating pipes GPC control. As a courtesy of the authors [342]. **a** Inside air temperature evolution. **b** Pipes temperature evolution

to 55 °C. The unknown outside conditions over the prediction horizon have been considered constant and equal to the actual measured value. Other different controller configurations have been tested obtaining similar results. Figure 3.36 presents illustrative results during four nights (the last one leading to actuator saturation). As is to be expected, the differences between both techniques are not quite considerable, although the predictive nature of the GPC algorithm and the fact that the constraints surpassing can be anticipated produce slightly better results that can help to save energy.

Illustrative results of heating with forced-air heaters: In this case, the tuning knobs of the GPC algorithms were selected taking into account the characteristic dynamics of the system (static gain 0.04 °C %$^{-1}$, time constant of about 15 min, representative delay of 2 min and settling time of 30 min): $N_1 = 3$, $N_2 = 30$ and $N_u = 30$. After several simulations and real tests, the selected values are: $N_2 = 10$ and $N_u = 6$, as no improvements are observed when increasing these values. The value of N_2 is a trade-off between tracking characteristics and number of activations of the controller. As in the previous case, two kind of implementations have been done, one without explicitly taking into account disturbances (then the model is only valid for a range of operating conditions) and other including the linear models of the disturbances within the GPC framework. In this last case, again the unknown outside conditions over the prediction horizon have been considered constant and equal to the actual measured value. Obviously, the DES method could also be used here to improve disturbance estimation.

Figure 3.37 shows a typical profile of the control using an on/off controller with dead zone of ±0.5 and sample time of 10 min. Many tests have been performed modifying the activation time till the minimum allowed by the vendor (4 min) and similar results have been obtained regarding number of commutations and activation times. Figure 3.38 shows representative results of the performance of the GPC-PWM controller (similar to those of the branch-and bound algorithms). This controller
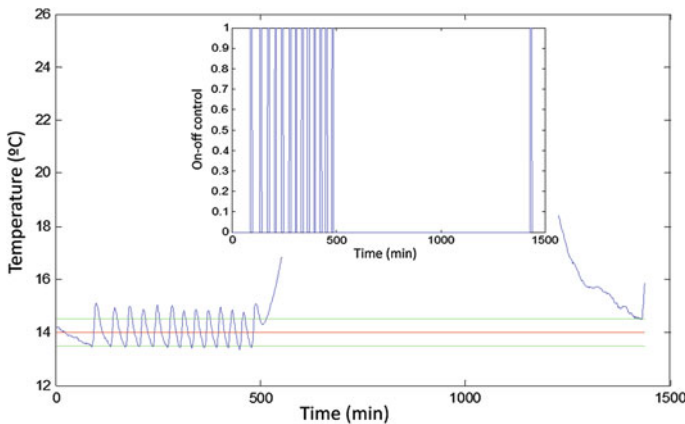

Fig. 3.37 On/off control with dead zone. As a courtesy of the authors [342]
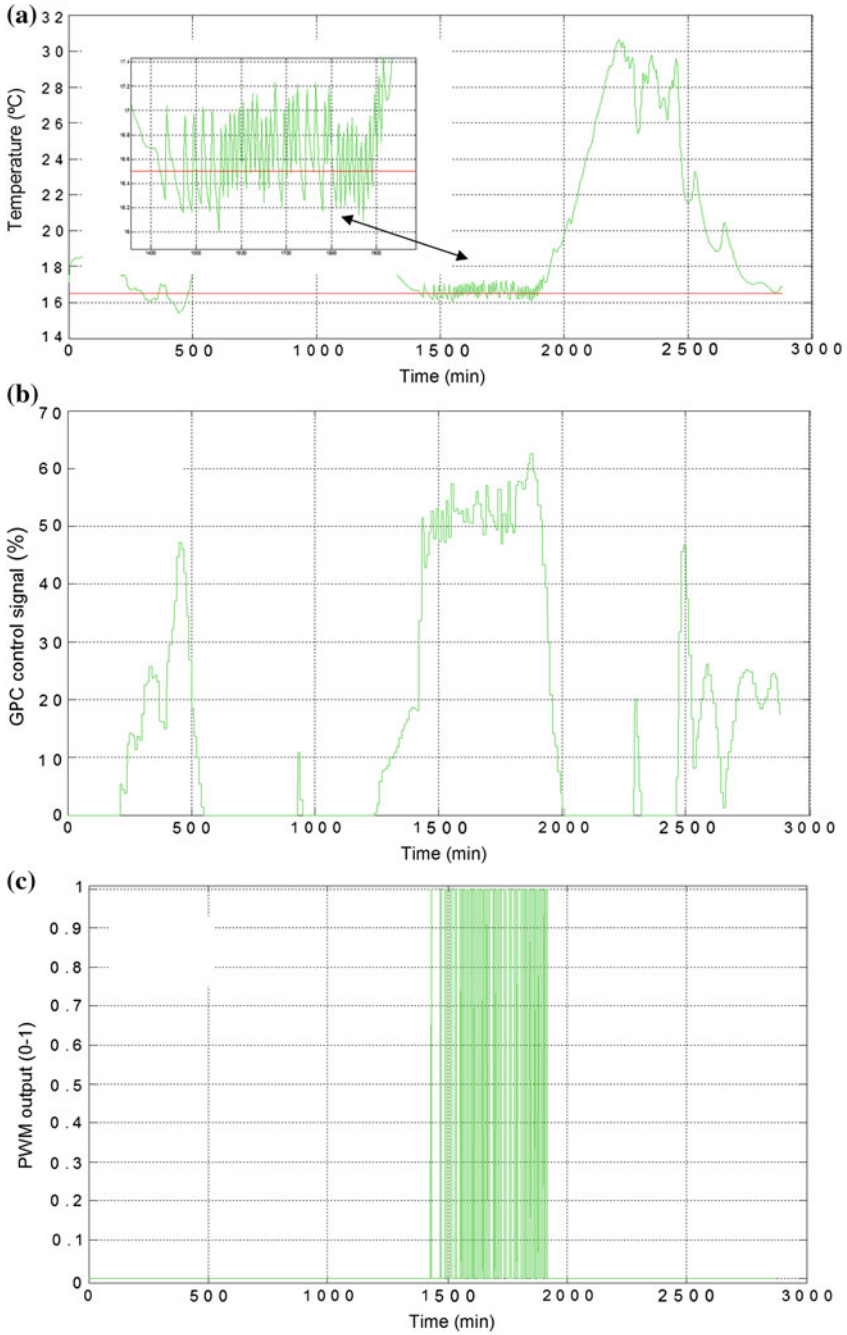
Fig. 3.38 Results using the GPC-PWM. As a courtesy of the authors [342]. **a** Inside air temperature evolution. **b** Continuous control signal. **c** Discrete control signal
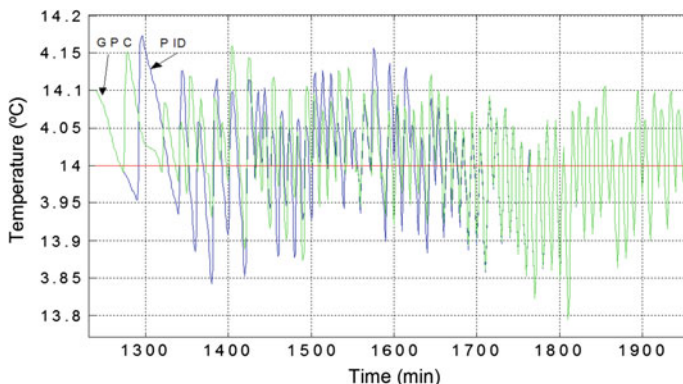
Fig. 3.39 Comparing GPC-PWM and PI. As a courtesy of the authors [342]

helps to achieve about 20 % of saving in fuel consumption, although it has been observed that, even using different tuning knobs in the GPC algorithm and different sample times and dead-zones in the on/off control, the GPC controller produces more commutations and less consumption than the on/off controller, the number of commutations being within the ranges recommended by the supplier. As an example, during a typical night the number of minutes during which the heating system is on with the on/off control is 221 min (11.27 € cost), while with the GPC controller is 164 min (8.36 € cost). There might also be effects on the crop, but not evident on the relatively short time scales used here.

It is common textbook knowledge that almost any control scheme will do better than an on/off control scheme. So, the comparison of MPC with an on/off controller may not be very convincing (despite decades of research, this point has not yet been fully accepted in horticultural industry, e.g., forced-air heaters still have on/off control, today). The effects of outdoor weather conditions such as outdoor temperature and wind speed have a relatively low-frequency behavior and a simple well-tuned PI algorithm could in principle do the job equally well. For instance, in Fig. 3.39, a comparison between the responses of a PI-PWM + AW controller and that of a GPC-PWM controller without incorporating models of the disturbances are shown using a validated nonlinear model of the greenhouse [355] explained in Chap. 2. As can be seen, at the beginning of the night the GPC controller anticipates the control action, while at the end of the night the control signals are similar in the case of PI and GPC controllers, and thus the operating costs. This is an expected result as the PI and the GPC are based on the same model and no input or output constraints are violated, although in this case the λ parameter tuning modulates the trade-off between costs and tracking. The advantages of GPC are more evident when reliable system and disturbance models are used and the operating conditions are such that minimum inside temperature constraints are violated.

3.2.8 *Event-Based Control of Daytime Temperature*

Event-based sampling and control has been receiving special attention since the last few years due to the necessity of reducing the exchange of information between sensors, controllers, and actuators, aimed at extending the lifetime of battery-powered wireless sensors, to reduce the computational load in embedded devices, or to cut down the network bandwidth [275]. In contrast to traditional computer control systems where the controller acts synchronously using a predefined sample time, the event-based control (EBC) systems is the proper dynamic evolution of the system that decides when the next control action will be executed, and thus the sampling period is governed by system events, and it is called event-based sampling. Under an event-based sampling framework, information is transmitted only when a significant change exists in the signal that justifies the acquisition of a new sample.

Traditionally, greenhouse installations require a great effort to connect and distribute all the sensors and data acquisition systems. These installations need many data and power wires to be distributed along the greenhouses making the system complex and expensive. For this reason, and others such as unavailability of distributed actuators, only individual sensors are usually located in a fixed point of the greenhouse selected as representative of greenhouse dynamics. On the other hand, the actuation system in many greenhouses are usually composed of mechanical devices controlled using relays, being desirable to reduce the number of commutations of the control signal from security and economical point of views. The greenhouse climate control can be represented as an event-based system, where low-frequency dynamics variables have to be controlled and this control usually acts against events governed by external disturbances. In the last few years, the authors have developed some applications in collaboration with other colleagues where wireless sensor networks (WSN) are used in a combination with event-based sampling and control approaches within the greenhouse climate control problem [127, 313, 314, 316–322]. As result, reductions by more than 80% on the number of changes in the control signal were reached in comparison with traditional time-based controllers. This result is a key issue for greenhouses since it helps decreasing electricity costs and increases the actuator lifetime. This section summarizes the application of an event-based predictive control algorithm for the greenhouse diurnal temperature control problem, which includes a combination of all the event-based sampling and control approaches developed by the authors and coworkers in this topic [313, 315, 316].

The control approach is composed by a complete event-based GPC control scheme that considers both sensor and actuator deadband at the same time [315]. This event-based structure is built first for the sensor deadband approach [316], and additionally, the actuator deadband in the optimization procedure for the developed controllers [313]. In this way, an event-based GPC controller manages two sources of events, related to process output and input, respectively. Thus, the complete event-based GPC control structure has two additional tuning parameters, β_y and β_u, which determine the deadband for the sensor and the actuator, respectively. Each of these
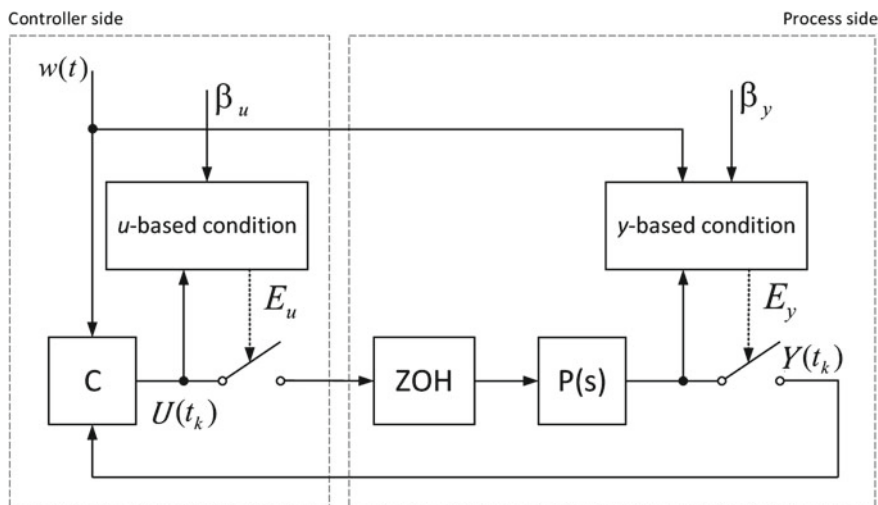
Fig. 3.40 Event-based control approach; t_k refers to time of events and t to discrete time (samples)

tuning parameters can be used to obtain the desired trade-off between control performance and the number of events for the sensor and the actuator, independently.

The EBC structure used is shown in Fig. 3.40, where C represents an EBC and $P(s)$ the controlled process. In this configuration, two types of events can be generated from *u-based* and *y-based* conditions. In the developed application, the actuator possesses a ZOH (Zero Order Hold), so the current control action is maintained until the arrival of a new one.

The *u-based* criterion is used to trigger the input side event, E_u, consisting of the transmission of a new control action, $U(t_k)$, when it is different enough (bigger than a threshold β_u) with respect to the previous control action. On the other hand, the *y-based* condition will trigger the output side event, E_y, when the difference between the reference $W(t)$ and the process output is out of the limit β_y. The adaptive sampling technique with deadband sampling/updating is used for *y-based* and *u-based* conditions [328].

Since the *u-based* condition is related to the actuator and the *y-based* condition with the sensor, three approaches to perform EBC strategies can be established: Sensor deadband approach, actuator deadband approach, and complete event-based approach.

3.2.8.1 Sensor Deadband Approach for Event-Based Control

In a general way, an EBC consists of two parts: An event detector and a controller [15]. The event detector deals with informing the controller when a new control signal must be calculated due to the occurrence of a new event. In this case, the controller is composed of a set of GPC controllers, in such a way that one of them will be selected

according to the time instant when a new event is detected, such as described below. This scheme operates using the following ideas [316]:

- The process output is sampled using a constant sampling time t_{base} at the event generator block, while the control action is computed and applied to the process using a variable sampling time, t_f, which is determined by an event occurrence.
- t_f is multiple of t_{base} ($t_f = f t_{\text{base}}$, $f \in [1, n_{\max}]$) and verifies $t_f \leq t_{\max}$, being $t_{\max} = n_{\max} t_{\text{base}}$ the maximum sampling time value. This maximum sampling time will be chosen to maintain a minimum performance and stability margins.
- t_{base} and $t_{\max}$ are defined considering process data and closed loop specifications, following classical methods for sampling time choice.
- After applying a control action at time t, the process output is monitored by the event generator block at each base sampling time, t_{base}. This information is used by the event detector block, which verifies if the process output satisfies some specific conditions. If these conditions are satisfied, an event is generated with a sampling period t_f and a new control action is computed. Otherwise, the control action is only computed by a timing event, at $t_k = t + t_{\max}$.
- Notice that according to the previous description, the control actions will be computed based on a variable sampling time, t_f. For that reason, a set of GPC controllers is used, where each GPC controller is designed for a specific sampling time $t_f = f t_{\text{base}}$, $f \in [1, n_{\max}]$. On the other hand, resampling of the signals is necessary to avoid undesirable jumps in the control action at each change among controllers.

As pointed out above, the proposed control structure is based on the use of the GPC algorithm as the feedback controller. Specifically, a set of GPC controllers is used to implement the proposed strategy, one for each sampling time t_f, $f \in [1, n_{\max}]$. Each individual controller in that set is implemented as a classical GPC algorithm. The GPC controller consists of applying a control sequence that minimizes a multistage cost function defined by Eq. (3.16), which in this case has the form [316]:

$$J = \sum_{j=N_1^f}^{N_2^f} \delta^f [\hat{Y}^f(t+j|t) - W(t+j)]^2 + \sum_{j=1}^{N_u^f} \lambda^f [\Delta U^f(t+j-1)]^2 \quad (3.35)$$

where $\hat{Y}^f(t+j|t)$ is an optimum j step ahead prediction of the system output on data up to time t, $\Delta U^f(t+j-1)$ are the future control increments and $W(t+j)$ is the future reference trajectory, considering all signals with a sampling time t_f ($t = k t_f, k \in Z^+$). Moreover, the tuning parameters are the minimum and maximum prediction horizons, N_1^f and N_2^f, the control horizon, N_u^f, and the future error and control weighting factors, δ^f and λ^f, respectively [316]. The objective of GPC is to compute the future control sequence $U^f(t), U^f(t+1), \ldots, U^f(t+N_u^f-1)$ in such a way that the future plant output $Y^f(t+j)$ is driven close to $W(t+j)$. This is accomplished by minimizing J.

Signal sampling and resampling technique: Such as described above, the computation of a new control action is done with a variable sampling period t_f. So, in order to implement the GPC control algorithm, the past values of the process variables and of the control signals must be available sampled with that sampling period t_f. Therefore, a resampling of the corresponding signals is required, such as described in the following.

Resampling of process output: As discussed previously, the controller block only receives the new state of the process output when a new event is generated. This information is stored in the controller block and is resampled to generate a vector $\mathbf{Y}^b$ including the past values of the process output with t_{base} samples. The resampling of the process output is performed by using a linear approximation between two consecutive events, and afterward this linear approximation is sampled with the t_{base} sampling period, resulting in $Y^b(k)$ with $k = 0, t_{\text{base}}, 2t_{\text{base}}, 3t_{\text{base}}, \ldots$. Once the process output signal is resampled, the required past information must be obtained according to the new sampling time t_f, resulting in a new signal, Y^f, with the past information of the process output every t_f samples. Hence, a vector $\mathbf{Y}^f$ is obtained as a result, which contains the past process information with the new sampling period t_f to be used in the calculation of the current control action.

Reconstruction of past control signals: The procedure is similar to that described for the resampling of the process output. There is a control signal, U^b, which is always used to store the control signal values every t_{base} samples. Nevertheless, the procedure for the control signal is done in the opposite way than for the process output. First, the required past information is calculated and afterward the signal U^b is updated. Lets consider that a new event is generated, which results in a new sampling period $t_f = f t_{\text{base}}$. Now, the past information for the new sampling period, t_f, is first calculated from the past values in U^b and stored in a variable called U_{p}^{f}. Afterward, this information, together with the past process output data given by $\mathbf{Y}^f$, will be used to calculate the new control action, $U^f(t_f) = U^b(k)$. Once the new control action has been calculated, the U^b signal is updated by keeping constant the values between the two consecutive events.

3.2.8.2 Actuator Deadband Approach for Event-Based Control

The main idea of this approach is to develop a control structure where the control signal is updated in an asynchronous manner. The main goal is to reduce the number of control signal updates, saving system resources, retaining acceptable control performance. Therefore, this section will focus on the actuator deadband approach, which tries to face these drawbacks regarding control signal changes. The actuator deadband can be understood as a constraint on control signal increments $\Delta U(t)$:

$$|\Delta U(t)| = |U(t-1) - U(t)| \geqslant \beta_u \qquad (3.36)$$

where β_u is the proposed deadband.

The introduced deadband, β_u, will be used as an additional tuning parameter for control system design, to adjust the number of actuator events (transmissions from controller to actuator). In this section, the presence of the actuator deadband is included into the controller design procedure in order to improve the EBC system performance.

The methodology presented here consists of the actuator virtual deadband into the GPC design framework [313]. The deadband nonlinearity can be handled together with other constraints on controlled process. The deadband can be expressed mathematically with a hybrid design framework developed by [36], that translates discrete rules into a set of linear logical constraints. The resulting formulation consists in a system containing continuous and discrete components, which is known as a Mixed Logical Dynamic (MLD) system [36] (MLD systems will be treated with more detail in Sect. 3.2.9).

Let us introduce two logical variables, φ_1 and φ_2, to determine a condition on control signal increments, $\Delta U(t)$. So, these logical variables are used to describe the different stages of the control signal with respect to the deadband, as following:

$$x(t) = \begin{cases} \Delta U(t) : \Delta U(t) \geqslant \beta & \varphi_2 = 1 \\ 0 : \Delta U(t) \leqslant \beta & \varphi_2 = 0 \\ 0 : \Delta U(t) \geqslant -\beta & \varphi_1 = 0 \\ \Delta U(t) : \Delta U(t) \leqslant -\beta & \varphi_1 = 1 \end{cases} \tag{3.37}$$

To make this solution more general, minimal m and maximal M values for control signal increments are included into the control system design procedure, resulting in $M = \max\{\Delta U(t)\}$ and $m = \min\{\Delta U(t)\}$. In this way, it is possible to determine the solution region based on binary variables. Figure 3.41 shows the virtual deadband in a graphical form, where each region can be distinguished. Thus, the proposed
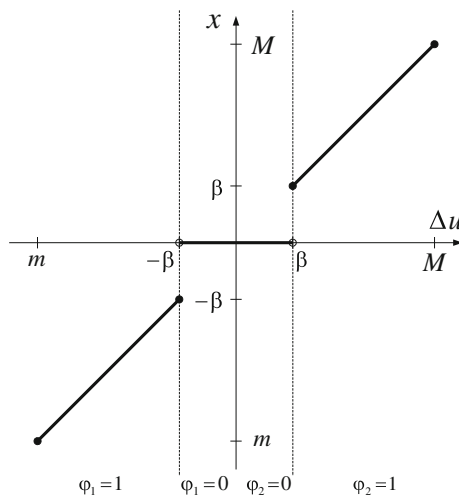

Fig. 3.41 Control signal increments with deadband

logic determined by Eq. (3.37) can be translated into a set of mixed-integer linear inequalities involving both continuous variables, $\Delta U \in \mathbb{R}$, and logical variables $\varphi_i \in \{0, 1\}$. Finally, a set of mixed-integer linear inequalities constraints for the actuator deadband are established as:

$$
\begin{aligned}
\Delta U - (M - \beta)\varphi_2 &\leqslant \beta \\
\Delta U + (M + \beta)\varphi_1 &\leqslant M \\
\Delta U - M\varphi_2 &\leqslant 0 \\
-\Delta U + (m + \beta)\varphi_1 &\leqslant \beta \\
-\Delta U - (m - \beta)\varphi_2 &\leqslant -m \\
-\Delta U + m\varphi_1 &\leqslant 0 \\
\varphi_1 + \varphi_2 &\leqslant 1
\end{aligned}
$$

Mixed-integer quadratic programming-based design for control signal deadband— The reformulated hybrid input constraints presented above are integrated in the GPC optimization problem, where the resulting formulation belongs to a mixed-integer quadratic programming (MIQP) optimization problem.

In the case where the control horizon is $N_u > 1$, the corresponding matrix becomes:

$$
\underbrace{\begin{bmatrix}
1\underline{\mathbf{D}} & 0\underline{\mathbf{D}} & -(M - \beta)\underline{\mathbf{D}} \\
1\underline{\mathbf{D}} & (M + \beta)\underline{\mathbf{D}} & 0\underline{\mathbf{D}} \\
1\underline{\mathbf{D}} & 0\underline{\mathbf{D}} & -M\underline{\mathbf{D}} \\
-1\underline{\mathbf{D}} & (m + \beta)\underline{\mathbf{D}} & 0\underline{\mathbf{D}} \\
-1\underline{\mathbf{D}} & 0\underline{\mathbf{D}} & -(m - \beta)\underline{\mathbf{D}} \\
-1\underline{\mathbf{D}} & m\underline{\mathbf{D}} & 0\underline{\mathbf{D}} \\
0\underline{\mathbf{D}} & 1\underline{\mathbf{D}} & 1\underline{\mathbf{D}}
\end{bmatrix}}_{\mathbf{C}}
\underbrace{\begin{bmatrix}
\Delta U \underline{\mathbf{d}} \\
\varphi_1 \underline{\mathbf{d}} \\
\varphi_2 \underline{\mathbf{d}}
\end{bmatrix}}_{\mathbf{x}}
\leqslant
\underbrace{\begin{bmatrix}
\beta \underline{\mathbf{d}} \\
M \underline{\mathbf{d}} \\
0 \underline{\mathbf{d}} \\
\beta \underline{\mathbf{d}} \\
-m \underline{\mathbf{d}} \\
0 \underline{\mathbf{d}} \\
1 \underline{\mathbf{d}}
\end{bmatrix}}_{\rho}
$$

where $\underline{\mathbf{D}}$ is a matrix ($N_u \times N_u$) of ones and $\underline{\mathbf{d}}$ is a vector of ones with size ($N_u \times 1$).

The previous matrices that contain linear inequality constraints can be expressed in a general form as

$$
\mathbf{Cx} \leqslant \rho \tag{3.38}
$$

with $\mathbf{x} = [\mathbf{x}_c, \mathbf{x}_d]^T$, where $\mathbf{x}_c$ represents the continuous variables ΔU, and $\mathbf{x}_d$ are those of the logical variables φ_i. Introducing the matrix $\mathbf{Q}_{(3N_u \times 3N_u)}$ and $\mathbf{l}_{(3N_u \times 1)}$ defined as:

$$
\mathbf{Q} = \begin{bmatrix}
\mathbf{H} & \underline{\mathbf{0}} & \underline{\mathbf{0}} \\
\underline{\mathbf{0}} & \underline{\mathbf{0}} & \underline{\mathbf{0}} \\
\underline{\mathbf{0}} & \underline{\mathbf{0}} & \underline{\mathbf{0}}
\end{bmatrix}; \quad \mathbf{l} = \begin{bmatrix}
\mathbf{b} \\
\hat{\mathbf{0}} \\
\hat{\mathbf{0}}
\end{bmatrix} \tag{3.39}
$$

where $\underline{\mathbf{0}} = N_u \times N_u$, $\hat{\mathbf{0}} = N_u \times 1$ both of zeros, $\mathbf{H}$ and $\mathbf{b}$ are a matrices used in classical QP optimization, the GPC optimization problem is expressed as:

$$\min_x x^T \mathbf{Q} x + \mathbf{l}^T x \tag{3.40}$$

subject to (3.38), which is a MIQP optimization problem [36]. The optimization problem involves a quadratic objective function and a set of mixed linear inequalities. Moreover, the classical set of constraints, $\mathbf{R}\Delta u \leq \mathbf{r}$ can also be included into the optimization procedure, introducing an auxiliary matrix $\hat{\mathbf{R}}$ of the form $[\mathbf{R}\,\bar{\mathbf{0}}\,\bar{\mathbf{0}}]$, where $\bar{\mathbf{0}}$ is a matrix of zeros with the same dimensions that $\hat{\mathbf{R}}$. Finally, all constraints that must be considered into the optimization procedure are grouped in:

$$\begin{bmatrix} \mathbf{C} \\ \hat{\mathbf{R}} \end{bmatrix} \mathbf{x} \leqslant \begin{bmatrix} \rho \\ \mathbf{r} \end{bmatrix}$$

In such a way, the event-based GPC with actuator deadband obtains optimal control signal values considering established deadband and classical constraints.

3.2.8.3 Complete Event-Based GPC Scheme and Results

The complete event-based GPC control scheme considers both sensor and actuator deadband at the same time [315]. To perform such an EBC structure, it is necessary to build the control structure introduced for the sensor deadband approach. Additionally, the developed controllers consider the actuator deadband in the optimization procedure. In this way, an event-based GPC controller manages two sources of events, related to process output and input, respectively. Thus, the complete event-based GPC control structure has two additional tuning parameters, β_y and β_u, which determine the deadband for the sensor and the actuator, respectively. Each of these tuning parameters, can be used to obtain the desired trade-off between control performance and the number of events for the sensor and the actuator, independently.

In this configuration, the process output is sampled using the intelligent sensor, where the deadband sampling logic is implemented. When one of the conditions becomes true, the event generator transmits the current process output to the controller node. The usage of the sensor deadband allows one to reduce the process output events, E_y. Afterward, the received information in the EBC node triggers the event detector to calculate the time elapsed since the last event. The obtained time value is used as the current sampling time and the corresponding controller is selected to calculate a new control signal. Because the virtual actuator deadband is also used in such a configuration, the corresponding constraints on the control signal are active for all controllers from the set. In this way, the resulting control signal takes into account the deadband and makes the reduction of process input events E_u possible.

The whole EBC scheme was applied to the greenhouse inside temperature control problem. The simulations have been performed using the TrueTime MATLAB/Simulink toolbox. TrueTime is a tool developed to simulate real-time systems, networked control systems, communication models, and wireless sensor networks [82].

To compare classical time-based (TB) and event-based (EB) configuration a specific performance indexes for this type of control strategies were considered [328]. As a first measure, the IAE is used to evaluate the control accuracy $IAE = \int_0^\infty |E(t)|dt$. The IAEP compares the EBC with the time-based control used as a reference $IAEP = \int_0^\infty |Y_{TB}(t) - Y_{EB}(t)|dt$, where $Y_{TB}(t)$ is the response of the time-based classical GPC. An efficiency measure index for EBC systems can be defined as $NE = \frac{IAEP}{IAE}$. Additionally, E_y and E_u measurements are considered to show the number of events for the process output and input, respectively.

The greenhouse inside temperature problem, used as the test bench, can be considered as a MISO system such as presented in Sect. 3.2.6, which is summarized in the Fig. 3.29 and described by the CARIMA model presented in (3.28).

The event-based GPC control structures were implemented with the following parameters. The sensor deadband configuration was implemented with $t_{base} = 1$ min, $t_{max} = 4$ min, $n_{max} = 4$, and thus $t_f \in [1, 2, 3, 4]$. The control horizon was selected to $N_u^{n_{max}} = 5$ samples. The prediction horizon was set to $N_2^c = 20$ min in continuous time, and the control weighting factor to $\lambda^f = 1$.

For the actuator deadband configuration, simulations were performed for the following system parameters: $N_2 = 10$, $N_u = 5$, and $\lambda = 1$. The minimum and maximum control signal increments of the vents opening percentage were set to $m = -20\%$ and $M = 20\%$, respectively. The actuator virtual deadband was set to $\beta_u = [0.1, 0.5, 1, 2]$ in order to check its influence on the control performance.

The complete event-based GPC considers actuator and sensor deadbands at the same time. In this case, the control system configuration is as follows: $t_{base} = 1$ min, $t_{max} = 4$ min, $n_{max} = 4$, and thus $t_f \in [1, 2, 3, 4]$. The control horizon was selected to $N_u^{n_{max}} = 5$ samples, the prediction horizon was set to $N_2^c = 20$, and the control signal weighting factor was adjusted to $\lambda^f = 1$. In this configuration, the actuator virtual deadband was set to $\beta_u = [0.1, 0.5, 1]$ and the sensor deadband $\beta_y = [0.2, 0.5]$.

Due to the physical limitation of the actuator, all controllers consider constraints on the control signal $0 \le U(t) \le 100\%$.

Table 3.5 collects performance indexes for all analyzed control configurations for 19 simulation days (using real data for disturbances) and Fig. 3.42 shows graphical results for a representative day. As can be observed, the deadband values have a direct influence on the control performance obtained for the different configurations. The event-based GPC with sensor deadband is characterized by an important reduction for process output events E_y, where the number of events depends directly on the deadband value. For this event-based configuration, the sensor deadband value represents a desired trade-off between control performance and number of events (see Fig. 3.42). The event-based GPC with actuator deadband is characterized by acceptable control performance for most of the tested deadband values, which is confirmed by the performance indexes from Table 3.5. Interesting results for this configuration are obtained for $\beta_u = 1$, where IAE increases about 15.9%, an event reduction of the order of 74% is obtained. Likewise in the previous configuration, the deadband value can be tuned to obtain a desired process input event reduction at an acceptable control accuracy. On the other hand, even the smaller actuator deadband, $\beta_u = 0.1$,

Table 3.5 Numerical results of the event-based GPC control scheme for 19 days

	Deadband		Performance indexes				
	β_u	β_y	IAE	E_u	E_y	IAEP	NE
TB	–	–	2,275	5,173	5,173	–	–
EB	–	0.1	2,292	4,383	4,383	715	0.31
	–	0.2	2,343	3,829	3,829	727	0.31
	–	0.5	2,799	2,656	2,656	1,013	0.36
	–	0.75	3,283	2,161	2,161	1,457	0.44
	0.1	–	2,277	4,665	5,173	12	0.01
	0.5	–	2,352	2,694	5,173	300	0.13
	1	–	2,637	1,317	5,173	845	0.32
	2	–	4,457	453	5,173	2,894	0.65
	0.1	0.2	2,307	4,411	4,530	489	0.21
	0.1	0.5	2,525	2,991	3,049	486	0.19
	0.5	0.2	2,416	3,435	4,271	717	0.29
	0.5	0.5	2,516	2,792	3,005	492	0.19
	1	0.2	2,597	2,028	4,957	939	0.36
	1	0.5	2,998	2,165	2,693	800	0.26

results in an important event reduction, E_u, where savings of 9.9 % are achieved compared to the time-based GPC.

The complete event-based configuration merges the advantages of both previously introduced methods. In the resulting configuration, the process input and output events can be tuned independently using the actuator or the sensor deadband, respectively. The analyzed scheme is characterized by acceptable control performance and obtains minimum and maximum IAE values between 1.4 and 33.6 % higher than the TB configuration. For the configuration with $[\beta_y = 0.5, \beta_u = 0.5]$, the best trade-off between control performance and the number of events was obtained. In this case, IAE increases 10.6 %, while E_y and E_u were reduced by about 41.3 and 46 %, respectively. The bottom graph on Fig. 3.42 shows how events are generated for this configuration.

3.2.9 Switching Control Approaches for Combined Daytime and Nighttime Temperature Control

To account both for daytime and nighttime greenhouse climate control, the previously explained adaptive and predictive control strategies can be used. The system dynamics at this level can be described with hybrid models that arise due to the different modes of operating/controlling the greenhouse climate (heating and ventilation). As a result, different choices for the state of the system can be considered where inner temperature, solar radiation, and optimized set points will act as logical conditions in the description of the hybrid system. The hybrid dynamics are described both in a general way and using a MLD representation, this result being useful for control pur-
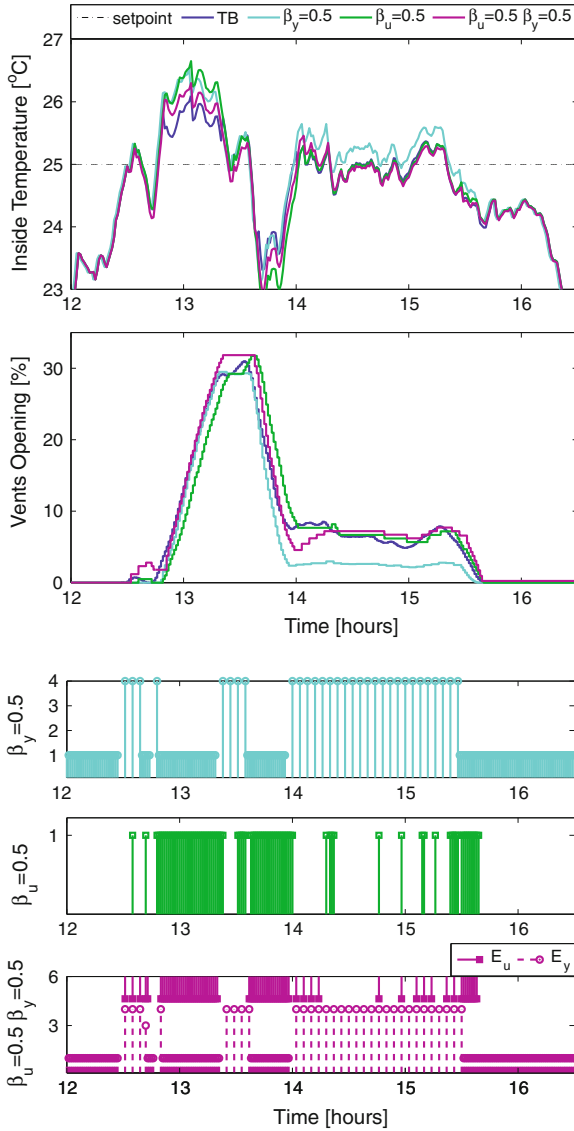
Fig. 3.42 Comparison of control results for different GPC configurations for a representative day [315]

poses in the greenhouse climate control community [165, 362]. A different switching approach evaluated in simulation can be found in [232, 474].

The switching operation modes may arise due to changes in the actuator, and thus in the source supplying the energy to the process under control. These changes in the operation mode may occur in the day/night transition or along the nominal daytime and nighttime operation due to the operating conditions or control objectives, and also

due to the crop evolution (slow time scale) requiring changes in the climate control policies. If the temperature set point or the inner temperature are outside certain security limits, the heating and ventilation systems will have to switch along the day; such security limits will take different values for the day and the night. The daytime and nighttime set points can be modified based on the humidity specifications [237]. So, the modified set points could reach low values during the night being difficult to track them using only heating, or high values during the day being also hard to reach them using the ventilation system. Therefore, some extreme situations could cause the commutation of the heating and ventilation system along the day. Note that, usually these two actuators never will be turned on together because their effects are the opposite.

In order to include this switching phenomenon into the control system architecture, a supervisory layer is devoted to detect when the commutation between the control systems must be performed, in such a way that the full temperature dynamics can be expressed as a hybrid system with the temperature set point, the heating control signal, the ventilation control signal, and the disturbances as inputs, where the system dynamics are switched based on the combination of the solar radiation (day or night), set point temperature, and the inner temperature. The greenhouse dynamics are thus represented as an hybrid system, which also expresses as a MLD system, where two different discrete variables produce the operation mode changes [362]. Other approaches can be found in [336].

In order to control temperature using natural ventilation, the adaptive plus FF control scheme explained in Sect. 3.2.2 can be used (see Fig. 3.12) [43]. The scheme to control temperature using heating has been explained in Sect. 3.2.7 [342].

Regarding humidity, the greenhouse air water content control has two main drawbacks previously commented in this text: The temperature and the humidity closely interact with each other presenting a correlation coefficient higher than -0.9. On the other hand, in order to control both variables, the same actuators are used (vents and heating). When the heating system is turned on, the vents are closed, so there is no mixing between the outside and inside of the greenhouse. The water content in the greenhouse air is constant, so if the temperature raises then the relative humidity decreases. In the opposite case, if the vents are opened (the heating system is turned off) the temperature decreases, but the water content of the internal air also decreases because there is a mixing with external air, generally with a humidity lower than that of the inside greenhouse air.

There exist several methods to control the humidity [215]; the modification of the nighttime and daytime temperature set points based on the priority given to humidity has been selected in this section [362]. This method consists in adapting the temperature set points in order to keep humidity in a specific range. So, the control schema described above have a supervisory control to modify the temperature set point based on the humidity control. As commented previously, the temperature control is usually performed using ventilation during the day and heating during the night. However, situations may occur being necessary to switch between both control systems along the day. For example, the relative humidity could increase too much in nighttime periods because the transpiration is stimulated under high-temperature
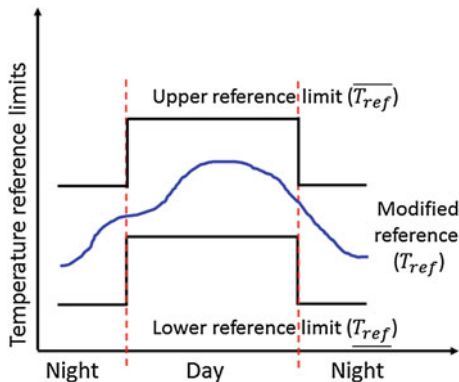
Fig. 3.43 Limits in the reference temperature for detecting changes in the dynamic behavior

conditions. Therefore, it should be necessary to remove the water vapor using the vents, and thus an additional nighttime set point is predetermined in order to force the use of the ventilation. On the other hand, the daytime set point can be modified to force the use of the heating system during the day in order to decrease the relative humidity or stimulate the photosynthesis if the greenhouse air temperature is very low. In summary, if the modified temperature set point or the inner temperature are outside certain security limits, the heating and the ventilation systems will have to switch along the day. Note that such security limits will take different values for the day and the night (see Fig. 3.43). In order to include this switching phenomenon in the control system architecture, a supervisory layer is devoted to detect when the commutation between the control systems must be performed considering a combination of the solar radiation, the inner temperature, and the humidity-based modified set point (see Fig. 3.44).

To account for the switching nature described in previous paragraphs, the hybrid systems framework can be used [362], as done in Sect. 3.2.8, by considering the greenhouse as a dynamical system whose state has two components: One that evolves in a continuous set such as $\mathbb{R}^n$ (typically, according to a differential or difference equation) and another one that evolves in a discrete set such as $\mathbb{N}$ (typically, according to some transition logic-based rule). Perhaps the simplest model for a hybrid system is of the form [251]

$$\begin{aligned}
\dot{\mathbf{X}}(t) &= f_{\sigma(t)}\big(\mathbf{X}(t)\big), & \mathbf{X} \in \mathbb{R}^n, \\
\sigma(t) &= \lim_{\tau \to t^-} \phi(\mathbf{X}(\tau), \sigma(\tau)), \ \sigma \in \mathbb{N}.
\end{aligned} \tag{3.41}$$

where $\mathbf{X} = \mathbf{x}_c$ and $\sigma = \mathbf{x}_d$ denote the continuous and discrete components of the state, respectively. Usually, $\{f_p : p \in P\}$ is a family (normally finite) of sufficiently regular functions from $\mathbb{R}^n$ to $\mathbb{R}^n$ that is parameterized by some index set P, and $\sigma : [0, \infty) \to P$ is a piecewise constant function of time, called a switching signal. Standard assumptions in this context are that the solution $\mathbf{X}(t)$ is everywhere continuous and that there are finite switches in finite time [251]. The particular value for
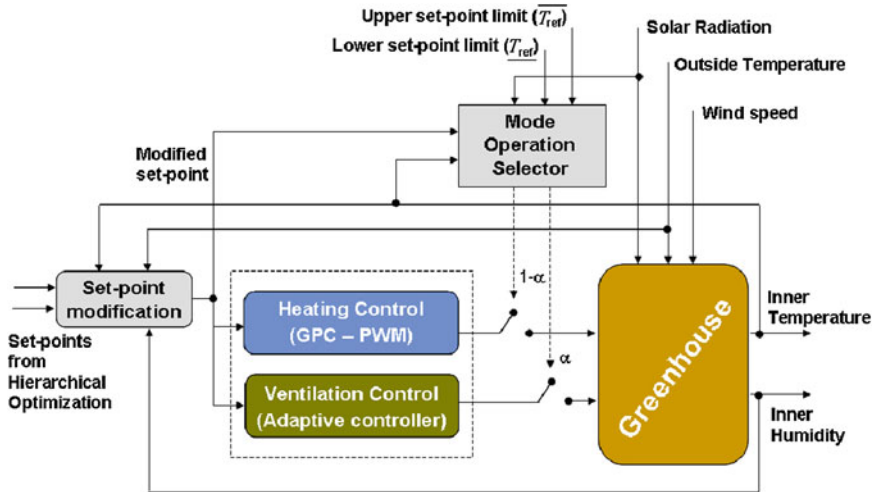
Fig. 3.44 Hybrid control scheme. As a courtesy of the authors [362]

σ may be chosen by some higher process, such as a controller, computer, or human operator, in which case the system is said to be controlled. It may also be a function of time or state or both, in which case the system is said to be autonomous.

A relevant framework for the representation of hybrid systems is the mixed logical dynamical (MLD) systems [36]. The MLD framework tries to specify the evolution of continuous variables through linear dynamic discrete-time equations, of discrete variables through propositional logic statements and automata, and the mutual interaction between the two. The key idea of the approach consists of embedding the logic part in the state equations by transforming Boolean variables into 0–1 integers, and by expressing the relations as mixed-integer linear inequalities. Therefore, MLD systems are capable to model a broad class of systems arising in many applications: Linear hybrid dynamical systems, hybrid automata, nonlinear dynamic systems where the nonlinearity can be approximated by a piecewise linear function, some classes of discrete event systems. The general MLD representation is given by

$$\mathbf{X}(t+1) = \mathbf{A}\mathbf{X}(t) + \mathbf{G}_1\mathbf{U}(t) + \mathbf{G}_2\delta(t) + \mathbf{G}_3\mathbf{Z}(t)$$
$$\mathbf{Y}(t) = \mathbf{H}\mathbf{X}(t) + \mathbf{D}_1\mathbf{U}(t) + \mathbf{D}_2\delta(t) + \mathbf{D}_3\mathbf{Z}(t) \qquad (3.42)$$

subject to

$$\mathbf{E}_2\delta(t) + \mathbf{E}_3\mathbf{Z}(t) \le \mathbf{E}_1\mathbf{U}(t) + \mathbf{E}_4\mathbf{X}(t) + \mathbf{E}_5$$

where $\mathbf{X} \in \mathbb{R}^{n_l} \times 0, 1^{n_l}$ is a vector of continuous and binaries states, $\mathbf{U} \in \mathbb{R}^{m_c} \times 0, 1^{m_l}$ are the inputs, $\mathbf{Y} \in \mathbb{R}^{p_c} \times 0, 1^{p_l}$ the outputs, $\delta \in 0, 1^{r_l}$, $\mathbf{Z} \in \mathbb{R}^{r_c}$ represent auxiliary binary and continuous variables respectively, which are introduced when

transforming logic relations into mixed-integer linear inequalities, and $\mathbf{A}$, $\mathbf{G}_1$, $\mathbf{G}_2$, $\mathbf{G}_3$, $\mathbf{H}$, $\mathbf{D}_1$, $\mathbf{D}_2$, $\mathbf{D}_3$, $\mathbf{E}_1$, $\mathbf{E}_2$, $\mathbf{E}_3$, $\mathbf{E}_4$, $\mathbf{E}_5$ are matrices of suitable dimensions.

In short, hybrid dynamics deals precisely with systems that result from the interconnection of differential equations with logic-based decision rules. This section is devoted to show that the greenhouse climatic control problem can be described as a hybrid system, where ventilation and heating dynamics are switched. First, it will be shown that the greenhouse dynamics can be represented in the form of (3.41) as an autonomous hybrid system, where two different discrete variables produce the operation mode changes. Afterward, the hybrid dynamics will be expressed as a MLD system.

In the temperature control problem in a greenhouse, heating dynamics and ventilation dynamics are switched during the day and the night based on the value of the temperature set point, the inner temperature, and several security limits. Typically, as has been previously explained, the switching between ventilation and heating, that is, the change of the energy source, is performed at dark and at dawn, in such a way that the heating system is working only during the night and the ventilation system is only working during the day. So, in this case the dynamics change is based on the solar radiation. However, there exist some situations where heating has to be used during the day and ventilation during the night, thus producing a commutation in the representative dynamics of the system. For instance, and as commented previously, the temperature set points (possibly optimized by the hierarchical layer explained in Chap. 4) are modified in order to keep the inner humidity within some specific limits. Therefore, it could be possible that after such modification, the new required set point takes too high values during the day or too low values during the night, being difficult to reach them using the ventilation and heating systems, respectively (see Fig. 3.43). In these cases the ventilation and heating dynamics should be switched in order to follow the new temperature references.

As described in previous sections, the greenhouse temperature dynamics can be represented as a set of several subdynamics including the effect of the heating system, the ventilation system, and disturbances such as outside temperature, wind speed, and solar radiation. The effect of the different disturbances can be represented as follows:

$$
\begin{aligned}
\dot{X}_{T,a-\mathrm{rs}} &= A_{\mathrm{rs}} X_{T,a-\mathrm{rs}} + B_{\mathrm{rs}} D_{\mathrm{rs,e}}; \\
Y_{T,a-\mathrm{rs}} &= C_{\mathrm{rs}} X_{T,a-\mathrm{rs}} + E_{\mathrm{rs}} D_{\mathrm{rs,e}}
\end{aligned}
\tag{3.43}
$$

$$
\begin{aligned}
\dot{X}_{T,a-\mathrm{ws}} &= A_{\mathrm{ws}} X_{T,a-\mathrm{ws}} + B_{\mathrm{ws}} D_{\mathrm{ws,e}}; \\
Y_{T,a-\mathrm{ws}} &= C_{\mathrm{ws}} X_{T,a-\mathrm{ws}} + E_{\mathrm{ws}} D_{\mathrm{ws,e}}
\end{aligned}
\tag{3.44}
$$

$$
\begin{aligned}
\dot{X}_{T,a-T_e} &= A_{T_e} X_{T,a-T_e} + B_{T_e} D_{T,e}; \\
Y_{T,a-T_e} &= C_{T_e} X_{T,a-T_e} + E_{T_e} D_{T,e}
\end{aligned}
\tag{3.45}
$$

where $X_{T,a-\mathrm{rs}}$, $X_{T,a-\mathrm{ws}}$, $X_{T,a-T_e}$, $Y_{T,a-\mathrm{rs}}$, $Y_{T,a-\mathrm{ws}}$, $Y_{T,a-T_e}$ represent the states and outputs of the dynamical system representing the influence on the inner temperature due to solar radiation, wind speed, and outside temperature respectively. $D_{\mathrm{rs,e}}$ is

the solar radiation, $D_{\text{ws,e}}$ the wind speed, $D_{T,\text{e}}$ the outer temperature, and A_x, B_x, C_x, and E_x are matrices of corresponding size. The proposed extended vector X_{d} including the disturbance dynamics is defined as

$$\mathbf{X_d} = [X_{T,a-\text{rs}} \; X_{T,a-\text{ws}} \; X_{T,a-T_e}]^\top \tag{3.46}$$

Then, the effect of disturbances can be expressed in the following way

$$\dot{\mathbf{X}}_{\text{d}} = A_{\text{d}}\mathbf{X}_{\text{d}} + \mathbf{B}_{\text{d}}\mathbf{D}_m \tag{3.47}$$
$$\mathbf{Y}_{\text{d}} = \mathbf{C}_{\text{d}}\mathbf{X}_{\text{d}} + \mathbf{E}_{\text{d}}\mathbf{D}_m \tag{3.48}$$

where $\mathbf{A_d}$, $\mathbf{B_d}$, $\mathbf{C_d}$, and $\mathbf{E_d}$ are diagonal matrices easily obtained from (3.43) to (3.45), and $\mathbf{D}_m = [D_{\text{rs,e}} \; D_{\text{ws,e}} \; D_{T,\text{e}}]^\top$ is the vector of measurable disturbances.

Certainly, and considering that ventilation and heating systems are usually not used together (as was justified in previous comments), the greenhouse temperature dynamic behavior is mainly described by two switched dynamics, heating dynamics, and ventilation dynamics, both affected by the previous disturbances (see Fig. 3.44). Therefore, the inner temperature will be represented by $X_{T,a-v}$ or $X_{T,a-h}$ when the ventilation or heating systems are working, respectively. Such dynamics can be represented as follows

$$\begin{aligned}
\dot{X}_{T,a-v} &= A_{\text{v}}X_{T,a-v} + B_{\text{v}}U_{\text{ven}} + \vartheta_x; \\
Y_{T,a-v} &= C_{\text{v}}X_{T,a-v} + E_{\text{v}}U_{\text{ven}} + \vartheta_y \\
\dot{X}_{T,a-h} &= A_h X_{T,a-h} + B_h U_{T,\text{heat}} + \vartheta_x; \\
Y_{T,a-h} &= C_h X_{T,a-h} + E_h U_{T,\text{heat}} + \vartheta_y
\end{aligned} \tag{3.49}$$

$$\tag{3.50}$$

where $\vartheta_x = \dot{\mathbf{X}}_{\text{d}}$, $\vartheta_y = \mathbf{Y}_{\text{d}}$, and U_{ven} and $U_{T,\text{heat}}$ are the ventilation and heating control signals, respectively.

Hence, considering the different dynamics described above, a preliminary representation for the switched inner temperature dynamics, $X_{T,\text{a}}$, is described as follows:

$$\begin{aligned}
\dot{X}_{T,\text{a}} &= (\alpha A_{\text{v}} + (1-\alpha)A_h)X_{T,\text{a}} + \alpha B_{\text{v}}U_{\text{ven}} \\
&\quad + (1-\alpha)B_h U_{T,\text{heat}} + \vartheta_x \\
Y_{T,\text{a}} &= (\alpha C_{\text{v}} + (1-\alpha)C_h)X_{T,\text{a}} + \alpha E_{\text{v}}U_{\text{ven}} \\
&\quad + (1-\alpha)E_h U_{T,\text{heat}} + \vartheta_y
\end{aligned} \tag{3.51}$$

$$\tag{3.52}$$

with $\alpha \in [0, 1]$, which is the discrete variable leading the commutation between both dynamics.

As described previously, the main objective is to regulate the inner temperature to a specific reference. Therefore, the following variable change $\tilde{X}_{T,\text{a}} = X_{T,a} - T_{\text{ref}}$ is considered, in order to include the reference as an input signal in the previous system description

$$\dot{\tilde{X}}_{T,a} = A_T \tilde{X}_{T,a} + (A_T - I)T_{\text{ref}} + \alpha B_v U_{\text{ven}} + (1 - \alpha)B_h U_{T,\text{heat}} + \vartheta_x \quad (3.53)$$
$$Y_{T,a} = C_T \tilde{X}_{T,a} + C_T T_{\text{ref}} + \alpha E_v U_{\text{ven}} + (1 - \alpha)E_h U_{T,\text{heat}} + \vartheta_y \quad (3.54)$$

where $A_T = (\alpha A_v + (1 - \alpha)A_h)$, $C_T = (\alpha C_v + (1 - \alpha)C_h)$ and I is the identity matrix of the corresponding size.

In summary, the full temperature dynamics can be expressed as a hybrid system with the temperature set point, the heating control signal, the ventilation control signal, and the disturbances as inputs, where the system dynamics is switched based on the combination of the solar radiation (day or night), set point temperature, and the inner temperature. Hence, and such as it can be observed from Fig. 3.44, the full hybrid description of the system can be expressed in the form of (3.41) as follows:

$$\dot{\tilde{X}}_{T,a} = A_T \tilde{X}_{T,a} + [(A_T - I)T_{\text{ref}} \ \alpha B_v \ (1 - \alpha)B_h] \begin{bmatrix} T_{\text{ref}} \\ U_{\text{ven}} \\ U_{T,\text{heat}} \end{bmatrix} + \vartheta_x \quad (3.55)$$

$$Y_{T,a} = C_T \tilde{X}_{T,a} + [C_T \ \alpha E_v \ (1 - \alpha)E_h] \begin{bmatrix} T_{\text{ref}} \\ U_{\text{ven}} \\ U_{T,\text{heat}} \end{bmatrix} + \vartheta_y$$

subject to

$$\eta = X_{T,\text{rs}} < \underline{X_{T,\text{rs}}}$$
$$\alpha = (\sim\eta \wedge T_{\text{ref}} \leq \overline{T_{\text{ref}}} \wedge X_{T,a} \geq \underline{T_{\text{ref}}}) \vee$$
$$\vee [\eta \wedge (T_{\text{ref}} \leq \overline{T_{\text{ref}}} \vee (T_{\text{ref}} \geq \underline{T_{\text{ref}}} \wedge X_{T,a} > \overline{T_{\text{ref}}}))]$$

where η indicates the nightfall and $[\underline{T_{\text{ref}}}, \overline{T_{\text{ref}}}]$ the set point limits which influence on the use of the ventilation during the night, and the use of the heating system during the day.

A graphical representation of the switched dynamics can be observed in Fig. 3.45, where the full dynamics commutation is provided and $[\underline{T_{\text{ref}}}, \overline{T_{\text{ref}}}]$ limits have been set to $[20, 30]\,°\text{C}$ for daytime and $[10, 20]\,°\text{C}$ for nighttime periods, respectively.

As commented above, MLD representations are becoming a standard way to model hybrid systems in the control community. The rules and properties proposed in [175, 273] to help the translation of hybrid systems into MLD representation have been followed in order to obtain a MLD model for the discrete version of system (3.55). The MLD model has resulted as follows (from here t represents sample time for the sake of simplicity):
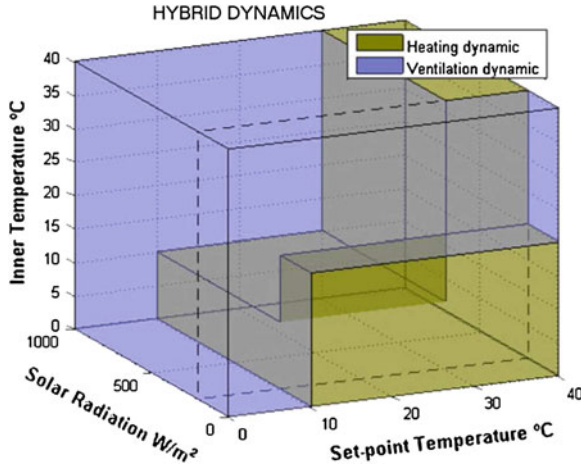
Fig. 3.45 3D representation for limits delimiting the switched inner temperature dynamics. *Dashed line* represents nightfall. As a courtesy of the authors [362]

$$\tilde{X}_{T,a}(t+1) = Z_1(t) + \vartheta_x(t)$$
$$Y_{T,a}(t) = Z_2(t) + \vartheta_y(t)$$

subject to

$(m_{h1}-M_{v1})\alpha(t)+Z_1(t)\le A_h X_{T,a-h}(t)+B_h U_{T,\text{heat}}(t)$ $\qquad\qquad \delta_7(t)-\alpha(t)\le 0$

$(m_{v1}-M_{h1})\alpha(t)-Z_1(t)\le -(A_h X_{T,a-h}(t)+B_h U_{T,\text{heat}}(t))$ $\qquad\qquad \delta_{10}(t)-\alpha(t)\le 0$

$(M_{h1}-m_{v1})\alpha(t)+Z_1(t)\le (A_v X_{T,a-v}(t)+B_v U_{\text{ven}}(t))+(M_{h1}-m_{v1})$ $\qquad \alpha(t)-\delta_7(t)-\delta_{10}(t)\le 0$

$(M_{v1}-m_{h1})\alpha(t)-Z_1(t)\le -(A_v X_{T,a-v}(t)+B_v U_{\text{ven}}(t))+(M_{v1}-m_{h1})$ $\qquad \delta_7(t)-\delta_2(t)\le 0$

$(m_{h2}-M_{v2})\alpha(t)+Z_2(t)\le C_h X_{T,a-h}(t)+B_h U_{T,\text{heat}}(t)$ $\qquad\qquad \delta_7(t)-\delta_3(t)\le 0$

$(m_{v2}-M_{h2})\alpha(t)-Z_2(t)\le -(C_h X_{T,a-h}(t)+B_h U_{T,\text{heat}}(t))$ $\qquad\qquad \delta_7(t)-\delta_6(t)\le 0$

$(M_{h2}-m_{v2})\alpha(t)+Z_2(t)\le (C_v X_{T,a-v}(t)+C_v U_{\text{ven}}(t))+(M_{h2}-m_{v2})$ $\qquad \delta_2(t)+\delta_3(t)+\delta_6(t)-\delta_7(t)\le 0$

$(M_{v2}-m_{h2})\alpha(t)-Z_2(t)\le -(C_v X_{T,a-v}(t)+C_v U_{\text{ven}}(t))+(M_{v2}-m_{h2})$ $\qquad \delta_8(t)-\delta_4(t)\le 0$

$(m_{\delta_1}-\xi)\delta_1(t)\le X_{T,\text{rs}}(t)-\underline{X_{T,\text{rs}}}(t)-\xi$ $\qquad\qquad \delta_8(t)-\delta_5(t)\le 0$

$-(\xi+M_{\delta_2})\delta_2(t)\le -(X_{T,\text{rs}}(t)-\underline{X_{T,\text{rs}}}(t))-\xi$ $\qquad\qquad \delta_4(t)+\delta_5(t)-\delta_8(t)\le 0$

$(m_{\delta_3}-\xi)\delta_3(t)\le T_{\text{ref}}(t)-\overline{T_{\text{ref}}}(t)-\xi$ $\qquad\qquad \delta_3(t)-\delta_9(t)\le 0$

$-(\xi+M_{\delta_4})\delta_4(t)\le -(T_{\text{ref}}(t)-\underline{T_{\text{ref}}}(t))-\xi$ $\qquad\qquad \delta_8(t)-\delta_9(t)\le 0$

$-(\xi+M_{\delta_5})\delta_5(t)\le -(X_{T,a}(t)-\overline{T_{\text{ref}}}(t))-\xi$ $\qquad\qquad \delta_9(t)-\delta_3(t)+\delta_8(t)\le 0$

$-(\xi+M_{\delta_6})\delta_6(t)\le -(X_{T,a}(t)-\underline{T_{\text{ref}}}(t))-\xi$ $\qquad\qquad \delta_1(t)-\delta_{10}(t)\le 0$

$\delta_9(t)-\delta_{10}(t)\le 0$ $\qquad\qquad \delta_1(t)-\delta_9(t)+\delta_{10}(t)\le 0$

$$(3.56)$$

This representation helps studying the hybrid dynamics of the greenhouse climatic control problem. Therefore, this result is suitable to be used for designing hybrid control algorithms, for example, using the well-known hybrid toolbox for *Matlab* [35]. In fact, the work presented in this section only covers heating and ventilation dynamics, but the approach can even be more useful if more control variables are taken into account (e.g., shade screen and humidifiers).

Figure 3.46 shows representative results of the performance of the GPC controller explained in Sect. 3.2.6 for controlling temperature using the heating system and of
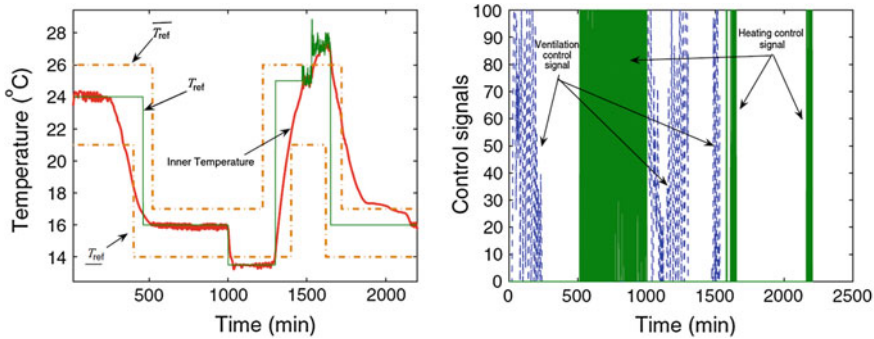
Fig. 3.46 Temperature control. Commutation between heating and ventilation systems. As a courtesy of the authors [362]

the AC treated in Sect. 3.2.2 for controlling temperature using ventilation system, respectively. In nominal operation, the heating controller helps to achieve about 20 % of saving in fuel consumption, the number of commutations being within the ranges recommended by the supplier. On the other hand, the results obtained with the AC have presented acceptable performance results, being tested to analyze both short-term and long-term objectives. In [43] multiple results and graphics can be found, being out of this section for saving space reasons. The most interesting results are shown in Fig. 3.46, that summarizes the approach shown in this section. It is possible to observe how heating and ventilation dynamics are switched along the day and the night. At the instant time 994 min ventilation control is switched on in order to reach a new required low set point that is impossible to achieve using the heating system. In the same way, at instant time 1,531 min the heating systems begin to work for a couple of hours in order to follow the new reference values modified based on the humidity control, which are quite high to reach using the ventilation system. This kind of behavior is not common in the greenhouse control field, but the hybrid systems theory provides a framework to easily accommodate such situations.

3.2.10 Fuzzy Logic Control of Nighttime Temperature

Fuzzy logic controllers (FLC) are widely used within the greenhouse climate control problem, as can be seen in the large number of references presented in Table 3.2. This sections presents a summary of the development of a FLC for temperature control using heating systems of forced-air type [291]. The designed controllers are Takagi-Sugeno (T–S) ones and the design method is iterative by solving a set of Linear Matrix Inequalities (LMIs) to ensure stability and performance in closed loop. As shown in some of the previous sections, most advanced control strategies make use of a linear model of the temperature for a particular operation point, and this can be a serious inconvenience given that the process is known to be nonlinear. Another disadvantage of some of these techniques is the complexity of implementing the controller. In this section, the nonlinear dynamics of greenhouse temperature are described by a set of

linear models with fuzzy interpolation (see Sect. 2.1.3.3), proportioning a nonlinear but easy to implement controller that ensures stability and performance [435, 438]. A previous attempt to use LMIs for greenhouse control was presented in [84], but only tested in simulation and practically complex to implement. Further developments can be found in [89].

The controller design procedure explained in this section interpolates linear controllers based on state feedback through membership functions that absorb the nonlinear terms (a technique known as Parallel Distributed Compensation (PDC) [472]). The gain of each local controller will in turn be obtained as the solution to an optimization problem formulated using LMIs, following an adaptation of the generic technique proposed in [289, 290]. The resulting controller will only be a series of state feedback controllers with nonlinear interpolation, thus enabling its implementation in these systems without the need for an excessive amount of calculation (like a typical gain-scheduling controller). The approach is directly based on preexisting physical models, and gives the region where the controller is ensured to be stable, so it is appealing for plant engineers.

For greenhouses, the proposal starts from a simple nonlinear model obtained from energy balances, which enables a TS model to be derived with only two fuzzy rules, which represent precisely the nonlinear model. The resulting controller is simple to implement in nighttime temperature control systems for greenhouses.

A T–S system in discrete time for a system with input vector $\mathbf{U}(t) \in \mathbb{R}^m$, output vector $\mathbf{Y}(t) \in \mathbb{R}^p$, and state vector $\mathbf{X}(t) \in \mathbb{R}^n$, consists of a fuzzy set of $\aleph$ rules that give rise to the following global dynamic model:

$$\mathbf{X}(t+1) = \sum_{i=1}^{\aleph} \mu_i(\varsigma)(\mathbf{A}_i\mathbf{X}(t) + \mathbf{B}_i\mathbf{U}(t)) \tag{3.57}$$

$$\mathbf{Y}(t) = \sum_{i=1}^{\aleph} \mu_i(\varsigma)\mathbf{C}_i\mathbf{X}(t)$$

where ς are the fuzzy variables (whose dependence on the state variables $\mathbf{X}(t)$ and possible disturbances is omitted for simplicity), μ_i are the corresponding normalized membership functions, and $\mathbf{A}_i$, $\mathbf{B}_i$ and $\mathbf{C}_i$ are the state matrices corresponding to each submodel (for details, see [435]). In this section, it is assumed that the state matrices are precisely known, and a methodology is used to derive them from the nonlinear dynamical model of a greenhouse. In the case where the parameters of the system are not perfectly known, techniques are available to cope with uncertainty (see [59, 385] and references therein). The output matrices $\mathbf{C}_i$ are not assumed to be the same for all the rules.

The controller shares the same fuzzy sets as the system model, so it is given by the interpolation of $\aleph$ linear compensators. Using a static output feedback, the resulting controller has the following structure:

$$\mathbf{U}(t) = \sum_{i=1}^{\aleph} \mu_i(\varsigma)\mathbf{K_i}\mathbf{Y}(t). \tag{3.58}$$

The complete algorithm to find stabilizing controllers is based on LMIs and provided in [291]. The result of the algorithm is then a set of gains $\mathbf{K_i}$ that ensure closed loop stability.

The development of T–S models is based on the simplified energy balances shown in Chap. 2. As shown in [291], an equivalent T–S model to the first principles one can be represented using a differential equation of the type:

$$X_{T,a}(t+1) = f(X_{T,a}, *)X_{T,a}(t) + Q_{max}U_{T,heat}(t) \tag{3.59}$$

where $f(\cdot)$ is a nonlinear function that depends on the temperature and on the rest of the variables an parameters of the nonlinear model (explicitly developed in [291], Q_{max} is the maximum energy that can be contributed by the system and $U_{T,heat}(t)$ is the heater's activation control signal (see Eq. (2.38)).

As $f(\cdot)$ is bounded between two values ($\underline{f} \le f \le \overline{f}$), then it can be written as:

$$f = \overline{f}\mu(X_{T,a}, *) + \underline{f}[1 - \mu(X_{T,a}, *)]. \tag{3.60}$$

It is thus sufficient to consider μ as a fuzzy function in order to obtain the proposed T–S model as the model of the greenhouse for designing the controllers:

$$X_{T,a}(t+1) = \overline{f}\mu(X_{T,a}, *) + \underline{f}[1 - \mu(X_{T,a}, *)]X_{T,a}(t) + Q_{max}U_{T,heat}(t) \tag{3.61}$$

where the membership function μ is simply evaluated as:

$$\mu(\cdot) = \frac{f(\cdot) - \underline{f}}{\overline{f} - \underline{f}} \tag{3.62}$$

The heating system used in the examples shown in this section consists of the hot air heater explained in Sect. 3.1.2.2. The actuation variable $U_{T,heat}(t)$ is, in fact, used as a reference for a simple control system that continuously turns the heater on and off. Except for the generation of small perturbations on the output, this does not significantly affect the design procedure used. In fact, it simplifies the procedure, as rapid variations of $U_{T,heat}(t)$ do not significantly affect the duration of the actuator (since it is continuously switching on and off in any case), so constraints on the dynamics of the control signal are not very relevant in this case.

The T–S model was validated using the first principles models and using data taken from the greenhouse during spring and autumn growing seasons (Fig. 2.17), providing extreme values of the nonlinear smooth function as $\overline{f} = 0.000135$ and $\underline{f} = 0.000108$, in order to obtain the corresponding membership functions following (3.62).

The structure of the regulator is thus:

$$U_{T,\text{heat}}(t) = [K_1\mu(\cdot) + K_2(1 - \mu(\cdot))]X_{T,\text{a}}(t) \tag{3.63}$$

where K_i are the gains to be designed (see [291]) and $\mu(\cdot)$ is a fuzzy membership function, evaluated at the current conditions of the greenhouse (internal and external temperatures, humidity, etc.). This regulator is simple to implement in greenhouse control systems, as it corresponds to a simple feedback of the variable measured using a variable gain (that depends on the measured variables). In fact, if necessary, this gain can be prerecorded using a single look-up table.
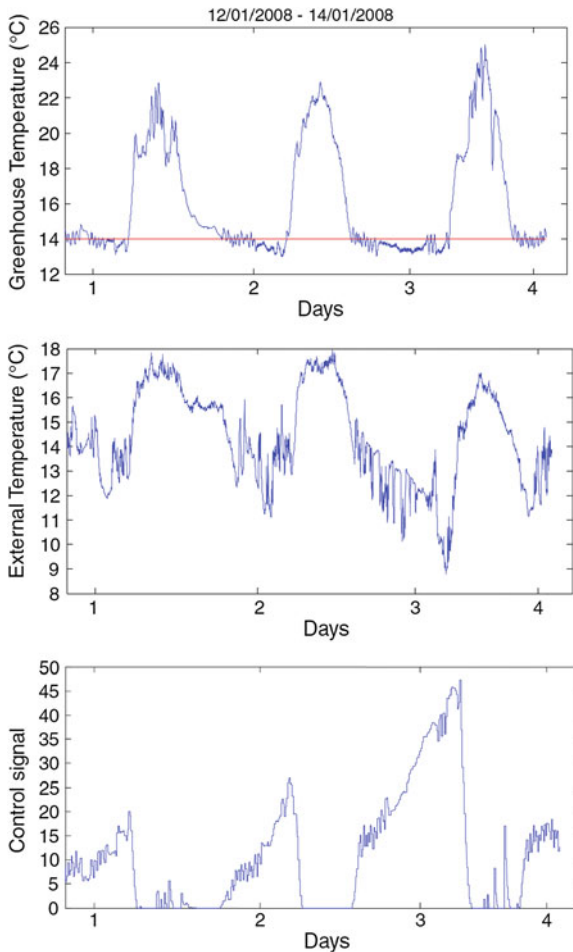
Fig. 3.47 Control test with the fuzzy logic controller on the greenhouse (nighttime reference: 14 °C). As a courtesy of the authors [291]

Figure 3.47 shows the results of three consecutive days when heating was required, using a set point of 14 °C, with a maximum deviation of 1 °C during nights with strong

external disturbances (the outside temperature is included in the plot and decreased down to 9 °C). The corresponding control signal calculated by the proposed controller is depicted in the same figure (this control signal corresponds to the activation time of a lower level PWM controller that switches on/off the heating system). The whole result is more than acceptable for this type of system.

3.2.11 Model-Based Irrigation Control

3.2.11.1 Introduction

In this section, an irrigation control algorithm based on evapotranspiration and relative humidity of substrate is developed, using computer-based on/off control based on a determined criterion, such as water level, amount of accumulated solar radiation, or transpiration.

Related works on water supply control techniques mainly deal with FF control [224, 400]. In [145], feedback control is implemented using drainage as feedback signal, while water absorption is treated as a disturbance. Other works deal with the application of FLC for fertigation purposes. In [487] FLC was used, so that the irrigation time and amount of water to supply were determined from measurements of soil moisture and the amount of drainage water and human experience. This FLC was applied to control ornamental plants in greenhouses developed in a substrate mixing peat and pine bark. In [366] the inputs to the fuzzy inference mechanism were the moisture content of the substrate and the estimated evapotranspiration from climatic data; decision rules were built to apply irrigation control on tomato grown in sand. In [493] a fuzzy PID algorithm was designed using as inputs flow rate of concentrated fertilizer solutions in mixing tank by Venturi regulated by a solenoid valve with PWM method. A fuzzy PID control algorithm was developed to regulate the fertilizer component ratio and the EC/pH value of the nutrient solution. In [488] a wireless sensor network is used for irrigation purposes also based on fuzzy PID control of soil temperature and humidity. In [166] a fuzzy controller is introduced to control greenhouse climate (using a shading screen) to reduce tomato cracking using as variables solar radiation, substrate temperature, and canopy temperature.

In soilless systems, control of irrigation water is closely linked to control of nutrient supply, so that many of the works carried out are aimed at gaining control of water and nutrients, as mentioned later.

In [224] FF control of the concentration of the nutrient solution is performed, using models of photosynthesis, absorbed water (estimated by a transpiration model) and assuming constant the content of main elements of the produced dry matter. Following the same approach, [223] shows results where water and nutrients demand is synchronized with their supply as a function of climatic parameters, producing set points of daily nutrient solution based on an empirical estimate of the ratio between water and nutrients demand [221]. Only FF control was implemented and authors indicated that no feedback based on leachate was necessary. Tests were carried out

in tomato and pepper reusing drainage water and compared with other in which constant concentration in the nutrient solution was used. Feedforward control helped to reduce blossom end rot of fruits and to increase fresh weight of fruit yield [222].

Other studies also used FF irrigation control using system identification in NFT and substrate crops. The amount of water supplied to the system is a direct function of solar radiation and control is performed to maintain a constant level of drainage. Tests were performed in a system without plants [142]. In [143] multivariable FF control was implemented to supply water and eight elements in the nutrient solution. Simulations are included showing the controller is capable of reaching a constant level in the potassium content in the leachate.

In [188] neural networks are proposed for controlling the supply of water and nutrients, based on the expertise of the farmer. The input variables to the network are solar radiation, temperature, relative humidity, water temperature, and carbon dioxide concentration in the greenhouse. The output variables are the amount of water and nutrients to be supplied to the system.

3.2.11.2 Algorithms and Illustrative Results

This section describes illustrative results of tests performed on irrigation based on a model of transpiration. Irrigation scheduling based on transpiration was performed in such a way that after the initial irrigation, water supply was done using an estimation of crop transpiration based on climatic data recorded every minute. Irrigation signal activates when the volume specified by the user is reached, providing an amount of water equivalent to the estimated transpiration plus a desired percentage of drainage. On/off control techniques were applied and the transpiration model used was the one described in Chap. 2, based on [419] but calibrated and validated for the system at hand.

Figure 3.48 shows the dynamics of transpiration and irrigation control during 2 days. The initial irrigation during the first day was done manually till reaching a drainage of around 10 %, while during the second day the desired drainage percentage was 20 %. The irrigation rate was set at $180\,\mathrm{ml\,m^{-2}}$, which was the equivalent of a 4 min irrigation, according to the characteristics of the irrigation system. Figure 3.48a shows the estimated crop transpiration, that is smaller in the first day. The irrigation activation signal and the water content in the substrate are included in Fig. 3.48b, while the vapor pressure deficit and global irradiance inside the greenhouse are shown in Fig. 3.48c. The variables associated with the dynamics of irrigation application (drainage, electrical conductivity in the substrate, temperature, and relative humidity of inside greenhouse air) can be seen in Fig. 3.49.

Transpiration dynamics showed a significant increase during the evening of the first day mainly associated with low vapor pressure deficit, which showed a rise at night, explained by the conditions of temperature and humidity. In response to this increase in transpiration, the control system applied three irrigations during the night of the first day (see Fig. 3.48a, b).

The environmental conditions during the second day increased transpiration, thus producing 13 irrigations, unlike the first day in which 9 were applied. The drainage
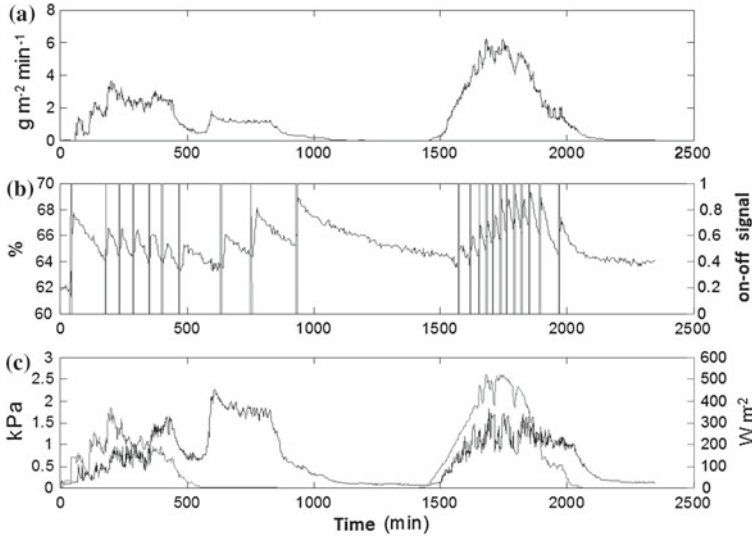
Fig. 3.48 Results using irrigation control based on transpiration during 2 days. **a** Crop transpiration. **b** Moisture content in the substrate and control signal. **c** Water pressure deficit and global irradiance in the greenhouse
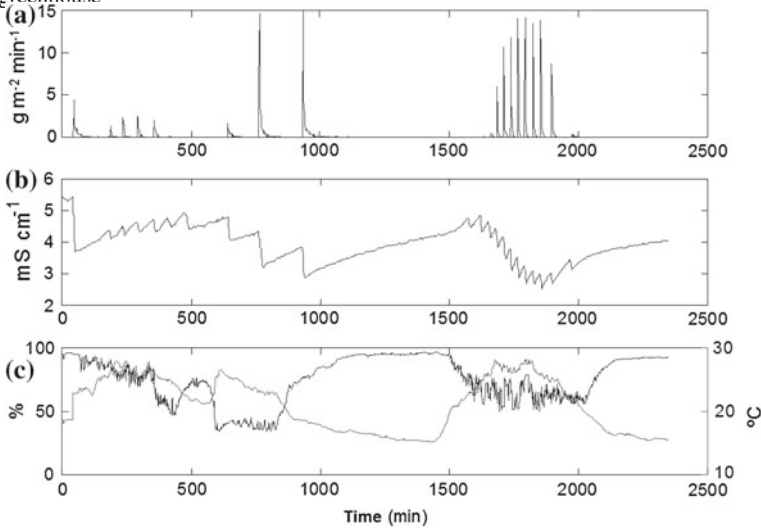

Fig. 3.49 Variables associated with irrigation control based on transpiration. **a** Dynamic drainage. **b** Electrical conductivity in the substrate. **c** Relative humidity and air temperature in the greenhouse

volume dynamics is shown in Fig. 3.49; obtaining 8 and 16 % in the first and second day. During the first three irrigations of the second day the drainage fraction was nil; however, when the moisture content of the substrate increased, the volume fraction of water drained and also showed a rising trend. The behavior of EC in the substrate is shown in Fig. 3.49b, decreasing in each irrigation applied to the system.
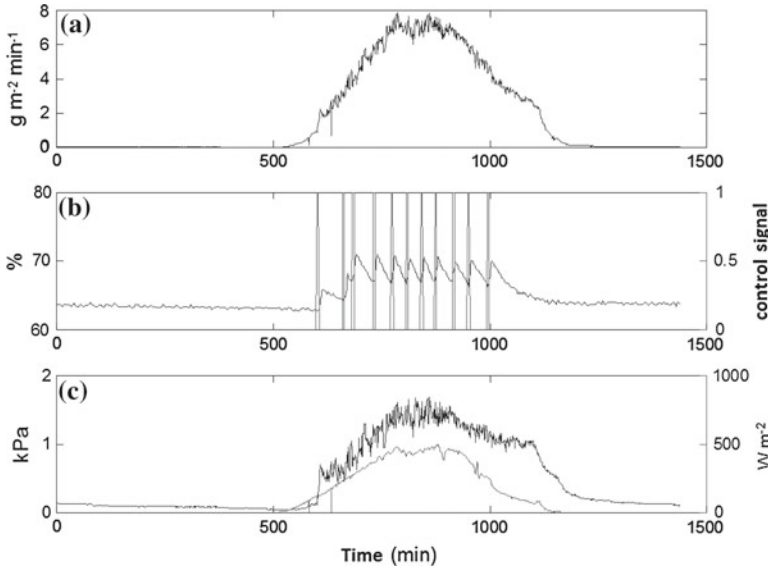
Fig. 3.50 Irrigation control based on demand tray. **a** Crop transpiration. **b** Moisture content in the substrate and control signal. **c** Vapor pressure deficit of water and global radiation in the greenhouse

Other tests showed a similar behavior to that described above, while the drainage fraction was 4–10 % lower than the set point established by the user.

The irrigation system applied using irrigation tray demand during daytime hours and responds to the amount of water that is absorbed by plants. The first irrigation is supplied at a fixed time and from this irrigation performance is determined by the level of water in the tray is detected by a sensor. Figure 3.50 shows the behavior of the irrigation system based on demand tray and the associated variables during day, while Fig. 3.51 represents the dynamics of the volume of drainage, EC in the substrate and greenhouse air temperature and humidity. The irrigation system based on demand tray supplies water during daytime and responds to the amount of water that is absorbed by the crop. The first irrigation is supplied at a fixed time and from this moment irrigation is determined by the water level in the tray.

The drainage volume dynamics is shown in Fig. 3.51a; during the first two irrigations there was no drainage and the fraction of drainage during the day was 18 %. Although drainage chart for a day shows some uniformity, variations in environmental conditions through the growing season cause this system does not conform to an established fraction of drains, being difficult to control them, as can be seen in Fig. 3.52, which shows the variation in the drainage fraction for several months using the demand try system.
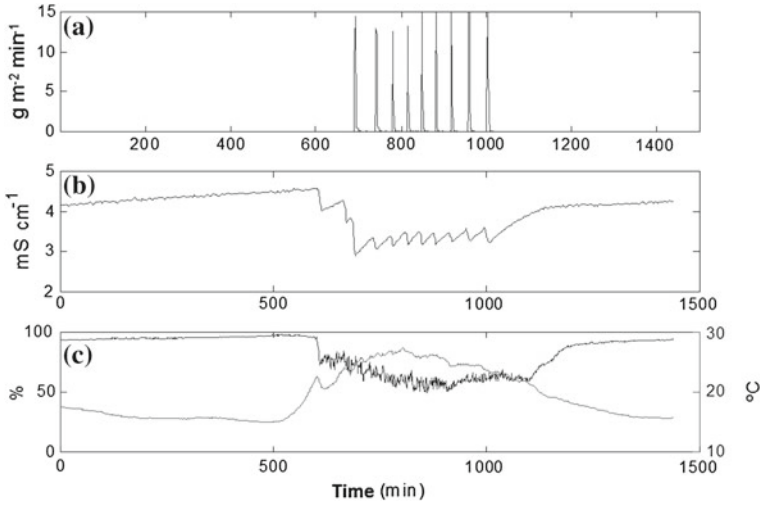
Fig. 3.51 Variables associated with irrigation. **a** Drainage. **b** Electrical conductivity in the substrate. **c** Relative humidity and air temperature in the greenhouse
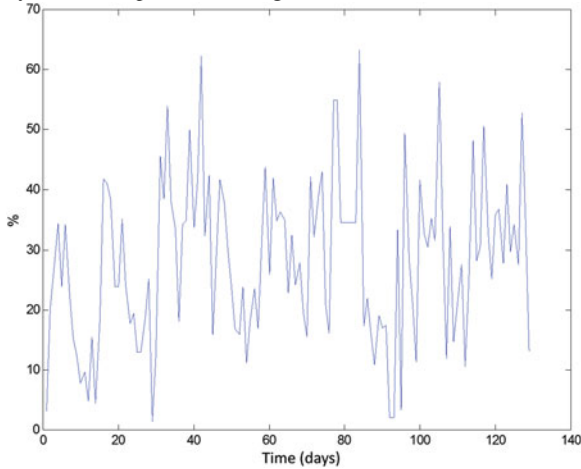

Fig. 3.52 Volume fraction of drainage during the growing season, applying irrigation based on demand tray

3.2.11.3 Simulation of Irrigation Control Based on the Moisture Content in the Substrate

A further possibility consists of controlling irrigation based on the moisture content in the substrate. The hydric balance model developed in Chap. 2 is used to determine the moisture content in the substrate, and to decide when to irrigate based on a set point established by the user. The simulations with this model were performed

using simple control techniques: On/off control with dead band and proportional control. When using on/off control with dead band it is established that irrigation is mainly performed during daytime, within a time interval during which humidity must evolve within maximum and minimum bounds defined by the user, constituting the control dead zone. Irrigation is activated when humidity is below the lower limit and deactivated when it reaches the upper limit. This strategy defines the amount of water, while the irrigation time is defined by the lower limit of the dead zone. Overnight, this strategy is switched off, but a security limit is defined so that, if it is surpassed, irrigation should be applied. Figure 3.53a shows a simulation using on/off control compared with the results obtained with demand try based control. Despite the controller simplicity, the humidity content is maintained within the range set by the user, and overnight prevents the amount of water in the substrate falls below the threshold, as shown in activation of the first irrigation of Fig. 3.53a. The on/off controller performs adequate control of moisture in the substrate relative to the demand tray application, since the maximum fluctuation in the moisture content is 0.6 over 3.3 % in demand tray.

Irrigation supply applying a proportional controller in which a moisture content set point is tracked has also been simulated. The approach is similar to the on/off controller in terms of a defined period during the day when irrigation should be applied. The simulation using this control technique can be seen in Fig. 3.53b; it is also compared with the demand try controller, including the evolution of the control signal. Figure 3.53 also includes other variables that are simulated by the water balance model and interact with the irrigation control system. It is possible to observe the dynamics of the structural dry matter in the root (Fig. 3.53c) and canopy (Fig. 3.53d), the dynamics of water reserve in the root and the canopy, in Fig. 3.53e, f, respectively, the temperature on the substrate (Fig. 3.53g) and transpiration (Fig. 3.53h).

Despite the apparent better performance of the proportional controller on on/off controller, which keeps the moisture content with small variations of the order of 0.05 %, the first one is difficult to use in irrigation systems because of the difficulty of finding proportional valves and pumps in this operating range and the associated costs.

Figure showing structural dry matter in the root and canopy (Fig. 3.53c, d) are typical of the dynamics of a day; during the night the breathing process predominates and simulated dry matter decreases, while during the light hours there is a sharp increase due to photosynthesis. On the other hand, the simulation of water in the canopy and root shows a close relationship between transpiration and the amount of water in the canopy by an inverse relationship, the water reservoir in the canopy decreases at noon and recovered overnight, while that of the root shows a temporal storage pattern with variations during the day than stabilizes at night (Fig. 3.53e, f).
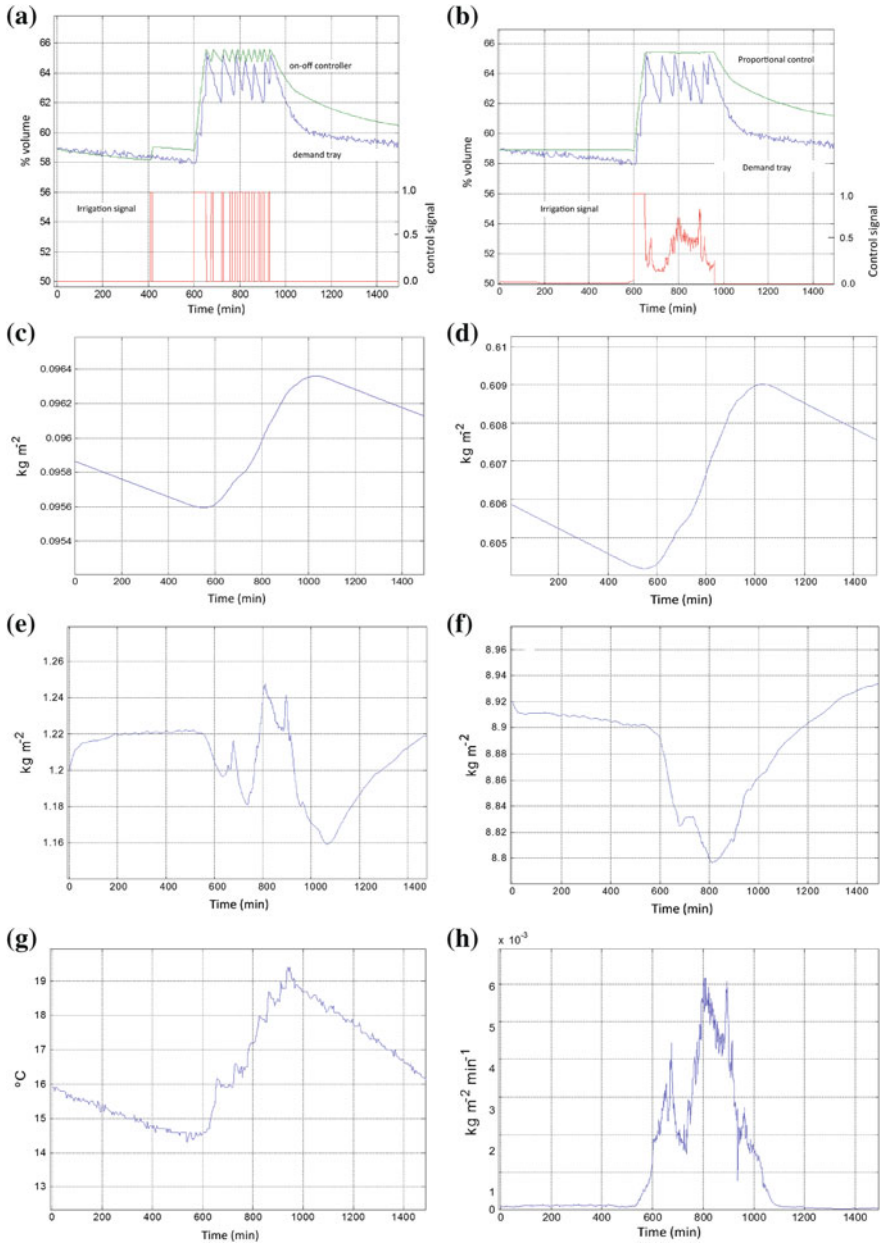
Fig. 3.53 Irrigation control based on moisture content in the substrate and other variables of the water balance model. **a** On/off control. **b** Proportional control. **c** Structural dry matter in the root. **d** Structural dry matter in the canopy. **e** Mass of water in the root. **f** Mass of water in the canopy. **g** Substrate temperature. **h** Transpiration

3.3 Conclusions

About ventilation control: The greenhouse crop production is influenced by the inside climate, so it is necessary to maintain the variables that characterize it within a given range considered ideal. This chapter has described the general problem of climate control, which is generated inside a greenhouse, and the problems particularly related to each of the climatic variables, which are usually controlled in southeastern Spain: temperature, relative humidity, and radiation. Furthermore, different strategies have been developed, implemented, and validated in both simulation and real tests. The algorithms developed have tried at all times to use information available of measurable disturbances, as they are the main source of energy required for crop growth, highlighting the proposal of FF and nonlinear controllers based on simplified models based on energy balances. All control strategies try to find a trade-off between performance and ease of understanding by users.

From all the experiences in this chapter, the following conclusions can be drawn:

- Although climate variables that affect crop growth are temperature, the PAR radiation and the CO_2 concentration, the main control is established on the indoor air temperature.
- The two main actuation systems are ventilation and heating, which exhibit reverse actions with respect to temperature, and do not usually act simultaneously.
- As in this application the temperature control specifications are not very restrictive and also considering the nature of the signals involved, it is possible to control greenhouse climate using classical strategies such as PID control or GS control (used in commercial control systems).
- The relative humidity of indoor air indirectly affects the development of the crop, so that it is convenient to maintain it within a predefined interval. The same actuators are used to control both temperature and humidity, and they are highly correlated with each other. Since temperature is the variable really affects the growth of plants, it is considered as the main controllable variable and humidity is maintained within a range, changing the set point temperature when required if humidity surpasses its bounds.

About heating control: Traditional heating systems in greenhouses are based on on/off control with dead zone. The evaluation of this kind of systems has shown that fuel consumption is high. MPC algorithms have demonstrated to be a valuable alternative for heating control minimizing fuel consumption, as the costs associated and outside climate variables are taken into account in the control design stage. The classical MPC algorithms have been modified to take into account the characteristics of the actuators, implementing both a PWM approach and a branch, and bound algorithm to obtain fuel savings of around 20 % when compared with on/off controllers.

About irrigation control: An irrigation control scheme has been developed in this chapter based on a model of transpiration. The influence of unmodeled dynamics and model accuracy has been studied in terms of subestimation of evapotranspiration or delays in water retention. Nevertheless, it has been established that irrigation based

on transpiration is a feasible method to control the water dynamics in the plants, interacting with climate control as there is a close feedback relationship between the transpiration process and the behavior of relative humidity and temperature inside the greenhouse, as indicated in [27] and demonstrated in [294, 422, 425].

The developed method can be improved by including the model within a MPC framework using a prediction horizon of around 30–40 min so that observed transport delays can be implicitly taken into account.

Chapter 4
Crop Growth Control

4.1 Hierarchical Control of Greenhouse Crop Growth

4.1.1 Introduction

As introduced in Chap. 1, the greenhouse crop production problem can be described as a hierarchical control system with three levels and different variations [177, 333, 355, 440, 461] (see Fig. 1.2). The existence of different timescales helps to decouple the climate control dynamics from those of crop growth and development, in such a way that the upper layer of a hierarchical control architecture calculates the climate setpoints for the lower layer, generally using static versions of crop growth and climate models. In this section, temperature setpoints are obtained based on economic criteria using a crop growth tomato model, economic data, and weather forecasts. Once the temperature setpoints are obtained (one for diurnal operation and another for nocturnal operation), these can be used by the climate control layer, but usually are subject to modifications due to grower preferences and/or to special operating conditions or security reasons, leading to changes in the mode of operation. The temperature control implemented by the lower layer of the hierarchical architecture is usually performed using ventilation during the day and heating during the night, although mixed approaches such as the switching control scheme explained in Sect. 3.2.9 can be implemented.

First, the hierarchical control architecture developed aimed at obtaining optimal nocturnal and diurnal setpoints is explained, describing in detail the proposed cost function and optimization procedure. Then, some experimental results representative of those obtained during the recent years are shown, where control results of both the optimization and regulatory layers are discussed.

4.1.2 Hierarchical Control Architecture to Maximize Profits

In [355], a hierarchical control architecture was proposed as an integral solution to crop growth control based on economic criteria. In this case, the control architecture was composed of two layers, as shown in Fig. 4.1, that control the system composed of crop and greenhouse climate, based on the existence of two different timescales. The upper layer (second layer) solves an optimization problem as a function of the expected production and associated costs or the desired date of harvesting. This optimization problem maximizes an objective function that represents the profit obtained based on the climatic variables, providing as results the setpoints that these climatic variables must follow along the season. The lower layer (first layer) includes the controllers that try to cancel tracking errors and compensate for disturbances considering the setpoints calculated by the upper layer. Several controllers have been proposed for this layer as described in Chap. 3. As shown in Fig. 4.1, the main actuators to control temperature and humidity are ventilation and heating. The shade screen is used to diminish the radiation onto the canopy, the reason that the crop growth rate also diminishes. This fact provides a new degree of freedom to control the production, delaying the harvesting date. Nevertheless, it is not considered in the optimization process because the system often tries to obtain the maximum
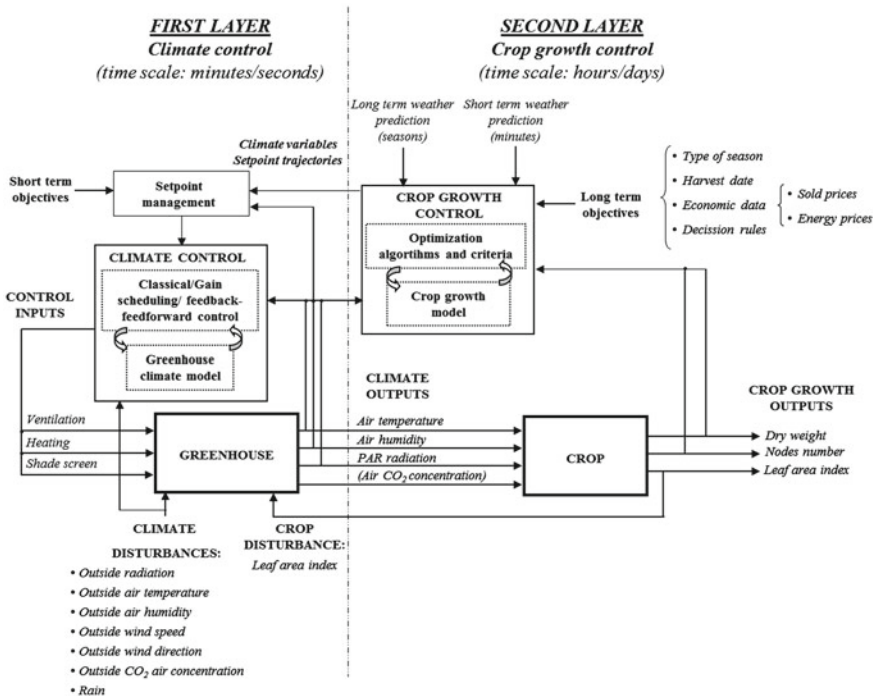
Fig. 4.1 Multilayer hierarchical system proposed to control the crop growth

production. So, the shade screen is only used under certain tactical circumstances based on the experience of the producer, as will be discussed in the following section where a three-layer hierarchical control approach is used.

The optimization problem follows a receding horizon strategy. Therefore, when a night–day transition (or vice versa) occurs, the optimization problem is again solved using new real measured data of climatic variables and crop growth, trying to reduce errors coming from plant-model mismatch, deviations in the weather forecast, or even because the climatic variables are not able to reach the setpoints.

The problem of crop growth control based on the greenhouse climatic conditions and considering economic criteria has different variants depending on the aspects to consider and the desired objective to reach. Particularly, the approach considered in this book is based on the following general hypotheses:

1. A single harvesting at the end of the season is considered (this is not a restrictive hypothesis, as the algorithm can easily manage continuous harvesting, as shown in Sect. 4.2).
2. The crop growth variable to be controlled is the global dry weight of the plant (measured using pattern plants or estimated using simplified models to simulate the tomato growth as proposed in [212]). There are different studies demonstrating that at the end of a season, the fraction of total dry weight that corresponds to the tomato fruits is approximately 60 %, as it is indicated in [184]. This fact has been corroborated in our own tests. On the other hand, the market prices are referred to the fresh weight. Some authors estimate that approximately the 6 % of the fruit weight correspond to dry matter (6.5 % [184], 5.5 % [213]). Our own experiences have estimated a fraction of 7 %, these data used to calculate the prices of the harvested products.
3. The optimization process obtains the optimal setpoint trajectories of the air temperature, which is the main control variable that affects the crop growth.
4. Two temperature setpoints per day are considered, one for diurnal time and another for nocturnal time (the plants do not make the same vital functions at night and at diurnal time). The commutation of the setpoints is made when the sun rises or falls (threshold of $100 \, \text{W m}^{-2}$, as the duration of the nocturnal and diurnal time periods is not constant along one year).
5. The system is well irrigated and fertilized.

One important component of the hierarchical control architecture is the coordination between the two layers. After analyzing and testing different alternatives, a receding horizon-based algorithm is selected, whose flow diagram is shown in Fig. 4.2.

At the beginning, some initial data must be set in order to initialize the control process of the crop growth: Type of season, date of harvesting, initial crop status, economic data (predicted final price of production sale and the price evolution of the electricity and the fuel throughout the season), and prediction horizon N (to generate $2N + 1$ initial intervals to compute setpoints). Based on these data and using a long-term weather prediction obtained from the AEMET weather forecast (according to the disturbance forecast models described in Sect. 2.4), an optimization problem is to determine the setpoints of temperature for all the time intervals along the prediction horizon.
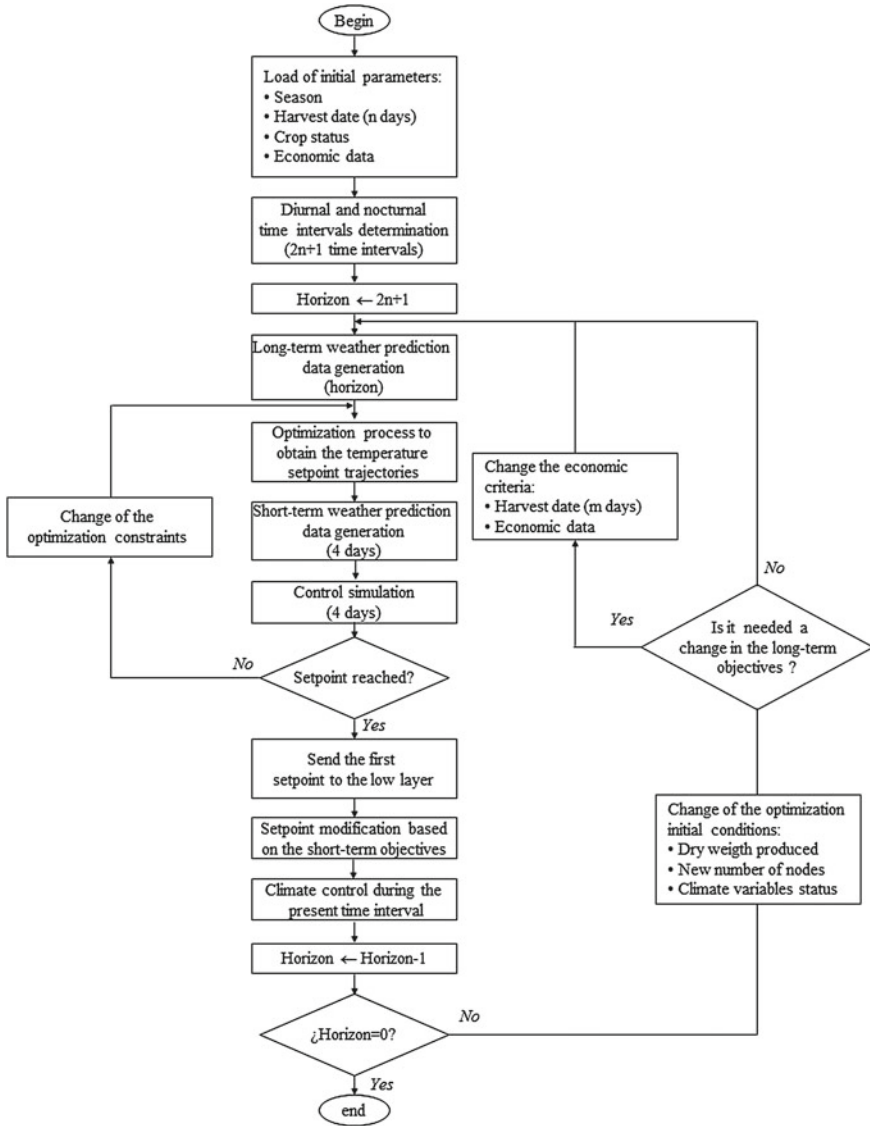
Begin

Load of initial parameters:
• Season
• Harvest date (n days)
• Crop status
• Economic data

Diurnal and nocturnal
time intervals determination
(2n+1 time intervals)

Horizon ← 2n+1

Long-term weather prediction
data generation
(horizon)

Optimization process to
obtain the temperature
setpoint trajectories

Change the economic
criteria:
• Harvest date (m days)
• Economic data

Change of the
optimization constraints

Short-term weather prediction
data generation
(4 days)

Control simulation
(4 days)

Setpoint reached?   No

Yes

Is it needed a
change in the long-term
objectives ?   No

Yes

Send the first
setpoint to the low layer

Setpoint modification based
on the short-term objectives

Climate control during the
present time interval

Change of the optimization
initial conditions:
• Dry weigth produced
• New number of nodes
• Climate variables status

Horizon ← Horizon-1

¿Horizon=0?   No

Yes

end

Fig. 4.2 Management algorithm of the hierarchical architecture. Courtesy of the authors of [360]

4.1.3 Cost Function and Optimization

The objective of the proposed hierarchical control problem consists in maximizing profits, that is, the differences between the incomes obtained from the final production sale and the associated production costs, which can be formulated as

$$J = c_{\text{area,ss}} V_{\text{price,cr}}(t_{\text{h}}) X_{\text{W}}(t_{\text{h}}) - \int_{t_{\text{i}}}^{t_{\text{h}}} V_{\text{cos}}(\tau)\, d\tau \qquad (4.1)$$

where $c_{\text{area,ss}}$ is the greenhouse soil surface, $V_{\text{price,cr}}$ are the sale prices of the production at the harvesting date, t_{h}, X_{W} is the dry weight (note that also fresh weight of fruits X_{FF} can be used here, as done in the following section), V_{cos} are the cost incurred by the actuators (electricity and fuel), and t_{i} is the initial time. It can be demonstrated [355] that all the variables present in the objectives are functions of the air temperature, as well as of measurable disturbances such as PAR radiation or CO_2 concentration. So, the cost function Eq. (4.1) can be expressed as a function of the temperature (and measurable disturbances) using a steady-state version of a crop growth model (Sect. 2.2.1.2).

The optimization problem is solved using SQP methods since a QP subproblem is solved at each major iteration. The constraints of this process are based on the internal air temperature, which must be between the lower and upper limits modified by a yearly pattern.

4.1.4 Representative Results

This section outlines representative control results from the evaluation of the hierarchical control structure in the greenhouse type Almería.

Several tests have been performed to study the response of the system under different conditions. The initial crop state is the same and the length of the crop cycle is 91 days.

The first tests were carried out to analyze the trends of the temperature setpoint trajectories along the autumn and winter seasons. Constant energy prices were considered. The results are shown in Fig. 4.3, considering constant constraints along the season. The optimal trajectories in each of the tests present a downward trend, maintaining maximum temperatures at the beginning of the season, diminishing them to the minimum allowed at the end. This result is not a common and typical strategy used in tomato crop in this zone, where the temperature setpoints are relatively constant and moderate along the season. The results improve the profit by around 12 %.

There are several situations when the lower layer is not able to reach the temperature setpoint calculated by the upper layer: The weather forecast is erroneous, the actuators are saturated, the temperature in diurnal intervals is less than the diurnal setpoint or the temperature in nocturnal intervals is greater than the nocturnal setpoint, the transitions between nocturnal and diurnal intervals are not immediate, etc. For example, if the weather forecast is erroneous, the system is unable to track the proposed setpoints, so the transition from high to low temperature is delayed. The system tends to maintain high temperatures to produce more dry weight due to the use of a receding horizon strategy. Similarly, if the harvesting date is modified, the system increases the temperature setpoint when the harvesting date is shortened
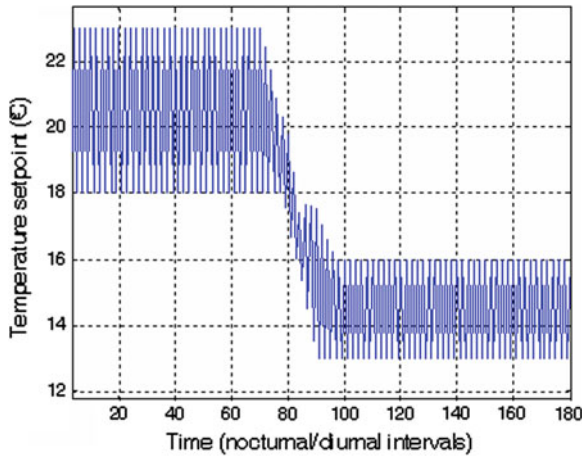
Fig. 4.3 Temperature setpoint trajectories. Courtesy of the authors of [360]
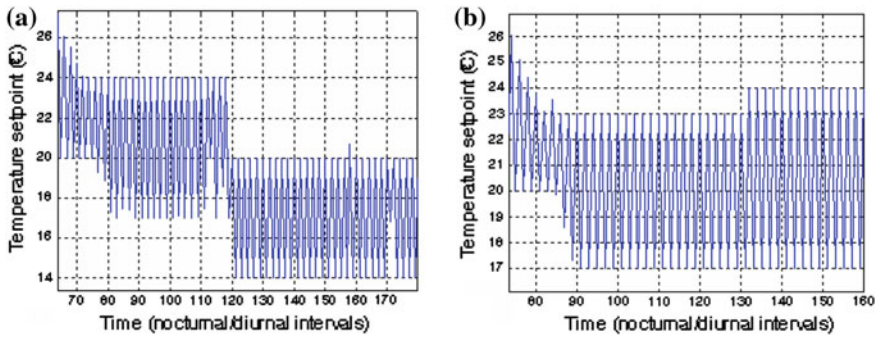

Fig. 4.4 Response when harvesting date is brought forward. Courtesy of the authors of [360]. **a** Season length = 90 days. **b** Season length = 80 days

to help the crop growth and diminishes it when this date is delayed to decrease the crop growth rate. For these reasons, sometimes it is better to use a three-layer hierarchical architecture as described in Chap. 1, where the middle layer checks these problems before providing the references to the lower layer and modifying them when necessary.

Figure 4.4 shows an example when on the 36th day the harvesting date is shortened by 10 days (the season is reduced from 90 to 80 days). Figure 4.4a shows the typical temperature setpoint trajectories calculated by the optimization process on the 35th day with a season length of 90 days. When in the next few days the harvesting date is changed, the system increases the diurnal and nocturnal temperature setpoints to maximize the profit, obtaining the maximum production.

4.2 Multiobjective Hierarchical Control of Greenhouse Crop Growth

4.2.1 Introduction

The problem of determining the trajectories to control greenhouse crop growth has traditionally been solved using constrained optimization or applying artificial intelligence techniques. As described in the previous section, the economic profit is used as the main criterion in most research on optimization to obtain adequate climatic control setpoints for crop growth. This section addresses the problem of greenhouse crop growth also through a hierarchical control architecture, but in this case governed by a high-level multiobjective (MO) optimization approach, where the solution to this problem is to find reference trajectories for diurnal and nocturnal temperatures (climate-related setpoints) and electrical conductivity (fertirrigation-related setpoints). The objectives are to maximize profit, fruit quality, and water-use efficiency, these being currently fostered by international rules. This hierarchical scheme is similar to that used in Fig. 4.1, but with an intermediate layer for setpoint adaptation. So, the resulting control architecture is composed of three layers according to the scheme presented in Fig. 4.5), where short- and long-term weather forecast tools are used to improve the prediction on the optimization process, and where the greenhouse climate simulators are also included to assure that the resulting setpoint profiles are reached by the local controllers at the greenhouse level. So, the first and the third layers work in the same way as described in Sect. 4.1.2, and in the new second layer the setpoints generated from the upper layer and sent to the lower layer for the next day are modified and updated in order to avoid unfeasibility problems and allow
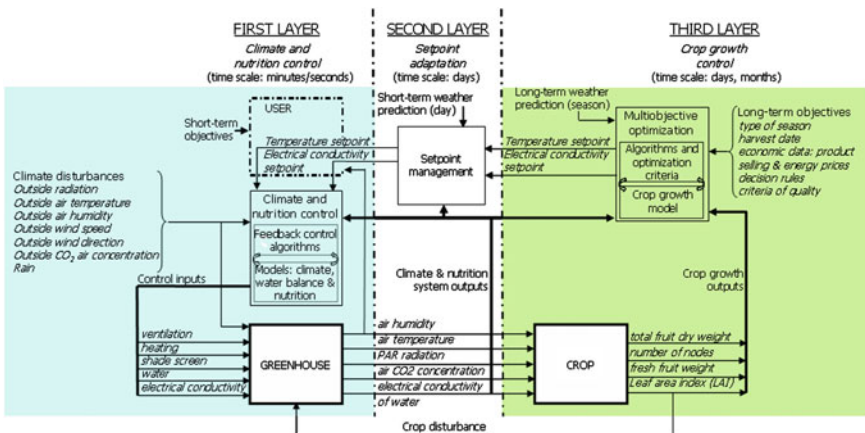
Fig. 4.5 Multilayer hierarchical control architecture with an adaptation layer. Courtesy of the authors of [343]

them to reach the reference values. These modifications are performed considering the trajectories generated in the upper layer, the short-term weather prediction (that has a lower degree of uncertainty), the current state of the crop, and the short-term grower goals (considering his/her skill and the crop status, this being a necessary degree of freedom to let the grower interact with the hierarchical control system). Then, this information is used within the greenhouse models presented in Chap. 2 to simulate the greenhouse behavior and to evaluate if the provided setpoints can be reached. The optimization process is repeated modifying the constraints (diminishing or increasing the setpoints) according to the simulation results. When the setpoints are reachable, they are sent to the lower layer.

The tomato crop model presented in Sect. 2.2.1 is used to relate the greenhouse crop production dynamics to the process decision variables. Finally, note that from a methodological point of view and considering that this framework has been designed in a modular and hierarchical way, it is straightforward to use this approach for other horticultural crops, other latitudes, as well as including other models or objective functions in the optimization process (for instance, to include additional variables related to the growth crop, such as CO_2, or considering objectives related to energy saving and/or plant disease control). Illustrative results selected from those obtained in an industrial greenhouse are shown and described in [343].

4.2.2 Multiobjective Optimization in Crop Production

An MO optimization problem can be defined as finding a vector of decision variables which satisfies constraints and optimizes a vector whose elements represent objective functions [47]. The problems characterized by competing measures of performance or objectives are considered as MO optimization problems, where n objectives $J_i(p)$ in the vector of variables $p \in P$ are simultaneously minimized (or maximized) [256]

$$\min_{p \in P}(J_1(p), J_2(p), \ldots, J_n(p)) \tag{4.2}$$

satisfying m inequality constraints, $g_i(p) \geq 0$, $i = 1, 2, \ldots, m$, and j equality constraints, $h_i(p) = 0$, $i = 1, 2, \ldots, j$.

The problem often has no optimal solution that simultaneously optimizes all objectives, but has a set of suboptimal or nondominated alternative solutions known as Pareto optimal set [256], where a compromise solution may be selected from that set by a decision process. Different criteria, such as physical yield, crop quality, product quality, timing of production process, or production costs and risks, can be formulated within greenhouse crop management. These criteria often give rise to controversial climate and fertirrigation requirements, which have to be solved explicitly or implicitly at the so-called tactical level where the grower has to make decisions about several conflicting objectives. The solution of this MO optimization process, $p \in P$, is the optimal diurnal and nocturnal present and future reference

trajectories of temperature, $X_{T,a}$, and EC, X_{EC}, for the rest of the crop cycle. That is, $p = [\mathbf{X}_{T,a}, \mathbf{X}_{EC}] \in P$, where $\mathbf{X}_{T,a}$ is a vector of the inside air temperature along the optimization intervals, and $\mathbf{X}_{EC}$ is a vector of the EC along the optimization intervals. Two temperature setpoints are considered: Diurnal and nocturnal [362]. It is necessary to emphasize that although the process optimization is presented in continuous time, it is solved in discrete time intervals for an optimization horizon, $N_f(t)$ (this horizon is variable and represents the remaining intervals until the end of the agricultural season). Thus, the solution vectors $\mathbf{X}_{T,a}$ and $\mathbf{X}_{EC}$ are obtained as

$$\mathbf{X}_{T,a} = [X_{T,a}(t), \ldots, X_{T,a}(t + N_f)]$$

$$\mathbf{X}_{EC} = [X_{EC}(t), \ldots, X_{EC}(t + N_f)]$$

where t is the current discrete time instant.

Note that, for the proposed optimization problem, a greenhouse crop production model is required to estimate the inner climate behavior and crop growth through the different steps of the algorithm and relate the different objective functions to the decision variables. Both climate conditions and crop growth influence each other and their dynamic behavior can be characterized by different timescales. Hence, as shown in Chap. 2, the crop growth in response to the environment can be described by two dynamic models, represented by two systems of differential equations with a timescale associated to their dynamics, which can be represented by [124, 341, 359, 363]

$$\frac{d\mathbf{X}_{cl}}{dt} = f_{cl}(\mathbf{X}_{cr}, \mathbf{X}_{cl}, \mathbf{U}, \mathbf{D}_m, \mathbf{V}, \mathbf{C}, t), \quad \mathbf{X}_{cl}(t_i) = \mathbf{X}_{cl,i} \tag{4.3}$$

$$\frac{d\mathbf{X}_{cr}}{dt} = f_{cr}(\mathbf{X}_{cr}, \mathbf{X}_{cl}, \mathbf{U}, \mathbf{D}_m, \mathbf{V}, \mathbf{C}, t), \quad \mathbf{X}_{cr}(t_i) = \mathbf{X}_{gr,i} \tag{4.4}$$

where $\mathbf{X}_{cl} = \mathbf{X}_{cl}(t)$ is an n_1-dimensional vector of greenhouse climate state variables (mainly the inside air temperature and humidity, CO_2 concentration, PAR radiation, soil surface temperature, cover temperature, and plant temperature), $\mathbf{X}_{cr} = \mathbf{X}_{cr}(t)$ is an n_2-dimensional vector of crop growth state variables (mainly number of nodes on the main stem, LAI or surface of leaves by soil area, total dry matter which represents all the plant constituents—root, stem, leaves, flower, and fruit—excluding water, fruit dry matter being the biomass of the fruits excluding water, and mature fruit dry matter or mature fruit biomass accumulation), $\mathbf{U} = \mathbf{U}(t)$ is an m-dimensional vector of input variables (natural vents and heating system in this work), $\mathbf{D}_m = \mathbf{D}_m(t)$ is an o-dimensional vector of measurable disturbances (outside temperature and humidity, wind speed and direction, outside radiation, and rain), $\mathbf{V} = \mathbf{V}(t)$ is a q-dimensional vector of system variables (related to transpiration, condensation, and other processes), $\mathbf{C}$ is an r-dimensional vector of system constants, t is the time, $\mathbf{X}_{cl,i}$ and $\mathbf{X}_{gr,i}$ are the known states at the initial time t_i, $f_{cl} = f_{cl}(t)$ is a nonlinear function based on mass and heat transfer balances, and $f_{cr} = f_{cr}(t)$ is a nonlinear function based on the basic physiological processes of the plants.

The following subsections show how the different objectives (cost functions) are expressed as functions of the decision variables of the optimization problem (present and future temperature and EC setpoints).

4.2.2.1 Maximization of Profits

Profits are calculated as the difference between the income from the selling of fresh fruits and the costs associated to their production

$$J_1 = \int_{t_i}^{t_h} V_{\text{price,cr}}(\tau) X_{\text{FF}}(\tau) \, d\tau - \int_{t_i}^{t_h} V_{\text{cos}}(\tau) \, d\tau \tag{4.5}$$

where $V_{\text{price,cr}}(t)$ is the selling price of the production (estimated from the market), $X_{\text{FF}}(t)$ is the fresh fruit production obtained from the crop growth model (such as described in Sect. 2.2.2.1), $V_{\text{cos}}(t)$ are the costs incurred by heating, electricity, fertilizers, and water (obtained from market and model estimations and measurements in the installations), t is the time, t_i is the initial time of crop cycle, and t_h is the latest harvesting time, both selected by the grower. Note that in practice, the tomato crop has multiple harvests during the growing season. For this reason, t_h represents the latest harvesting time in Eq. (4.5). An alternative is to consider the next harvesting time (t_n) in the cost function and restart the optimization process once the previous harvest has been produced. Both alternatives are valid for multiple harvest. The income depends on the price of tomato fruits ($\$ \, \text{kg}^{-1}$, $€ \, \text{kg}^{-1}$), the harvesting dates, and on the yield in fresh weight per surface unit ($\text{kg} \, \text{m}^{-2}$). The price policy requires market models or historical data, this being a difficult prediction problem. The following subsections describe how the fresh fruit production, $X_{\text{FF}}(t)$, and the process costs, $V_{\text{cos}}(t)$, can be estimated and related to the decision variables, $p = [\mathbf{X}_{\text{T,a}}, \mathbf{X}_{\text{EC}}]$.

As a first approximation, the fresh fruit production, X_{FF}, can be estimated as a linear relationship, $X_{\text{FF}} \simeq f_1(X_{\text{MF}}) = c_{\text{MF}} X_{\text{MF}}$, on the mature fruit dry weight with different values for spring and autumn seasons (note that the time dependence has been removed in this section for space reasons), where c_{MF} is the conversion factor between fresh and dry matter, and X_{MF} is the mature fruit dry weight. This function assumes that crop growth is developed in optimal conditions with enough water of good quality. However, there are some areas, such as in the Mediterranean regions, where bad quality water or lack of water with nonoptimal nutritive dissolution can be provided to the plants. Hence, the calculation of the fresh fruit production must be modulated by the effects of the electrical conductivity, $f_2(X_{\text{EC}})$, the vapor pressure deficit of the greenhouse air, $f_3(V_{\text{vpd}})$, and the crop transpiration, $f_4(V_{\text{ET}})$ (note that in cases in which the soil surface is mulched [421], evapotranspiration can be considered equal to crop transpiration, $M_{\text{trp,cr}} = V_{\text{ET}}$), in the following way:

$$X_{\text{FF}} = f_1(X_{\text{MF}}) f_2(X_{\text{EC}}) f_3(\text{VPD}) f_4(\text{ET}), \tag{4.6}$$

where $f_2(X_{EC})$ is given by [262]

$$f_2(X_{EC}) = \begin{cases} 0.67X_{EC} & X_{EC} < 1.5 \\ 1 & 1.5 \le X_{EC} \le 2.5 \\ -0.07X_{EC} + 1.18 & X_{EC} > 2.5 \end{cases} \qquad (4.7)$$

Regarding the functions $f_3(V_{vpd})$ [110] and $f_4(V_{ET})$ [286], the variables V_{vpd} and V_{ET} can be estimated based on humidity and solar radiation, respectively (see Sect. 2.1.1.6 and Eq. (2.44)). Therefore, these functions can be considered disturbances where their future values, to be used along the prediction horizon, are estimated based on the short-term weather forecast included within the hierarchical control architecture.

For estimation of X_{MF} in f_1, the *Tomgro* model described in Sect. 2.2.1 has been used, see Eq. (2.90).

Note how X_{FF} is related to the decision variables $X_{T,a}$ and X_{EC} through the functions f_1 and f_2 (Eq. (4.7) and those of the *Tomgro* model).

The costs, $V_{cos}(t)$, usually include those of heating (fuel cost), electricity, fertilizers, and water. Such costs can be estimated in the following way:

$$V_{cos}(t) = \underbrace{V_{fcos}(t)H_{heat}(t) + V_{ecos}(t)E_{ee}(t)}_{f(X_{T,a})} + \underbrace{V_{wcos}(t)U_{sw}(t) + V_{fecos}(t)U_{sf}(t)}_{f(X_{EC})}$$
$$(4.8)$$

where $H_{heat}(t)$ is the fuel consumption of the heating system, $E_{ee}(t)$ is the electrical energy consumed by the heating system, $U_{sw}(t)$ is the supplied water (see Eq. (4.10)), $U_{sf}(t)$ are the supplied fertilizers, and $V_{fcos}(t)$, $V_{ecos}(t)$, $V_{wcos}(t)$, and $V_{fecos}(t)$ are the fuel, electricity, water, and fertilizer costs, respectively. As mentioned above, the costs can be estimated from the market and the consumed fungibles are estimated from energy and mass steady-state balance and measurements in the installations. Note that, electrical consumption by the ventilation system is negligible. The estimation of fuel consumption, $H_{heat}(t)$, and wasted electrical energy, $E_{ee}(t)$, is based on the activation of the heating system, and thus the function of the greenhouse air temperature and other measurable climate variables and model calibration constants using an energy and mass steady-state balance [363], assuming that the heating system only works during the night and the vents are closed. In the same way, the estimation of the supplied fertilizers, $U_{sf}(t)$, is based on the concentration of the ions for nutrient dissolution supplied by the fertirrigation system in order to reach the desired electrical conductivity.

The supplied water volume, $U_{sw}(t)$, is calculated considering the water absorbed by the plants, $V_{abs,cr}(t)$, the drainage volume, $V_{dr}(t)$, and the increase in water content in the substrate $\Delta V_{H,s}(t)$ in the optimization interval (these variables can be easily obtained from water mass balances in Sect. 2.3.4),

$$U_{sw}(t) = V_{abs,cr}(t) + V_{dr}(t) + \Delta V_{w,s}(t). \qquad (4.9)$$

However, for the optimization process, we consider that the substrate is always saturated with water ($\Delta V_{w,s}(t) \simeq 0$), and knowing that $V_{dr}(t) = c_{df} V_{abs,cr}(t)$, the estimated supplied water volume Eq. (4.9) is obtained as follows:

$$U_{sw}(t) = (1 + c_{df}) V_{abs,cr}(t) \tag{4.10}$$

$$V_{abs,cr}(t) = (V_{ET}(t) + \Delta X_F(t))(1 - (X_{EC}(t) - c_{suwa})c_{srwa}) \tag{4.11}$$

where c_{df} is a constant value representing the drainage fraction calculated based on the quality of the irrigation water, fertilizers, and substrate [411], $V_{ET}(t) = M_{trp,cr}(t)$ is the crop transpiration that can be estimated based on solar radiation as mentioned above, $\Delta X_F(t)$ is the estimated increment of the fruit dry weight based on *Tomgro* model (Eq. (2.89)) in the optimization interval, c_{suwa} is a constant threshold of X_{EC} over which there is a decrease in water absorption, and c_{srwa} is the reduction coefficient of water absorption per unit of X_{EC}.

Thus, from Eqs. (4.10) to (4.11), how the second term in Eq. (4.8) is related to the decision variable X_{EC} can be seen.

4.2.2.2 Maximization of Quality

Although maximizing profits can be understood as the main objective from the growers' point of view, this cannot always be used as the only target. The growers usually belong to cooperatives or agrarian societies that facilitate the introduction of horticultural products into the market. These associations fix the policies on quality products based on the different market requirements, and thus the growers must adapt their production process to these policies in order to reach some minimum quality levels. Food quality embraces both sensory attributes that are readily perceived by the human senses and hidden attributes such as health and nutrition [394]. In fruits and vegetables, the sensory properties are determined by the amount of sugars, organic acids, and volatile compounds, as well as color, shape, and texture. However, sugars and acids are those reflecting overall taste preferences for a fruit. For tomato crop, soluble solids have been related to sugars [249, 250, 411] and titratable acidity to main organic acids [19, 411]; thus, they can be used as indicators of fruit quality. Firmness of the fruit is another important quality parameter in the chain grower-dealer-consumer. Nevertheless, some works have shown that in horticultural vegetables, as tomato or flowers, some important parameters of sensory quality are in conflict with yield [113, 249, 250, 411]. Hence, the fruit quality can be expressed as

$$J_2 = \int_{t_i}^{t_h} (w_{ssol} V_{ssol}(\tau) + w_{ta} V_{ta}(\tau) + w_{ff} V_{ff}(\tau) + w_{fs} V_{fs}(\tau)) \, d\tau \tag{4.12}$$

where $V_{ssol}(t)$ is the soluble solids concentration in the fruit, $V_{ta}(t)$ is the titratable acidity in fruits, $V_{ff}(t)$ is the fruit firmness, $V_{fs}(t)$ is fruit size, and w_{ssol}, w_{ta},

w_{ff}, and w_{fs} are weighting parameters. The weighting of the quality criteria has been established based on interviews with consumers, retailers, farmers, agricultural technicians, and academics, and we have determined the following values: $w_{ssol} = 0.3$, $w_{ta} = 0.3$, $w_{ff} = 0.3$, and $w_{fs} = 0.1$.

In tomato fruits, soluble solids, titratable acidity, fruit firmness, and size may be related to $X_{T,a}(t)$ and $X_{EC}(t)$ (decision variables) using the following linear approach [113, 411]:

$$Y(t) = a_q + b_q(X(t) - g(X(t))) \tag{4.13}$$

where $Y(t)$ is the variable to be calculated (soluble solids, titratable acidity, fruit firmness, or size), $X(t)$ is the related decision variable ($X_{EC}(t)$ for $V_{SSol}(t)$, $V_{ta}(t)$, $V_{fs}(t)$; and $X_{T,a}(t)$ for $V_{ff}(t)$), a_q is a constant increment coefficient in $Y(t)$, b_q is the increment coefficient in $Y(t)$ per unit of increment in $X(t)$, and $g(X(t))$ is a piecewise function representing a threshold of $X(t)$ over which there is an increment in $Y(t)$ (a_q and b_q of adequate units).

4.2.2.3 Maximization of Water-Use Efficiency

The explicit inclusion of this objective in the optimization problem has an environmental purpose. In semi-arid climates, such as Mediterranean ones, water is a scarce and expensive resource, mainly during some seasons of the year. Some authors maintain that productivity in such regions is determined by the available water and the water efficiency use [191]. Thus, adequate management of water is required. With the explicit inclusion of this objective, the grower can select a solution from the Pareto front providing the desired water consumption during the growing cycle. This objective tries to use the water quantities adequate to the crop growth in close relationship with the supplied concentration of nutrient solution. In this section, the water-use efficiency (WUE) is considered like the biomass efficiency defined as the relationship between fresh fruit matter production and the water supplied. The supplied water objective depends on multiple factors, including the EC and the inside air temperature, as described in the following function:

$$J_3 = \int_{t_i}^{t_h} \frac{X_{FF}(\tau)}{U_{sw}(\tau)}\, d\tau \tag{4.14}$$

where $X_{FFP}(t)$ is the fresh fruit production given by Eq. (4.6) and $U_{sw}(t)$ is the supplied water given by Eq. (4.10).

4.2.2.4 Multiobjective Optimization Problem

Therefore, the MO optimization problem presented in this section is composed of the previous objective functions described by Eqs. (4.5), (4.12) and (4.14). All the variables presented in these objectives are functions of the air temperature, $X_{T,a}$, and/or the EC, X_{EC}, $\left(X_{FF}(t), U_{sf}(t), U_{sw}(t), V_{ta}(t), V_{ssol}(t), V_{fs}(t), V_{ff}(t) \right)$, as well as of measurable disturbances such as PAR radiation or CO_2 concentration. That is, the objective functions can be expressed as $J_i(X_{T,a}, X_{EC}, D_m)$ for $i = 1, 2, 3$, where $X_{T,a}$ is a vector of the inside air temperature along the optimization interval, X_{EC} is a vector of the EC along the optimization interval, and D_m is a vector of the measurable disturbances that have to be predicted along the optimization horizon. The solution to the MO optimization problem provides both diurnal and nocturnal setpoint trajectories of EC and inside air temperature for the rest of the control horizon. Constant diurnal and nocturnal setpoints are defined, and steady-state models of greenhouse climate and tomato crop summarized in Eqs. (4.3) and (4.4) are used for optimization purposes [360, 362, 363]. Although several techniques have been evaluated to solve the MO optimization problem [256], in this case, a goal attainment algorithm has been used (SQP-based). Priorities for each objective are determined using weights that are sequentially modified in each iteration. The constraints are defined by maximum and minimum values of temperature and EC obtained from expert knowledge that indicates "optimal" growing temperatures for tomato and by analyzing local data from historical series. The resulting constraints are changing with time with a yearly pattern designed on the basis of the last 20 years' collected data.

4.2.3 Representative Results

The results included in this section were obtained using a tomato crop *Lycopersicon esculentum*, grown in Rockwool® substrate at a density of 2 plants m^{-2} and for autumn–winter period when the external temperatures are low and there is a need for heating at night to avoid reaching the vital temperature of the plants or for optimization purposes. No carbon dioxide was applied and running water is used for irrigation. There is an important time interval for vegetative growth that must be considered to optimize profits. The initial conditions were: Four nodes at initial time, LAI was 0.002, and total dry weight was 0.5 g m^{-2}. Figure 4.6 shows an example of long-and short-term predictions (solar radiation patterns and temperature respectively), for the dates where the tests presented in this section were performed. As expected, for the long-term predictions, there are relevant prediction errors, mainly at the end of the prediction horizon. Therefore, the use of the receding horizon strategy included in the optimization problem is an important factor to compensate for the uncertainty induced by these prediction deviations. Note that the optimization problem is solved each day for a horizon including the rest of the season.
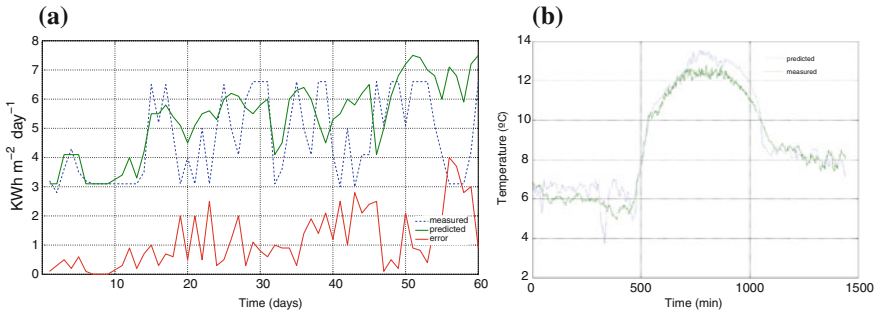
(a)

(b)

Fig. 4.6 Example of long-(*left*) and short-(*right*) term climate prediction

Figure 4.7 shows the 3D Pareto front. From this figure, it can be seen how, when profits and water-use efficiency increase, quality decreases; thus, it is possible to achieve tradeoff solutions avoiding a drastic decrease of quality while keeping acceptable levels of profits and water-use efficiency. When the different objectives are analyzed in groups of two objectives, some interesting conclusions can be obtained. For instance, it can be deduced that there is a proportional relation between water-use efficiency and profit, making it difficult to determine a Pareto front for such objectives. When the crop quality and profit are analyzed, it can be concluded that maximum values of quality imply decreasing values of profit. Table 4.1 shows different values of the objectives obtained from some of the nondominated solutions. The quality values never reach the maximum (100 %), being the quality range between 68 % and 96 %. Profits fluctuate between 1.11 and 2.65 €m^{-2}, while the water-use
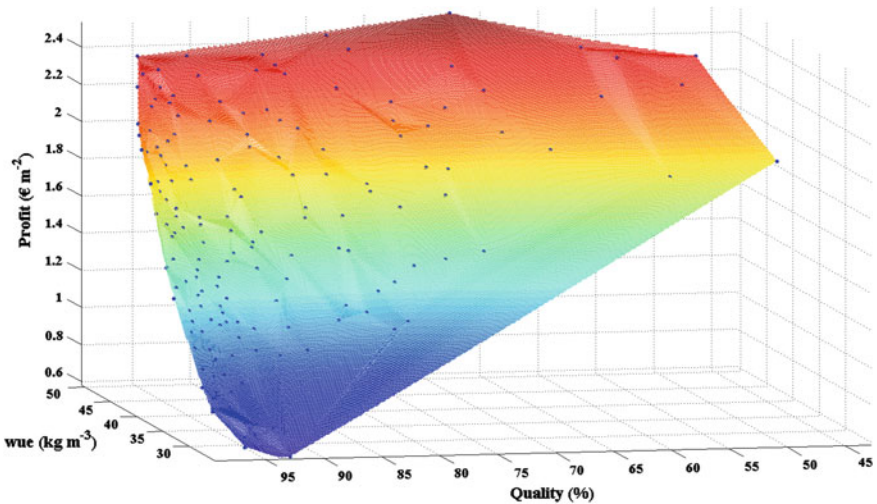
Fig. 4.7 Pareto fronts obtained from the optimization process

Table 4.1 Objectives by nondominated solutions

Profits ($\text{€}\,\text{m}^{-2}$)	WUE ($\text{kg}\,\text{m}^{-3}$)	Quality index (%)
1.113	26.539	**96.062**
1.752	36.926	95.963
–	–	–
2.606	**50.837**	84.563
–	–	–
2.657	44.051	78.641
2.659	37.864	68.435

efficiency varies between 26.5 and $50.8\,\text{kg}\,\text{m}^{-3}$. Note that these values are for a season, and thus, the total profits per year are twice these quantities. On the other hand, Fig. 4.8 shows the day/night setpoint trajectories for temperature and EC obtained using the MO optimization for a cycle of 65 days (130 setpoint intervals for each variable). The figure shows the resulting trajectories for different solutions, maximizing each objective individually (Fig. 4.8a–c) and maximizing the three objectives simultaneously (Fig. 4.8d).

When the main objective is maximizing profits (Fig. 4.8a), the diurnal temperature is regulated between 22 and 25 °C to improve fruit growth. Once the fruits are well formed, and from the mincemeat of fruits, the temperature profile tends to gradually diminish looking for suitable temperatures to obtain a better nutrient distribution. The EC is maintained through the whole horizon at $2.0\,\text{mS}\,\text{cm}^{-1}$, which is the recommended value for the tomato crop in order to maintain production performance and avoid reduction in yield due to salinity (note that there is an inverse relation-
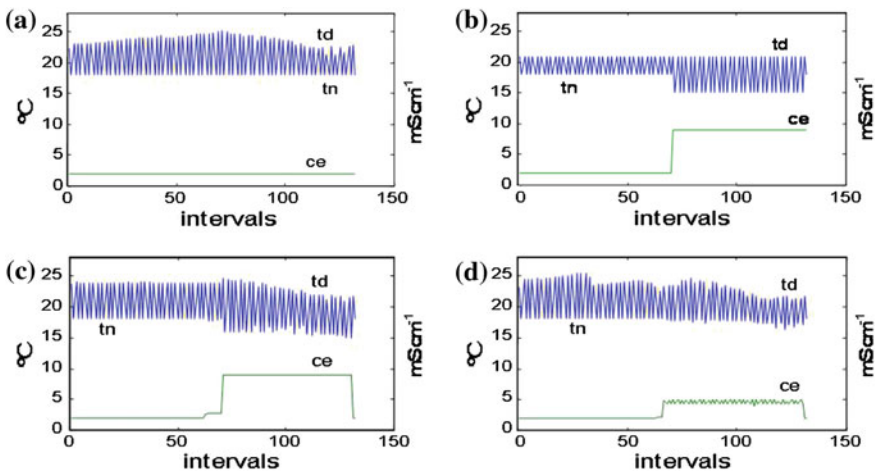
Fig. 4.8 Resulting reference trajectories: Diurnal temperatures (td), nocturnal temperatures (tn), electrical conductivity (ce). Courtesy of the authors of [343]
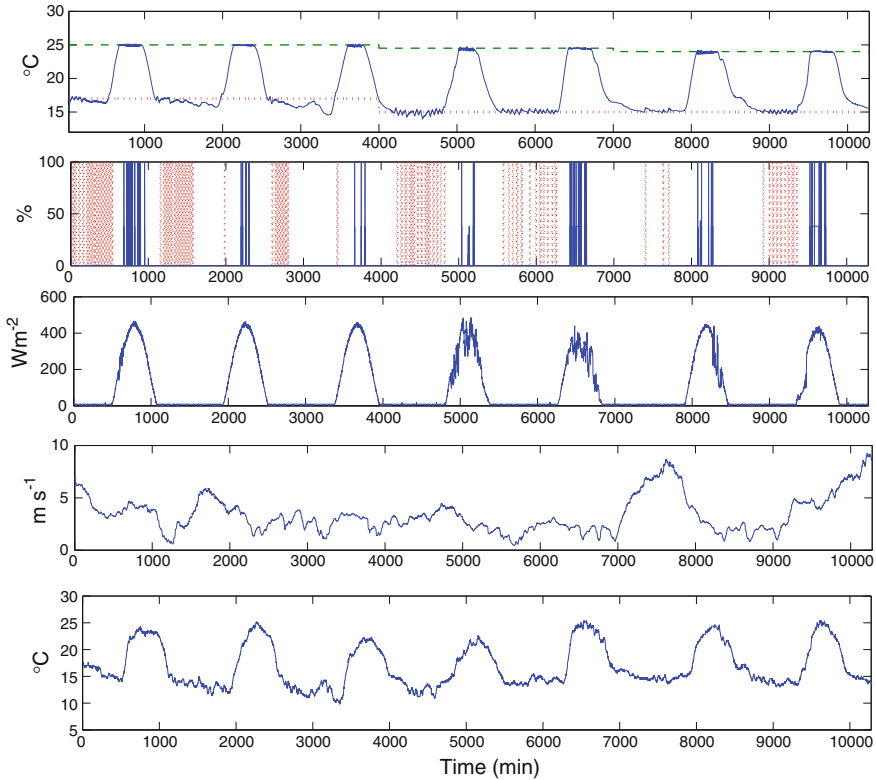
Fig. 4.9   Real tests for climate control (04–11 December 2009). From *top* to *bottom*: (1) greenhouse temperature (*solid*), diurnal temperature setpoint (*dashed*), nocturnal temperature setpoint (*dotted*) [°C]; (2) ventilation (*solid*) and heating (*dotted*) control signals [%]; (3) solar radiation [W m^{-2}]; (4) wind speed [m s^{-1}]; (5) and outside temperature [°C]. As a courtesy of the authors [343]

ship between EC and production). If maximum quality is prioritized (Fig. 4.8b), the diurnal temperature trajectories stay at the minimum values given by constraints (21 °C) through the complete planning horizon, whereas the nocturnal temperature trajectories remain at the allowed maximum. From the fruition stage, an evolution is produced reaching the minimum values (15 °C), because through that policy, fruit firmness is enhanced. The EC trajectory increases until reaching the maximum limit to harness the maximum accumulation of sugar and titratable acidity, both being important characteristics of fruit quality. If the water-use efficiency is the main objective (Fig. 4.8c), temperatures between 24 and 15 °C are combined during the day and the night to achieve maximum growth in the first stage. When the first fruits appear, the temperature profile should decrease to the lower allowed limits to reduce the water consumption by decreasing transpiration. The EC increases to the maximum limit from fruition as a consequence of decrease in water consumption when salinity is increased. In Fig. 4.8d, the trajectories of a nondominated solution are shown.

In this case, the diurnal temperature stays at high values at the beginning of the horizon and diminishes at the end of the cycle, while the nocturnal temperature is at the maximum limit and slightly diminishes at the end of the cycle. The EC value is $2.0\,mS\,cm^{-1}$ at the first stage of growth, and at the stage of fruition and maturation increases to 4.5–$5.0\,mS\,cm^{-1}$ until the end of the horizon. This trajectory corresponds to one of the nondominated solutions in which there seems to be good balance between the different objectives. Figure 4.9 shows some representative real experiments for temperature control. The diurnal temperature reference is slightly decreasing from 25 to 24–23 °C and the nocturnal temperature reference is also decreasing from 18–17 to 15 °C. For these tests, a gain scheduling controller and a predictive control algorithm [362] were used for diurnal and nocturnal temperature control [342] respectively.

4.3 Conclusions

This chapter presented two different hierarchical control solutions for the greenhouse crop growth control problem. First, a solution based only on a single objective, to maximize profit, was presented. In this case, optimal setpoint temperatures were obtained and for whole seasons of 80 and 90 days. Although this solution provides better results than classical nonhierarchical control approaches, some disadvantages were observed. First, the setpoints from the upper layers cannot sometimes be reached by the lower layer control algorithms. This fact was because of the lack of a middle layer to check the feasibility of the resulting setpoints. On the other hand, some other important aspects on the greenhouse crop growth problem were missing in the optimization layer, such as fruit quality and water-use efficiency. Therefore, in the second part of the chapter, an MO optimization problem is proposed and tested for greenhouse crop growth management, obtaining tradeoff solutions of three objectives: Maximization of economic benefits, fruit quality, and water-use efficiency. This optimization scheme is integrated into a hierarchical control architecture that automatically generates setpoints for diurnal and nocturnal temperatures and EC through a whole crop cycle (using a receding horizon strategy). The obtained results showed logical trajectories both in short and long crop cycles.

Chapter 5
Advice and Suggestions for Greenhouse Technicians and Producers

5.1 Main Conclusions, Advice, and Suggestions

The first suggestion to producers is to consider the problem as an integration of three main interrelated systems, such as the greenhouse (climate and fertigation), crop, and market, which have different timescales. The problem is to determine the control signals to be sent to the actuation systems so that climate variables reach the climate and fertigation optimal setpoints providing the maximum profit, which is related to the crop (because the incomes come from the sale of production) and actuators (because operation costs depend on their state). The solution to this problem depends on the selected approach, either by obtaining the desired trajectories of climate and fertigation variables, as in this book, or by directly obtaining the control signals, as done by other authors (e.g., [147, 431]). What is really important is to address the crop growth control in greenhouses from this point of view. This is a typical hierarchical control problem, so it is needed to define a multilayer architecture. A key and limiting issue is the need for developing reliable models describing the main dynamics of these main subsystems. As mentioned above, there exist several climate, fertirrigation, and different crops growth models and well-known methodologies to develop them. The main drawback of the hierarchical architecture is to have a good model of the market behavior to predict the selling prices of production; the tasks included in the tactical layer may be developed by technicians and producers, which should provide the economic setpoints to the lower layers. This is an important change in the actual working scheme, as the managing of crops is performed from a business point of view instead of using the traditional view based on changing the climate and fertigation setpoints. It is important to point out that these control systems do not account for the occurrence of pests and diseases or other short-term objectives that may arise, so the system must be flexible allowing for manual modification of the control decisions proposed by the control algorithm.

Another important aspect to consider in this approach is that, as the control systems work with a crop growth planning with timescales corresponding to agricultural seasons (months), it is also necessary to have a good weather forecast system

in the location where the greenhouse is installed in order to predict the behavior of the indoor climate and hence crop growth. Although there are tools available for this purpose, meteorological forecast on these timescales (months) are vague and erroneous, making it necessary to compensate the underlying uncertainty by implementing receding horizon approaches, repeating the whole optimization process to determine future setpoints at least once a day (to also take into account manual modifications in setpoints performed by farmers due to pests and diseases or other short-term objectives). Moreover, this also allows the producer to modify the initial conditions of optimization such as expected harvesting date depending on trends in selling prices to advance or delay the fruit maturing process. Furthermore, the user can also change the electricity and fuel prices (or other operation-related costs); these changes are published a few days in advance. On the other hand, errors in the climate prediction involve errors in the estimation of the variables describing crop growth, so that it is advisable to make biweekly real measurements of these variables (LAI, dry matters, etc.) although they could require destructive testing of some plants.

Although the main goal of crop growth control in greenhouses is to obtain the maximum profit (defined as the difference between the incomes from the sale of the product and the associated operation cost), in a second phase it would also be useful that the high-level controller should consider other objectives such as production quality, efficiency in the use of basic resources such as water and energy, emission of pollutants or other objectives depending on the local conditions or facilities (which should be also converted into operational costs). Thus, the original formulation becomes a multiobjective problem that can be implemented on the same proposed hierarchical control architecture by modifying the cost functions of the upper layer of the controller where the optimal control algorithm runs. Changing this approach, more degrees of freedom are provided to the managers of the greenhouse to adapt both to the different trade scenarios as the local environment conditions (e.g., continental or Mediterranean climate, availability of renewable energy sources, semi-desert areas with water problems, crop varieties for localized areas with demanding requirements of quality taste, production for canning industry, etc.).

With respect to the lower layer of the proposed architecture, which corresponds to climate and fertigation controllers, there are many commercial systems widely installed in greenhouse facilities. These systems use classical controllers whose parameters are modified using heuristics based on the farmer and technicians experience. Furthermore, in many cases it is necessary to define hundreds of parameters related to the trajectories of climate and the actuators. The main problems identified in these systems are [339, 355, 441]:

- Tracking of setpoints is not perfect, because the system is dynamic and there are many interactions between the control loops and constraints on control devices.
- The climate, irrigation, and fertilizer setpoints are not scientifically defined regarding the behavior of the crop, therefore, problems may arise regarding inefficiency in the use of energy and other resources.

- The number of setpoints and controller parameters to set up these systems is so large that the system is not transparent and, therefore, the effects on energy efficiency or performance are not easy to discern.
- Most commercial systems are not open (their control algorithms are not modifiable), neither are they interoperable with third-party systems. They do not allow integration with the supervisory system of a hierarchically higher level, although from the authors' point of view, they must evolve following the process industry standards.
- Systems installed outside the conditions under which where they were developed require a process of adaptation and calibration of their different operating parameters to achieve acceptable results.

Some of these problems can be solved using successful proposals from other industrial areas presented in this book. Some of the control algorithms shown are intuitive and easy to understand and apply. Furthermore, the implementation of the optimal control layer takes into account the crop growth and therefore the optimal setpoints to be achieved by the different control variables. Even so, it should be noted that it is essential to tune the controller, performing various tests to obtain the parameters that relate the control variables (actuators) with the controlled variables. All controllers (both commercial tools and new proposals) may work correctly, but adequate tuning for each particular case is imperative. It is impossible that a control system works properly without previously modifying the default configuration parameters. For this, there are numerous techniques, although with a simple test like reaction curve method [16], acceptable results can be obtained.

Another important issue, which is essential to correct, is that currently greenhouse climate control systems are completely independent of fertigation control systems. It is unthinkable that if crop growth and organoleptic properties depend on both sets of variables, both systems do not communicate with each other to establish coordinated control strategies. This is another reason why it is necessary to introduce a higher layer that integrates all greenhouse systems.

Regarding actuators, some considerations can also be made:

- The actuators must be appropriately sized. It is believed that a control system can regulate a variable with any actuator, but this is not true. In the past, as actuation systems were undersized the control system operated in saturation (open loop), and hence the influence on greenhouse climate was not relevant. Nowadays, there is a trend to install oversized actuators with which there should be no problems to conveniently control a particular variable, but usually they have drawbacks related to nonlinear behavior, efficient use of energy, water, or fertilizers. When the installation of an actuator is planned, it would be advisable that a control engineer is involved in the process and not a posteriori (as is the typical situation).
- Climate variables inside a greenhouse are not homogeneous in the air volume enclosed in the structure, mainly due to different vertical and horizontal air flow patterns. Thereby, a spatial climate is produced. Obviously, this fact influences the homogeneity of production in the different sectors of the greenhouse, which is undesirable. Moreover, the control systems only regulate the variables using

information about the area of influence where the sensors are installed. It would be advisable the installation of distributed actuators that enable distributed control of the different greenhouse sectors. For this, it should be necessary to extend the sensorial subsystems and controllers (replicate the set of sensors and controllers in each sector). Furthermore, new cooperative and coordinated control algorithms must be designed. However, in the case where distributed actuators are not available (as in most installations), it is advisable to use sets of sensors to obtain an average value of the different greenhouse sectors so that the control system makes an "average" decision. For example, it is useful the installation of at least three temperature sensors at crop height forming an "L" (East, West, and North) spaced the same distance, being possible to obtain information about the temperature distribution at every moment.

- In most greenhouse facilities, actuators to regulate the greenhouse air temperature and humidity are installed, but the use of CO_2 enrichment systems is not widespread, especially in locations with warm or semi-arid climates. It has been demonstrated that the use of CO_2 may increase by up to 20 % the production, along with quality. By recycling plant residues as biomass, the costs associated to the CO_2 production decreases, making it convenient and advisable to consider using such actuators, as recently done in [376].

Finally, and related to the physical implementation of the proposed hierarchical architecture, the data acquisition, and control system to be installed must fulfill the following conditions:

- Interoperability, understood as the ability of two or more systems or components to exchange information and use the information exchanged [196].
- Maximum level of decentralization with the objective of minimizing wiring between the controller and the sensors and actuators. It can be suitable to merge them (sensor, controller, and actuator) into a single component. The use of wireless sensor networks is also an alternative to this problem.
- The use of a single communication bus, where all the sensors, actuators, and control systems can be connected.
- Maximum flexibility to allow any topological configuration, simplify the cable layout, easy reconfiguration of the system, and installation of a new device, involving a simple electrical connection to the bus and further configuration from the main control system.
- It must be a deterministic network communication understood as one in which data transmission is ensured in a given time [197].
- Ease of maintenance, so as to permit fault detection and diagnosis and, system reconfiguration, remotely.
- The installed equipment must have a good life span, as well as maintenance and good flexibility to adapt to market changes.
- Electrical and mechanical normalization must be fulfilled so as to ensure maximum modularity and interchangeability of components.
- Operation in hostile environments (high temperature and humidity, dust, presence of abrasive plant protection products, electromagnetic Interference, etc.).

As a final remark, this book proposes an approach to what should be the new model for greenhouse crop production, in which all systems must be integrated, taking into account economic criteria and other objectives of local and/or general interest. As discussed above, this is not a unique solution, since there are different approaches and all are valid. The authors are convinced that this is the way this field must evolve and encourages technicians and producers involved in the process to analyze their facilities and decide to perform a step in this direction.

Appendix A
Main Characteristics of the Greenhouses Used in This Book

Greenhouse	Araba	Inamed	Almería
Location			
Coordinates	36°42′N, 2°47′O	36°42′N, 2°47′O	36°48′N, 2°43′O
Locality	El Ejido (Almería)	El Ejido (Almería)	Santa María del Águila (Almería)
Structure			
Cover	Symmetric curve	Asymmetric curve	Symmetric plane
Ridge orientation	North–South	East–West	East–West
Surface shape	Rectangular	Rectangular	Irregular
Cover material	Polyethylene 800 gauges	Polyethylene 800 gauges	Polyethylene 720 gauges
Surface area [m^2]	1500	1575	877
Width [m]	37.5	45	23.2
Length [m]	40	35	37.8
Ridge height [m]	5.50	5.60	4.4
Lateral height [m]	3.75	4	2.8
Number of chapels	5	6	5
Chapel width [m]	7.5	7.5	7.6
Chapel length [m]	40	35	23.2
Actuators			
Cenit natural ventilation	• Zip • One per chapel • 2.22 [m] × 40 [m] • Aperture of 38°	• Zip • One per chapel • 2.75 [m] × 35 [m] • Aperture of 33°	• Zip • One per chapel to the West • 2.75 [m] × 35 [m] • Aperture of 45°

(continued)

(continued)

(continued)

Greenhouse	Araba	Inamed	Almería
Actuators			
Lateral natural ventilation	• Two (N-S) • Rolling • 1.8 [m] × 37.5 [m]	• Two (N-S) • Rolling • 1.7 [m] × 37.5 [m]	• Two (N-S) • Rolling • 1.7 [m] × 37.5 [m]
Aerial pipes heating system	• Heater of $2\ 10^6$ kcal • Diesel as combustible • Heater temperature of 80°C • Steel pipes: 5.2 cm diameter, 11 cm on the ground		• Heater of 150 kW • Biomass combustible • Heater temperature of 60°C • Steel pipes: 5.2 cm diameter, 11 cm on the ground
Air heating system			• Power of $95\ 10^3$ kcal • Diesel as combustible • Fan for air distribution
Shade screen	• 10 Thermo-reflected screens of 4 [m] • Transmission coefficient of 0.5		• 5 Thermo-reflected screens of 7 [m] • Transmission coefficient of 0.5
Fertirrigation system	• NFT (Nutrient Film Technique) • Programmed irrigation • Typical fertigation of 5.5 pH and EC of 2 dS m^{-1}		• Hydroponic • On demand irrigation • Typical fertigation of 6 pH and EC of 2.2 dS m^{-1}
Measurement system			
Inside greenhouse	• 1 air temperature • 1 soil temperature • 1 humidity • 1 solar radiation • 1 PAR radiation		• 3 air temperature • 1 soil temperature • 8 cover temperature • 4 leaves temperature • 1 soil temperature at 40 cm • 3 humidity • 2 solar radiation • 2 PAR radiation • 1 CO_2 concentration • 1 air speed • 1 air speed by heat wire • 1 air speed by ultrasonics
Outside greenhouse	• Temperature • Humidity • Solar radiation • PAR radiation • Wind speed • Wind direction • Rain detection		• Temperature • Humidity • Solar radiation • PAR radiation • Wind speed • Wind direction • Rain detection • CO_2 concentration

(continued)

Greenhouse	Araba	Inamed	Almería
Hydric requirements			• 1 lysimeter • 1 drainage balance • 4 substrate water contents • 1 substrate temperature
Fertilizers	• EC of water and drainage • pH of water and drainage • Water counter		• EC of water and drainage • pH of water and drainage • Water counter • EC of substrate
Measurement system			
Actuator state	• Boiler water temperature • Pipe water temperature		• Boiler water temperature • Pipe water temperature • Lateral vents position • CO_2 tank pressure • Flow and temperature of • CO_2 pipe

References

1. J.M. Aaslyng, J.B. Lund, N. Ehler, E. Rosenqvist, IntelliGrow: a greenhouse component-based climate control system. Environ. Model. Softw. **18**, 657–666 (2003)
2. A.M. Abdel-Ghany, T. Kozai, Dynamic modeling of the environment in a naturally ventilated, fog-cooled greenhouse. Renew. Energy **31**, 1521–1539 (2006)
3. G. Ahmadi, P.G. Glockner, Dynamic simulation of the performance of an inflatable greenhouse in the southern part of Alberta. I. Analysis and average winter conditions. Agric. Meteorol. **27**, 155–180 (1982)
4. G. Ahmadi, P.G. Glockner, Dynamic simulation of the performance of an inflatable greenhouse in the southern part of Alberta. III. Efects of cloudiness factor. Agric. For. Meteorol. **31**, 183–191 (1984)
5. G. Ahmadi, P.G. Glockner, K.O. Kessey, Dynamic simulation of the performance of an inflatable greenhouse in the southern part of Alberta. II. Comparisons with experimental data. Agric. Meteorol. **27**, 181–190 (1982)
6. L.D. Albright, R.S. Gates, K.G. Arvanitis, A.E. Drysdale, Environmental control for plants on Earth and in Space. IEEE Control Syst. Mag. **21**, 28–47 (2001)
7. A. Alessandri, F. Bini, T. Parisini, A. Torrini, Neural approximation for the optimal control of heating systems. In 3rd IEEE Conference on Control Applications (Glasgow, UK, 1994), pp. 1613–1618
8. M. Alipour, M. Loghavi, Development and evaluation of a comprehensive greenhouse climate control system using artificial neural network. Univ. J. Control Autom. **1**(1), 10–14 (2013)
9. A. Anastaiou, K.P. Ferentinos, K.G. Arvantis, N. Sigrimis, DSS-Hortimed for on-line management of hydroponic systems. In Proceedings of Greensys 2004 (Leuven, Belgium, 2004)
10. M.J. Ansorena, *Sustratos* (Propiedades y caracterización, Mundi Prensa, 1994)
11. M.R. Arahal, M. Berenguel, F. Rodríguez, Técnicas de Predicción con Aplicaciones en Ingeniería (Prediction Techniques with Applications to Engineering) (Servicio de Publicaciones de la Universidad de Sevilla, 2006)
12. M.R. Arahal, F. Rodríguez, A. Ramírez-Arias, M. Berenguel, Discrete-time nonlinear FIR models with integrated variables for greenhouse indoor temperature simulation. In 44th IEEE Conference on Decision and Control and the European Control Conference 2005 CDC-ECC'05 (Seville, Spain, 2005), pp. 4158–4162
13. K.G. Arvanitis, P.N. Paraskevopoulos, A.A. Vernados, Multirate adaptive temperature control of greenhouses. Comput. Electron. Agric. **26**, 303–320 (2000)
14. ASAE, Heating, Ventilating, and Cooling Greenhouses (EP406.3) (American Society of Agricultural Engineering Standards, Michigan, USA, 1998)
15. K.J. Aström, In Analysis and Design of Nonlinear Control Systems, chapter Event-Based Control (Springer, 2007), pp. 127–147

16. K.J. Aström, T. Hägglund. In The Control Handbook, ed. by S. Levine, chapter PID control. (CRC Press/IEEE Press, 1996)

17. K.J. Aström, T. Hägglund, Advanced PID Control. ISA-The Instrumentation, Systems, and Automation Society, Research Triangle Park, NC 27709 (2005)

18. K.J. Aström, B. Wittenmark, Adaptive Control (Addison-Wesley, 1995)

19. H. Auerswald, D. Schwarz, C. Kornelson, A. Krumbein, B. Brückner, Sensory analysis, sugar and acid content of tomato at different EC values of the nutrient solution. Sci. Hortic. **82**, 227–242 (1999)

20. R. Avila-Miranda, O. Begovich, J. Ruiz-León, An optimal and intelligent control strategy to ventilate a greenhouse. In 2013 IEEE Congress on Evolutionary Computation (Cancún, México, 2013), pp. 779–782

21. B.J. Bailey, Limiting the relative humidity in insulated greenhouse at night. Acta Hortic. **148**, 411–419 (1984)

22. B.J. Bailey, I. Seginer, Optimum control of greenhouse heating. Acta Hortic. **245**, 418–512 (1989)

23. A. Baille, Irrigation management strategy of greenhouse crops in Mediterranean countries. Acta Hortic. **361**, 105–122 (1994)

24. A. Baille, B. von Elsner, In Energy Conservation and Renewable Energies for Greenhouse Heating. European Cooperative Networks an Rural Energy, CNRE Guideline ed. by von Zabeltitz, vol. 2, chapter Low temperature heating systems (Academic Press, 1988), pp. 149–167

25. M. Baille, A. Baille, J.C. Laury, A simplified model for predicting evapotranspiration rate of nine ornamental species vs. climate factors and leaf area. Sci. Hortic. **59**, 217–232 (1994)

26. M. Baille, A. Baille, J.C. Laury, Influence of whitening on greenhouse microclimate and crop energy partitioning. Agric. For. Meteorol. **107**(4), 293–306 (2001)

27. M. Baille, J.C. Laury, A. Baille, Some comparative results on evapotranspiration of greenhouse ornamental crops, using lysimeter, greenhouse H_2O balance and LVDT sensors. Acta Hortic. **304**, 199–208 (1992)

28. J.C. Bakker, H. Challa, In Greenhouse Climate Control: An Integrated Approach ed. by J.C. Bakker, G.P.A. Bot, H. Challa, N.J. van de Braak, Chapter Aim of the Greenhouse Climate Control (Wageningen Press, 1995), pp. 1–3

29. F.J. Baptista, B.J. Bailey, J.F. Meneses, Effect of nocturnal ventilation on the occurrence of Botrytis cinerea in Mediterranean unheated tomato greenhouses. Crop Prot. **32**, 144–149 (2012)

30. B.R. Barmish, New tools for robustness analysis. In Proceedings of the 27th IEEE Conference on Decision and Control (Austin, Texas, 1988)

31. T. Bartzanas, M. Tchamitchian, C. Kittas, Influence of the heating method on greenhouse climate and energy consumption. Biosys. Eng. **91**(4), 487–499 (2005)

32. D. Bastien, A.K. Athienitis, A control algorithm for optimal energy performance of a solarium/greenhouse with combined interior and exterior motorized shading. Energy Procedia **30**, 995–1005 (2012)

33. D. Beckles, Factors affecting the postharvest soluble solids and sugar content of tomato (Solanum lycopersicum L.) fruit. Postharvest Biol. Technol. **63**, 129–140 (2012)

34. A. Belhani, N.K. M'Sirdi, Backstepping-based multi-criteria decision analysis for greenhouse control with real weather data. Int. Rev. Autom. Control Theor. Appl. **2**(5), 592–599 (2009)

35. A. Bemporad, Hybrid Toolbox-User's Guide. http://www.dii.unisi.it/hybrid/toolbox (2004)

36. A. Bemporad, M. Morari, Control of systems integrating logic, dynamics, and constraints. Automatica **35**(3), 407–427 (1999)

37. A. Ben-Gal, L. Karlberg, P.E. Jansson, U. Shani, Temporal robustness of linear relationship between production and transpiration. Plant Soil **251**, 211–218 (2003)

38. N. Bennis, J. Duplaix en G. Eneá, H. Haloua, H. Youlai, Greenhouse climate modelling and robust control. Comput. Electron. Agric. 61, 96–107 (2008)

39. M. Berenguel, E.F. Camacho, F. García-Martín, F.R. Rubio, Temperature control of a solar furnace. IEEE Control Syst. Mag. **19**(1), 8–24 (1999)

40. M. Berenguel, F. Rodríguez, F.G. Acién, J.L. García, Model predictive control of pH in tubular photobioreactors. J. Process Control **14**, 377–387 (2004)

41. M. Berenguel, F. Rodríguez, M. Cantón, Experiences in greenhouses automation for hydroponic crop in mediterranean greenhouses. In I IFAC International Conference on Technology Automation and Control of Wastewater and Drinking Water Systems TIASWIK'02 (Gdansk, Poland, 2002), pp. 89–94

42. M. Berenguel, F. Rodríguez, J.L. Guzmán, D. Lacasa, J. Pérez-Parra, Greenhouse diurnal temperature control with natural ventilation based on empirical models. Acta Hortic. **719**, 57–64 (2006)

43. M. Berenguel, L.J. Yebra, F. Rodríguez, Adaptive control strategies for greenhouse temperature control. In European Control Conference ECC'03 (Cambridge, UK, 2003)

44. N. Bertin, S. Guichard, C. Leonardi, J.J. Longuenesse, D. Langlois, B. Navez, Seasonal evolution of the quality of fresh glasshouse tomatoes under Mediterranean conditions, as affected by air vapour pressure deficit and plant fruit load. Ann. Bot. **85**, 741–750 (2000)

45. R.G.S. Bidwell, *Plant Physiol* (Macmillan Publishing Co., London, 1974)

46. T.E. Bilderback, S.L. Warren, J.H. Daniels, Managing irrigation by electrical conductivity. Acta Hortic. **481**, 403–408 (1999)

47. X. Blasco, J. Herrero, J. Sanchis, M. Martínez, In Lecture Notes in Computer Science, vol. 4527, Chapter decision making graphical tool for multiobjective optimization problems (Springer, Berlin, 2007), pp. 568–577

48. X. Blasco, M. Martínez, J.M. Herrero, C. Ramos, J. Sanchis, Model-based predictive control of greenhouse climate for reducing energy and water consumption. Comput. Electron. Agric. **55**, 49–70 (2007)

49. J. Boaventura, C. Couto, A.E.B. Ruano, Real-Time parameters estimation of dynamic temperature models for greenhouse environmental control. Control Eng. Pract. **5**(10), 1473–1481 (1997)

50. J. Boaventura, C. Couto, A.E.B. Ruano, A greenhouse climate multivariable predictive controller. Acta Hortic. **534**, 269–276 (2000)

51. J. Boaventura-Cunha, Greenhouse climate models: An overview. In Proceedings of the EFITA Conference (Debrecen, Hungary, 2003), pp. 823–829

52. J. Boaventura-Cunha, A.E.B. Ruano, C. Couto, Identification of greenhouse climate dynamic models. In Proceedings of the Sixth International Congress on Computers in Agriculture (Cancún, México, 1996), pp. 161–171

53. J. Boaventura-Cunha, A.E.B. Ruano, E.A. Faria, C. Couto, Dynamic temperature models of a soilless greenhouse. In Proceedings of the 2nd Portuguese Conference on Automatic Control (Porto, Portugal, 1996), pp. 77–81

54. J. Boaventura-Cunha, M. Santos, M. Cordeiro, P. Salgado, C. Serodio, C. Couto, Computerised management of greenhouses. Acta Hortic. **440**, 147–152 (1996)

55. D. Boisson, Etudes de la climatisation de serres par ventilation naturelle en periodo estivale: Modelisations et similations. PhD thesis (University of Perpignan, France, 1991)

56. C. Borguesani, Y. Chait, O. Yaniv, *The Quantitative Feedback Theory Toolbox for MATLAB* (The MathWorks, MA, 1995)

57. G.P.A. Bot, Greenhouse Climate from Physical Processes to a Dynamic Model (Ph.D. thesis, Agricultural University of Wageningen, The Netherlands, 1983)

58. G.P.A. Bot, N.J. van de Braak, In Greenhouse Climate Control: An Integrated Approach (Eds. J.C. Bakker, G.P.A. Bot, H. Challa, N.J. van de Braak), chapter Physics of greenhouse climate (Wageningen Press, 1995), pp. 125–162

59. T. Bouarar, K. Guelton, N. Manamanni, Robust fuzzy Lyapunov stabilization for uncertain and disturbed Takagi-Sugeno descriptors. ISA Trans. **49**(4), 447–461 (2010)

60. T. Boulard, A. Baille, A simple greenhouse climate control model incorporating effects on ventilation and evaporative cooling. Agric. For. Meteorol. **65**, 145–157 (1993)

61. T. Boulard, A. Baille, Modelling the air exchange rate in a greenhouse equipped with continuous roofs vents. J. Agric. Eng. Res. **61**, 37–48 (1995)

62. T. Boulard, B. Draoui, F. Neirac, Calibration and validation of a greenhouse climate control model. Acta Hortic. **406**, 49–62 (1996)
63. T. Boulard, S. Wang, Greenhouse crop transpiration simulations from external climate conditions. Agric. For. Meteorol. **100**, 25–35 (2000)
64. A. Brandelik, C. Hübner, Soil moisture determination-accurate, large and deep. Phys. Chem. Earth **21**(3), 157–160 (1996)
65. K.E. Brenan, S.L. Campbell, L.R. Petzold, Numerical Solution of Initial-Value Problems in Differential-Algebraic Equations (North-Holland, 1989)
66. R. Brun, J.J. Longuenesse, L. Barthelemy, P. Reich, Distribution of water in rockwool slabs. In Proceedings of Greensys 2004 (Leuven, Belgium, 2004)
67. R. Brun, J.P. Tournier, Micrometric measurement of stem diameter changes as a means to detect nutritional stress of tomato plants. Acta Hortic. **304**, 265–272 (1992)
68. S. Burés, Sustratos (Agrotecnia S.L., 1997)
69. F. Buwalda, A.A. Rijsdijk, J.V.M. Vogelezang, A. Hattendorf, L.G.G. Batta, An energy efficient heating strategy for cut rose production based on crop tolerance to temperature fluctuations. Acta Hortic. **507**, 117–125 (1999)
70. E.F. Camacho, M. Berenguel, F.R. Rubio, *Advanced Control of Solar Plants* (Springer, New York, 1997)
71. E.F. Camacho, M. Berenguel, F.R. Rubio, D. Martínez, *Control of Solar Energy Systems* (Springer, London, 2012)
72. E.F. Camacho, C. Bordóns, *Model Predictive Control in the Process Industry* (Springer, London, 1999)
73. E.F. Camacho, C. Bordóns, *Model Predictive Control* (Springer, London, 2004)
74. E.F. Camacho, F.R. Rubio, F.M. Hughes, Self-tuning control of a solar power plant with a distributed collector field. IEEE Control Syst. Mag. **12**(2), 72–78 (1992)
75. R. Cameron, *Model validation (XVI Course of Automatic Control in Industries* (University of Cádiz, Spain, Technical report, 1996)
76. R. Caponetto, L. Fortuna, G. Nunnari, L. Occhipinti, A fuzzy approach to greenhouse climate control. In Proceedings of the American Control Conference (Philadelphia, Pennsylvania, USA, 1998), pp. 1866–1870
77. R. Caponetto, L. Fortuna, G. Nunnari, L. Occhipinti, M.G. Xibilia, Soft computing for greenhouse climate control. IEEE Trans. Fuzzy Syst. **8**(6), 753–760 (2000)
78. M. Carvajal, F. del Amor, G. Fernández-Ballester, V. Martínez, A. Cerdá, Time course of solute accumulation and water relations in muskmelon plants exponed to salt during different growth stages. Plant Sci. **138**, 103–112 (1998)
79. R. Castañeda, E. Ventura, R. Peniche, G. Herrera, Greenhouse climate control system based on a field programmable gate array. Biosyst. Eng. **94**(2), 165–177 (2006)
80. M.M. Castilla, J.D. Álvarez, F. Rodríguez, *M* (Berenguel, Comfort Control in Buildings (Springer, 2014)
81. N. Castilla, *Manejo del Cultivo Intensivo con Suelo* (El Cultivo del Tomate. Mundi-prensa, Madrid, Spain, 1995)
82. A. Cervin, D. Henriksson, M. Ohlin, TrueTime 2.0 beta 5 - Reference Manual (2010)
83. D.E. Chaabane, Influence d'un ecran thermique sur le microclimat nocturne d'une serre agricole, Ph.D. thesis (Universite of Perpignan, France, 1986)
84. M. Chaabane, M. Souissi, D. Mehdi, Control of greenhouse climate with guaranteed H_∞ performance and D-stability. Int. J. Autom. Control **3**(1), 56–72 (2009)
85. Z.S. Chalabi, B.J. Bailey, Simulation of the energy balance in a greenhouse. Divisional note, 1516. Technical Report (Silsoe Research Institute, Silsoe, Bedford, MK45 4HS, 1989)
86. Z.S. Chalabi, B.J. Bailey, D.J. Wilkinson, A real-time optimal control algorithm for greenhouse heating. Comput. Electron. Agric. **15**(1), 1–13 (2005)
87. H. Challa, E. Heuvelink, U. van Meeteren, In Greenhouse Climate Control: An Integrated Approach ed. by J.C. Bakker, G.P.A. Bot, H. Challa, N.J. van de Braak, Chapter Crop growth and development (Wageningen Press, 1995), pp. 62–84

88. H. Challa, G. van Straten, In The Computerized Greenhouse ed. by Y. Hashimoto, G. Bot, H.J. Tantau, W. Day, H. Nonami, Chapter Optimal climate control in greenhouses as related to greenhouse management and crop requirements (Academic Press, 1993), pp. 119–137

89. A. Chouchine, E. Feki, A. Mami, A feedback linearization control based on a Takagi-Sugeno system to control the inside temperature of a greenhouse. In 16th IEEE Mediterranean Electrotechnical Conference (MELECON) (Yasmine Hammamet, Tunisia, 2012), pp. 693–698

90. V.T. Chow, D.R. Maidment, L.W. Mays, *Applied Hydrology* (Mc Graw-Hill, New York, 1994)

91. D.W. Clarke, C. Mohtadi, P.S. Tuffs, Generalized predictive control - i, ii. Automatica **23**(2), 137–160 (1987)

92. W. Claussen, Proline as a measure of stress in tomato plants. Plant Sci. **168**, 241–248 (2005)

93. J.P. Coelho, J. Boaventura-Cunha, P.B. de Moura-Oliveira, Solar radiation prediction methods applied to improve greenhouse climate control. In World Congress of Computers in Agriculture and Natural Resources (Iguacu Falls, Brazil, 2002), pp. 154–160

94. J.P. Coelho, P.B. de Moura-Oliveira, J. Boaventura-Cunha, Greenhouse air temperature predictive control using the particle swarm optimisation algorithm. Comput. Electron. Agric. **49**, 330–344 (2005)

95. J.P. Coelho, P.B. Moura, J. Boaventura-Cunha, Greenhouse air temperature control using the particle swarm optimization algorithm. In 15th IFAC World Congress (Barcelona, Spain, 2002)

96. C.A. Coello, Guest editorial: Special issue on evolutionary multiobjetive optimization. IEEE Trans. Evol. Comput. **7**(2), 97–99 (2003)

97. M. Cohen, R. Savé, C. Biel, O. Marfá, Simultaneuous measurements of water stress with LVDT sensors and electrotensiometers: applications in pepper plants grown in two types of perlites. Acta Hortic. **421**, 193–199 (1998)

98. M. Coomans, K. Allaerts, L. Wittermans, D. Pinxteren, Monitoring and energetic performance of two similar semi-closed greenhouse ventilation systems. Energy Convers. Manag. **76**, 128–136 (2013)

99. Y. Cormary, C. Nicolas, *La Thermique des Serres* (Editions Eyrolles, Paris, 1985)

100. D.L. Corwin, S.M. Lesch, Applications of apparent soil electrical conductivity measurements in agriculture. Comput. Electron. Agric. **46**(1–3), 11–44 (2005)

101. R.B. Curry, Dynamic simulation of plant growth. Part I. Development of a model. Trans. Am. Soc. Agric. Eng. **14**, 946–959 (1971)

102. D. Dannehl, J. Suhl, S. Huyskens-Keil, C. Ulrichs, U. Schmidt, Effects of a special solar collector greenhouse on water balance, fruit quantity and fruit quality of tomatoes. Agric. Water Manag. **134**, 14–23 (2014)

103. P.F. Davis, A technique of adaptive control of the temperature on a greenhouse using ventilator adjustements. J. Agric. Eng. Res. **29**(3), 241–248 (1984)

104. P.F. Davis, A.W. Hooper, Improvement of greenhouse heating control. IEE Proc. Control Theor. Appl. **138**(3), 249–255 (1991)

105. E. Dayan, H. van Keulen, J.W. Jones, I. Zipori, D. Simuel, H. Challa, Development, calibration and validation of a greenhouse tomato growth model: I. Description of the model. Mod. Agric. Syst. **43**, 145–163 (1993)

106. E. Dayan, H. van Keulen, J.W. Jones, I. Zipori, D. Simuel, H. Challa, Development, calibration and validation of a greenhouse tomato growth model: II. Field calibration and validation. Agri. Syst. **43**, 165–183 (1993)

107. W. Delin, M. Hanping, L. Pingping, Environmental regulation techniques based on economic optimization in greenhouse. Trans. Chinese Soc. Agric. Mach. **38**(2), 115–119 (2007)

108. J. DellAmico, A. Torrecillas, P. Rodríguez, D. Morales, M.J. Sánchez-Blanco, Differences in the effects of flooding the soil early and late in the photoperiod on the water relations of pot-grown tomato plants. Plant Sci. **160**, 481–487 (2001)

109. J. Doorenbos, A.H. Kassam, Efectos del Agua sobre el Rendimiento de los Cultivos FAO, Estudio FAO Riego y Drenaje 33 (1986)

110. J. Doorenbos, A.H. Kassam, C.L.M. Bentvelsen, V. Branscheid, J.M.G.A. Plusje, Yield Response to Water (FAO, 1979)

111. M. Dorais, J. Caron, G. Begin, A. Gosselin, L. Gaudreau, C. Ménard, Equipment performance for determining water needs of tomato plants grown in sawdust based substrates and rockwool. Acta Hortic. **692**, 293–304 (2004)

112. M. Dorais, R. Dorval, D.A. Demers, D. Micevic, G. Turcott, X. Hao, A. Papadopoulos, D.L. Ehret, A. Gosselin, Improving tomato fruit quality by increasing salinity: effects on ion uptake, growth and yield. Acta Hortic. **511**, 185–195 (2000)

113. M. Dorais, A.P. Papadopoulus, A. Gosselin, Influence of electrical conductivity management on greenhouse tomato yield and fruit quality. Agronomy **21**, 367–383 (2001)

114. F.J. Doyle, R.K. Pearson, B.A. Ogunnaike, *Identification and Control Using Volterra Models* (Springer, London, 2002)

115. C. Duarte-Galvan, I. Torres-Pacheco, R.G. Guevara-Gonzalez, R.J. Romero-Troncoso, L.M. Contreras-Medina, M.A. Rios-Alcaraz, J.R. Millan-Almaraz, Review. Advantages and disadvantages of control theories applied in greenhouse climate control systems. Span. J. Agric. Res. **19**(4), 926–938 (2012)

116. Dynasim. Dynasim Dymola http://www.dynasim.se (2003)

117. Dynasim. Dynasim Modelica http://www.dynasim.se/www/modelica.html (2003)

118. D. Ehret, A. Lau, S. Bittman, W. Lin, T. Shelford, Automated monitoring of greenhouse crops. Agronomie **21**, 403–414 (2001)

119. M.Y. El Ghoumari, H.J. Tantau, D. Megías, J. Serrano, Real time non linear constrained model predictive control of a greenhouse. In 15th IFAC World Congress (Barcelona, Spain, 2002)

120. R.Z. Eltez, T. Tuzel, A. Gül, I.H. Tuzel, H. Duyar, Effects of different EC levels of nutrient solution on greenhouse tomato growing. Acta Hortic. **573**, 443–448 (2002)

121. S.H. Emerman, T.E. Dawson, Experiments using split-root chambers on water uptake from soil macropores by sunflowers. Plant Soil **189**, 57–63 (1997)

122. X. Fang, C. Jiaoliao, Z. Libin, Z. Hongwu, Self-tuning fuzzy logic control of greenhouse temperature using real-coded genetic algorithm. In 9th International Conference on Control, Automation, Robotics and Vision, 2006-ICARCV'06 (Singapore, 2006)

123. X. Fang, S. Junqiang, C. Jiaoliao, Rough sets based fuzzy logic control for greenhouse temperature. In Proceedings of the 2nd IEEE/ASME International Conference on Mechatronic and Embedded Systems and Applications (Beijing, China, 2006)

124. I. Farkas, Modelling and control in agricultural processes. Comput. Electron. Agric. **49**(3), 315–316 (2005)

125. B. Farneti, R.E. Schouten, T. Qian, J.A. Dieleman, L.M.M. Tijskens, E.J. Woltering, Greenhouse climate control affects postharvest tomato quality. Postharvest Biol. Technol. **86**, 354–361 (2013)

126. J.E. Fernández, M.J. Palomo, A. Díaz-Espejo, B.E. Clothier, S.R. Green, L.F. Girón, F. Moreno, Heat pulse measurements of sap flow in olives for automating irrigation: tests, root flow and diagnostics of water stress. Agric. Water Manag. **51**, 99–123 (2001)

127. J.A. Ferre, A. Pawlowski, J.L. Guzmán, F. Rodríguez, M. Berenguel, A wireless sensor network for greenhouse climate monitoring. In 5th International Conference on Broadband and Biomedical Communications (Málaga, Spain, 2010)

128. P.M. Ferreira, A.E. Faria, A.E.B. Ruano, Neural network models in greenhouse air temperature prediction. Neurocomputing **43**, 51–75 (2002)

129. P.M. Ferreira, A.E.B. Ruano, Choice of RBF model structure for predicting greenhouse inside air temperature. In 15th IFAC World Congress (Barcelona, Spain, 2002)

130. F. Fourati, M. Chtourou, A greenhouse control with feed-forward and recurrent neural networks. Simul. Model. Pract. Theor. **15**, 1016–1028 (2007)

131. H.U. Frausto, J.G. Pieters, Modeling greenhouse temperature using system identification by means of neural networks. Neurocomputing **56**, 423–428 (2004)

132. S. Gal, A. Angel, I. Seginer, Optimal control of greenhouse climate: Methodology. Eur. J. Oper. Res. **17**, 45–56 (1984)

133. M. Gallardo, *Uso de indicadores del estado hídrico de la planta para la programación del riego*, In Jornadas Técnicas de Agricultura (Almería, Spain, 2004)

134. J.L. García, A. Perdigones, M. Pastor, R.M. Benavente, L. Luna, C. Chaya, S. de la Plaza, Effect of heating control strategies on greenhouse energy efficiency: Experimental results and modelling. Trans. ASAE **49**(1), 143–155 (2006)

135. C. Gary, A. Baille, M. Navarrete, R. Espanet, *"Tompousse", un modele simplifie de previous du rendement et du calibre de la tomate*, in Actes du Seminaire de IAIP Serres (Avignon, France, 1996)

136. C. Gary, J.F. Barczi, N. Bertin, M. Tchamitchian, Simulation of individual organ growth and development on a tomato plant: a model and a user-friendly interface. Acta Hortic. **399**, 199–205 (1995)

137. C. Gary, J.W. Jones, M. Tchamitchian, Crop modeling in horticulture: state of the art. Sci. Hortic. **74**, 3–20 (1998)

138. K.V. Garzoli, J. Blackwell, An analysis of the nocturnal heat loss from a single skin plastic greenhouse. J. Agric. Eng. Res. **26**, 203–214 (1981)

139. R.S. Gates, K. Chao, N. Sigrimis, Identifying design parameters for fuzzy control of staged ventilation control systems. Comput. Electron. Agric. **31**, 61–74 (2001)

140. A. de Gelder, J.A. Dieleman, G.P.A. Bot, L.F.M. Marcelis, An overview of climate and crop yield in closed greenhouses. J. Hortic. Sci. Biotechnol. **87**(3), 193–202 (2012)

141. M.T. van Genutchen, A closed-form equation for predicting the hydraulic conductivity of unsaturated soils. Soil Sci. Soc. Am. J. **44**, 892–898 (1980)

142. Th.H. Gieling, Control of Water Supply and Specific Nutrient Application in Closed Growing Systems Ph.D. thesis (Wageningen University, The Netherlands, 2001)

143. ThH Gieling, J. Bontsema, T.W.B.M. Bouwmans, R.H. Steeghs, Modelling and simulation for control of nutrient application in closed growing systems. Neth. J. Agric. Sci. **45**, 127–142 (1997)

144. Th.H. Gieling, F.J.M. Corver, H.J.J. Janssen, Hydrion-line, towards a closed system for water and nutrients: feedback control of water and nutrients in the drain. In Proceedings of Greensys 2004 (Leuven, Belgium, 2004)

145. Th. H Gieling, H.J.J. Janssen, G. van Straten, M. Suurmond, Identification and simulated control of greenhouse closed water supply systems. Comput. Electron. Agric. **26**, 361–374 (2000)

146. H. Gijzen, Simulation of photosynthesis and dry matter production of greenhouse crops. Technical Report, Simulation Reports, CABOT No. 28 (Agricultural University of Wageningen, The Netherlands, 1992)

147. R. González, F. Rodríguez, J.L. Guzmán, M. Berenguel, Robust constrained economic receding horizon control applied to the two time-scale dynamics problem of a greenhouse. Optimal Control Applications & Methods page http://dx.doi.org/10.1002/oca.2080 (2013)

148. E. Gorrostieta, J.C. Pedraza, M.A. Aceves, J.M. Ramos, S. Tovar, A. Sotomayor, In Emerging Technologies and Applications, Chapter Greenhouse fuzzy and neuro-fuzzy modeling techniques (Intech, 2012), pp. 309–322

149. J. Goudrian, H.H. van Laar, *Modelling Potential Crop Growth Processes* (Kluwer Academic Publishers, Dordrecht, 1994)

150. R. de Graaf, M.H. Esmeijer, Calculated and measured water comsumption in a study of the (minimal) transpiration of cucumbers grown in rockwool. Acta Hortic. **458**, 103–112 (1998)

151. C.J. Graves. In Horticultural Reviews ed. by J. Janick, volume 5, chapter The Nutrient Film Technique. (Wiley, Hoboken, 1983)

152. C. Grimholt, S. Skogestad, Optimal PI-Control and Verification of the SIMC Tuning Rule. In Proceedings of the IFAC Conference on Advances in PID control (PID'12) (Brescia, Italy, 2012)

153. J.K. Gruber, J.L. Guzmán, F. Rodríguez, M. Berenguel, C. Bordóns, Nonlinear model predictive control of greenhouse temperature using a Volterra model. In European Control Conference ECC'09 (Budapest, Hungary, 2009), pp. 1299–1304

154. J.K. Gruber, J.L. Guzmán, F. Rodríguez, C. Bordóns, M. Berenguel, J. Sánchez, Nonlinear MPC based on a Volterra series model for greenhouse temperature control using natural ventilation. Control Eng. Prac. **19**(4), 354–366 (2011)

155. J.K. Gruber, F. Rodríguez, C. Bordóns, J.L. Guzmán, M. Berenguel, Modelling greenhouse temperature using Volterra series. In IFAC 2nd International Conference AGRICONTROL 2007 (Osijek, Croatia, 2007), pp. 41–46

156. J.K. Gruber, F. Rodríguez, C. Bordóns, J.L. Guzmán, M. Berenguel, E.F. Camacho, A Volterra model of the greenhouse temperature using natural ventilation. In 17th IFAC World Congress (Seoul, Korea, 2008), pp. 2925–2930

157. F. Güohler, A. Heibner, H. Schmeil, Control of water and nutrient supply in greenhouse vegetable production by means of hydroponic systems. Acta Hortic. **260**, 237–254 (1989)

158. E.H. Gurban, G.D. Andreescu, Employing 2DoF PID controllers to improve greenhouse climate system robustness. In IEEE International Conference on System Science and Engineering-ICSSE 2013 (Budapest, Hungary, 2013), pp. 93–98

159. P.O. Gutman, P.O. Lindber, I. Ioslovich, I. Seginer, A non-linear optimal greenhouse control problem solved by linear programming. J. Agric. Res. **55**, 335–351 (1993)

160. J.L. Guzmán, M. Berenguel, S. Dormido, Interactive teaching of constrained predictive control. IEEE Control Syst. Mag. **25**(2), 52–66 (2005)

161. J.L. Guzmán, T. Hägglund, Simple tuning rules for feedforward compensators. J. Process Control **21**, 92–102 (2011)

162. J.L. Guzmán, T. Hägglund, A. Visioli, *In PID Control in the Third Millenium: Lessons Learned and New Approaches Chapter Feedforward compensation for PID control loops* (Springer, New York, 2012)

163. J.L. Guzmán, D. Rivera, S. Dormido, M. Berenguel, ITSIE: An interactive software tool for system identification education. In Proceedings of the 15th IFAC Symposium on System Identification (St. Malo, France, 2009)

164. J.L. Guzmán, D. Rivera, S. Dormido, M. Berenguel, Teaching system identification through interactivity. In Proceedings of the 8th IFAC Symposium on Advances in Control Education (ACE09) (Kumamoto, Japan, 2009)

165. J.L. Guzmán, F. Rodríguez, M. Berenguel, M.R. Arahal, A hybrid control approach to the greenhouse climatic control problem. In IFAC 2nd International Conference AGRICONTROL 2007 (Osijek, Croatia, 2007)

166. F. Hah, Fuzzy controller decreases tomato cracking in greenhouses. Comput. Electron. Agric. **77**, 21–27 (2011)

167. D. Halleaux, Modele dynamique des échanges énergétiques des serres: Étude théorique et expérimentale, Ph.D. thesis (Faculté des Sciencies Agronomiques de Gembloux, Belgium, 1989)

168. I.A. Hameed, Simplified architecture of a type-2 fuzzy controller using four embedded type-1 fuzzy controllers and its application to a greenhouse climate control system. Proc. IMechE Part I J. Syst. Control Eng. **223**(5), 619–631 (2009)

169. I.A. Hameed, Using the extended Kalman filter to improve the efficiency of greenhouse climate control. Int. J. Innovative Comput. Inf. Control **6**(6), 2671–2680 (2010)

170. J.C.P. Hamer, Validation of a model used for irrigation control of a greenhouse crop. Acta Hortic. **458**, 75–82 (1998)

171. Y. Hashimoto, In The Computerized Greenhouse ed. by Y. Hashimoto, G. Bot, H.J. Tantau, W. Day, H. Nonami, Chapter Computer integrated system for the cultivation process in agriculture and horticulture. Approach to "Intelligent Plant Factory" (Academic Press, London, 1993), pp. 175–196

172. A. Hasni, B. Draoui, F. Bounaama, M. Tamali, T. Boulard, Evolutionary algorithms in the optimization of natural ventilation parameters in a greenhouse with continuous roof vents. Acta Hortic. **719**, 49–56 (2006)

173. M. Hast, T. Hägglund, Design of optimal low-order feedforward controllers. In IFAC Conference on Advances in PID Control (Brescia, Italy, 2012)

174. T. Hägglund, K.J. Åström, Industrial adaptive controllers based on frequency response techniques. Automatica **27**(4), 599–609 (1991)

175. W.P.M.H. Heemels, B. de Schutter, A. Bemporad, On the equivalence of classes of hybrid dynamical models. In 40th IEEE Conference on Decision and Control (Orlando, Florida, USA, 2001)

176. M. Heinen, Dynamics of Water and Nutrients in Closed, Recirculating Cropping Systems in Glasshouse Horticulture, Ph.D. thesis (Agricultural University of Wageningen, The Netherlands, 1997)

177. E.J. van Henten, Greenhouse Climate Management: An Optimal Control Approach Ph.D. Thesis (Agricultural University of Wageningen, The Netherlands, 1994)

178. E.J. van Henten, J. Bontsema, Singular perturbation methods applied to a variational problem in greenhouse climate control. In Proceedings of the 31st Conference on Decision and Control (Tucson, Arizona, USA, 1992)

179. E.J. van Henten, J. Bontsema, A time-scale decomposition of an optimal control problem in greenhouse climate management. Control Eng. Pract. **17**, 88–96 (2009)

180. A.S. Hernández, R.E.J. Fernández, V.J. Fernández, In Innovaciones Tecnológicas en Cultivos de Invernadero ed. by E.J. Fernández, Chapter El uso del laptómetro como alternativa a la bandeja de demanda para el control del riego en sistemas de cultivo sin suelo (Cajamar, 2003), pp. 97–120

181. E. Heuveling, Dry matter production in a tomato crop: measurements and simulation. Ann. Botany **73**, 369–379 (1993)

182. E. Heuveling, Dry matter partitioning in tomato: Validation of a dynamic simulation model. Ann. Botany **77**, 71–80 (1996)

183. E. Heuveling, Evaluation of a dynamic simulation model for tomato crop growth and development. Ann. Botany **83**, 413–422 (1999)

184. E. Heuvelink, Tomato Growth and Yield: Quantitative Analysis and Synthesis Ph.D. Thesis (Agricultural University of Wageningen, The Netherlands, 1996)

185. E. Heuvelink, L.M.M. Tijskens, M. Kang, Modelling product quality in horticulture: an overview. Acta Hortic. **654**, 19–30 (2004)

186. L.C. Ho, In Genetic and Environment Manipulation of Horticultural Crops ed. by K. Cockshull, D. Gray, G. Seynor, B. Thomas, Chapter Improving tomato fruit quality by cultivation (Cabi Publishers, 1996), pp. 17–29

187. L.C. Ho, D.J. Hand, M. Fusell, Improvement of tomato fruit quality by calcium nutrition. Acta Hortic. **481**, 463–468 (1999)

188. T. Honjo, T. Takakura, In Mathematical and Control Applications in Agriculture and Horticulture ed. by Y. Hashimoto, W. Day, Chapter Identification of water and nutrient supply to hydroponic tomato plants by using neural nets, (Pergamon Press, 1991), pp. 285–288

189. I. Horowitz, Quantitative feedback theory. IEEE Proc. 129(D-6), 215–226 (1982)

190. C. Houck, J. Joines, M. Kay, The genetic algorithm for function optimization: a Matlab implementation. Technical Report http://www.ie.ncsu.edu/mirage/GAToolBox/gaot/, Industrial Engineering (North Carolina State University, 1995)

191. T.C. Hsiao, L.K. Xu, Predicting water use efficiency of crops. Acta Hortic. **537**, 199–206 (2000)

192. H. Hu, L. Xu, R. Wei, B. Zhu, Multi-objective control optimization for greenhouse environment using evolutionary algorithms. Sensors **11**, 5792–5807 (2011)

193. H. Hu, L. Xu, B. Zhu, R. Wei, A compatible control algorithm for greenhouse environment control based on MOCC strategy. Sensors **11**(3), 3281–3302 (2011)

194. R.G. Hurd, C.J. Graves, The influence of different temperature patterns having the same integral on the earliness and yield of tomatoes. Acta Hortic. **148**, 547–554 (1984)

195. I.A. Ibrahim, C.G. Sorensen, A more energy efficient controller for the greenhouses climate control system. Appl. Eng. Agric. **25**(3), 491–498 (2010)

196. Institute of Electrical and Electronics Engineers IEEE, *IEEE Standard Computer Dictionary: A Compilation of IEEE Standard Computer Glossaries* (IEEE, New York, USA, 1990)

197. Institute of Electrical and Electronics Engineers IEEE, *IEEE Standard Glossary of Computer Networking Terminology* (IEEE, New York, USA, 1995)

198. I. Impron, S. Hemming, G.P.A. Bot, Simple greenhouse climate model as a design tool for greenhouses in tropical lowland. J. Biosyst. Eng. **98**(1), 79–89 (2007)

199. I. Ioslovich, P.O. Gutman, R. Linker, Hamilton-Jacobi-Bellman formalism for optimal climate control of greenhouse crop. Automatica **45**(5), 1227–1231 (2009)

200. I. Ioslovich, P.O. Gutman, I. Seginer, A non-linear optimal greenhouse control problem with heating and ventilation. Opt. Control Appl. Meth. **17**, 157–169 (1996)

201. I. Ioslovich, I. Seginer, Acceptable nitrate concentration of greenhouse lettuce: Two optimal control policies. Biosyst. Eng. **83**, 199–215 (2002)

202. I. Ioslovich, I. Seginer, P.O. Gutman, M. Borshchevsky, Sub-optimal CO_2 enrichment of greenhouses. J. Agric. Eng. Res. **60**, 117–136 (1995)

203. K. Iwao, Application of fuzzy theory to a plant factory with artificial intelligence. Electrothecnol. Application. **1**, 317–320 (1994)

204. M. Jackson, W. Davies, M. Else, Pressure-flow relationships, xylem solutes and root hydraulic conductance in flooded tomato plants. Ann. Botany **77**, 17–24 (1996)

205. P. Javadikia, A. Tabatabaeefar, M. Omid, R. Alimardani, M. Fathi, Evaluation of intelligent greenhouse climate control system based fuzzy logic in relation to conventional systems. In 2009 International Conference on Artificial Intelligence and Computational Intelligence (Budapest, Hungary, 2009), pp. 146–150

206. R. Jemaa, T. Boulard, A. Baille, Some results on water and nutrient consumption of a greenhouse tomato crop grown in rockwool. Acta Hortic. **408**, 137–146 (1995)

207. T.J. Jewett, W.R. Jarvis, Management of the greenhouse microclimate in relation to disease control: a review. Agronomie **21**, 351–366 (2001)

208. S. Ji, G. Ciovanu, Conformon-driven biopolymer shape changes in cell modelling. BioSystems **70**, 165–181 (2003)

209. Y. Jiaqiang, J. Yulong, G. Jian, An intelligent greenhouse control system. TELKOMNIKA **11**(8), 4627–4632 (2013)

210. H.G. Jones, F. Tardieu, Modelling water relations of horticultural crops: A review. Scientia Hortic. **74**, 21–46 (1998)

211. J.W. Jones, E. Dayan, L.H. Allen, H. van Keulen, H. Challa, A dynamic-tomato growth and yield model (TOMGRO). Trans. ASAE **34**(2), 663–672 (1991)

212. J.W. Jones, A. Kening, C.E. Vallejos, Reduced state-variable tomato growth model. Trans. ASAE **42**(1), 255–265 (1999)

213. P. Jones, J.W. Jones, Y. Hwang, Simulation for determining greenhouse temperature setpoints. Trans. ASAE **33**(5), 1722–1728 (1990)

214. M. Kacira, S. Sase, L. Okushima, P.P. Ling, Plant response-based sensing for control strategies in sustainable greenhouse production. J. Agric. Meteorol. **61**(1), 15–22 (2005)

215. P.G.H. Kamp, G.J. Timmerman, *Computerized Environmental Control in Greenhouses (A Step by Step Approach)* (IPC Plant, Netherlands, 1996)

216. A. Kenig, J.W. Jones, In Optimal Environmental Control for Indeterminate Greenhouse Crops ed. by I. Seginer, J.W. Jones, P. Gutman, C.E. Vallejos, Chapter TOMGRO v3.0 A dynamic model of tomato growth and yield. BARD Research Report No. IS-1995-91RC. (Haifa, Israel, 1997)

217. M. Kindelan, Dynamic modeling of greenhouse environment. Trans. ASAE **23**, 1232–1239 (1980)

218. C. Kirda, M. Cetin, Y. Dasgan, S. Topcu, H. Kaman, B. Ekici, M.R. Derici, A.I. Ozguven, Yield response of greenhouse grown tomato to partial root drying and conventional deficit irrigation. Agric. Water Manag. **69**, 191–201 (2004)

219. C. Kittas, T. Boulard, G. Papadakis, Natural ventilation of a greenhouse with ridge and side openings: sensitivity to temperature and wind effects. Trans. ASAE **40**(2), 415–425 (1997)

220. H.P. Kläring, Strategies to control water and nutrient supplies to greenhouse crops. A Rev. Agrono. **21**, 311–321 (2001)

221. H.P. Kläring, W. Cierpinsky, Control of nutrient solution concentration depending on greenhouse climate in sweet pepper crop. Acta Hortic. **458**, 141–146 (1998)

222. H.P. Kläring, D. Schwarz, Model based control of concentration of nutrient solution in glasshouse tomato cultivation. Acta Hortic. **507**, 127–132 (1999)

223. H.P. Kläring, D. Schwarz, W. Cierpinsky, Control of concentration of nutrient solution in soilless growing systems, depending on greenhouse climate: advantages and limitations. Acta Hortic. **507**, 133–140 (1999)

224. H.P. Kläring, D. Schwarz, A. Heibner, Control of nutrient solution concentration in tomato crop using models of photosynthesis and transpiration-a simulation study. Acta Hortic. **450**, 329–334 (1997)
225. D. Kolokotsa, G. Saridakis, K. Dalamagkidis, S. Dolianitis, I. Kaliakatsos, Development of an intelligent indoor environment and energy management system for greenhouses. Energy Conv. Manag. **51**, 155–168 (2010)
226. A.N.M. de Koning, Long term temperature integration of tomato. Growth and development under alternating temperature regimes. Sci. Hortic. **45**, 117–128 (1990)
227. A.N.M. de Koning, Development and Dry Matter Distribution in Glasshouse Tomato: A Quantitative Approach Ph.D. thesis (Wageningen Agricultural University, The Netherlands, 1994)
228. O. Körner, H. Challa, Design for an improved temperature integration concept in greenhouse cultivation. Comput. Electron. Agric. **39**, 39–59 (2003)
229. O. Körner, H. Challa, Process-based humidity control regime for greenhouse crops. Comput. Electron. Agric. **39**(3), 173–192 (2003)
230. O. Körner, N. Holst, Model based humidity control of Botrytis in greenhouses. In Proceedings of Greensys 2004 (Leuven, Belgium, 2004)
231. O. Körner, G. Van Straten, Decision support for dynamic greenhouse climate control strategies. Comput. Electron. Agric. **60**(1), 18–30 (2008)
232. F.N. Koumboulis, M.P. Tzamtzi, Towards step-wise safe switching climate control for a greenhouse. In IEEE International Conference on Emerging Technologies and Factory Automation, 2008-ETFA 2008 (Hamburg, Germany, 2008), pp. 1400–1407
233. P. Kramer, J. Boyer, *Water Relations of Plants and Soils* (Academic Press, San Diego, 1995)
234. M.J. Kurtz, M.A. Henson, Input-output linearizing control of constrained nonlinear processes. J. Process Control **7**, 3–17 (1996)
235. E.J. Kyriannakis, K.G. Arvanitis, N. Sigrimis, On-line improvement for the descentralized predictive control of the heat dynamics of a greenhouse. In 15th IFAC World Congress (Barcelona, Spain, 2002)
236. M.C. van Labeke, P. Dembre, Gerbera cultivation on coir recirculation of nutrient solution: a comparison with rockwool culture. Acta Hortic. **458**, 357–362 (1998)
237. R. Lacroix, R. Kok, Simulation-based control of enclosed ecosystems-a case study: Determination of greenhouse heating setpoints. Can. J. Agric. Eng. **41**, 175–183 (1999)
238. F. Lafont, J.F. Balmat, Optimized fuzzy control of a greenhouse. Fuzzy Sets Syst. **128**, 47–59 (2002)
239. F. Lafont, J.F. Balmat, Fuzzy logic to the identification and the commande of the multidimensional systems. Int. J. Comput. Cogn. **2**, 21–47 (2004)
240. F. Lafont, N. Pessel, J.F. Balmat, M. Fliess, On the model-free control of an experimental greenhouse. in Proceedings of World Congress on Engineering and Computer Science 2013-WCECS 2013, vol. 2 (San Francisco, USA, 2013)
241. H. Lambers, S. Chapin, *T* (Pons, Springer, Plant Physiological Ecology, 1998)
242. I. Laribi-Maatoug, R. Mhiri, An explicit solution for the optimal control of greenhouse temperature relying on embedded system. ICGST Int. J. Autom. Control. Syst. Eng. **3**, 27–34 (2008)
243. R.U. Larsen, Plant grow modelling by light and temperature. Int. J. Comput. Cogn. **272**, 235–242 (1990)
244. J. Leal-Iga, Modeling of the climate for a greenhouse in the northeast of Mexico. In Proceedings of the 17th World Congress (Seoul, Korea, 2008), pp. 9558–9563
245. A. Lecomte, J. Flaus, E. Brajeul, R. Brun, P. Reich, L. Barthelemy, Multivariable greenhouse control: applications to fertigation and climate management. Acta Hortic. **691**, 249–258 (2005)
246. B.W. Lee, J.H. Shin, Optimal irrigation management system of greenhouse tomato based on stem diameter and transpiration monitoring. Agric. Inf. Technol. Asia Oceania **23**, 87–90 (1998)
247. S. Li, S. Liu, L. Ju, Application of adaptive fuzzy controller in intelligent greenhouse control system. In Proceedings of the IEEE International Conference on Automation and Logistics, (Qingdao, China, 2008) pp. 1708–1712

248. Y.L. Li, L.F.M. Marcelis, C. Stanghellini, Plant water relations as affected by osmotic potential of the nurient solution and potential transpiration in tomato (Lycopersicon esculentum Mill). J. Hortic. Sci. Biotech. **79**, 211–218 (2004)
249. Y.L. Li, C. Stanghellini, Analysis of the effect of EC and potential transpiration on vegetative growth of tomato. Sci. Hortic. **89**, 9–21 (2001)
250. Y.L. Li, C. Stanghellini, H. Challa, Effect of electrical conductivity and transpiration on production of greenhouse tomato. Sci. Hortic. **88**, 11–29 (2001)
251. D. Liberzon, *Switching in Systems and Control* (Springer, Berlin, 2003)
252. W. Ling, D.E. Rivera, Control relevant model reduction of Volterra series models. J. Process Control **8**(2), 79–88 (1998)
253. R. Linker, P.O. Gutman, I. Seginer, Robust controllers for simultaneous control of temperature and CO_2 concentration in greenhouses. Control Eng. Pract. **7**, 851–862 (1999)
254. R. Linker, I. Seginer, P.O. Gutman, Neural network and hybrid adaptive modeling of greenhouse air temperature. In Proceedings of the AgEng'98 Conference, (Oslo, Norway, 1998)
255. R. Linker, I. Seginer, P.O. Gutman, Optimal CO_2 control in a greenhouse modeled with neural networks. Comput. Electron. Agric. **19**, 289–310 (1998)
256. G.P. Liu, J.B. Yang, J.F. Whidborne, *Multiobjective Optimisation and Control* (Research Studies Press, Hertfordshire, 2003)
257. L. Ljung, *System Identification* (Theory For The User. Prentice Hall, Englewood Cliffs, New Jersey, USA, 1999)
258. I.L. Lopez, L. Hernández, Neuro-fuzzy models for air temperature and humidity of a greenhouse. Acta Hortic. **927**, 611–617 (2012)
259. I. López-Cruz, L.G. van Willigenburg, G. van Straten, Optimal control of nitrate in lettuce by a hybrid approach: differential evolution and adjustable control weight gradient algorithms. Comput. Electron. Agric. **40**, 179–197 (2003)
260. X.L. Luan, P. Shi, F. Liu, Robust adaptive control for greenhouse climate using neural networks. Int. J. Robust Nonlinear Control **21**(7), 815–826 (2011)
261. C.J.J. Magán, In Mejora de la Eficiencia en el Uso del Agua en Cultivos Protegidos, ed. by F.M. Fernández, M.P. Lorenzo, G.M.I. Cuadrado, chapter Efectos de la salinidad sobre el tomate en cultivo en sustrato en las condiciones del sudeste peninsular: Resultados experimentales, (Almería, Spain, 2003), pp. 169–187
262. C.J.J. Magán, N. Moreno, D. Meca, F. Cánovas, Response to salinity of a tomato crop in Mediterranean greenhouse climate conditions. Acta Hortic. **644**, 479–484 (2004)
263. B.R. Maner, F.J. Doyle, B.A. Ogunnaike, R.K. Pearson, Nonlinear model predictive control of a simulated multivariable polymerization reactor using second-order Volterra models. Automatica **32**(9), 1285–1301 (1996)
264. C. Manera, P. Picuno, G. Scarascia, Analysis of nocturnal microclimate in a single skin cold greenhouse in Mediterranean countries. Acta Hortic. **281**, 47–56 (1990)
265. L.F.M. Marcelis, E. Heuvelink, J. Goudriaan, Modelling biomass production and yield of horticultural crops: a review. Sci. Hortic. **74**, 83–111 (1998)
266. M. Martínez-Ballesta, V. Martínez, M. Carvajal, Osmotic adjustment, water relations and gas exchange in pepper plants grown under NaCl or KCl. Env. Exp. Biol. **52**, 161–174 (2004)
267. The MathWorks Inc, *Using Matlab* (The Language of Technical Computing, USA, 1998)
268. The MathWorks Inc, *Using Simulink* (Dynamic Systems Simulation for Matlab, USA, 1998)
269. K. Matous, M. Leps, J. Zeman, M. Sejnoha, Applying genetic algorithm to selected topics commonly encountered in engineering practice. Comput. Methods Appl. Mech. Eng. **190**, 1629–1650 (2000)
270. R.F. Mechlouch, A.B. Brahim, A global solar radiation model for the design of solar energy systems. Asian J. Sci. Res. **1**(3), 231–238 (2008)
271. E. Medrano, P. Lorenzo, M.C. Sánchez-Guerrero, J.I. Montero, Evaluation and modelling of greenhouse cucumber crop transpiration under high and low radiation conditions. Sci. Hortic. **105**(2), 163–175 (2005)
272. U. Meier, *Growth Stages of Mono-and Dicotyledonous Plants* (BBCH Monograph, Federal Biological Research Centre for Agriculture and Forestry, Braunschweig, Germany, 2001)

273. D. Mignone, The REALLY BIG Collection of Logic Propositions and Linear Inequalities, (2002)
274. R.C. Miranda, E. Ventura-Ramos, R.R. Peniche-Vera, G. Herrera-Riuz, Fuzzy greenhouse climate control system based on a field programmable gate array. Biosyst. Eng. **94**, 165–177 (2006)
275. M. Miskowicz, Sampling of signals in energy domain. In 10th IEEE Conference on Emerging Technologies and Factory Automation, (Catania, Italy, 2005), pp. 263–266
276. H. Mohr, P. Schopfer, *Plant Physiology* (Springer, Berlin, 1995)
277. J. Monteith, *In The State and Movement of Water in Living Organism, Evaporation and environment*, vol. 19 (Cambridge University Press, Cambridge, 1965), pp. 205–234
278. J.I. Montero, A. Antón, P. Muñoz, Curso Superior de Especialización: Tecnología de Invernaderos II, chapter Refrigeración de invernaderos (Greenhouse cooling) (Dirección General de Investigación y Formación Agroalimentaria de la Junta de Andalucía, FIAPA y Caja Rural de Almería, 1998), pp. 313–338
279. J.I. Montero, A. Antón, P. Muñoz, P. Lorenzo, Transpiration from geranium grown under high temperatures and low humidities in greenhouses. Agric. For. Meteorol. **107**, 323–332 (2001)
280. A.P. Montoya, J.L. Guzmán, F. Rodríguez, J.A. Sánchez, Hybrid modelling and control of greenhouse temperature combining aerial-pipes and air-fan heater systems. In International Conference of Agricultural Engineering, CIGR-AgEng 2012, (Valencia, Spain, 2012)
281. A.P. Montoya, F. Rodríguez, J.L. Guzmán, *Obtención de modelos reducidos para el diseño de controladores de la temperatura interior de invernaderos* (In V Congreso Nacional y II Congreso Ibérico Agroingeniería, Lugo, Spain, 2009)
282. J.J. Moré, In Numerical Analysis. Lecture Notes in Mathematics, The Levenberg-Marquardt algorithm: Implementation and theory, vol. 630 (Springer, Heidelberg, 1978), pp. 105–116
283. J.C. Moreno, A. Baños, F.J. Montoya, An Algorithm for Computing QFT Multiple-valued Performance Bounds, In Proceedings of the Symposium on QFT and other Frequency Domain Methods and Applications, (Stratchclyde, Scotland, 1997), pp. 29–32
284. J.C. Moreno, M. Berenguel, F. Rodríguez, A. Baños. Robust control of greenhouse climate exploiting measurable disturbances, In 15th IFAC World Congress, (Barcelona, Spain, 2002)
285. Y. Mualem, A new model for predicting the hydraulic conductivity of unsaturated porous media. Water Resour. Res. **12**(3), 513–522 (1976)
286. B.J. Mulholland, M. Fusell, R.N. Edmonson, J. Basahm, J.M. Mckee, Effects of vpd, K nutrition and root-zone temperature on leaf area development, accumulation of Ca and K and yield in tomato. J. Hortic. Sci. Biotechnol. **76**(5), 641–647 (2001)
287. P. Muñoz, J.I. Montero, A. Antón, F. Giuffrida, Effect of insect-proof screens and roof openings on greenhouse ventilation. J. Agric. Eng. Res. **73**, 171–178 (1998)
288. M. Nachidi, A. Benzaouia, F. Tadeo, Temperature and humidity control in greenhouses using the Takagi-Sugeno fuzzy model, In IEEE International Conference on Control Applications, (Munich, Germany, 2006), pp. 2150–2154
289. M. Nachidi, A. Benzaouia, F. Tadeo, M. Ait-Rami, LMI-based approach for output feedback stabilization for discrete time Takagi-Sugeno systems. In Proceedings of the 45th IEEE Conference on Decision and Control, (San Diego, CA, 2006), pp. 6301–6306
290. M. Nachidi, F. Rodríguez, F. Tadeo, A. Benzaouia, Modeling of a Greenhouse climate using Takagi-Sugeno Fuzzy models, In Conference on Systems and Control, (Marrakech, Marocco, 2007)
291. M. Nachidi, F. Rodríguez, F. Tadeo, J.L. Guzmán, Takagi. Sugeno control of nocturnal temperature in greenhouses using air heating. ISA Trans. **50**, 315–320 (2011)
292. M. Nachidi, F. Rodríguez, F. Tadeo, J.L. Guzmán, R. González. Modeling and control of nocturnal temperature inside a greenhouse using Takagi-Sugeno fuzzy models. In 8th Portuguese Conference on Automatic Control CONTROLO'08, (Vila Real, Portugal, 2008), pp. 518–523
293. P.V. Nelson, *Greenhouse Operation and Management* (Prentice Hall, New Jersey, 2002)
294. K.S. Nemali, M.W. van Iersel, Physiological responses to different substrate water contents: screening for high water-use efficiency in bedding plants. J. Am. Soc. Hortic. Sci. **133**(3), 333–340 (2008)

295. B. Nielsen, H. Madsen, Identification of transfer functions for control of greenhouse air temperature. J. Agric. Eng. Res. **60**(1), 25–34 (1995)
296. B. Nielsen, H. Madsen, Predictive control of air temperature in greenhouses, In 13th IFAC World Congress, (San Francisco, USA, 1996)
297. NI/SEMATECHST: e-Handbook of Statistical Methods (2006), http://www.itl.nist.gov/div898/handbook/
298. L. Occhipinti, G. Nunnari, Synthesis of a greenhouse climate controller using AI-based techniques, In Proceedings of the IEEE International Conference MELECON96, (Bari, Italy, 1996), pp. 230–233
299. A. O'Dwayer, *Handbook of PI and PID Controller Tuning Rules* (Imperial College Press, London, 2006)
300. R. Olfati-Saber, Distributed Kalman Filter with embedded consensus filters. In 44th IEEE Conference on Decision and Control and European Control Conference. CDC-ECC'05. (Seville, Spain, 2005), pp. 8179–8184
301. M. Ooba, H. Takahashi, Effect of asymmetric stomatal response on gas exchange dynamics. Ecol. Model. **164**, 65–82 (2003)
302. R.J.C. Ooteghem, J.D. Stigter, L.G. van Willigenburg, G. van Straten, *Receding horizon optimal control of a solar greenhouse* (In Proceedings of Greensys, Leuven, Belgium, 2004)
303. C. Osorio, Implantación y puesta a punto de un sistema de control jerárquico del crecimiento del cultivo de un invernadero regulando las variables climáticas. Master's thesis, (Universidad de Almería, Spain, 2011)
304. B. Ozkhan, R. Fige, H. Kizalay, Energy inputs and crop yield relationships in greenhouse winter crop tomato production. Renew. Energy **36**, 3217–3221 (2011)
305. E. Palomo, Desarrollo de una metodología teórico experimental de caracterización de invernaderos. Ph.D. thesis, (Universidad Complutense de Madrid, Spain, 1992)
306. N.L. Panwar, S.C. Kaushika, S. Kotharib, Solar greenhouse an option for renewable and sustainable farming. Renew. Sustain. Energy Rev. **15**, 3934–3945 (2011)
307. C. Paoli, C. Voyant, M. Muselli, M.L. Nivet, Lecture Notes in Computer Science-ICIC 2009. Solar Radiation Forecasting Using ad-hoc Time Series Preprocessing and Neural Networks, vol. 5754 (Springer, Berlin, 2009), pp. 898–907
308. S. de Pascale, A. Maggio, *Sustainable protected cultivation at a Mediterranean climate perspectives and challenges* (In Proceedings of Greensys, Leuven, Belgium, 2004)
309. P.J. Paschold, K.H. Zengerle, Sweet pepper production in a closed system in mound culture with special consideration to irrigation scheduling. Acta Hortic. **458**, 329–334 (1998)
310. G.D. Pasgianos, K.G. Arvanitis, P. Polycarpou, N. Sigrimis, A nonlinear feedback technique for greenhouse environmental control. Comput. Electron. Agric. **40**, 153–177 (2003)
311. A. Patakas, B. Noistakis, A. Chouzouri, Optimization of irrigation water use in grapevine using the relationship between transpiration and plant water status. Agric. Ecosyst. Environ. **106**(2–3), 159–170 (2005)
312. S. Patil, H. Tantau, V. Salokhe, Modelling of tropical greenhouse temperature by autoregressive and neural network models. J. Biosyst. Eng. **99**(3), 423–431 (2008)
313. A. Pawlowski, A. Cervin, J.L. Guzmán, M. Berenguel, Generalized predictive control with actuator deadband for event-based approaches. IEEE Trans. Ind. Inform. **10**(1), 523–537 (2014)
314. A. Pawlowski, J.L. Guzmán, F. Rodríguez, M. Berenguel, J. Sánchez, S. Dormido, Simulation of greenhouse climate monitoring and control with wireless sensor network and event-vased control. Sensors **9**, 232–252 (2009)
315. A. Pawlowski, J.L. Guzmán, M. Berenguel, S. Dormido, Event-based predictive control triggered by input and output deadband conditions, In Proceedings of 19th IFAC World Congress. (Cape Town, South Africa, 2014)
316. A. Pawlowski, J.L. Guzmán, J.E. Normey-Rico, M. Berenguel, A practical approach for generalized predictive control within an event-based framework. Comput. Chem. Eng. **41**, 52–66 (2012)

317. A. Pawlowski, J.L. Guzmán, J.E. Normey-Rico, M. Berenguel, Improving feedforward disturbance compensation capabilities in generalized predictive control. J. Process Control **22**(3), 527–539 (2012)
318. A. Pawlowski, J.L. Guzmán, F. Rodríguez, M. Berenguel, Event-based control and wireless sensor network for greenhouse diurnal temperature control: a simulated case study, In IEEE International Conference on Emerging Technologies and Factory Automation EFTA'08, (Hamburg, Germany, 2008)
319. A. Pawlowski, J.L. Guzmán, F. Rodríguez, M. Berenguel, Event-based packet scheduling for wireless sensor networks, In 4th International Conference on Broadband Communication, Information Technology and Biomedical Applications, (Wroclaw, Poland, 2009)
320. A. Pawlowski, J.L. Guzmán, F. Rodríguez, M. Berenguel, S. Dormido, In Factory Automation. Study of Event-based Sampling Techniques and theirs Influence on Greenhouse Climate Control with Wireless Sensors Network. (Intech, 2009)
321. A. Pawlowski, J.L. Guzmán, F. Rodríguez, M. Berenguel, S. Dormido. The influence of event-based sampling techniques on data transmission and control performance, In 14th International Conference on Emerging Technologies and Factory Automation ETFA'09, (Mallorca, Spain, 2009)
322. A. Pawlowski, J.L. Guzmán, F. Rodríguez, M. Berenguel, J.E. Normey-Rico, *Predictive control with disturbance forecasting for greenhouse diurnal temperature control, in 18th IFAC World Congress* (Milano, Italy, 2011)
323. A. Pawlowski, J.L. Guzmán, F. Rodríguez, M. Berenguel, J. Sánchez, *Application of time-series methods to disturbance estimation in predictive control problems, In IEEE Symposium on Industrial Electronics IECON'10* (Bari, Italy, 2010)
324. R.K. Pearson, Nonlinear input/output modelling. J. Process Control **5**(4), 197–211 (1995)
325. J. Pérez Parra, E. Baeza, J.I. Montero, B.J. Bailey, Natural ventilation of parral greenhouses. Biosyst. Eng. 87(3), 355–366 (2004)
326. J. Pérez-Parra, M. Berenguel, F. Rodríguez, A. Ramírez-Arias, Ventilation rate models of Mediterranean greenhouses for control purposes. Acta Hortic. **719**, 197–204 (2006)
327. S.M. Piñón, E.F. Camacho, B. Kuchen, Constrained predictive control of a greenhouse. Comput. Electron. Agric. **49**, 317–329 (2005)
328. J. Ploennigs, V. Vasyutynskyy, K. Kabitzsch, Comparative study of energy-efficient sampling approaches for wireless control networks. IEEE Trans. Ind. Inform. **6**(3), 416–424 (2010)
329. H. Pohlheim, A. Heibner, Optimal control of greenhouse climate using real-world weather data and evolutionary algorithms, In Proceedings of the Genetic and Evolutionary Computation Conference-GECCO '99, (San Francisco, CA, 1999), pp. 1672–1677
330. W.H. Press, S.A. Teukolsky, T.W. Vetterling, B.P. Flannery, *Numerical Recipes in C: The Art of Scientific Computing* (Cambridge University Press, Cambridge, 1995)
331. E. Pressman, A. Bar-Tal, R. Shaked, K. Rosenfeld, The development of tomato root system in relation to the carbohydrate status of the whole plant. Ann. Bot **80**, 533–538 (1997)
332. A. Pross, The driving force for life-s emergence: kinetic and thermodynamic considerations. J. Theoretichal Biol. **220**, 393–406 (2002)
333. J.A. Pucheta, C. Schugurensky, R. Fullana, H.D. Patiño, B. Kuchen, Optimal greenhouse control of tomato-seedling crops. Comput. Electron. Agric. **50**(1), 70–82 (2006)
334. S.J. Qin, T.A. Badgwell, Using proportional integral derivative and fuzzy logic with optimization for greenhouse temperature control. Int. J. Latest Trends Agric. Food Sci **2**(2), 103–112 (2012)
335. R. Rabbinge, W.A.H. Rossing, W. van der Werf, Systems approaches in epidemiology and plant disease management. Neth. J. Plant Pathol. **99**(3), 161–171 (1993)
336. L.H. Rajaoarisoa, K.N.K. M'Sirdi, J.F. Balmat. A case study of a hybrid controller design of a class of hybrid system. Application to a greenhouse micro-climate control, In 2nd International Conference on Communications, Computing and Control Applications CCCA 2012, (Marseilles, France, 2012)
337. L.H. Rajaoarisoa, N.K. M'Sirdi, J. Balmat, Micro-climate optimal control for an experimental greenhouse automation, In 2nd International Conference on Communications, Computing and Control Applications (CCCA) (Marseilles, France, 2012), pp. 1–6

338. A. Ramírez, Control de calefacción en invernadero (heating control in greenhouses). Master's Ph.D. thesis, (Fundación Arturo Rosenblueth, México, 1998)
339. A. Ramírez-Arias, Control jerrquico multiobjetivo de cultivos en invernadero (Hierarchical multiobjective control of greenhouse crop production). Ph.D. thesis, (University of Almería, Spain, 2005)
340. A. Ramírez-Arias, F. Rodríguez, M. Berenguel, M.D. Fernández, A modified water model to control the irrigation supply in soilless systems, In Conference on Agricultural Engineering, (Wageningen, The Netherlands, 2004)
341. A. Ramírez-Arias, F. Rodríguez, M. Berenguel, E. Heuvelink, Calibration and validation of complex and simplified tomato growth models for control purposes in the southeast of Spain. Acta Hortic. **654**, 147–154 (2004)
342. A. Ramírez-Arias, F. Rodríguez, J.L. Guzmán, M.R. Arahal, M. Berenguel, J.C. López, *Improving efficiency of greenhouse heating systems using model predictive control, In 16th IFAC World Congress* (Czech Republic, Prague, 2005)
343. A. Ramírez-Arias, F. Rodríguez, J.L. Guzmán, M. Berenguel, Multiobjective hierarchical control architecture for greenhouse crop growth. Automatica **48**(3), 490–498 (2012)
344. P. de Reffye, D.G. Hu, Relevant qualitative and quantitative choices for building an efficient dynamic crop growth model: Green Lab case, In Proceedings of International Symposium on Plant Growth Modelling, Simulation and Visualization and their Applications, (Beijing, China, 2003)
345. G. Reikard, Predicting solar radiation at high resolutions: a comparison of time series forecasts. Sol. Energy **83**(3), 342–349 (2009)
346. A. Reina-Sánchez, R. Romero-Aranda, J. Cuartero, Plant water uptake and water use efficiency of greenhouse tomato cultivars irrigated with saline water. Agric. Water Manag. **78**, 54–66 (2005)
347. M. Rieger, P. Litvin, Root system hydraulic conductivity in species with contrasting root anatomy. J. Exp. Bot. **50**, 201–209 (1999)
348. G. de Rijck, E. Schrevens, Distribution of nutrients and water in rockwool slabs. Sci. Hortic. **72**, 277–285 (1998)
349. A.A. Rijsdijk, J.V.M. Vogelezang, Temperature integration on a 24-hour base: A more efficient climate control strategy. Acta Hortic. **519**, 163–169 (2000)
350. D.E. Rivera, H. Lee, M. Braun, H. Mittelmann, *Plant-friendly system identification: A challenge for the process industries, In 13th IFAC Symposium on System Identification* (Rotterdam, Netherlands, 2003), pp. 25–37
351. L. Roca, J.L. Guzmán, J.E. Normey-Rico, M. Berenguel, L. Yebra, Robust constrained predictive feedback linearization controller in a solar desalination plant collector field. Control Eng. Pract. **17**, 1076–1088 (2009)
352. C. Rodríguez, J.L. Guzmán, M. Berenguel, T. Hägglund, Generalized feedforward tuning rules for non-realizable delay inversion. J. Process Control **23**, 1241–1250 (2013)
353. C. Rodríguez, J.L. Guzmán, M. Berenguel, T. Hägglund, Optimal feedforward compensators for systems with right-half plane zeros. J. Process Control **24**, 368–374 (2014)
354. C. Rodríguez, J.L. Guzmán, F. Rodríguez, M. Berenguel, M.R. Arahal, Diurnal greenhouse temperature control with predictive control and online constraints mapping, In IFAC Conference on Control Methodologies and Technology for Energy Efficiency. (Vilamoura, Portugal, 2010)
355. F. Rodríguez, Modelado y control jerárquico de crecimiento de cultivos bajo invernadero (Modeling and hierarchical control of greenhouse crop production). Ph.D. thesis, (University of Almería, Spain, 2002)
356. F. Rodríguez, M.R. Arahal, M. Berenguel, *Application of artificial neural networks for greenhouse climate modeling, In European Control Conference ECC'99* (Karlsruhe, Germany, 1999)
357. F. Rodríguez, M. Berenguel, Sistemas de control climático de invernaderos (I). Riegos y Drenajes, XX **I**(115), 30–36 (2000)

358. F. Rodríguez, M. Berenguel, Sistemas de control climático de invernaderos (II). Sus efectos en el crecimiento del cultivo. Riegos y Drenajes, XX I(116), 28–37 (2000)

359. F. Rodríguez, M. Berenguel, Design, implementation, calibration and validation of a dynamic model of greenhouse climate based on physical principles. Technical report, (University of Almería, Spain, 2002) http://aer.ual.es/techreport/greenhouseclimatemodel02.pdf

360. F. Rodríguez, M. Berenguel, M.R. Arahal, A hierarchical control system for maximizing profit in greenhouse crop production. In European Control Conference ECC'03. (Cambridge, UK, 2003)

361. F. Rodríguez, M. Berenguel, M.R. Arahal, Feedforward controllers for greenhouse climate control based on physical models. In European Control Conference ECC'01. (Porto, Portugal, 2001)

362. F. Rodríguez, J.L. Guzmán, M. Berenguel, M.R. Arahal, Adaptive hierarchical control of greenhouse crop production. Int. J. Adapt. Control Signal Process. **22**, 180–197 (2008)

363. F. Rodríguez, L. Yebra, M. Berenguel, S. Dormido, Modelling and simulation of greenhouse climate using Dymola. In 15th IFAC World Congress, (Barcelona, Spain, 2002)

364. R. Romero-Aranda, T. Soria, J. Cuartero, Tomato plant-water relationships under saline growth conditions. Plant Sci. **160**, 265–272 (2001)

365. C. Ruggiero, S. de Pascale, M. Fagnano, Plant and soil resistance to water flow in faba bean (Vicia faba L. major). Plant Soil **210**, 219–231 (1999)

366. A. Ruiz, A. Ramírez-Arias, A. Rojano-Aguilar, W. Ojeda, *Amount of Water Supply in Soilless Irrigation System with Fuzzy Logic* (In ASAE Annual Meeting. Milwakee, USA, 2000)

367. J. Rumbaugh, M. Blaha, W. Premerlani, F. Eddy, W. Lorensen, *Object-Oriented Modeling and Design* (Prentice Hall, Englewood, 1991)

368. J. del Sagrado, F. Rodríguez, M. Berenguel, R. Mena, Bayesian networks for greenhouse temperature control. In International Conference on Soft Computing Models in Industrial and Environmental Applications, SOCO 2013 (Salamanca, Spain, 2013)

369. Ö Sahin, P. Sayan, A.N. Buluctu, Application of genetic algorithms for determination of mass transfer coefficients. J. Cryst. Growth 216, 475–482 (2000)

370. C. Salas San Juan, G.M. Urrestarazu, In Manual de Cultivos sin Suelo, chapter Métodos de riego y fertirrigación en cultivos sin suelo, (Mundiprensa, 1997), pp. 186–243

371. R. Salazar, U. Schmidt, C. Huber, A. Rojano, I. Lopez, Network models for temperatures and CO_2 control. Int. J. Agric. Res. **5**(4), 191–200 (2010)

372. P. Salgado, J. Boaventura-Cunha, Greenhouse climate hierarchical fuzzy modelling. Control Eng. Pract. **13**, 613–628 (2005)

373. J.A. Sánchez, F. Rodríguez, F.G. Acién, J.L. Guzmán, J.C. López, Biomass-based system design. In Agricultural Engineering-CIGR-AgEng 2012: Agriculture and Engineering for a Healthier Life, vol. C-0367. (Valencia, Spain, 2012)

374. J.A. Sánchez, F. Rodríguez, J.L. Guzmán, M.R. Arahal, Virtual sensors for designing irrigation controllers in greenhouses. Sensors **12**(11), 15244–15266 (2012)

375. M.J. Sánchez-Blanco, M.A. Morales, A. Torrecillas, J.J. Alarcón, Diurnal and seasonal osmotic potencial changes in Lotus creticus creticus plants grown under saline stress. Plant Sci. **136**, 1–10 (1998)

376. J.A. Sánchez-Molina, J.V. Reinoso, F.G. Acién, F. Rodríguez, J.C. López, Development of a biomass-based system for nocturnal temperature and diurnal CO_2 concentration control in greenhouses

377. S. Sarkka, A. Vehtari, J. Lampinen, Time series prediction by Kalman smoother with cross-validated noise density, In IEEE International Joint Conference on Neural Networks, vol. 2 (Budapest, Hungary, 2004), pp. 1615–1619

378. I. Seginer, Optimal control of the greenhouse environment: an overview. Acta Hortic. **406**, 191–198 (1996)

379. I. Seginer, Alternative design formulae for the ventilation rate of greenhouse. J. Agric. Eng. Res. **68**, 355–365 (1997)

380. I. Seginer, Some artificial neural network applications to greenhouse environmental control. Comput. Electron. Agric. **18**, 167–186 (1997)

381. I. Seginer, T. Boulard, B.J. Bailey, Neural network models of the greenhouse climate. J. Agric. Eng. Res. **59**, 203–216 (1994)
382. I. Seginer, I. Ioslovich, Seasonal optimisation of the greenhouse environment for a simple two-stage crop growth model. J. Agric. Eng. Res. **70**, 145–155 (1998)
383. I. Seginer, G. Shina, L.D. Albright, L.S. Marsh, Optimal temperature setpoints for greenhouse lettuce. J. Agric. Eng. Res. **49**, 209–226 (1991)
384. J.S. Senent, M.A. Martínez, X. Blasco, J. Sanchís. MIMO predictive control of temperature and humidity inside a greenhouse using Simulated Annealing (SA) as optimiser of a multi-criteria index. In 11th International Conference on Industrial and Engineering Applications of Artificial Intelligence and Expert Systems (Castellón, Spain, 1998)
385. D. Senthilkumar, Ch. Mahanta, Identification of uncertain nonlinear systems for robust fuzzy control. ISA Trans. **49**(1), 27–38 (2010)
386. V.P. Sethi, S.K. Sharma, Survey of cooling technologies for worldwide agricultural greenhouse applications. Sol. Energy **81**, 1447–1459 (2007)
387. V.P. Sethi, S.K. Sharma, Survey and evaluation of heating technologies for worldwide agricultural greenhouse applications. Sol. Energy **82**, 833–859 (2008)
388. V.P. Sethi, K Sumathy, C. Lee, D.S. Pal, Thermal modeling aspects of solar greenhouse microclimate control: a review on heating technologies. Sol. Energy **96**, 56–82 (2013)
389. A. Setiawan, L.D. Albright, R.M. Phelan, Simulation of greenhouse air temperature control using PI and PDF algorithms. In Proceedings of the 1st IFAC Workshop on Control Applications and Ergonomics in Agriculture (Athens, Greece, 1998), pp. 111–116
390. A. Setiawan, L.D. Albright, R.M. Phelan, Application of pseudo-derivative-feedback algorithm in greenhouse air temperature control. Comput. Electron. Agric. **26**(3), 283–302 (2000)
391. R. Shamshiri, W.I.W. Ismail, A review of greenhouse climate control and automation systems in tropical regions. J. Agric. Sci. Appl. **2**(3), 175–183 (2013)
392. P.K. Sharme, G.N. Tiwari, V.P.S. Sorayan, Temperature distribution in different zones of the microclimate of a greenhouse: a dynamic model. Energy Convers. Manag. **40**, 348–355 (1999)
393. Y. Sharon, B. Bravdo, A fully-automated orchard irrigation system based on constinuous monitoring of turgor potential with a leaf sensor. Acta Hortic. **562**, 55–61 (2001)
394. R.L. Shewfelt, What is quality? Postharvest Biol. Technol. **18**(3), 299–308 (1999)
395. P. Shi, X. Luan, F. Liu, H.R. Karimi, Kalman filtering on greenhouse climate control. In Proceedings of the 31st Chinese Control Conference (Hefei, China, 2012), pp. 779–784
396. M. Shuying, M. Yuquan, C. Lidong, L. Shiguang, Design of a new measurement and control system of CO_2 for greenhouse based on fuzzy control. In International Conference on Computer and Communication Technologies in Agriculture Engineering (Nanchang, China, 2010), pp. 128–131
397. M.Y. Siddiqi, H.J. Kronzucker, D.T. Britto, A.D.M. Glass, Growth of a tomato crop at reduced nutrient concentrations as a strategy to limit eutrophication. J. Plant Nutr. **21**(9), 1879–1895 (1998)
398. A. Siemens, J.J. Zwiazek, Effects of water deficit stress and recovery on the root water relations of trembling aspen (Populus tremuloides) seedlings. Plant Sci. **165**, 113–120 (2003)
399. N. Sigrimis, A. Anastaiou, N. Rerras, Energy saving in greenhouse using temperature integration: a simulation survey. Comput. Electron. Agric. **26**, 321–341 (2000)
400. N. Sigrimis, P. Antsaklis, P. Groumpos, Control advances in agriculture and the environment. IEEE Control Syst. Mag. Spec. Issue **21**(5), 8–12 (2001)
401. N. Sigrimis, K. G. Arvanitis, A. Anastasiou, G. D. Pasgianos. A comparison of optimal greenhouse heating set point generation algorithms for energy conservation. In 2nd IFAC/CIGR Conference on Intelligent Control in Agriculture Applications (Bali, Indonesia, 2001)
402. N. Sigrimis, K.G. Arvanitis, R.S. Gates, A learning technique for a general purpose optimizer. Comput. Electron. Agric. **26**(2), 83–103 (2000)
403. N. Sigrimis, K.G. Arvanitis, G.D. Pasgianos, Synergism of high and low level systems for the efficient management of greenhouses. Comput. Electron. Agric. **29**, 21–39 (2000)
404. N. Sigrimis, K.G. Arvanitis, G.D. Pasgianos, K.P. Ferentinos, Computer integrated management and intelligent control of greenhouses. Environ. Control Biol. **40**(1), 39–53 (2002)

405. N. Sigrimis, K.G. Arvanitis, G.D. Pasgianos, K. Ferentios, Hydroponics water management using adaptive scheduling with an on-line optimizer. Comput. Electron. Agric. **31**(1), 31–46 (2001)
406. N. Sigrimis, R. King. Advances in greenhouse environment control. Comput. Electron. Agric. Special Issue 26(3), (1999)
407. N. Sigrimis, P.N. Paraskevopoulos, K.G. Arvanitis, N. Rerras. Adaptive temperature control in greenhouses based on multirate-output controllers. In 14th IFAC World Congress (Beijing, China, 1999), pp. 571–576
408. N. Sigrimis, N. Rerras, A linear model for greenhouse control. Trans. ASAE **39**(1), 253–261 (1996)
409. F.F. da Silva, R. Wallach, Y. Chen, Hydraulic properties of roockwool slabs used as substrates in horticulture. Acta Hortic. **401**, 71–75 (1995)
410. J. Slotine, W. Li, *Applied Nonlinear Control* (Prentice Hall, New Jersey, 1991)
411. C. Sonneveld. Effects of salinity on substrate grown vegetables and ornamentals in greenhouse horticulture. PhD thesis (Wageningen University, The Netherlands, 2000)
412. C. Sonneveld, G. Swinkels, J. Campen, B. Tujil, H. Janssen, G.P.A. Bot, Performance results of a solar greenhouse combining electrical and thermal energy production. Biosyst. Eng. **106**, 48–57 (2010)
413. C. Sonneveld, C.A.M.N. van der Burg, Sodium chloride salinity in fruit vegetable crops in soilles culture. Netherlands J. Agric. Sci. **39**, 115–122 (1991)
414. C. Sonneveld, M.N.J. Verhoyen, Cult. tech. spec. emphasis environ. implications Nutr. manage. In Proceedings of the XXV International Horticultural Congress. (Brussels, Belgium, 1998)
415. T. Soria, J. Cuartero, Tomato fruit yield and water consumption with salty water irrigation. Acta. Hortic. **458**, 215–219 (1998)
416. S.L. Speetjens, J.D. Stigter, G. van Straten, Towards an adaptive model for greenhouse control. Comput. Electron. Agric. **67**(1–2), 1–8 (2009)
417. A. Sriraman, R.V. Mayorga, A fuzzy inference system approach for greenhouse climate control. Environ. Inform. Arch. **2**, 699–710 (2004)
418. A. Stamatakis, N. Papadantonakis, D. Savvas, N. Lidakis, P. Kefalas, Effects of silicon and salinity on fruit yield and quality of tomato grown hydroponically. Acta. Hortic. **609**, 141–147 (2003)
419. C. Stanghellini, *Transpiration Greenhouse Crops* (IMAG Publication, Wageningen, Holland, 1987)
420. C. Stanghellini, Evapotranspiration in greenhouses with special reference to Mediterranean conditions. Acta. Hortic. **335**, 295–304 (1992)
421. C. Stanghellini, A model of humidity and its applications in a greenhouse. Agric. For. Meteorol. **76**, 129–148 (1993)
422. C. Stanghellini, T. de Jong, A model of humidity and its applications in a greenhouse. Agric. For. Meteorol. **76**, 120–148 (1995)
423. C. Stanghellini, F. de Lorenzi, A comparison of soil-and canopy temperature - based methods for early detection of water stress in a simulated patch of pasture. Irrig. Sci. **14**, 141–146 (1994)
424. C. Stanghellini, F.L.K. Kempkes, P. Knies, Enhancing environmental quality in agricultural systems. Acta. Hortic. **609**, 277–283 (2003)
425. C. Stanghellini, ThM van Meurs, Environmental control of greenhouse crop transpiration. J. Agric. Eng. Res. **51**, 297–311 (1992)
426. E. Steudle, Water uptake by plant roots: an integration of views. Plant. Soil. **226**, 45–56 (2000)
427. E. Steudle, C.A. Peterson, How does water get through roots? J. Exp. Bot. **49**, 775–788 (1998)
428. G. van Straten, Acceptance of optimal operation and control methods for greenhouse cultivation. Ann. Rev. Control **23**, 83–90 (1999)
429. G. van Straten, H. Challa, F. Buwalda, Towards user accepted optimal control of greenhouse climate. Comput. Electron. Agric **26**, 221–238 (2000)

430. G. van Straten, F. Tap, L.G. van Willigenburg. Sensitivity of on-line RHOC of greenhouse climate to adjoint variables for the crop. In 14th IFAC World Congress (Beijing, China, 1999), pp. 383–387

431. G. van Straten, G. van Willigenburg, E. van Henten, R. van Ooteghem, *Optimal Control Greenhouse Cultivation* (CRC Press, USA, 2010)

432. G. van Straten, L.G. van Willigenburg, F. Tap, The significance of crop co-state for receding horizon optimal control of greenhouse climate. Control Eng. Pract. **20**, 625–632 (2002)

433. C. Sweetapple, G. Fu, D. Butler, Multi-objective optimisation of wastewater treatment plant control to reduce greenhouse gas emissions. Water Res. **55**, 52–62 (2014)

434. L. Taiz, E. Zeiger, *Plant Physiology* (Sinauer Associates Publishers, USA, 1998)

435. T. Takagi, M. Sugeno, Fuzzy identification of systems and its applications to modeling and control. IEEE Trans. Syst. Man Cybern. **15**, 116–132 (1985)

436. T. Takakura, *Climate Under Cover* (Kluwer Academic Publishers, Holland, 1993)

437. T. Takakura, K.A. Jordan, L.L. Boyd, Dynamic simulation of plant growth and environment in the greenhouse. Trans. ASAE **5**, 964–971 (1971)

438. K. Tanaka, H.O. Wang, *Fuzzy control systems design and analysis: a linear matrix inequality approach* (Wiley, New York, 2001)

439. H.J. Tantau, Analysis and synthesis of climate control algorithms. Acta. Hortic. **174**, 375–380 (1985)

440. H.J. Tantau. in The Computerized greenhouse Eds. Y. Hashimoto, G. Bot, H.J. Tantau, W. Day, H. Nonami), chapter Optimal control for plant production in greenhouses. (Academic Press, 1993), 139–152

441. R.F. Tap. Economics-based optimal control of greenhouse tomato crop production. PhD thesis (Agricultural University of Wageningen, The Netherlands, 2000)

442. R.F. Tap, L.G. van Willigenburg, G. van Straten, Experimental results of receding horizon optimal control of greenhouse climate. Acta. Hortic. **406**, 229–238 (1996)

443. R.F. Tap, L.G. van Willigenburg, G. van Straten. Receding horizon optimal control of greenhouse climate based on the lazy man weather prediction. In 13th IFAC World Congress (San Francisco, USA, 1996)

444. R.F. Tap, L.G. van Willigenburg, G. van Straten, G. van Henten. Optimal control of greenhouse climate: computation of the influence of fast and slow dynamics. In 12th IFAC World Congress (Sydney, Australia, 1993)

445. F. Tardieu, Why work and discuss the basic principles of plant modelling 50 years after the first plant models? J. Exp. Bot. **61**(8), 2039–2041 (2010)

446. C. Tavares, A. Gonzalves, P. Castro, D. Loureiro, A. Joyce, Modelling an agriculture production greenhouse. Renew. Energy **22**, 15–20 (2001)

447. M. Tchamitchian, H.J. Tantau. Optimal control of the daily greenhouse climate: physical approach. In 13th IFAC World Congress (San Francisco, USA, 1996) 471–475

448. M. Tchamitchian, L.G. van Willigenburg, G. van Straten, Optimal control applied to tomato crop production in a greenhouse. In European Control Conference ECC'93, vol. 3, (Groningen, Holland, 1993), pp. 1324–1348

449. M. Teitel, I. Segal, A. Shklyar, M. Barak, A comparison between pipe and air heating methods for greenhouses. J. Agric. Eng. Res. **72**, 259–273 (1999)

450. R.D. Thompsom, Programación de riegos mediante sensores de humedad en suelo. In Jornadas Técnicas de Agricultura. (Almería, Spain, 2004)

451. J.H.M. Thornley. Mathematical models in plant physiology. A quantitative approach to problems in Plant and Crop Physiology (Blackburn Press, London, 1976)

452. J.H.M. Thornley, Modelling water in crops and plant ecosystems. Ann. Bot. **77**, 261–275 (1996)

453. B.T. Tien, G. van Straten, A neuro-fuzzy approach to identify lettucce growth and greenhouse climate. Artif. Intell. Rev. **12**, 71–93 (1998)

454. Y. Ton, M. Kopyt, Phytomonitoring: A bridge from sensors to information technology for greenhouse control. Acta. Hortic. **614**, 639–644 (2003)

455. Y. Ton, N. Nilov, M. Kopyt, Phytomonitoring: the new information technology for improving crop production. Acta. Hortic. **562**, 257–262 (2001)
456. A. Torrecillas, C. Guillaume, C., J.J. Alarcón, and M.C. Ruíz-Sánchez. Water relations of two tomato species under water stress and recovery. Plant. Sci. 105, 169–176 (1995)
457. A. Trabelsi, F. Lafont, M. Kamoun, G. Enea, Fuzzy identification of a greenhouse. Appl. Soft Comput. **7**(3), 192–201 (2010)
458. M. Trigui. Strategy for the optimal climate control of greenhouse tomatoes PhD Thesis (McGill University, Montreal, Canada, 2000)
459. M. Trigui, S. Barrington, L. Gauthier, A strategy for greenhouse climate control, Part I: Model development. J. Agric. Eng. Res. **78**(4), 407–423 (2001)
460. M. Trigui, S. Barrington, L. Gauthier, A strategy for greenhouse climate control, Part II: Model validation. J. Agric. Eng. Res. **79**(1), 99–105 (2001)
461. A.J. Udink ten Cate. Modeling and (adaptive) control of greenhouse climates. PhD Thesis (Agricultural University of Wageningen, The Netherlands, 1983)
462. A.J. Udink ten Cate, *In Computer applications in agricultural environments, chapter analysis and synthesis of greenhouse climate controllers* (Butterworths, London, 1987), pp. 1–19
463. R.K. Ursen, B. Filipic, T. Krink, Exploring the performance of an evolutionary algorithm for greenhouse control. J. Comput. Inf. Technol. CIT **10**(3), 195–201 (2002)
464. R. Vadakkoot, M.D. Shah, S. Shrivastava, Enhanced moving average computation.In World Congress on Computer Science and Information Engineering. (Los Angeles, USA, 2009)
465. A. Vadiee, V. Martin, Energy management strategies for commercial greenhouses. Appl. Energy **114**, 880–888 (2014)
466. T.L.C. Valdéz. Medidas continuas del estado hídrico de la planta y del suelo para la programación del riego en cultivos hortícolas de invernaderos. PhD Thesis (Universidad de Almería, Spain, 2005)
467. R.L.M. van Uffelen, A.A. van der Mass, P.C.M. Vremeulen, J.C.J. Ammerlaan, TQM applied to the Dutch glasshouse industry: State of the art in 2000. Acta Hortic. **536**, 679–686 (2000)
468. B.H.E. Vanthoor, C. Stanghellini, E.J. van Henten, P.H.B. de Visser, A methodology for model-based greenhouse design: Part 1, a greenhouse climate model for a broad range of designs and climates. Biosyst. Eng. **10**(4), 363–377 (2011)
469. R. Vilanova, A. Visioli, *PID control in the third millennium: lessons learned and new approaches* (Springer, Berlin, 2012)
470. T.L.S. Vincent, T. Vincent, Using the ESS maximum principle to explore root-shoot allocation, competition and coexistence. J. Theor. Biol. **180**, 111–120 (1996)
471. W. Wan-Liang, W. Qi-Di. Neural network modelling and intelligence control of the distributed parameter greenhouse climate. In 14th IFAC World Congress, (Beijing, China, 1999), pp. 479–484
472. H.O. Wang, K. Tanaka, M.F. Griffin, An approach to fuzzy control of nonlinear systems: Stability and design issues. IEEE Trans. Fuzzy Syst. **4**, 14–23 (1996)
473. J.Z. Wang, P.P. Li, H.P. Mao, Decision support system for greenhouse environment management based on crop growth and control cost. Trans. Chin. Soc. Agri. Eng. **22**, 168–171 (2006)
474. J.Z. Wang, L.L. Qin, G. Wu, X.T. Lu, Modeling of greenhouse temperature-humid system and model predictive control based on switching system control. Trans. Chin. Soc. Agri. Eng. **24**, 182–192 (2008)
475. Q.J. Wang, Using genetic algorithms to optimise model parameters. Environ. Model. Softw. **12**(1), 27–34 (1997)
476. S. Wang, T. Boulard, Predicting the microclimate in a naturally ventilated plastic house in a Mediterranean climate. J. Agric. Eng. Res. **75**, 27–38 (2000)
477. S. Wang, T. Boulard, R. Haxaire, Air speed profiles in a naturally ventilated greenhouse with a tomato crop. Agric. Forest. Meteorol **96**, 181–188 (1999)
478. H. Xiao, L. Feng, Y. Zhi, Flexible time-triggered sampling in smart sensor-based wireless control system. Sensors **7**, 2548–2564 (2007)

479. H. Xu, L. Gauthier, A. Gosselin, Effects of fertigation management on growth and photsynthesis of tomato plants grown in peat rockwool and NFT. Sci. Horti. **63**, 11–20 (1995)

480. Z.T. Xu, Z.Y. Yao, L.J. Chen, S.F. Du. Greenhouse air temperature predictive control using the Dynamic Matrix Control. In 2013 fourth international conference on intelligent control and information processing (ICICIP), (Beijing, China, 2013) pp. 349–353

481. Q. Yi, N. Duo, L. Zhanchi, C. Qi, M. Lining, Neural networks based on PID control for greenhouse temperature. Trans. CSAE **27**(2), 307–311 (2011)

482. P. Young, A. Chotai, Data-based mechanistic modeling, forecasting and control. IEEE Control Syst. Mag. **21**(5), 14–26 (2001)

483. P. Young, M. Lees, A. Chotai, W. Tych, The modelling and multivariable control of glasshouse systems. In 12th IFAC World Congress, 10 (Sidney, Australia, 1993), pp. 313–316

484. A. Zaharim, A.M. Razali, T.P. Gim, K. Sopian, Time series analysis of solar radiation data in the tropics. Eur. J. Sci. Res. **25**(4), 672–678 (2009)

485. S. Zeng, H. Hu, L. Xu, G. Li, Nonlinear adaptive PID control for greenhouse environment based on RBF network. Sensors **12**, 5328–5348 (2012)

486. Q. Zengshuai, W. Xiangdong. Environmental parameter control of the greenhouse. In 2013 Fifth conference on measuring technology and mechatronics automation, (Hong Kong, 2013) pp. 93–98

487. Q. Zhang, C.H. Wu. Application of fuzzy logic in an irrigation control system. In Proceedings of IEEE international conference on industrial technology, (Shanghai, 1996) pp. 593–597

488. X. Zhang, C. Chang, Design of water-saving irrigation monitoring system based on CC2430 and fuzzy-PID. J. Control Eng. Technol **2**(3), 124–129 (2012)

489. Y. Zhang, Y. Mahrer, M. Margolin, Predicting the microclimate inside a greenhouse: an application of a one-dimensional numerical model in an unheated greenhouse. Agr. For. Meteorol **86**, 291–297 (1997)

490. X. Zhou, C. Wang, H. Lan. The research and PLC application of fuzzy control in greenhouse environment. In 2009 sixth international conference on fuzzy systems and knowledge discovery, (Tianjin, China, 2009) pp. 340–344

491. J. Zhuang, K. Nakayama, G.R. Yu, T. Urushisaki, Estimation of root water uptake of maize: An ecophysiological perspective. Field Crop Res. **69**, 201–213 (2001)

492. Q. Zou, J. Ji, S. Zhang, M. Shi, Y. Luo. Model predictive control based on particle swarm optimization of greenhouse climate for saving energy consumption. In Proceedings of world automation congress (WAC 2010), (Marseilles, France, 2010), pp. 1–6

493. Z. Zuo, H. Mao, X. Zhang, W. Huang, X. Guan, Y. Hu. Design of a new measurement and control system of CO_2 for greenhouse based on fuzzy control. In ASABE annual international meeting (Dallas, Texas, USA, 2012), pp. 12–1341219

494. H.F. de Zwart. Analyzing Energy-saving Options in Greenhouse Cultivation Using a Simulation Model. PhD Thesis, (Wageningen University, The Netherlands, 1996)

Index